

LIBRARY OF THE
UNIVERSITY OF ILLINOIS
AT URBANA-CHAMPAIGN

537.12
H19i

Engin.



The person charging this material is responsible for its return to the library from which it was withdrawn on or before the **Latest Date** stamped below.

Theft, mutilation, and underlining of books are reasons for disciplinary action and may result in dismissal from the University.

UNIVERSITY OF ILLINOIS LIBRARY AT URBANA-CHAMPAIGN

ENGINEERING

NOV 22 1976

MAR - 1 1981

APR 13 REC'D

DEC 04 1985

DEC 06 REC'D

APR 21 1987

MAY 12 1987

MAY 12 REC'D

IRRC NOV 20 2009

SEP 26 REC'D

APR 30 REC'D

L161—O-1096

© Copyright by

Donald Farness Hanson

1976

AN INVESTIGATION OF THE CURRENT SOURCE-FUNCTION TECHNIQUE
FOR SOLVING PROBLEMS OF ELECTROMAGNETIC SCATTERING

BY

DONALD FARNESS HANSON

B.S., University of Illinois, 1969

M.S., University of Illinois, 1972

THESIS

Submitted in partial fulfillment of the requirements
for the degree of Doctor of Philosophy in Electrical Engineering
in the Graduate College of the
University of Illinois at Urbana-Champaign, 1976

Urbana, Illinois

27.12
H172

ENGINEERING LIBRARY

UNIVERSITY OF ILLINOIS AT URBANA-CHAMPAIGN

THE GRADUATE COLLEGE

May, 1976

WE HEREBY RECOMMEND THAT THE THESIS BY

DONALD FARNES HANSON

ENTITLED AN INVESTIGATION OF THE CURRENT SOURCE-FUNCTION TECHNIQUE

FOR SOLVING PROBLEMS OF ELECTROMAGNETIC SCATTERING

BE ACCEPTED IN PARTIAL FULFILLMENT OF THE REQUIREMENTS FOR

THE DEGREE OF DOCTOR OF PHILOSOPHY

Paul E. Mayne

Director of Thesis Research

Ed Jordan

Head of Department

Committee on Final Examination†

Paul E. Mayne

Chairman

Joseph C. Deschamps

Harvey Belford

Paul W. Klock

† Required for doctor's degree but not for master's.

UNIVERSITY OF ILLINOIS
Urbana-Champaign Campus
The Graduate College
330 Administration Building

FORMAT APPROVAL

To the Graduate College:

The format of the thesis submitted by DONALD FARNESS HANSON
for the degree of DOCTOR OF PHILOSOPHY is acceptable to the
department of Electrical Engineering.

4/30/76

Date

(Signed)

Harold S. Weir
Departmental Representative

ACKNOWLEDGMENT

I would like to express my appreciation to my adviser, Professor P. E. Mayes. The many hours spent in discussion were fundamental to the development and completion of this dissertation. I would like to thank Professor G. A. Deschamps, Professor G. G. Belford, and Professor P. W. Klock for their helpful comments and suggestions.

The typing skills of Mrs. Brenda Masters and the artistic abilities of S. J. Holland are gratefully acknowledged.

I am indebted to the Departments of Electrical Engineering and Architecture at the University of Illinois for providing me with teaching positions during the course of this work and to the University of Illinois Research Board for providing computer time.

TABLE OF CONTENTS

CHAPTER	Page
1. INTRODUCTION.....	1
2. LITERATURE SURVEY AND BACKGROUND MATERIAL.....	5
2.1 Integral and Integro-differential Equation Formulations.....	5
2.2 The Wave Equation and a Magnetic Field Source-Function.....	10
2.3 The Edge Condition.....	17
2.4 Divergent Integrals and the Finite Part.....	19
2.5 Conclusion.....	27
3. THE CURRENT SOURCE-FUNCTION TECHNIQUE APPLIED TO THE HALF-PLANE PROBLEM.....	28
3.1 Maxwell's Equations and the Current Source-Function Technique.....	28
3.2 The E- and H-polarization Current Source-Functions.....	29
3.3 The Solution of the Integral Equations for $u(z)$	32
3.3.1 Solution of the Homogeneous Finite Part Integral Equation by the Wiener-Hopf Technique.....	34
3.3.2 The Solution of the Homogeneous Finite Part Integral Equation from Belward's Results.....	39
3.3.3 The Solution of the Homogeneous Finite Part Integral Equation by Differentiation.....	40
3.4 The Consistency Condition.....	41
3.5 The Current in Terms of the Current Source-Function.....	48
3.6 Discussion of the Results and Conclusions.....	51
4. THE NUMERICAL SOLUTION OF THE HALF-PLANE PROBLEM: E-POLARIZATION	54
4.1 The Integral Equation Formulation for the E-polarization....	54
4.1.1 The Physical Optics Current, I_{p0}	55
4.1.2 The Integral Equation for the Difference $\{I_E - I_{p0}\}$..	56
4.1.3 The Choice of Expansion Functions.....	57
4.2 Matrix Element Approximations.....	61
4.2.1 Matrix Element Approximations for Pulse Basis Functions.....	61
4.2.2 Matrix Elements Associated with the Inverse Square Root Basis Function.....	63
4.3 The Right-Hand Side.....	66

CHAPTER	Page
4.3.1 Computation of the U_k 's.....	68
4.3.2 Computation of the J_k 's.....	68
4.3.3 The Computation of the S_k 's.....	69
4.3.4 Final Remarks on RHS.....	70
4.4 The Efficient Inversion of the Almost-Toeplitz Matrix.....	70
4.5 The Results.....	74
4.5.1 Accuracy of the Moment Method Results.....	75
4.5.2 The Relation Between the Hybrid Expansion Solution and the All-Pulse Expansion Solution.....	89
4.6 Conclusion.....	105
5. THE NUMERICAL SOLUTION OF THE HALF-PLANE PROBLEM BY THE CURRENT SOURCE-FUNCTION TECHNIQUE: H-POLARIZATION.....	106
5.1 The Current Source-Function Technique Applied to the Half- Plane Problem.....	106
5.1.1 The Physical Optics Current for the H-polarization, I_{po}	107
5.1.2 The Solution for u_H , the Current Source-Function, in Terms of $\{I_E - I_{po}\}$	107
5.1.3 The Solution for $\{I_H - I_{po}\}$ in Terms of $\{I_E - I_{po}\}$...	111
5.2 The Numerical Evaluation of $\{I_H - I_{po}\}$	112
5.2.1 The Evaluation of the Integral Weighted by $h(y,y')$...	115
5.2.2 The Evaluation of the Integral Weighted by $g(y,y')$...	117
5.2.3 The Numerical Evaluation of the Integrals Used to Find A, the Consistency Constant.....	118
5.3 The Numerical Results for I_H	119
5.3.1 Accuracy of the Numerical Results for the Consist- ency Constant, A.....	120
5.3.2 Accuracy of the Numerical Results for $\{I_H - I_{po}\}$	122
5.4 Conclusion.....	132
6. SCHWARTZ DISTRIBUTION THEORY AND THE STRIP PROBLEM.....	133
6.1 The Strip Problem.....	133
6.2 Pertinent Concepts in Schwartz Distribution Theory.....	136
6.2.1 The Definition of a Distribution.....	137
6.2.2 The Differentiation of a Distribution.....	140
6.2.3 The Convolution of Distributions.....	142
6.2.4 Convolution Equations.....	144

CHAPTER	Page
6.3 Maxwell's Equations and the Convolution Equation for the Current Source-Function.....	146
6.4 An Attempt to Solve for $u(z)$	150
6.5 The Consistency Condition.....	154
6.6 The Solution for the Current.....	157
6.6.1 Off Resonance.....	157
6.6.2 The Case of Resonance.....	159
6.7 Conclusion.....	160
7. THE THREE-DIMENSIONAL TIME-DEPENDENT CURRENT SOURCE-FUNCTION.....	162
7.1 Maxwell's Equations and the Current Source-Function.....	162
7.2 The Expression for the Current in Terms of the Current Source-Function.....	163
7.3 Conclusions.....	165
8. CONCLUSION AND SUGGESTIONS FOR FURTHER DEVELOPMENT.....	166
APPENDICES	
A. ANALYSIS OF ACCURACY.....	169
B. APPROXIMATIONS TO THE MATRIX ELEMENTS.....	173
B.1 The Self Terms for a Pulse Basis Function.....	174
B.2 The Mutual Terms for a Pulse Basis Function.....	175
B.3 The Self Terms for an Inverse Square Root Basis Function....	179
B.4 The Mutual Terms for an Inverse Square Root Basis Function..	181
C. THE CHEBYSHEV APPROXIMATION FOR $\int_0^H t^{-\frac{1}{2}} H_0^{(1)}(t) dt$	185
D. COMPUTER PROGRAMS.....	190
REFERENCES.....	238
VITA.....	244

LIST OF TABLES

Table	Page
4.1 Digits of Accuracy for RHS by Double Precision Evaluation of Equations (3.4) and (3.6).....	71
4.2 Accuracy of the Inverse Square Root Expansion Function Coefficient.....	85
4.3 Average Digits of Accuracy for the Hybrid Expansion Solution Over Several Ranges.....	87
4.4 Average Digits of Accuracy for the All-Pulse Expansion Solution Over Several Ranges.....	88
4.5 A Relation Between the Coefficient for the Inverse Square Root Basis Function and the Edge Coefficient for the All-Pulse Expansion.....	93
4.6 Comparison of the Empirical Formula for $(T^{-1}\underline{r})_1$ with Numerical Results.....	96
4.7 Comparison of the Empirical Formula for $(T^{-1}\underline{r})_2$ with Numerical Results.....	97
4.8 Comparison of the Empirical Formula for $(T^{-1}\underline{p})_1$ with Numerical Results.....	98
4.9 Comparison of the Empirical Formula for $(T^{-1}\underline{p})_2$ with Numerical Results.....	99
4.10 Comparison of the Values of the First Two Elements in the Solution Vector for the Hybrid Expansion with the Values Obtained Using the Corresponding Elements for the All-Pulse Expansion and the Empirical Formulas.....	101
4.11 Comparison of the Values of the First Two Elements in the Hybrid and All-Pulse Expansion Solution Vectors with the Values Obtained Using the Corresponding Elements in the Toeplitz Solution Vector..	103
4.12 Number of Matching Digits in the Magnitudes of Elements of T^{-1} as Matrix Order is Varied.....	104
5.1 Accuracy of the Numerical Results for $kZ_0 F_{kL}(\theta)$	121
5.2 Accuracy of the Numerical Results for ikA_θ , the Consistency Constant.....	123
5.3 Accuracy of $Z_0\{I_H - I_{po}\}$ for $\theta = 45^\circ$ and $\theta = 90^\circ$	131

Table		Page
B.1	Digits of Accuracy and Decimal Offset Factors for Pulse Expansion Function Self Term Matrix Element Approximations.....	176
B.2	Digits of Accuracy and Decimal Offset Factors for Pulse Expansion Function Matrix Element Approximations--the Mutual Terms.....	178
B.3	Digits of Accuracy and Decimal Offset Factors for Pulse Expansion Function Matrix Element Approximations for Small H and D.....	180
B.4	Digits of Accuracy and Decimal Offset Factors for Inverse Square Root Expansion Function Self Term Matrix Element Approximations....	182
B.5	Digits of Accuracy and Decimal Offset Factors for Inverse Square Root Expansion Function Matrix Element Approximations--the Mutual Terms.....	184
C.1	The Chebyshev Coefficients for $H_0^{(1)}(t)$	186
C.2	The Chebyshev Coefficients for $\int_0^x t^{-\frac{1}{2}} H_0^{(1)}(t) dt$	188

LIST OF FIGURES

Figure		Page
2.1	The Geometry of the Half-plane Problem for (a) the E-polarization, and (b) the H-polarization.....	7
3.1	Integration Path for (a) $z < 0$, and (b) $z > 0$; (c) Deformed Path for $z > 0$	38
4.1	The Expansion Function Sets. (a) The Hybrid Expansion. (b) The All-Pulse Expansion.....	58
4.2	Plots of $Z_0 \cdot \text{RHS}$ for Angles of Incidence of 45° , 90° , 135° and 180° .	72
4.3	Comparison of the Exact with the Hybrid Expansion Moment Method Solution for $\theta = 45^\circ$	76
4.4	Comparison of the Exact with the Hybrid Expansion Moment Method Solution for $\theta = 90^\circ$	77
4.5	Comparison of the Exact with the Hybrid Expansion Moment Method Solution for $\theta = 135^\circ$	78
4.6	Comparison of the Exact with the Hybrid Expansion Moment Method Solution for $\theta = 180^\circ$	79
4.7	Comparison of the Exact with the Hybrid Expansion Solution and the All-Pulse Expansion Solution for the First Eleven Subsections and $\theta = 45^\circ$	81
4.8	Comparison of the Exact with the Hybrid Expansion Solution and the All-Pulse Expansion Solution for the First Eleven Subsections and $\theta = 180^\circ$	82
4.9	Comparison of the Exact with the Hybrid Expansion Solution and the All-Pulse Expansion Solution for $\theta = 45^\circ$ and the Edge Subsection....	83
4.10	Comparison of the Exact with the Hybrid Expansion Solution and the All-Pulse Expansion Solution for $\theta = 180^\circ$ and the Edge Subsection...	84
4.11	Comparison of the Exact with the Hybrid Expansion Solution and with the All-Pulse Expansion Solution for the Edge Subsection, $\theta = 135^\circ$, and $H = 0.05$	92
5.1	Comparison of the Exact with the Numerical Results Corresponding to the Hybrid and the All-Pulse Expansion Solutions for $\theta = 45^\circ$	124
5.2	Comparison of the Exact with the Numerical Results Corresponding to the Hybrid and the All-Pulse Expansion Solutions for $\theta = 90^\circ$	125

Figure	Page
5.3 Comparison of the Exact with the Numerical Results Corresponding to the Hybrid and the All-Pulse Expansion Solutions for $\theta = 135^\circ$...	126
5.4 Comparison of the Exact Edge Behavior for $\{I_H - I_{po}\}$ with that of the Numerical Results Corresponding to the Hybrid and the All-Pulse Expansion Solutions for $\theta = 45^\circ$	128
5.5 Comparison of the Exact Edge Behavior for $\{I_H - I_{po}\}$ with that of the Numerical Results Corresponding to the Hybrid and the All-Pulse Expansion Solutions for $\theta = 90^\circ$	129

1. INTRODUCTION

In the years since 1965, a great deal of work in electromagnetic theory has been based on the moment method for the numerical solution of integral equations. For certain classes of problems, the electric field integral equation, derived by requiring the tangential component of the electric field to vanish on perfectly conducting surfaces, is most advantageous. The cylindrical antenna problem is an example. Previous studies of this problem have considered one of two standard representations for the electric field integral equation, or some slight modification of one of them. If azimuthal variation in the field can be neglected, the integral equations are

$$\left(\frac{d^2}{dt^2} + k^2 \right) \int_L I(z) K(|z-t|) dz = i\omega\epsilon E_{\tan}^i(t), \quad t \in L, \quad (1.1)$$

and

$$\int_L I(z) K(|z-t|) dz = A \cos(kt) + B \sin(kt) + i\omega\epsilon \int_L E_{\tan}^i(z) g(t,z) dz, \quad (1.2)$$

$t \in L,$

where $e^{-i\omega t}$ time dependence with radian frequency ω is assumed, k is the free space wave number, and ϵ is the permittivity of the medium. These two equations are due to Pocklington (1897) and Hallén (1938), respectively. $I(z)$ is the induced current due to the incident electric field which has tangential component E_{\tan}^i . The kernel $K(|z-t|)$ is

$$K(|z-t|) = \frac{1}{8\pi^2} \int_0^{2\pi} \frac{e^{ik\sqrt{4a^2 \sin^2(\phi/2) + (z-t)^2}}}{\sqrt{4a^2 \sin^2(\phi/2) + (z-t)^2}} d\phi \quad (1.3)$$

where ϕ is the azimuthal angle and a is the cylinder radius. A and B are constants. $g(t,z)$ is a Green's function for the one-dimensional harmonic operator $(d^2/dt^2 + k^2)$. Discussions of these integral equations may be found in many sources, for example, in Mittra (1973, pp. 9-14).

In 1972, Mayes (1972) proposed an alternate integral equation formulation for the cylindrical rod scatterer or antenna. This formulation is

$$\int_L u(z) K(|z-t|) dz = i\omega \epsilon E_{\tan}^i(t), \quad t \in L \quad (1.4)$$

where

$$\frac{d^2 I}{dz^2} + k^2 I = u(z). \quad (1.5)$$

Note that the integral equation (1.4) has the same kernel as (1.1) and (1.2) and that there are no differential operators involved. The left-hand side of (1.4) has the same form as the left-hand side of Hallén's equation (1.2) and the right-hand side is identical to the right-hand side of Pocklington's equation (1.1). The unknown quantity in (1.4), however, is not the induced current, but rather an auxiliary function, called the "current source-function," from which the current can be obtained by solving the inhomogeneous differential equation (1.5). If a solution for the current source-function $u(z)$ is found from the integral equation (1.4), then the current is found from (1.5) to be

$$I(z) = \int_L u(t) g(t,z) dt, \quad z \in L, \quad (1.6)$$

where $g(t,z)$ is a Green's function for the operator $(d^2/dz^2 + k^2)$.

The current source-function (CSF) technique differs from previous procedures in that the vector and scalar potentials are not used. Instead, direct relationships between the fields \underline{E} and \underline{H} and the electric and magnetic current sources, \underline{J} and \underline{K} , respectively, and their derivatives, are introduced. Although these direct relationships are not new, their application to integral equations apparently is. Collin (1960, Eq. (51b), p. 21) gives such a direct relation between \underline{E} and \underline{J} . It is

$$\nabla^2 \underline{E} + k^2 \underline{E} = \frac{1}{i\omega\epsilon} \{ \nabla \nabla \cdot \underline{J} + k^2 \underline{J} \} = \frac{1}{i\omega\epsilon} \underline{U} \quad (1.7)$$

where

$$\underline{U} = \nabla \nabla \cdot \underline{J} + k^2 \underline{J}. \quad (1.8)$$

This \underline{U} is the vector current source-function. The solution for \underline{E} in terms of \underline{U} is

$$\underline{E} = - \frac{1}{4\pi i\omega\epsilon} \iiint_V \underline{U}(\underline{r}') \frac{e^{ikR}}{R} dV' \quad (1.9)$$

where $R = |\underline{r} - \underline{r}'|$ is the source-point to observation-point distance. Equation (1.9) may be used to form electric field integral equations for antennas and scatterers which are shapes other than finite circular cylinders.

Since the form of the CSF integral equation, Equation (1.4), is simpler than either that of Pocklington or of Hallén, it has been conjectured

that the numerical solution of CSF integral equations should be more efficient. However, the CSF formulation is not without difficulties. The current density function \underline{J} may not be twice-differentiable throughout all of space. Hence, the current source-function may not exist everywhere. This may require that the concept of functions be generalized according to the rules of Schwartz distribution theory. Furthermore, differentiation of \underline{J} may produce singularities in \underline{U} of such order that the integral (1.9) is divergent. In this case either the theory of distributions or the concept of the finite part of divergent integrals is required.

The work reported here was undertaken to establish the validity and feasibility of the CSF technique. For this purpose, some classical problems of electromagnetic scattering are attacked using the CSF approach so that comparisons can be made. The validation of the CSF formulation for scattering by a semi-infinite conducting plane is reported here in detail. Chapter 2 surveys previous work on certain aspects of the half-plane problem and its relation to the CSF technique. Chapter 3 details the analytic solution to the half-plane problem using the current source-function technique. Chapters 4 and 5 discuss the numerical solution of the half-plane problem by the CSF technique for the E-polarization and the H-polarization, respectively. An attempt to extend the CSF technique to the strip problem is described in Chapter 6. Chapter 7 presents a discussion of the possible extension of the CSF technique to the three-dimensional time-dependent case. Conclusions and suggestions for further work are given in Chapter 8.

2. LITERATURE SURVEY AND BACKGROUND MATERIAL

The solution for the current induced on a perfectly conducting half-plane by an incident plane wave was chosen as a first test of the CSF technique. A number of mathematical procedures have previously been established to provide solutions to this classic problem. Some early authors developed results which, accepted as proper at the time, were later shown to be improper because they did not satisfy the edge condition. After the development of the edge condition, other researchers published papers that corrected such results of the early authors. In order to make the earlier results obey the edge condition, the later authors sometimes found that another function which satisfied the requirements of the problem had to be subtracted from the original solution. It turns out that a similar function must be added to have the current source-function exhibit the correct edge behavior. [For example, see Equation (4.2) of Chapter 3.] This additional function is not integrable in the ordinary sense, so that the theory of divergent integrals must be used. Integral equation and integro-differential equation formulations for the half-plane problem are given in Section 2.1. The partial differential equation CSF formulation for the half-plane problem is discussed in Section 2.2. The findings of the authors who altered early results to make them conform to the edge condition are described in Section 2.3. Divergent integrals are discussed in Section 2.4.

2.1 Integral and Integro-differential Equation Formulations

Consider a perfectly conducting half-plane subjected to an incident plane wave of radian frequency ω polarized with either the electric or the

magnetic field parallel to the edge of the conductor. These will be referred to as the E-polarization and the H-polarization, respectively.

Figure 2.1 shows the geometry and the coordinate system for each of these polarizations. Throughout this chapter, M denotes the metal or perfectly conducting sheet defined by $x = 0$, $z > 0$ in Figure 2.1.

The integral equation and integro-differential equation formulations for, respectively, the E-polarization and the H-polarization half-plane currents are well known. For the E-polarization [see Figure 2.1(a)], the integral equation for the current I_E is

$$\int_0^{\infty} I_E(z') H_0^{(1)}(k|z-z'|) dz' = \frac{4}{kZ_0} E_y^i, \quad z > 0. \quad (1.1)$$

For the H-polarization [see Figure 2.1(b)], the integro-differential equation for the current I_H is

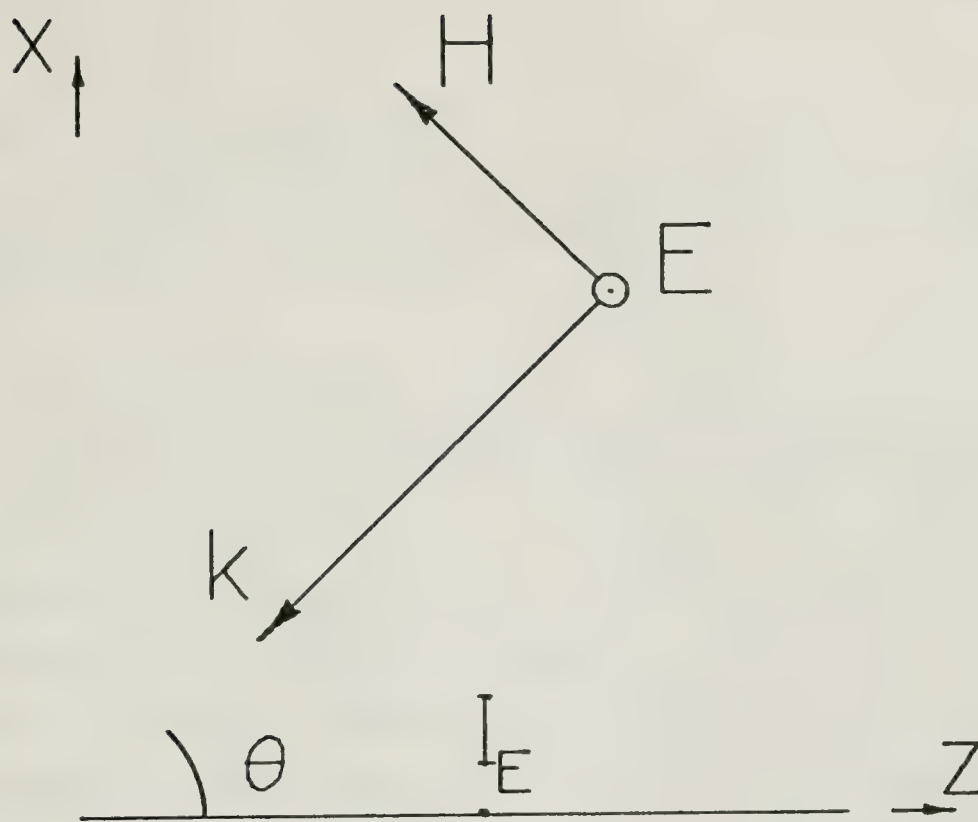
$$\left(\frac{d^2}{dz^2} + k^2 \right) \int_0^{\infty} I_H(z') H_0^{(1)}(k|z-z'|) dz' = \frac{4k}{Z_0} E_z^i, \quad z > 0. \quad (1.2)$$

$H_0^{(1)}$ is the Hankel function of the first kind and order zero and is the kernel for the equations. Z_0 is the intrinsic impedance of the (free-space) medium. $I_E(z')$ and $I_H(z')$, respectively, are the unknown E- and H-polarization currents. E_y^i and E_z^i are the tangential incident electric fields evaluated at $x = 0$. For plane wave incident fields, these are

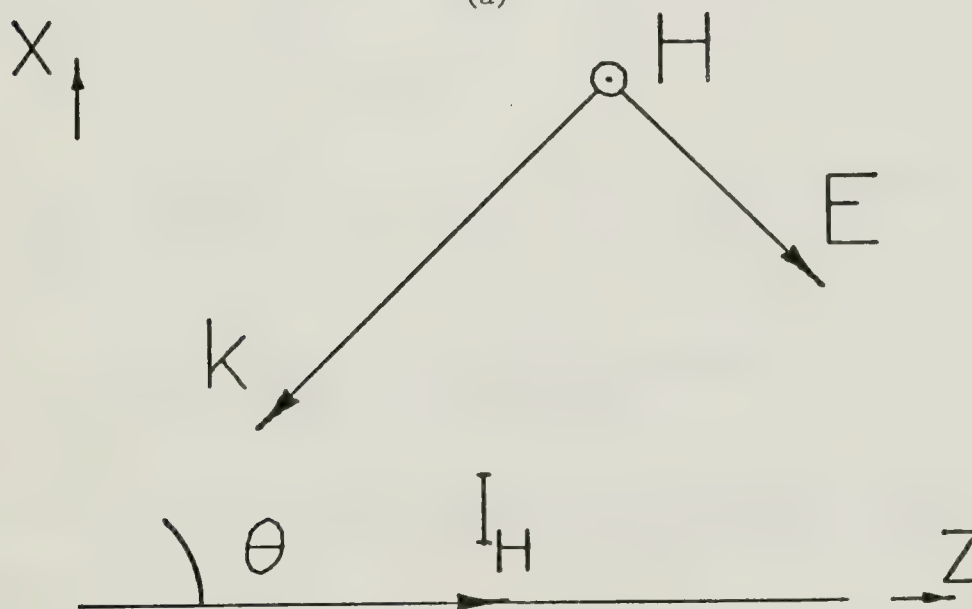
$$E_y^i = e^{-ikz \cos \theta} \quad \text{Volts/meter} \quad (1.3)$$

and

$$E_z^i = \sin \theta e^{-ikz \cos \theta} \quad \text{Volts/meter} \quad (1.4)$$



(a)



(b)

Figure 2.1. The Geometry of the Half-plane Problem for (a) the E-polarization, and (b) the H-polarization.

Equations (1.1) and (1.2) become

$$\int_0^{\infty} I_E(z') H_0^{(1)}(k|z-z'|) dz' = \frac{4}{kZ_0} e^{-ikz \cos\theta}, \quad z > 0 \quad (1.5)$$

and

$$\left(\frac{d^2}{dz^2} + k^2 \right) \int_0^{\infty} I_H(z') H_0^{(1)}(k|z-z'|) dz' = \frac{4k}{Z_0} \sin\theta e^{-ikz \cos\theta}, \quad z > 0. \quad (1.6)$$

The integral equations for the CSF formulation for the half-plane problem follow from (1.8) and (1.9) of Chapter 1. For the E-polarization, the current \underline{J}_E , which has z -variation $I_E(z)$, flows in the y -direction and is independent of y . This makes $\nabla \cdot \underline{J}_E = 0$ so that the current source-function, given by (1.8) of Chapter 1, is equal to $k^2 \underline{J}_E$. If the z -variation of the current source-function is denoted by $u_E(z)$, then

$$u_E(z) = k^2 I_E(z). \quad (1.7)$$

Hence, for the E-polarization, the CSF integral equation is identical in form to (1.5)

$$\int_0^{\infty} u_E(z') H_0^{(1)}(k|z-z'|) dz' = \frac{4k}{Z_0} e^{-ikz \cos\theta}, \quad z > 0. \quad (1.8)$$

The solution for the current source-function u_E is trivially different from the solution for I_E .

For the H-polarization, the current \underline{J}_H flows normal to the edge of the conducting half-plane and must be zero at the edge. Hence, $\nabla \nabla \cdot \underline{J}_H \neq 0$ so that the current source-function, given by (1.8) of Chapter 1, contains

partial derivatives of the current \underline{J}_H . For this polarization, the CSF technique for the half-plane problem is a two-step process. First, the integral equation

$$\int_0^{\infty} u_H(z') H_0^{(1)}(k|z-z'|) dz' = \frac{4k}{Z_0} \sin\theta e^{-ikz \cos\theta}, \quad z > 0, \quad (1.9)$$

must be solved for $u_H(z')$ and then the inhomogeneous differential equation

$$\frac{d^2 I_H}{dz^2} + k^2 I_H = u_H(z) \quad (1.10)$$

must be solved for $I_H(z)$. The reader is referred to Section 3.2 for the complete discussion. Using the known behavior of the current I_H near the edge, and differentiating twice according to (1.10) yields a current source-function $u_H(z)$ which is not locally integrable. This requires a special interpretation for the integral in (1.9). The interpretation of this integral is treated in Section 2.4.

Equations (1.5) and (1.6) have been solved by a variety of methods. One popular method has been the Wiener-Hopf technique. Copson (1946) was apparently the first to use the Wiener-Hopf technique to solve the integral equation (1.5). The use of the Wiener-Hopf technique for solving (1.5) and (1.6) is given by Noble (1958). Both Noble and Karp (1950, p. 418) comment on the non-uniqueness of Wiener-Hopf solutions. In treating the H-polarization half-plane problem, Karp shows how terms of the form $H_{\frac{1}{2}}^{(1)}(kr) \times \cos(\phi/2)$ and certain of its derivatives arise due to the Wiener-Hopf solution technique. (r and ϕ are the polar coordinates of a point in space.)

He indicates that all such terms satisfy all of the conditions of the problem and that each term has its own singular edge behavior. Karp concludes that "for uniqueness it is necessary to specify the behavior of the solution at the origin also." Thus, an additional condition, the edge condition, is needed to rule out all terms having the improper singularity at the edge. Several such terms must be included, however, in the Wiener-Hopf solution of the integral equation (1.9) for u_H . This is given in Chapter 3. The next section shows how such terms arise when the classical solution of the half-plane problem is differentiated. Each differentiation introduces a higher order singularity at the edge.

2.2 The Wave Equation and a Magnetic Field Source-Function

In the last section, an integral equation for the H-polarization half-plane current source-function u_H was developed. In this section, the current source-function for the same problem is found using a differential equation approach instead of the integral equation approach. To do this, a "magnetic field source-function" which satisfies the scalar Helmholtz equation subject to the Neumann boundary condition is introduced. Once the solution for the magnetic field source-function is found, the current source-function is derived from the magnetic field source-function in the same way that the current is obtained from the magnetic field.

For the E-polarization half-plane problem, the total electric field E_y^t is

$$E_y^t = E_y^s + E_y^i \quad (2.1)$$

where E_y^i and E_y^s are the incident and scattered fields, respectively. The total field must satisfy the scalar Helmholtz equation

$$(\nabla^2 + k^2)E_y^t = 0 \quad (2.2)$$

subject to the Dirichlet boundary condition

$$E_y^t = 0 \quad \text{on } M. \quad (2.3)$$

Here, $\nabla^2 = \frac{\partial^2}{\partial x^2} + \frac{\partial^2}{\partial z^2}$ and $k = \omega/c$ where c is the speed of light. Conditions on the behavior of the field near the edge and near infinity are also required. If the field is known, the E-polarization current I_E may be found from the field by using the equation for the discontinuity in the tangential magnetic field

$$I_E(z) = \frac{1}{i\omega\mu} \left\{ \frac{\partial E_y^t}{\partial x} (x = 0+, z) - \frac{\partial E_y^t}{\partial x} (x = 0-, z) \right\} \quad (2.4)$$

where μ is the permeability of the (free-space) medium. The current source-function for this case is given by (1.7) to be

$$u_E(z) = k^2 I_E(z). \quad (2.5)$$

I_E is given by (2.4).

For the H-polarization, the total magnetic field H_y^t is

$$H_y^t = H_y^s + H_y^i \quad (2.6)$$

where H_y^s and H_y^i are the scattered and incident magnetic fields, respectively.

The incident magnetic field can be written as

$$H_y^i = e^{-ikr \cos(\phi - \theta)} \quad (2.7)$$

where (r, ϕ) are the polar coordinates of the observation point and θ is the angle of incidence given in Figure 2.1. The field must satisfy the scalar Helmholtz equation

$$(\nabla^2 + k^2)H_y^t = 0 \quad (2.8)$$

subject to the Neumann boundary condition

$$\frac{\partial H_y^t}{\partial x} = 0 \quad \text{on } M. \quad (2.9)$$

For this polarization the current I_H on the half-plane is

$$I_H = H_y^t(x = 0+, z) - H_y^t(x = 0-, z), \quad (2.10)$$

and the current source-function u_H , given by (1.10), is

$$u_H(z) = \frac{d^2 I_H}{dz^2} + k^2 I_H \quad (2.11)$$

where I_H is given by (2.10). An expression for the current source-function, which is analogous to (2.10) for the current, can be found if a magnetic field source-function

$$T_y(x, z) = \frac{\partial^2 H_y(x, z)}{\partial z^2} + k^2 H_y(x, z) \quad (2.12)$$

is introduced. The expression for the current source-function then becomes

$$u_H(z) = T_y^t(x = 0+, z) - T_y^t(x = 0-, z). \quad (2.13)$$

Bouwkamp (1946) shows that any solution of the wave equation may be differentiated to obtain another solution. This was apparently first mentioned by Lord Rayleigh (1897). In discussing the half-plane problem, Bouwkamp indicates that an n^{th} order derivative with respect to z of H_y^t , for example, still satisfies the scalar Helmholtz equation (2.8) subject to the Neumann boundary condition (2.9). The order of the singularity at the edge of the half-plane becomes higher and higher after each differentiation.

It is easily shown that $T_y^t(x, z)$, given by (2.12), obeys the scalar Helmholtz equation (2.8) subject to (2.9). Clearly, if H_y^t satisfies (2.8), then $(\nabla^2 + k^2)(\frac{\partial^2}{\partial z^2} + k^2)H_y^t = 0$ and the magnetic field source-function T_y^t also satisfies scalar Helmholtz equation

$$(\nabla^2 + k^2)T_y^t = 0. \quad (2.14)$$

Since $\frac{\partial T_y^t}{\partial x} = \left(\frac{\partial^2}{\partial z^2} + k^2\right) \frac{\partial H_y^t}{\partial x}$ and $\frac{\partial H_y^t}{\partial x} = 0$ on M , the boundary condition on the magnetic field source-function T_y^t becomes

$$\frac{\partial T_y^t}{\partial x} = 0 \quad \text{on } M. \quad (2.15)$$

It is seen that the magnetic field source-function satisfies exactly the same conditions as does the magnetic field H_y . For this case, however, the incident field (the incident magnetic field source-function), found from (2.7) and (2.12), is

$$T_y^i = \left(\frac{\partial^2}{\partial z^2} + k^2\right)H_y^i = k^2 \sin^2 \theta e^{-ikr} \cos(\phi - \theta). \quad (2.16)$$

This has the same spatial variation as H_y^i . The only difference is the constant $k^2 \sin^2 \theta$. It becomes apparent that it might be possible to handle certain problems by a field source-function approach, i.e., solving for T_y and then finding H_y from (2.12).

In order to find the current source-function u_H using a differential equation approach, the scalar Helmholtz equation (2.14) with the Neumann boundary condition (2.15) and the incident field (2.16) must be solved for T_y^t . With T_y^t known, Equation (2.13) is used to find the current source-function. Instead of actually solving the differential equation (2.14) subject to the boundary condition (2.15), both Equation (2.12) and the known solution for H_y^t of the half-plane problem are used.

Sommerfeld (1896) was the first to give the exact solution of the half-plane problem. For the H-polarization problem, Sommerfeld's solution for the total magnetic field due to the incident field (2.7) is

$$H_y^t(r, \phi, \theta) = \frac{e^{-i\pi/4}}{\sqrt{\pi}} \left\{ e^{-ikr \cos(\phi-\theta)} \int_{-\infty}^{\sqrt{2kr} \cos \frac{1}{2}(\phi-\theta)} e^{i\tau^2} d\tau \right. \\ \left. + e^{-ikr \cos(\phi+\theta)} \int_{-\infty}^{\sqrt{2kr} \cos \frac{1}{2}(\phi+\theta)} e^{i\tau^2} d\tau \right\} \quad (2.17)$$

The solution for the magnetic field source-function can be obtained from (2.12) and (2.17). Bouwkamp (1946, Equation (6), page 471) gives expressions for the partial derivatives of Sommerfeld's solution. By using

these expressions, $\partial^2 H_y^t / \partial z^2$ can be straightforwardly found. The required solution for the magnetic field source-function becomes

$$T_y^t(r, \phi, \theta) = k^2 \sin^2 \theta H_y^t(r, \phi, \theta) + \hat{T}_N(r, \phi, \theta) \quad (2.18)$$

where

$$\begin{aligned} \hat{T}_N(r, \phi, \theta) = \\ = k^2 \left(\frac{2}{\pi}\right)^{\frac{1}{2}} \cos^{\frac{1}{2}} \theta \frac{e^{i(kr + \pi/4)}}{\sqrt{kr}} \left\{ \cos^{\frac{1}{2}} \phi (\cos \phi - \cos \theta) - \frac{\cos^{\frac{3}{2}} \phi}{2ikr} \right\}. \end{aligned} \quad (2.19)$$

H_y^t on the right-hand side of (2.18) is given by (2.17). It may be shown that \hat{T}_N obeys the scalar Helmholtz equation subject to a Neumann boundary condition. The subscript N is a reminder of this fact. \hat{T}_N may also be written in terms of Hankel functions $H_{\nu}^{(1)}$ as

$$\hat{T}_N(r, \phi, \theta) = k^2 \cos^{\frac{1}{2}} \theta e^{i\pi/4} \sum_{n=0}^{\infty} a_n \cos[(n + \frac{1}{2})\phi] H_{n+\frac{1}{2}}^{(1)}(kr) \quad (2.20)$$

where

$$a_0 = i(\frac{1}{2} - \cos \theta) \text{ and } a_1 = -\frac{1}{2}. \quad (2.21)$$

The current source-function may be obtained by substituting (2.18) and (2.20) in (2.13) after changing (r, ϕ) to (x, z) . It then becomes

$$u_H(z) = k^2 \sin^2 \theta I_H + \frac{2}{Z_0} k^2 \cos^{\frac{1}{2}} \theta e^{i\pi/4} \sum_{n=0}^{\infty} a_n H_{n+\frac{1}{2}}^{(1)}(kz) \quad (2.22)$$

where the a_i are again given by (2.21) and the current I_H is given in terms of H_y^t by (2.10). This gives the current source-function by a differential equation approach in terms of the previously derived results of Sommerfeld (1896) and Bouwkamp (1946). The last terms in (2.22) have been divided by the free space intrinsic impedance Z_0 to conform with the notation of Chapter 3. From (2.19), both the magnetic field and current source-functions become infinite as

$$z^{-\frac{3}{2}} \quad \text{as } z \rightarrow 0,$$

i.e., as the edge is approached.

If the scalar Helmholtz equation subject to the Neumann boundary condition had somehow been solved instead of just differentiating Sommerfeld's solution, the summation index on the series in (2.20) would have extended from zero to infinity. From (2.18), it is seen that the solution for T_y^t is composed of two parts. The first part is that due to the incident field T_y^i . Note that the first term in (2.18) is just the magnetic field H_y^t multiplied by $k^2 \sin^2 \theta$. This makes sense because the incident field T_y^i is just the incident magnetic field H_y^i multiplied by the same constant. The second part is just comprised of terms of the form $\cos(n+\frac{1}{2})\phi H_{n+\frac{1}{2}}^{(1)}(kr)$. Such terms satisfy the Helmholtz equation, the boundary condition, and the radiation condition independently of the incident field. As n in the series (2.20) becomes larger, however, the order of the singularity at the edge becomes higher and higher. The edge condition, the subject of the next section, places an upper limit on the values allowed for n .

2.3 The Edge Condition

Since its development in the 1940's, the edge condition has played a crucial role in electromagnetics problems for objects with edges. It should be expected to be equally important in the source-function development.

A number of papers were written in the late 1940's and early 1950's that obtained results which obeyed the edge condition from those that did not. In the case of half-plane problems, the proper results were often obtained from the improper ones by adding or subtracting functions, such as those in (2.20) with radial variation $H_{n+\frac{1}{2}}^{(1)}(kr)$, that cancel the improper singularity at the edge.

For example, Copson (1950, p. 283) uses integral equation techniques to find a solution to the half-plane problem which has $z^{-\frac{3}{2}}$ edge behavior. By subtracting a term which has this same edge behavior and which also satisfies all of the conditions of the problem, he is able to obtain the correct solution.

The procedure which Bromwich (1915) used to deduce the field of a dipole in the presence of a wedge yields inadmissible edge singularities. Bromwich's solution satisfies the edge condition only for the case when the axis of the electric dipole is parallel to the edge of the half-plane. Woods (1957) extends Bromwich's method to handle arbitrary orientations of the dipole. She finds that appropriate solutions of the wave equation must be subtracted from the Bromwich solution to satisfy the edge condition. These solutions are of the form

$$H_{n+\frac{1}{2}}^{(1)}(kr) \begin{cases} \sin(n+\frac{1}{2})\phi \\ \cos(n+\frac{1}{2})\phi. \end{cases} \quad (3.1)$$

It is terms of this type which appear in (2.20) and are part of the magnetic field source-function in (2.18).

In the Copson and Woods papers, each author finds that his solution has a singularity of too high an order at the edge. Each then finds another function with this same singularity which otherwise satisfies all of the requirements of the problem and subtracts this from the original solution to obtain the correct solution. The situation with the CSF technique is just the opposite. The straightforward solution of the integral equation (1.9) yields a result with an edge singularity that is not high enough. A term with the proper edge behavior must be added to the first part of the solution to obtain the correct solution. This is described in Section 3.3.

The edge conditions for the E-polarization and H-polarization currents on the half-plane are

$$I_E = O(z^{-\frac{1}{2}}), \quad z \rightarrow 0, \quad (3.2)$$

and

$$I_H = O(z^{\frac{1}{2}}), \quad z \rightarrow 0, \quad (3.3)$$

respectively. [See Mittra and Lee (1971, pp. 4-11).] The edge conditions for the E- and H-polarization current source-functions of (2.5) and (2.11), respectively, are

$$u_E = O(z^{-\frac{1}{2}}), \quad z \rightarrow 0, \quad (3.4)$$

and

$$u_H = O(z^{-\frac{3}{2}}), \quad z \rightarrow 0. \quad (3.5)$$

Equation (2.22) for u_H satisfies the edge condition. It is the edge condition which prohibits the addition of terms like those of (3.1) for $n > 1$ to the magnetic field source-function of (2.18).

A function is said to be locally integrable if it is integrable in the Lebesgue sense over every finite interval. The current source-function $u_H(z)$ of (2.11), satisfying the edge condition (3.5), is not locally integrable. The formal integration of u_H near the edge gives

$$\int_0^{\delta} z^{-\frac{3}{2}} dz = 2 \lim_{\epsilon \rightarrow 0} \epsilon^{-\frac{1}{2}} - 2\delta^{-\frac{1}{2}}. \quad (3.6)$$

Since the limit does not exist this is a divergent integral. Such integrals are discussed in the next section.

2.4 Divergent Integrals and the Finite Part

Some authors writing in the early 1950's commented that integrals of the type (1.9) may be divergent. In several places¹ Bouwkamp (1954) points out that if the d^2/dz^2 operator of (1.6), for example, is taken under the integral sign, the resulting kernel is non-integrable. This is true, but it has been shown that the integral can be assigned a meaning by introducing the concept of the finite part. This concept dates back to A. L. Cauchy (1826) who used it to assign a meaning to the gamma function for negative values of the argument. Hadamard (1923) extends the concept to the multi-dimensional case. A lengthy bibliography and a general discussion of the history of the finite part of divergent integrals is given by Bureau (1955,

¹p. 40; pp. 68-69.

pp. 143-146). Both Hadamard (1923) and Bureau (1955) use the finite part concept in connection with solving partial differential equations.

Friedlander (1951) uses a modification of the method developed by Hadamard for Cauchy's problem to solve the half-plane problem with time-dependent excitation. He shows that the integrals arising in the solution process must be interpreted as finite part integrals.

Equation (1.9) must be a finite part integral equation because $u(z')$ is not locally integrable. If the notation "Fp" is used for the finite part, this equation becomes

$$\text{Fp} \int_0^{\infty} u_H(z') H_0^{(1)}(k|z-z'|) dz' = \frac{4k}{z_0} \sin\theta e^{-ikz \cos\theta}, \quad z > 0. \quad (4.1)$$

This is a Fredholm finite part integral equation of the first kind over semi-infinite range.

Methods for solving finite part integral equations have been studied by several authors. Butzer (1959) and Boehme (1963) use operational calculus to study the finite part of divergent convolution integrals. They both treat finite part singular integral equations of Volterra type. Wiener (1962) treats linear finite part integral equations of Fredholm second kind and Volterra types. In a series of over thirty papers² published over the last fifteen years, he and his colleagues treat many finite part integral equations. However, it appears as if Fredholm finite part integral equations of the first kind with Hankel function kernels, such as

²Generally published in Wiss. Z. M.-L. Univ. Halle--Wittenberg, Math. Nachr., or Beiträge zur Analysis.

(4.1), have not yet been treated explicitly.

Belward (1972) obtains both the classical and generalized function solutions of the integral equation

$$\int_0^{\infty} G(t) K_0(|z-t|) dt = F(z), \quad 0 < z < \infty, \quad (4.2)$$

by using the properties of fractional integrals. Here K_0 is the MacDonald (modified Bessel) function. It is related to the Hankel function $H_0^{(1)}(x)$ by

$$K_0(x) = \frac{i\pi}{2} H_0^{(1)}(ix). \quad (4.3)$$

The solution of the finite part integral equation (4.1) is obtained by just making the indicated change of variable in Belward's generalized function solution. Generalized functions use the finite part concept in their definition. [See, for example, Schwartz (1966a, pp. 33-43)]. A discussion of the Schwartz distribution theory formulation of the current source-function technique is presented in Section 6.3.

Hadamard (1923, pp. 134-141) introduces the theory of the finite part of divergent integrals and discusses several examples at length. This excellent discussion should be consulted by those interested in the total theory. Several examples of finite part integration which are relevant to the present work are given here. As a first example, consider the integral

$$\int_a^b \frac{dt}{(b-t)^{\frac{3}{2}}} = \frac{2}{(b-t)^{\frac{1}{2}}} \bigg|_a^b. \quad (4.4)$$

The right-hand side goes to infinity when it is evaluated at the upper limit. The finite part of this expression is found by retaining only the value obtained when the right-hand side is evaluated at the lower limit. Hence,

$$\text{Fp} \int_a^b \frac{dt}{(b-t)^{\frac{3}{2}}} = \frac{-2}{(b-a)^{\frac{1}{2}}} . \quad (4.5)$$

As another example of finite part calculation, consider the integral

$$\int_0^x \frac{e^{it}}{t^{\frac{3}{2}}} dt, \quad x > 0, \quad (4.6)$$

Making the lower limit ϵ and formally integrating by parts gives

$$\int_{\epsilon}^x \frac{e^{it}}{t^{\frac{3}{2}}} dt = -2 \frac{e^{it}}{\sqrt{t}} \Big|_{\epsilon}^x + 2i \int_{\epsilon}^x \frac{e^{it}}{\sqrt{t}} dt. \quad (4.7)$$

Clearly, in the limit as $\epsilon \rightarrow 0$, the first term becomes infinite. The finite part of this integral is defined as

$$\text{Fp} \int_0^x \frac{e^{it}}{t^{\frac{3}{2}}} dt = \lim_{\epsilon \rightarrow 0} \left\{ \int_{\epsilon}^x \frac{e^{it}}{t^{\frac{3}{2}}} dt - \frac{2}{\sqrt{\epsilon}} \right\}, \quad x > 0. \quad (4.8a)$$

Substituting (4.7) in this expression and taking the limit gives

$$\text{Fp} \int_0^x \frac{e^{it}}{t^{\frac{3}{2}}} dt = -2 \frac{e^{ix}}{\sqrt{x}} + 4i \int_0^{\sqrt{x}} e^{it^2} dt, \quad x > 0. \quad (4.8b)$$

A $t^{-5/2}$ singularity in the integrand obtains

$$\text{Fp} \int_0^x \frac{e^{it}}{t^{5/2}} dt = -\frac{2}{3} \frac{e^{ix}}{x^{3/2}} + \frac{2}{3}i \text{Fp} \int_0^x \frac{e^{it}}{t^{3/2}} dt, \quad x > 0. \quad (4.9)$$

More terms are added as still higher order singularities are considered.

If both sides of (4.8b) are formally differentiated, note that equality is obtained.

The above calculation is carried out by using integration by parts. This calculation may also be done by expanding e^{it} in its Taylor series around $t = 0$, integrating term by term, and retaining only the well behaved terms. This approach is valid in the complex plane and is described by Zemanian (1965, p. 58). For some finite part calculations, the Taylor series approach would be preferred to the integration by parts approach. Integration by parts will generally be used here.

The nonlocally integrable portion of the integrand will be labelled a "pseudofunction" and denoted by "Pf." For example, consider the pseudofunction $\text{Pf}[l_0^x(t) \frac{e^{it}}{t^{3/2}}]$ where $l_0^x(t)$ is the unit characteristic function of the interval $[0, x]$. The integral of this pseudofunction is defined by

$$\int_{-\infty}^{\infty} \text{Pf} [l_0^x(t) \frac{e^{it}}{t^{3/2}}] dt = \text{Fp} \int_0^x \frac{e^{it}}{t^{3/2}} dt. \quad (4.10)$$

The Pf notation is useful as a reminder to indicate that the finite part must be taken if the function is integrated over limits including the singular point.

A useful property of finite part integrals with difference kernels is that they may be differentiated under the integral sign as long as the finite part is taken of the resulting integral. Consider the integral

$$\int_0^{\infty} \text{Fp} \int_0^t \frac{e^{i\tau}}{\tau^{\frac{3}{2}}} d\tau H_0^{(1)}(|z-t|) dt = -4\sqrt{\pi} e^{-i\pi/4}, \quad z > 0. \quad (4.11)$$

Differentiating both sides of this equation with respect to z and using the fact that

$$\frac{\partial}{\partial z} H_0^{(1)}(|z-t|) = -\frac{\partial}{\partial t} H_0^{(1)}(|z-t|) \quad (4.12)$$

obtains

$$0 = \int_0^{\infty} \text{Fp} \int_0^t \frac{e^{i\tau}}{\tau^{\frac{3}{2}}} d\tau \frac{\partial}{\partial t} H_0^{(1)}(|z-t|) dt, \quad z > 0. \quad (4.13)$$

Integrating by parts with ϵ as the lower limit yields

$$\begin{aligned} & \int_{\epsilon}^{\infty} \text{Fp} \int_0^t \frac{e^{i\tau}}{\tau^{\frac{3}{2}}} d\tau \frac{\partial}{\partial t} H_0^{(1)}(|z-t|) dt = \\ & = H_0^{(1)}(|z-t|) \text{Fp} \int_0^t \frac{e^{i\tau}}{\tau^{\frac{3}{2}}} d\tau \Big|_{\epsilon}^{\infty} - \int_{\epsilon}^{\infty} \frac{e^{it}}{t^{\frac{3}{2}}} H_0^{(1)}(|z-t|) dt. \end{aligned} \quad (4.14)$$

Substituting (4.8b) in the first term on the right-hand side shows that this term goes to infinity as $\epsilon^{-\frac{1}{2}}$ as ϵ goes to zero. The other terms at ϵ and the terms at infinity vanish. The right-hand side becomes

$$- \left\{ \int_{\epsilon}^{\infty} \frac{e^{it}}{t^{\frac{3}{2}}} H_0^{(1)}(|z-t|) dt - \frac{2H_0^{(1)}(|z|)}{\sqrt{\epsilon}} \right\}. \quad (4.15)$$

In the limit as ϵ goes to zero, this is just

$$- \text{Fp} \int_0^{\infty} \frac{e^{it}}{t^{\frac{3}{2}}} H_0^{(1)}(|z-t|) dt. \quad (4.16)$$

This can be seen by expanding e^{it} and $H_0^{(1)}(|z-t|)$ in their Taylor's series. The first term in each series is, respectively, 1 and $H_0^{(1)}(|z|)$. Substituting these in (4.15) shows that the divergent part of the integral in (4.15) is just given by $2H_0^{(1)}(|z|)/\sqrt{\epsilon}$. Thus, by the four equations above,

$$\text{Fp} \int_0^{\infty} \frac{e^{it}}{t^{\frac{3}{2}}} H_0^{(1)}(|z-t|) dt = 0, \quad z > 0. \quad (4.17)$$

Using (4.15) and (4.17), it can be shown that

$$\text{Fp} \int_0^{\infty} \frac{e^{it}}{t^{\frac{3}{2}}} H_0^{(1)}(|z-t|) dt = \int_0^{\infty} \frac{e^{it} H_0^{(1)}(|z-t|) - H_0^{(1)}(|z|)}{t^{\frac{3}{2}}} dt = 0, \quad z > 0. \quad (4.18)$$

In convolution notation, this is

$$\text{Pf} [1_+(t) e^{it}/t^{\frac{3}{2}}] * H_0^{(1)}(|t|) = 0, \quad z > 0, \quad (4.19)$$

where $1_+(t)$ is the unit step function. This example shows that there are non-zero functions which yield zero on the right-hand side, i.e., the

homogeneous finite part integral equation has non-zero solutions. It also illustrates that the derivative operator may be taken under the integral sign as long as the finite part is taken of the resulting integral.

Consider the integral of (1.6). Taking the second derivative under the integral sign as described above shows that

$$\frac{d^2}{dz^2} \int_0^\infty I_H(t) H_0^{(1)}(k|z-t|) dt = \text{Fp} \int_0^\infty \left(\frac{d^2}{dt^2} I_H(t) \right) H_0^{(1)}(k|z-t|) dt, \quad z > 0, \quad (4.20)$$

where

$$\begin{aligned} \text{Fp} \int_0^\infty \left(\frac{d^2}{dt^2} I_H(t) \right) H_0^{(1)}(k|z-t|) dt = \\ = \lim_{\epsilon \rightarrow 0} \left\{ \int_\epsilon^\infty \left(\frac{d^2}{dt^2} I_H(t) \right) H_0^{(1)}(k|z-t|) dt + \left(\frac{d}{dt} I_H(t) \right) \Big|_\epsilon H_0^{(1)}(k|z|) \right\} \end{aligned} \quad (4.21)$$

In this case, the last term must be included because $dI_H/dt = 0(t^{-\frac{1}{2}})$ as $t \rightarrow 0$ by the edge condition on $I_H(t)$. In this way, the integral equation (1.6) may be written in the form

$$\text{Fp} \int_0^\infty u_H(t) H_0^{(1)}(k|z-t|) dt = \frac{4k}{z_0} \sin\theta e^{-ikz \cos\theta}, \quad z > 0 \quad (4.22)$$

where

$$\frac{d^2 I_H}{dt^2} + k^2 I_H = u_H(t). \quad (4.23)$$

These are the basic equations involved in the current source-function technique for the half-plane problem.

2.5 Conclusion

For the H-polarization half-plane problem, a "magnetic field source-function" is introduced which allows the current source-function to be found from field quantities. In this way, a differential equation approach to finding the current source-function is derived. It is noted that all terms of the form $H_{n+\frac{1}{2}}^{(1)}(kr)\cos(n+\frac{1}{2})\phi$ satisfy the source-free scalar Helmholtz equation with the Neumann boundary condition, but that the edge condition restricts n to be at most one. The term for $n = 1$ has $t^{-\frac{3}{2}}$ edge behavior and, therefore, is not integrable in the ordinary sense. The concept of the finite part of divergent integrals is introduced so that integral equations for the current source-function can be interpreted. The CSF technique requires that a finite part integral equation must be solved for $u_H(z)$. It is shown that this integral equation may be found from Pocklington's integral equation by taking the $(\partial^2/\partial z^2 + k^2)$ operator under the integral sign. The next chapter treats the solution of the half-plane problem by the CSF technique.

3. THE CURRENT SOURCE-FUNCTION TECHNIQUE APPLIED TO THE HALF-PLANE PROBLEM

In this chapter, the problem of diffraction of a plane wave by a perfectly conducting half-plane is solved analytically by the current source-function (CSF) technique. This problem is chosen because it may be solved exactly. It serves as a good example to illustrate the solution procedures required in the CSF technique. The harmonic problem with $e^{-i\omega t}$ time dependence is considered.

3.1 Maxwell's Equations and the Current Source-Function Technique

The solution of electromagnetic field problems is based on Maxwell's equations. Assuming that any conducting inhomogeneities in a region have been replaced with the induced electric current \underline{J} acting in a homogeneous medium with constitutive parameters ϵ and μ , Maxwell's equations for the electric and magnetic fields \underline{E} and \underline{H} produced by these currents are

$$\nabla \times \underline{H} = \gamma \underline{E} + \underline{J} \quad (1.1)$$

$$\nabla \times \underline{E} = -Z \underline{H} \quad (1.2)$$

$$\nabla \cdot \underline{E} = \rho / \epsilon \quad (1.3)$$

$$\nabla \cdot \underline{H} = 0 \quad (1.4)$$

where $\gamma = -i\omega\epsilon$, $Z = -i\omega\mu$, $Z\gamma = -k^2$, and ρ is the electric charge density which is related to the current by

$$\nabla \cdot \underline{J} = i\omega\rho. \quad (1.5)$$

The CSF technique arises from a direct relationship between the fields and the sources. The curl of (1.2) is

$$\nabla \times \nabla \times \underline{E} = -Z \nabla \times \underline{H} = -Z (\gamma \underline{E} + \underline{J}) \quad (1.6)$$

or

$$\nabla \nabla \cdot \underline{E} - \nabla^2 \underline{E} = k^2 \underline{E} - Z \underline{J}. \quad (1.7)$$

The divergence of (1.1) is

$$\nabla \cdot \nabla \times \underline{H} = 0 = \gamma \nabla \cdot \underline{E} + \nabla \cdot \underline{J} \quad (1.8)$$

or

$$\nabla \cdot \underline{E} = -\frac{1}{\gamma} \nabla \cdot \underline{J}. \quad (1.9)$$

Using this in (1.7) gives

$$\nabla^2 \underline{E} + k^2 \underline{E} = -\frac{1}{\gamma} \{ \nabla \nabla \cdot \underline{J} + k^2 \underline{J} \} \equiv -\frac{1}{\gamma} \underline{U}. \quad (1.10)$$

where \underline{U} is the vector current source-function. Solving for the electric field \underline{E} due to the current \underline{J} yields

$$\underline{E} = \frac{1}{4\pi\gamma} \iiint_V \underline{U}(\underline{r}') \frac{e^{ikR}}{R} dV' \quad (1.11)$$

where $R = |\underline{r} - \underline{r}'|$ is the source-point to observation-point distance. A discussion of this result for three dimensions is given in Chapter 7. The present discussion is limited to the one-dimensional case.

3.2 The E- and H-polarization Current Source-Functions

The geometry for the E- and H-polarization half-plane problems is given in Figure 2.1. For the E-polarization, the current flows in the

y-direction only. The expression for \underline{J}_E can be written as

$$\underline{J}_E = I_E(z) \underline{1}_+(z) \delta(x) \hat{y} \quad (2.1)$$

where $\underline{1}_+$ is the unit step function and δ is the Dirac delta function. The current source-function becomes

$$\underline{U}_E = \nabla \nabla \cdot \underline{J}_E + k^2 \underline{J}_E = k^2 \underline{J}_E \quad (2.2)$$

because \underline{J}_E is divergence-free. For the H-polarization, the current flows in the z-direction only. The current \underline{J}_H can be expressed as

$$\underline{J}_H = I_H(z) \underline{1}_+(z) \delta(x) \hat{z} \quad (2.3)$$

and the current source-function for this case becomes

$$\begin{aligned} \underline{U}_H &= \nabla \nabla \cdot \underline{J}_H + k^2 \underline{J}_H = \\ &= \frac{\partial}{\partial z} (I_H \underline{1}_+) \frac{\partial}{\partial x} \delta(x) \hat{x} + \delta(x) \left(\frac{d^2}{dz^2} + k^2 \right) (I_H \underline{1}_+) \hat{z} \end{aligned} \quad (2.4)$$

For a proper interpretation, these derivatives should be performed using Schwartz distribution theory. The reader is referred to Section 6.2 for a discussion of Schwartz distribution theory.

Substituting (2.2) in (1.11) yields the expression for the E-polarization scattered field. After using the fact that

$$\int_{-\infty}^{\infty} \frac{e^{ik \sqrt{x^2 + \eta^2 + z^2}}}{\sqrt{x^2 + \eta^2 + z^2}} d\eta = i\pi H_0^{(1)}(k \sqrt{x^2 + z^2}), \quad (2.5)$$

the expression becomes

$$\underline{E}^s = - \hat{y} \frac{Z_0}{4k} \int_0^\infty u_E(z') H_0^{(1)}(k \sqrt{x^2 + (z-z')^2}) dz' \quad (2.6)$$

where

$$u_E = k^2 I_E. \quad (2.7)$$

The total field \underline{E}^t is equal to the sum of the incident and scattered fields, or $\underline{E}^t = \underline{E}^i + \underline{E}^s$. On the half-plane, the tangential component of the total electric field must be zero. Applying this boundary condition gives the integral equation for $u_E(z')$,

$$\int_0^\infty u_E(z') H_0^{(1)}(k|z-z'|) dz' = \frac{4k}{Z_0} E_y^i(x=0, z) = \frac{4k}{Z_0} e^{-ikz \cos\theta}, \quad z > 0, \quad (2.8)$$

where θ is the angle of incidence defined in Figure 2.1(a). If $u_E(z')$ is found, then the current $I_E(z')$ can be found from (2.7). In this case, the CSF formulation is only trivially different from the usual formulation.

For the H-polarization, however, the CSF formulation differs greatly from the customary integral equations. Substituting (2.4) in (1.11), the expression for the scattered electric field becomes

$$\begin{aligned} \underline{E}^s = & - \hat{x} \frac{Z_0}{4k} \int_z \int_{x'} \frac{\partial}{\partial z'} (I_H^{1+}) \frac{\partial}{\partial x'} \delta(x') H_0^{(1)}(k \sqrt{(x-x')^2 + (z-z')^2}) dx' dz' \\ & - \hat{z} \frac{Z_0}{4k} \int_0^\infty u_H(z') H_0^{(1)}(k \sqrt{x^2 + (z-z')^2}) dz' \end{aligned} \quad (2.9)$$

where

$$u_H = \frac{d^2 I_H}{dz'^2} + k^2 I_H. \quad (2.10)$$

The integrals in (2.9) must be taken as finite part integrals. The integral equation for $u_H(z')$ is obtained by applying the boundary condition that the tangential electric field must be zero on the half-plane. The integral equation becomes

$$\text{Fp} \int_0^\infty u_H(z') H_0^{(1)}(k|z-z'|) dz' = \frac{4k}{Z_0} E_z^i(x=0, z) = \frac{4k}{Z_0} \sin\theta e^{-ikz \cos\theta}, \quad z > 0, \quad (2.11)$$

where θ is the angle of incidence defined in Figure 2.1(b). If $u_H(z')$ is found from this integral equation, then the current $I_H(z')$ may be found from (2.10). The integral equations (2.8) and (2.11) for u_E and u_H are remarkably similar in form. The main difference is that (2.8) is an ordinary integral equation while (2.11) is a finite part integral equation.

3.3 The Solution of the Integral Equations for $u(z)$

In this section, the integral equations (2.8) and (2.11) are solved for u_E and u_H , respectively. For the finite part equation (2.11), one or more solutions of the homogeneous equation

$$\text{Fp} \int_0^\infty w(z') H_0^{(1)}(k|z-z'|) dz' = 0, \quad z > 0, \quad (3.1)$$

may be added to the solution of the ordinary integral equation to obtain another solution. The number of solutions that may be added is related to

the edge condition on the current source-function. The homogeneous integral equation (3.1) is solved by three related methods. These are (1) the Wiener-Hopf technique, (2) an application of the method of Belward (1972), and (3) the differentiation of a (locally integrable) solution to the ordinary integral equation.

Both the integral equation for the E-polarization and the ordinary part of the integral equation for the H-polarization may be written as

$$\int_0^{\infty} f(z') H_0^{(1)}(k|z-z'|) dz' = \kappa \frac{4k}{Z_0} e^{-ikz \cos \theta}, \quad z > 0, \quad (3.2)$$

where $\kappa = 1$ for the E-polarization and $\kappa = \sin \theta$ for the H-polarization. The solution of this integral equation has been found in several different ways. Magnus (1941), for example, solves it using series of Bessel functions. Copson (1946) and Noble (1958, p. 228) use the Wiener-Hopf technique. It has also been solved using the Kontorovich-Lebedev transform by Lebedev et al. (1966, pp. 389-390). The solution is

$$f(z) = 1_+(z) \frac{\kappa k^2}{Z_0} \frac{4e^{-i\pi/4}}{\sqrt{\pi}} \left\{ \frac{i \sin(\theta/2)}{\sqrt{2}} \frac{e^{ikz}}{\sqrt{kz}} + \sin \theta e^{-ikz \cos \theta} \int_0^{\sqrt{kz(1+\cos \theta)}} e^{it^2} dt \right\}, \quad (3.3a)$$

$$= 1_+(z) \frac{\kappa k}{Z_0} \frac{4e^{i\pi/4}}{\sqrt{\pi}} \tan \frac{\theta}{2} e^{ikz} \frac{d}{dz} \left[e^{-ikz(1+\cos \theta)} \int_0^{\sqrt{kz(1+\cos \theta)}} e^{it^2} dt \right], \quad (3.3b)$$

$$= 1_+(z) \frac{2\kappa k^2}{Z_0} e^{i\pi/4} \sin \frac{\theta}{2} \left[i H_{\frac{1}{2}}^{(1)}(kz) + \sqrt{2} \cos \frac{\theta}{2} e^{-ikz \cos \theta} \int_0^{kz(1+\cos \theta)} H_{\frac{1}{2}}^{(1)}(t) dt \right], \quad (3.3c)$$

$$= 1_+(z) \frac{\kappa k^2}{z_0} \frac{4e^{i\pi/4} \sin(\theta/2)}{\sqrt{2k}} e^{ikz} \frac{d^{\frac{1}{2}}}{dz^{\frac{1}{2}}} e^{-ikz(1+\cos\theta)}. \quad (3.3d)$$

In (3.3d), the operator $d^{\frac{1}{2}}/dz^{\frac{1}{2}}$ is the semiderivative operator of Oldham and Spanier (1974, pp. 115-131). $H_{\frac{1}{2}}^{(1)}(t)$ is the Hankel function of the first kind and order $\frac{1}{2}$.

The function $f(z)$ has edge behavior

$$z^{-\frac{1}{2}} \quad \text{as } z \rightarrow 0. \quad (3.4)$$

Since u_E , as given by (2.7), is allowed to have this same edge behavior, the solution for u_E is

$$u_E(z) = f(z) \Big|_{\kappa=1}. \quad (3.5)$$

From (3.5) of Chapter 2, the current source-function for the H-polarization, given by (2.10), must satisfy the edge condition $u_H = O(z^{-\frac{3}{2}})$ as $z \rightarrow 0$. This means that the function $f(z)$ of (3.3) alone does not have to be the total solution of (2.11). Solutions of (3.1) which behave as $z^{-\frac{3}{2}}$ as $z \rightarrow 0$ may be added to $f(z)$ without violating any of the conditions of the problem. The solutions of the homogeneous finite part integral equation are found in each of the next three sections by different methods.

3.3.1 Solution of the Homogeneous Finite Part Integral Equation by the Wiener-Hopf Technique

The Fourier transform pair that will be used here is

$$F(\alpha) = \frac{1}{\sqrt{2\pi}} \int_{-\infty}^{\infty} f(z) e^{i\alpha z} dz, \quad (3.6a)$$

$$f(z) = \frac{1}{\sqrt{2\pi}} \int_{-\infty}^{\infty} F(\alpha) e^{-i\alpha z} d\alpha. \quad (3.6b)$$

When $f(z)$ or $F(\alpha)$ are pseudofunctions these transforms must be defined either in the sense of distributions or as finite part integrals. The theory and calculation of pseudofunction transforms, along with a large table of transform pairs, is given by Lavoine (1963). For a general description of the Wiener-Hopf technique, the reader is referred to Mittra and Lee (1971, pp. 73-84).

The homogeneous finite part integral equation (3.1) may be rewritten as

$$\int_{-\infty}^{\infty} \text{Pf } w_+(z') H_0^{(1)}(k|z-z'|) dz' = b_-(z), \quad -\infty < z < \infty \quad (3.7)$$

where

$$\text{Pf } w_+(z') = \begin{cases} w(z') & z' > 0 \\ 0 & z' < 0 \end{cases} \quad (3.8)$$

and

$$b_-(z) = \begin{cases} 0 & z > 0 \\ b(z) = \int_{-\infty}^{\infty} \text{Pf } w_+ H_0^{(1)}(k|z-z'|) dz' & z < 0. \end{cases} \quad (3.9)$$

Taking the Fourier transform of (3.7) yields

$$\sqrt{2\pi} W_+(\alpha) G(\alpha) = B_-(\alpha), \quad \tau_- < \text{Im}\alpha < \tau_+, \quad (3.10)$$

where

$$W_+(\alpha) = \frac{1}{\sqrt{2\pi}} \text{Fp} \int_0^{\infty} w(z) e^{i\alpha z} dz, \quad (3.11)$$

$$G(\alpha) = \frac{1}{\sqrt{2\pi}} \int_{-\infty}^{\infty} H_0^{(1)}(k|z|) e^{i\alpha z} dz = \sqrt{\frac{2}{\pi}} \frac{1}{\sqrt{k^2 - \alpha^2}}, \quad (3.12)$$

and

$$B_-(\alpha) = \frac{1}{\sqrt{2\pi}} \int_{-\infty}^0 b(z) e^{i\alpha z} dz. \quad (3.13)$$

Equation (3.10) holds in the strip $\tau_- < \text{Im}\alpha < \tau_+$ where the regions of regularity of W_+ , $G(\alpha)$, and B_- overlap. Factorizing $\sqrt{2\pi} G(\alpha)$ into $G_+(\alpha)$ and $G_-(\alpha)$ gives

$$\sqrt{2\pi} G(\alpha) = G_+(\alpha) G_-(\alpha) = \frac{\sqrt{2}}{\sqrt{k+\alpha}} \frac{\sqrt{2}}{\sqrt{k-\alpha}}. \quad (3.14)$$

Equation (3.10) become

$$W_+(\alpha) G_+(\alpha) = \frac{B_-(\alpha)}{G_-(\alpha)}, \quad \tau_- < \text{Im}\alpha < \tau_+. \quad (3.15)$$

Since the left-hand side is regular in the lower half plane $\text{Im}\alpha < \tau_+$ and the right-hand side is regular in the upper half plane $\text{Im}\alpha > \tau_-$, then by analytic continuation, both sides must equal the same entire function $P(\alpha)$. Thus,

$$W_+(\alpha) G_+(\alpha) = \frac{B_-(\alpha)}{G_-(\alpha)} = P(\alpha), \quad \text{for all } \alpha. \quad (3.16)$$

To determine the nature of $P(\alpha)$, consider the asymptotic form of the above equation and look at the asymptotic representations of W_+ and G_+ . The asymptotic form of $W_+(\alpha)$ is related to the edge behavior of $w(z)$, which is required to be

$$w(z) = O(z^{-\frac{3}{2}}) \text{ as } z \rightarrow 0+. \quad (3.17)$$

Using a generalization of the Abelian initial value theorem, it is found that

$$W_+(\alpha) \sim (-i\alpha)^{\frac{1}{2}}, \quad |\alpha| \rightarrow \infty \text{ with } \text{Im}\alpha > 0.$$

Since $G_+(\alpha) \sim (\alpha)^{-\frac{1}{2}}$, $|\alpha| \rightarrow \infty$, it follows that $P(\alpha) = W_+(\alpha) G_+(\alpha) \sim C$, $|\alpha| \rightarrow \infty$, where C is a constant.

The solution for $W_+(\alpha)$ becomes

$$W_+(\alpha) = C \sqrt{k+\alpha} / \sqrt{2}. \quad (3.18)$$

Taking the generalized inverse transform gives the required homogeneous solution, which is

$$w(z) = \frac{C}{2\sqrt{\pi}} \int_{-\infty}^{\infty} \sqrt{k+\alpha} e^{-i\alpha z} d\alpha = \frac{C}{2} \frac{e^{ikz}}{\sqrt{\pi}} \int_{-\infty}^{\infty} \sqrt{\alpha} e^{-i\alpha z} d\alpha. \quad (3.19)$$

The branch cut for $\sqrt{\alpha}$ will be taken along the negative imaginary axis in the α -plane. For $z < 0$, the path of integration must be closed in the upper half of the α -plane and for $z > 0$ it must be closed in the lower half. These paths are shown in Figures 3.1(a) and 3.1(b), respectively. For $z < 0$, the integral in (3.19) is identically zero, as expected. For $z > 0$, the path of integration may be deformed to enclose the branch cut as shown in Figure 3.1(c). The integral in (3.19) becomes

$$\begin{aligned} \int_{P_1+P_2} \sqrt{\alpha} e^{-i\alpha z} d\alpha &= -2ie^{-i\pi/4} \int_0^{\infty} \sqrt{\beta} e^{-\beta z} d\beta = \\ &= -2ie^{-i\pi/4} \Gamma(\frac{3}{2})/z^{\frac{3}{2}}. \end{aligned} \quad (3.20)$$

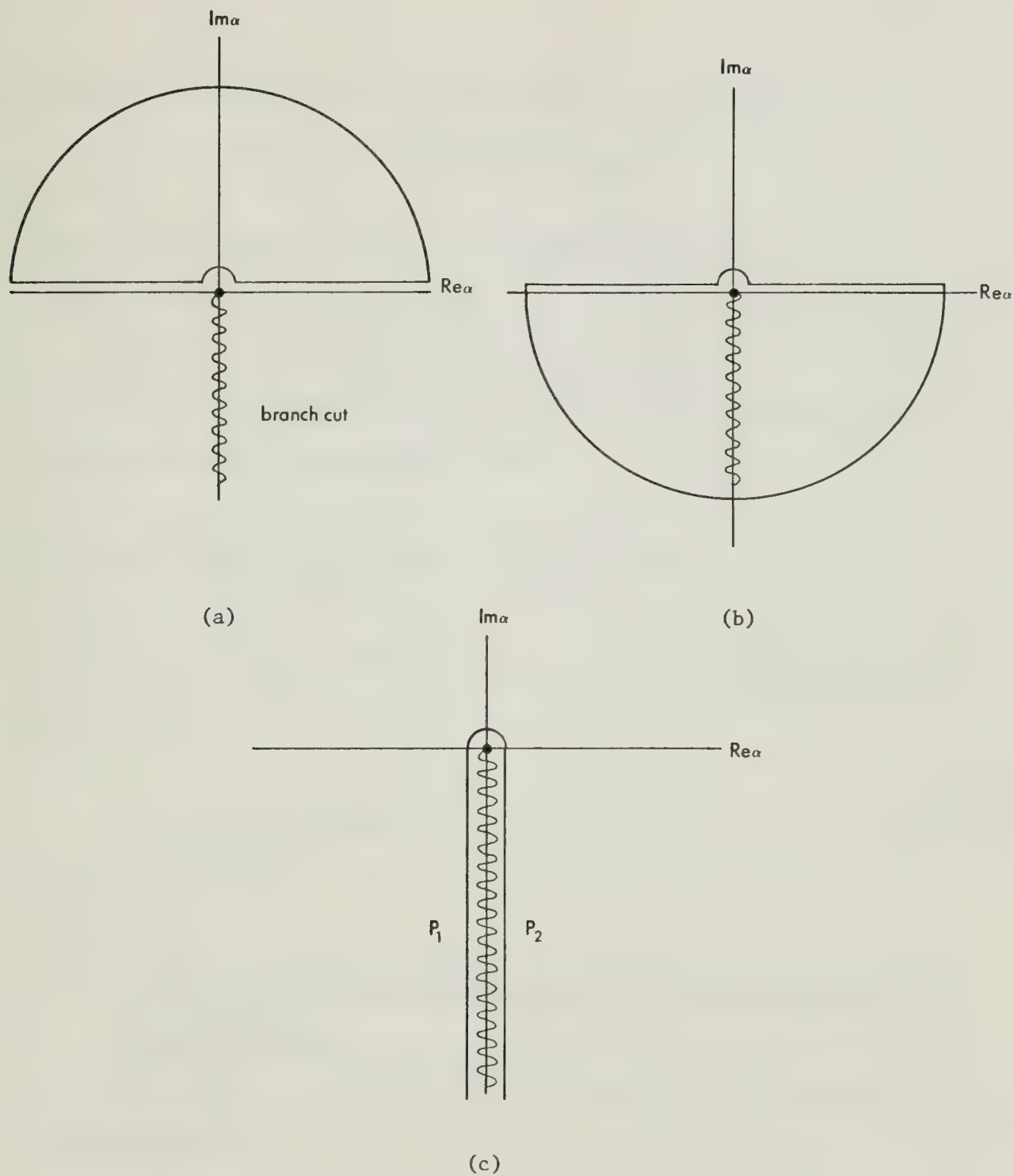


Figure 3.1. Integration Path for (a) $z < 0$, and (b) $z > 0$; (c) Deformed Path for $z > 0$.

where Γ is the gamma function. The expression for $w(z)$ then becomes

$$w(z) = -\frac{C}{2} e^{i\pi/4} \text{Pf} \frac{e^{ikz}}{z^{\frac{3}{2}}} 1_+(z) \quad (3.21)$$

where C is a constant. This is the required homogeneous solution of the finite part integral equation. Note that it has the required edge behavior.

This same result may also be obtained by using the fact that multiplication by α in the transform domain is the same as differentiation with respect to z in the spatial domain. Thus,

$$\begin{aligned} \text{Fp} \int_{-\infty}^{\infty} \sqrt{\alpha} e^{-i\alpha z} d\alpha &= \int_{-\infty}^{\infty} \frac{\alpha}{\sqrt{\alpha}} e^{-i\alpha z} d\alpha = i \frac{d}{dz} \int_{-\infty}^{\infty} \frac{e^{-i\alpha z}}{\sqrt{\alpha}} d\alpha = \\ &= 2\sqrt{\pi} e^{i\pi/4} \frac{d}{dz} (z^{-\frac{1}{2}} 1_+(z)) = -\sqrt{\pi} e^{i\pi/4} \text{Pf} (z^{-\frac{3}{2}} 1_+(z)) \end{aligned} \quad (3.22)$$

and

$$w(z) = -\frac{C}{2} e^{i(kz+\pi/4)} \text{Pf} z^{-\frac{3}{2}} 1_+(z) \quad (3.23)$$

as before.

3.3.2 The Solution of the Homogeneous Finite Part Integral Equation from Belward's Results

Belward (1972, pp. 908-911) finds the solutions of the homogeneous integral equation

$$\int_0^{\infty} G_H(t) K_0(|z-t|) dt = 0, \quad z > 0, \quad (3.24)$$

in a space of generalized functions, where $K_0(t)$ is the MacDonald (modified Bessel) function. He uses the term "generalized function" in the sense

defined by Jones (1966), i.e., that "a generalized function is an equivalence class of regular sequences." This definition may be shown to be equivalent to the definition of a distribution as a continuous linear functional [see Antosik, Mukusiński, and Sikorski (1973, p. 235)]. He finds

$$G_H(t) = \left(a_n \frac{d^n}{dt^n} + \cdots + a_0 \right) \frac{e^{-t}}{t^{\frac{3}{2}}}, \quad t > 0, \quad (3.25)$$

where n and the a_j are arbitrary. Since $H_0^{(1)}(x) = \frac{2}{i\pi} K_0(-ix)$, it could be argued that the solution of (3.1) would be obtained if "t" in (3.25) were replaced by $-ikz$. Although it is not clear whether this procedure can be justified mathematically, it gives the same result as was obtained with the Wiener-Hopf technique. Application of the edge condition gives $a_j = 0$ for $j > 0$. The solution becomes

$$w(z) = C' \frac{e^{ikz}}{(kz)^{\frac{3}{2}}}, \quad z > 0, \quad (3.26)$$

where C' is a constant.

3.3.3 The Solution of the Homogeneous Finite Part Integral Equation by Differentiation

Consider the integral equation

$$\int_0^\infty f(z') H_0^{(1)}(k|z-z'|) dz' = \frac{4k}{z_0} e^{-ikaz}, \quad z > 0, \quad (3.27)$$

where $-1 \leq a \leq 1$. The solution of this integral equation is given by (3.3) except with $\cos\theta$ replaced by a . Applying the operator $L = \frac{d}{dz} + ika$ to both

sides of (3.27) yields

$$\text{Fp} \int_0^{\infty} Lf(z') H_0^{(1)}(k|z-z'|) dz' = 0, \quad z > 0, \quad (3.28)$$

so that the solution of the homogeneous finite part integral equation is

$$\begin{aligned} w(z) &= \left(\frac{d}{dz} + ika \right) f(z) \\ &= - \frac{\kappa k^3 e^{i\pi/4} \sqrt{1-a}}{Z_0 \sqrt{\pi}} \frac{e^{ikz}}{(kz)^{\frac{3}{2}}}, \quad z > 0. \end{aligned} \quad (3.29)$$

For any $a \neq 1$, this procedure yields the same solution as before. The expression for $w(z)$ for the special case $a = 0$ was developed in Section 2.4.

3.4 The Consistency Condition

Redefining $w(z)$, the homogeneous solution of the finite part integral equation, to be the value given by (3.29) for $a = 0$ and $\kappa = 1$ gives

$$w(z) = - \frac{k^3 e^{i\pi/4}}{Z_0 \sqrt{\pi}} \text{Pf} \frac{e^{ikz}}{(kz)^{\frac{3}{2}}} 1_+(z). \quad (4.1)$$

The solution of the finite part integral equation (2.11) for $u_H(z)$ becomes

$$u_H(z) = \sin\theta v(z) + A w(z) \quad (4.2)$$

where A is a constant and $v(z) = f(z)/\kappa$. $f(z)$ is given by (3.3).

The relation between the current source-function $u_H(z)$ and the current $I_H(z)$ is, from (2.10),

$$\frac{d^2 I_H}{dz^2} + k^2 I_H = u_H(z), \quad z > 0. \quad (4.3)$$

This is an inhomogeneous second order differential equation for I_H , the half-plane current. The inverse of the operator $\mathcal{L} = (d^2/dz^2 + k^2)$ can be represented as an integral operator with a Green's function kernel. This Green's function $g(z, z')$ is a solution of the inhomogeneous differential equation

$$\mathcal{L}^* g = \delta(z - z') \quad (4.4)$$

subject to certain boundary conditions where \mathcal{L}^* is the adjoint of \mathcal{L} .

The adjoint boundary conditions are found by determining boundary conditions such that

$$\langle \mathcal{L}\eta_+, \psi \rangle = \langle \eta_+, \mathcal{L}^*\psi \rangle \quad (4.5)$$

where $\langle \alpha, \beta \rangle$ is shorthand for $\int_{-\infty}^{\infty} \alpha \beta dz$ and $\mathcal{L} = (d^2/dz^2 + k^2)$. The $+$ subscript denotes that η is multiplied by the unit step function. In (4.5) η takes the place of I_H and ψ is the function for which the adjoint boundary conditions are to be found. The fact that the current $I_H = O(z^{\frac{1}{2}})$ as $z \rightarrow 0$ for the H-polarization gives $\eta(0) = 0$ and $\eta = O(z^{\frac{1}{2}})$ as $z \rightarrow 0$. Clearly, $\mathcal{L}\eta_+$ is allowed to be a pseudofunction because

$$\mathcal{L}\eta = O(z^{-\frac{3}{2}}) \quad \text{as } z \rightarrow 0+. \quad (4.6)$$

For arbitrary ψ , this means that $\langle \mathcal{L}\eta_+, \psi \rangle$ must be interpreted as the finite part integral

$$\text{Fp} \int_0^{\infty} \left(\frac{d^2 \eta}{dz^2} + k^2 \eta \right) \psi(z) dz. \quad (4.7)$$

Setting the lower limit to ϵ and integrating by parts yields

$$\begin{aligned}
\int_{\epsilon}^{\infty} \left(\frac{d^2 \eta}{dz^2} + k^2 \eta \right) \psi(z) dz &= \left. \frac{d\eta}{dz} \psi(z) \right|_{\epsilon}^{\infty} - \eta(z) \left. \frac{d\psi}{dz} \right|_{\epsilon}^{\infty} \\
&+ \int_{\epsilon}^{\infty} \eta(z) \left(\frac{d^2 \psi}{dz^2} + k^2 \psi \right) dz.
\end{aligned} \tag{4.8}$$

Because of the edge condition on η ,

$$\frac{d\eta}{dz} = O(z^{-\frac{1}{2}}) \text{ as } z \rightarrow 0+,$$

the finite part integral becomes

$$\begin{aligned}
\text{Fp} \int_0^{\infty} (\mathcal{L}\eta) \psi(z) dz &= \lim_{\epsilon \rightarrow 0} \left\{ \int_{\epsilon}^{\infty} (\mathcal{L}\eta) \psi(z) dz + \left. \frac{d\eta}{dz} \psi(z) \right|_{\epsilon} \right\} = \\
&= \left. \frac{d\eta}{dz} \psi(z) \right|_{\infty} - \eta(z) \left. \frac{d\psi}{dz} \right|_0^{\infty} + \int_0^{\infty} \eta(z) \mathcal{L}^* \psi dz.
\end{aligned} \tag{4.9}$$

In order for (4.5) to hold, the boundary terms in (4.9) must vanish.

The boundary conditions to be satisfied are

$$\eta(z) \frac{d\psi}{dz} \rightarrow 0 \text{ as } z \rightarrow 0, \tag{4.10a}$$

$$\frac{d\eta}{dz} \psi(z) \rightarrow 0 \text{ as } z \rightarrow \infty, \tag{4.10b}$$

$$\text{and } \eta(z) \frac{d\psi}{dz} \rightarrow 0 \text{ as } z \rightarrow \infty. \tag{4.10c}$$

The first condition is always satisfied because $\eta(0) = 0$. The current asymptotically behaves like

$$I_H \sim e^{-ikz \cos \theta} \text{ as } z \rightarrow \infty.$$

After limiting θ to be in the range $90^\circ < \theta < 270^\circ$, a small imaginary part may be introduced in k such that $k = k_k + ik_2$. This gives

$$\eta, \frac{d\eta}{dz} \sim e^{k_2 z \cos\theta} \quad \text{as } z \rightarrow \infty \text{ with } \cos\theta < 0.$$

From (4.10), ψ and $d\psi/dz$ must exhibit the exponential form

$$\psi, \frac{d\psi}{dz} \sim e^{-\zeta z} \quad \text{as } z \rightarrow \infty$$

with $\zeta > k_2 \cos\theta$ in order for the boundary terms to vanish. It turns out that $\zeta = k_2$ so that this condition is always satisfied. This is the only adjoint boundary condition that is required. A condition at zero is not required for the adjoint problem. The above restriction on θ is necessary because a plane wave incident field in a lossy medium appears to become infinite at plus infinity for angles of incidence $\theta < 90^\circ$ [See Figure 2.1]. If the incident plane wave itself exhibits this behavior, then it makes sense that the current does also. It is assumed here that θ is initially restricted to the range $90^\circ < \theta < 270^\circ$ so that the incident field and the current approach zero at infinity. θ is extended to all angles of incidence only after the calculations have been completed.

The solvability of the second order differential equation $(d^2/dz^2 + k^2)y = f(z)$, $a < z < b$, such that certain boundary conditions are satisfied is closely related to the existence of solutions to the homogeneous system and to the adjoint homogeneous system. In the case of a scatterer of finite extent, solutions of the homogeneous system arise only at resonance, i.e., when the physical extent of the scatterer matches a multiple of a half wavelength of the incident field. For the semi-infinite case, the homogeneous system has no nontrivial solutions. For non-singular differential equations, it may be shown that if the homogeneous system has only the trivial (zero) solution, then the adjoint homogeneous

system has only the trivial (zero) solution. For the details, the reader is referred to Stakgold (1967, Volume I, pp. 84-85). For problems involving pseudofunctions and the finite part, this is no longer true. The adjoint homogeneous system usually has solutions even though the homogeneous system has only the trivial (zero) solution.

For the half-plane problem, the homogeneous, inhomogeneous, and adjoint homogeneous systems are

The homogeneous system

$$\mathcal{L}\rho = 0 \quad 0 < z < \infty \quad \rho(0) = 0 \quad \rho \rightarrow 0 \text{ as } z \rightarrow \infty \quad (4.11a)$$

The inhomogeneous system

$$\mathcal{L}\eta = f \quad 0 < z < \infty \quad \eta(0) = 0 \quad \eta \rightarrow 0 \text{ as } z \rightarrow \infty \quad (4.11b)$$

The adjoint homogeneous system

$$\mathcal{L}^*\psi = 0 \quad 0 < z < \infty \quad \psi \rightarrow 0 \text{ as } z \rightarrow \infty \quad (4.11c)$$

where $\mathcal{L}^* = \mathcal{L} = (d^2/dz^2 + k^2)$. The radiation condition must also be satisfied. As was shown previously, the adjoint homogeneous system does not have a boundary condition to be satisfied at $z = 0$. The differential equation of (4.11a) has solutions $[e^{-ikz}, e^{+ikz}]$ or $[\sin(kz), \cos(kz)]$, but none of these satisfy the boundary conditions so (4.11a) has only the trivial solution $\rho \equiv 0$. The adjoint homogeneous differential equation also has the above solutions, but in this case one of them does satisfy the given boundary condition (again assuming that $k = k_1 + i k_2$, $0 < k_2 \ll 1$, and that θ is restricted). The non-zero solution of the adjoint homogeneous system (4.11c) is

$$\psi = e^{+ikz}.$$

The following theorem is similar to one given by Stakgold (1967, Volume I, p. 85).

Theorem: System (4.11b) has no solution unless the consistency condition $\int_0^{\infty} f(z) \psi(z) dz = 0$ is satisfied for every $\psi(z)$ which is a solution of (4.11c).

Proof: \mathcal{L} is a second order differential operator and hence can have no more than two non-zero linearly independent homogeneous solutions. Only one of these goes to zero and is an outgoing wave as $z \rightarrow \infty$. These are the only conditions required on ψ by (4.11c). Multiplying (4.11b) by ψ and (4.11c) by η , subtracting, and integrating from 0 to ∞ gives

$$\int_0^{\infty} (\psi \mathcal{L} \eta - \eta \mathcal{L}^* \psi) dz = \int_0^{\infty} f(z) \psi(z) dz. \quad (4.12)$$

The left side is zero by applying the results of (4.10) to (4.9). Therefore,

$$\int_0^{\infty} f(z) \psi(z) dz = 0 \quad (4.13)$$

must hold for every ψ that satisfies (4.11c). Note that for the trivial solution $\psi(z) \equiv 0$, the consistency condition is always satisfied.

The constant A in the current source-function (4.2) can now be found.

The system

$$\mathcal{L} I_H = u_H(z) \quad 0 < z < \infty \quad I_H(0) = 0 \quad I_H \rightarrow 0 \text{ as } z \rightarrow \infty \quad (4.14)$$

is exactly of the form of (4.11b). Here the current source-function $u_H(z)$ takes the place of $f(z)$. In order for the system (4.14) to have a solution, the consistency condition (4.13) must be satisfied with u_H in place of f .

Substituting (4.2) in (4.13), the consistency condition becomes

$$0 = \int_0^{\infty} u_H(z) \psi(z) dz = \sin\theta \int_0^{\infty} v(z) e^{ikz} dz + A \int_0^{\infty} w(z) e^{ikz} dz. \quad (4.15)$$

Solving for A obtains

$$A = - \frac{\sin\theta \int_0^{\infty} v(z) e^{ikz} dz}{\int_0^{\infty} w(z) e^{ikz} dz}. \quad (4.16)$$

Therefore, there is only one value of A for which a solution for I_H exists. The integrals of $w(z)$ and $v(z)$ with respect to e^{ikz} , where $w(z)$ and $f(z) = \kappa v(z)$ are given by (4.1) and (3.3), respectively, become

$$\int_0^{\infty} v(z) e^{ikz} dz = \frac{2ik}{Z_0 \sin(\theta/2)} \quad (4.17)$$

and

$$\text{Fp} \int_0^{\infty} w(z) e^{ikz} dz = \frac{2\sqrt{2} k^2}{Z_0}. \quad (4.18)$$

Substituting these in (4.16) and simplifying yields

$$A = \frac{\sqrt{2} \cos(\theta/2)}{ik}. \quad (4.19)$$

The unique solution for $u_H(z)$ becomes

$$u_H(z) = \sin\theta v(z) + \frac{\sqrt{2} \cos(\theta/2)}{ik} w(z). \quad (4.20)$$

This is the required result. The solution for I_H is found in the next section.

3.5 The Current in Terms of the Current Source-Function

The solutions for u_E and u_H , the E- and H-polarization current source-functions, are given by (3.5) and (4.20), respectively. The relations between u_H and I_H and u_E and I_E are given by

$$I_E = \frac{1}{k^2} u_E(z) \quad (5.1)$$

and

$$\frac{d^2 I_H}{dz^2} + k^2 I_H = u_H(z). \quad (5.2)$$

The first expression is trivial. In the second, the solution for I_H may be found using Green's function techniques. The solution is

$$I_H(z) = \int_0^{\infty} u_H(z') g(z, z') dz' \quad (5.3)$$

where $g(z, z')$ is the Green's function for the operator in (5.2). This Green's function may be found by solving the inhomogeneous distributional second order differential equation

$$\mathcal{L}^* g = \delta(z - z'), \quad 0 < z, z' < \infty, \quad g \text{ outgoing as } z' \rightarrow \infty, \quad (5.4)$$

subject to the adjoint boundary conditions. No boundary condition is required at $z' = 0$ and only a radiation type boundary condition is required at infinity. The constraints on the Green's function are

$$\begin{aligned}
(1) \quad & g(z, z') \text{ continuous at } z' = z, \\
(2) \quad & \left. \frac{dg}{dz'} \right|_{z'=z+} - \left. \frac{dg}{dz'} \right|_{z'=z-} = 1,
\end{aligned} \tag{5.5}$$

and (3) $g(z, z')$ is an outgoing wave near infinity.

For $z' \neq z$, (5.4) becomes

$$\mathcal{L}^* g = 0.$$

This has solutions $e^{ikz'}$, $e^{-ikz'}$, $\sin(kz')$, or $\cos(kz')$. Although a boundary condition at $z'=0$ is not required, one may be imposed. If the condition $g(z, z'=0) = 0$ is imposed on g , then

$$g(z, z') = \begin{cases} A(z) \sin(kz') & z > z' \\ B(z) e^{ikz'} & z < z'. \end{cases} \tag{5.7}$$

Enforcing the conditions (5.5) gives

$$g(z, z') = \frac{1}{2ik} (e^{ik|z-z'|} - e^{ik(z+z')}). \tag{5.8}$$

The current I_H is found from (5.3). It is interesting to note that since $\int_0^\infty u_H e^{ikz'} dz' = 0$ by the consistency condition (4.15), the current may also be written as

$$I_H = \int_0^\infty u_H(z') E(z-z') dz' \tag{5.9}$$

where $E(z) = \frac{1}{2ik} e^{ik|z|}$. This is just the "fundamental solution" for the operator \mathcal{L} as is used in the theory of distributions. The current I_H is just the convolution of u_H with E . Thus, the integral in (5.3) has been reduced to the convolution integral in (5.9).

Substituting (4.20) for u_H in (5.9) obtains

$$I_H(z) = \frac{\sin\theta}{2ik} \int_0^\infty v(z') e^{ik|z-z'|} dz' + \frac{\sqrt{2} \cos(\theta/2)}{ik(2ik)} \int_0^\infty w(z') e^{ik|z-z'|} dz'. \quad (5.10)$$

The integrals in this expression are found to be

$$\begin{aligned} \int_0^\infty v(z') e^{ik|z-z'|} dz' &= \frac{4ke^{i\pi/4}}{z_0\sqrt{\pi}} \left[\frac{e^{-ikz} (F_2(\infty) - 1_+(z)F_2(2kz))}{\sin(\theta/2)} \right. \\ &\quad \left. + \frac{2}{\sin\theta} 1_+(z) e^{-ikz \cos\theta} F_2(kz(1+\cos\theta)) \right] \end{aligned} \quad (5.11)$$

and

$$\begin{aligned} \text{Fp} \int_0^\infty w(z') e^{ik|z-z'|} dz' &= \\ &= \frac{4k^2 e^{-i\pi/4}}{z_0\sqrt{\pi}} \sqrt{2} e^{-ikz} (F_2(\infty) - 1_+(z)F_2(2kz)) \end{aligned} \quad (5.12)$$

where

$$\begin{aligned} F_2(x) &= \int_0^{\sqrt{x}} e^{it^2} dt = \frac{e^{i\pi/4}}{2} \left(\sqrt{\pi} - e^{ix} U\left(\frac{1}{2}, \frac{1}{2}, -ix\right) \right) \\ &= \sqrt{x} M\left(\frac{1}{2}, \frac{3}{2}, ix\right). \end{aligned} \quad (5.13)$$

U and M are Kummer's functions and $F_2(\infty) = \sqrt{\pi} e^{i\pi/4}/2$. Substituting (5.11) and (5.12) in (5.10) and simplifying gives

$$I_H(z) = \frac{4e^{-i\pi/4}}{Z_0\sqrt{\pi}} l_+(z) e^{-ikz \cos\theta} \int_0^{\sqrt{kz(1+\cos\theta)}} e^{it^2} dt \quad (A/m)/(V/m) \quad (5.14a)$$

$$= \frac{\sqrt{2}}{Z_0} e^{i\pi/4} l_+(z) e^{-ikz \cos\theta} \int_0^{kz(1+\cos\theta)} H_{\frac{1}{2}}^{(1)}(t) dt \quad (5.14b)$$

$$= \frac{2\sqrt{(2k)}}{Z_0} e^{-i\pi/4} \cos\frac{\theta}{2} l_+(z) e^{ikz} \frac{d^{-\frac{1}{2}}}{dz^{-\frac{1}{2}}} e^{-ikz(1+\cos\theta)} \quad (5.14c)$$

where $H_{\frac{1}{2}}^{(1)}(t)$ is the Hankel function and the $d^{-\frac{1}{2}}/dz^{-\frac{1}{2}}$ operator is the semiintegral operator of Oldham and Spanier (1974, pp. 115-131). It is important to note that

$$I_H(z) = \frac{e^{-ikz}}{2ik} \int_0^{\infty} u_H(z') e^{ikz'} dz' = 0, \quad z < 0. \quad (5.15)$$

The integral is identically zero for all negative z . This is true because of the consistency condition (4.15). Thus,

$$I_H(z) = \int_0^{\infty} u_H(z') E(z-z') dz', \quad -\infty < z < \infty. \quad (5.16)$$

The current is given by the integral for all values of z .

3.6 Discussion of the Results and Conclusions

The main result of this chapter is the solution for the current $I_H(z)$ induced on a perfectly conducting half-plane due to an incident plane wave. The solution to the integral equation

$$\text{FP} \int_0^{\infty} u_H(z') H_0^{(1)}(k|z-z'|) dz' = \frac{4k}{Z_0} \sin\theta e^{-ikz \cos\theta}, \quad z > 0$$

is found by adding the solution of the ordinary integral equation to a solution of the homogeneous finite part integral equation such that the edge condition is satisfied. The success of this procedure requires that the form of the solution of the homogeneous finite part integral equation be unique to within an arbitrary multiplicative constant. All three ways of obtaining the homogeneous solution strongly suggest that this is true since they all exhibit z -dependence of the form $\text{Pf } l_+(z)e^{ikz}/(kz)^{\frac{3}{2}}$. One part of a source-free solution to the wave equation (described in Section 2.2) also has z -dependence of this form.

The constant multiplying the homogeneous solution is found by enforcing the consistency condition

$$\langle u_H(z), e^{ikz} \rangle = 0.$$

The current is found by inverting the $d^2/dz^2 + k^2$ operator to obtain

$$I_H = u_H * E, \quad \text{all } z.$$

The fundamental solution E may be used instead of a Green's function because of the consistency condition. The result for I_H , given by (5.14), is identical with the results obtained by other methods.

The current source-function technique has several possible advantages over the Hallén or Pocklington integral equation techniques for numerical solution. The CSF technique retains the simplicity of the kernel of the Hallén-type integral equation and does not require a differentiation operation in evaluating the matrix elements in the moment method as the Pocklington approach does. Furthermore, the forcing function of the CSF

integral equation is just the incident field. No operation on the incident field is required as is the case with the Hallén formulation. Since the integral operator is simplified, the behavior of the current source-function is expected to be somewhat similar to that of the incident field. Of course, the CSF technique requires an additional operation to find the current, but this is a straight-forward integration and may be separated from the considerations involved in the moment method. Local inaccuracies in the moment method solution for the current source-function should not drastically effect the overall accuracy of the current since the induced current is obtained by integrating over the (approximately represented) source-function.

4. THE NUMERICAL SOLUTION OF THE HALF-PLANE PROBLEM: E-POLARIZATION

The closed form solution of the half-plane problem with E-polarization plane wave incidence is discussed in Chapter 3. The present chapter is devoted to the moment method numerical solution of the same problem. The method of moments discretizes an integral equation into a matrix equation. This procedure has been widely discussed by Harrington (1968) and others and so is not discussed here in an introductory sense. The transform domain numerical solution of the half-plane problem is discussed by Li (1972).

The results obtained here are used later to solve for the H-polarization current by the current source-function technique. The half-plane problem is chosen primarily because its exact solution is known and can be used as a standard to judge the accuracy of the numerical procedures described in this chapter. The computer programs used in this work appear in Appendix D.

4.1 The Integral Equation Formulation for the E-polarization

The geometry for the E-polarization half-plane problem with plane wave incidence is given in Figure 2.1. The integral equation for the current is derived in Chapter 3 and is given by (2.7) and (2.8) of that chapter. It is

$$\int_0^{\infty} I_E(z') H_0^{(1)}(k|z-z'|) dz' = \frac{4}{kZ_0} e^{-ikz \cos\theta}, \quad z > 0, \quad (1.1)$$

where $I_E(z')$ is the y-directed E-polarization current. From energy considerations for this structure and polarization

$$|I_E(z)| = O(z^{-\frac{1}{2}}) \quad \text{as} \quad z \rightarrow 0. \quad (1.2)$$

This edge condition on the current is used to construct an appropriate expansion function set for the method of moments.

4.1.1 The Physical Optics Current, I_{PO}

A moment method numerical solution may be obtained only if the problem is reformulated to make the range of integration in (1.1) finite. Far from the edge, the current on the conducting half-plane is about the same as it would be if the conducting plane extended to infinity in all directions. Applying this concept allows us to say that the current $I_E(z)$ approaches a known function, the so-called physical optics current $I_{PO}(z)$, as z becomes large.

The geometry for solving for the physical optics current $I_{PO}(z)$ for the half-plane problem is just that of Figure 2.1(a) except that the metal is extended to infinity in all directions. For an incident plane wave

$$\underline{E}^i = e^{-ikx \sin\theta} e^{-ikz \cos\theta} \hat{y}, \quad (1.3)$$

the total tangential magnetic field is

$$H_z^t = H_z^i + H_z^r = -(2/Z_0) \sin\theta \cos(kx \sin\theta) e^{-ikz \cos\theta}. \quad (1.4)$$

The physical optics current is the difference in the tangential magnetic field above (H_2) and below (H_1) the metal surface. It becomes

$$\underline{I}_{PO} = \hat{x} \times [H_2^t - H_1^t] = \frac{2}{Z_0} \sin\theta e^{-ikz \cos\theta} \hat{y}. \quad (1.5)$$

The physical optics current for the E-polarization is seen to be directed in the y direction with magnitude $2\sin\theta/Z_0$.

4.1.2 The Integral Equation for the Difference $\{I_E - I_{PO}\}$

The integral equation for the E-polarization half-plane current is given by (1.1). Adding and subtracting terms in I_{PO} in the unknown yields

$$\begin{aligned} \int_0^{\infty} \{I_E - I_{PO}\}(z') H_0^{(1)}(k|z-z'|) dz' = \\ = \frac{4}{kZ_0} e^{-ikz \cos\theta} - \frac{2}{Z_0} \sin\theta \int_0^{\infty} e^{-ikz' \cos\theta} H_0^{(1)}(k|z-z'|) dz'. \end{aligned} \quad (1.6)$$

Transforming variables and substituting the identity

$$\begin{aligned} \int_0^{\infty} e^{-ix \cos\theta} H_0^{(1)}(|kz - x|) dx = \\ = e^{-ikz \cos\theta} \left\{ \frac{2}{\sin\theta} - \int_{kz}^{\infty} e^{iy \cos\theta} H_0^{(1)}(y) dy \right\} \end{aligned} \quad (1.7)$$

in (1.6), one obtains the integral equation

$$\begin{aligned} \int_0^{\infty} \{I_E - I_{PO}\} H_0^{(1)}(k|z-z'|) dz' = \\ = \frac{2}{kZ_0} \sin\theta e^{-ikz \cos\theta} \int_{kz}^{\infty} e^{iy \cos\theta} H_0^{(1)}(y) dy, \quad z > 0. \end{aligned} \quad (1.8)$$

The closed form solution of (1.8) may be obtained from Equation (3.3) of Chapter 3 and (1.5). In (1.8) the unknown is the quantity $\{I_E - I_{PO}\}$. This difference should approach zero for large z' , making it possible to truncate the integral at some finite distance kL . If the upper limit kL is chosen large enough, then

$$\begin{aligned}
\int_0^{\infty} \{I_E - I_{PO}\}(t) H_0^{(1)}(|kz-t|) dt &\approx \\
&\approx \int_0^{kL} \{I_E - I_{PO}\}(t) H_0^{(1)}(|kz-t|) dt = \text{RHS}(kz), \quad z > 0, \quad (1.9)
\end{aligned}$$

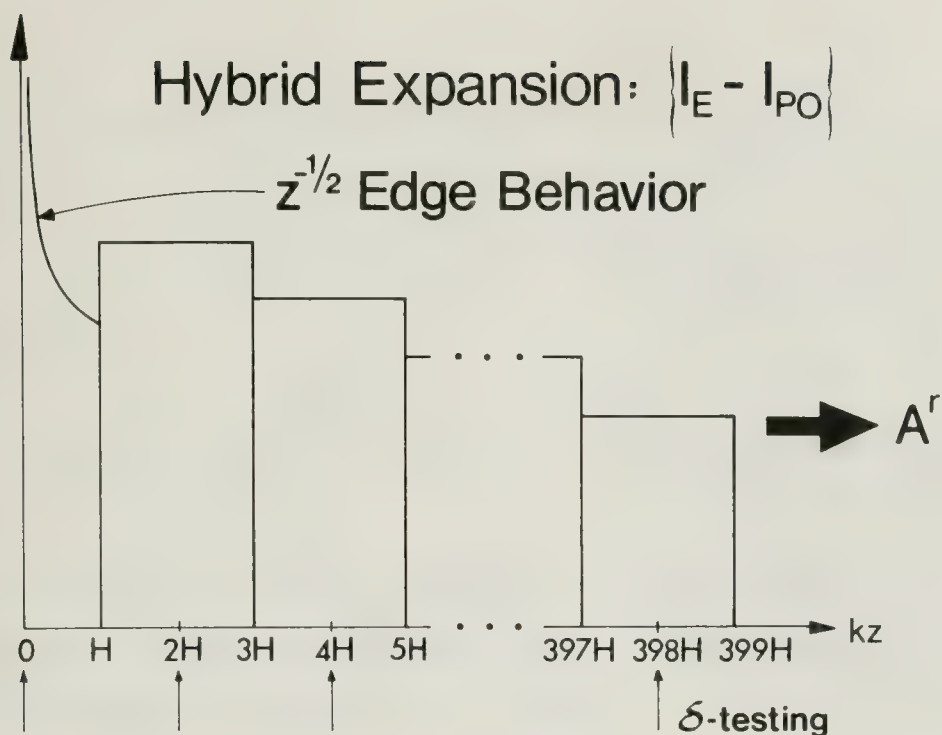
where RHS is the right-hand side of (1.8).

4.1.3 The Choice of Expansion Functions

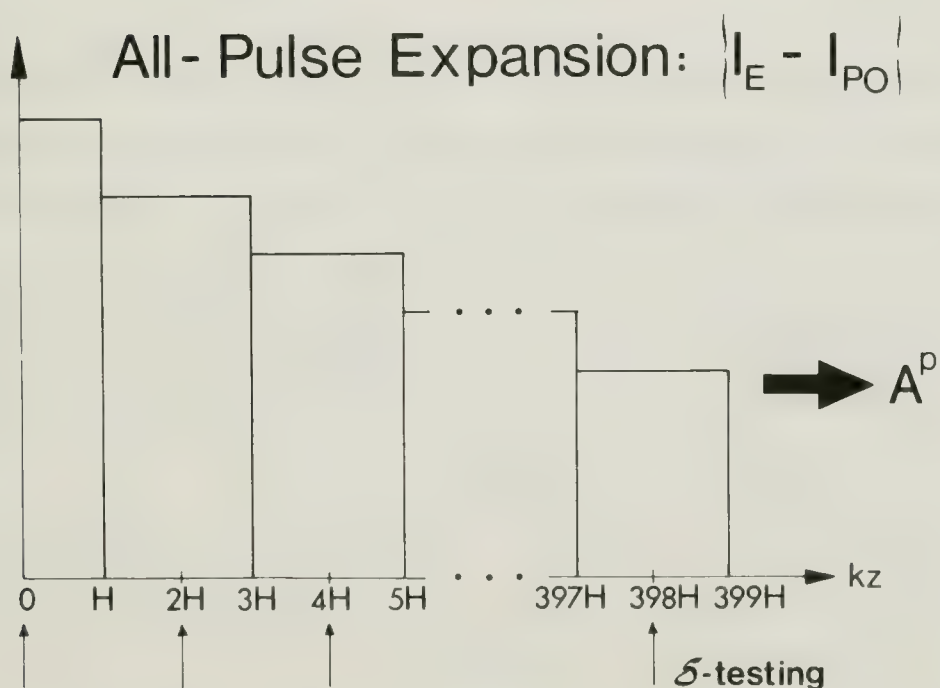
The integral equation (1.9) is solved numerically by the method of moments. The unknown, $\{I_E - I_{PO}\}$, is expanded in two similar basis function sets. The first is a hybrid expansion function set based on edge condition considerations. The second is an all-pulse expansion function set which is chosen because of the simplicity of matrix element evaluation. Point matching is used in both cases starting at the edge. The hybrid expansion function set that is used is one with a half-width $t^{-\frac{1}{2}}$ expansion function at the edge and with full-width pulse expansion functions away from the edge. This expansion is shown in Figure 4.1(a). The use of a half-width edge subsection was suggested by Pearson (1975). This allows the match points to be uniformly distributed. The all-pulse expansion function set that is used is one with a half-width pulse expansion function at the edge and with full-width pulse expansion functions away from the edge. This expansion is shown in Figure 4.1(b). It is of interest to observe the effect that such a crude edge expansion function has on the solution away from the edge.

The hybrid basis function expansion may be written as

$$\{I_E - I_{PO}\}(t) \approx \begin{cases} x_1^r t^{-\frac{1}{2}} & 0 < t < H \\ x_j^r & (2j-3)H < t < (2j-1)H, \quad 2 \leq j \leq 200, \end{cases} \quad (1.10a)$$



(a)



(b)

Figure 4.1. The Expansion Function Sets. (a) The Hybrid Expansion. (b) The All-Pulse Expansion.

where $H (=0.05)$ is the subsection half-width and the x_j^r 's are unknown constants. "r" is used because the hybrid expansion has a one over square root expansion function at the edge. The all-pulse expansion may be written as

$$\{I_E - I_{PO}\}(t) \approx \begin{cases} x_1^p & 0 < t < H \\ x_j^p & (2j-3)H < t < (2j-1)H, 2 \leq j \leq 200, \end{cases} \quad (1.10b)$$

where the x_j^p 's are unknown constants. "p" is used because the all-pulse expansion is composed of pulse functions. Substituting (1.10a) in (1.9), the approximate integral equation becomes

$$x_1^r \int_0^H t^{-\frac{1}{2}} H_0^{(1)}(|kz-t|) dt + \sum_{j=2}^N x_j^r \int_{(2j-3)H}^{(2j-1)H} H_0^{(1)}(|kz-t|) dt = \text{RHS}(kz), \quad z > 0, \quad (1.11)$$

where $kL = (2N-1)H$ and $N = 200$. The corresponding expression for the all-pulse basis function set is obtained by replacing the $t^{-\frac{1}{2}}$ under the integral sign by unity and the x_j^r by x_j^p . The moment method solution is obtained by requiring Equation (1.11) to hold at $kz = 2(i-1)H$ for $i = 1, 2, \dots, N$ (point matching). This results in N equations in N unknowns which may be written in matrix form as

$$A^r \underline{x}^r = \underline{y} \quad (1.12)$$

for the hybrid expansion and as

$$A^p \underline{x}^p = \underline{y} \quad (1.13)$$

for the all-pulse expansion. A^r and A^p are almost-Toeplitz matrices of integrals of the kernel weighted with respect to the basis functions. The

Toeplitz matrix is a matrix with all of the elements in any diagonal equal.

A^r and A^p are

$$A^r = \begin{bmatrix} r_1 & t_2 & \cdots & t_N \\ r_2 & t_1 & \cdots & t_{N-1} \\ \cdots & \cdots & \cdots & \cdots \\ r_N & t_{N-1} & \cdots & t_1 \end{bmatrix} \quad \text{and} \quad A^p = \begin{bmatrix} p_1 & t_2 & \cdots & t_N \\ p_2 & t_1 & \cdots & t_{N-1} \\ \cdots & \cdots & \cdots & \cdots \\ p_N & t_{N-1} & \cdots & t_1 \end{bmatrix}. \quad (1.14)$$

These would be Toeplitz matrices except for the fact that the first column is different. The individual matrix elements are

$$r_j = \int_0^H t^{-\frac{1}{2}} H_0^{(1)}(|D_j - t|) dt, \quad (1.15)$$

$$p_j = \int_0^H H_0^{(1)}(|D_j - t|) dt, \quad (1.16)$$

and

$$t_j = \int_{-H}^H H_0^{(1)}(|D_j - t|) dt \quad (1.17)$$

where H is the subsection half-width and $D_j = 2(j-1)H$ for $j = 1, 2, \dots, N$. y is a vector of the right-hand side evaluated at these points. Matrix element approximations are discussed in the next section. The evaluation of the right-hand side is discussed in Section 4.3. A treatment of the almost-Toeplitz matrix is given in Section 4.4. Finally, Section 4.5 discusses the results of the calculations. Complete listings of the computer programs referred to in the following are given in Appendix D.

4.2 Matrix Element Approximations

Matrix elements must be calculated as accurately as possible in order to have the moment method results turn out reasonably accurate. This section describes the method of calculating the matrix elements. Matrix element approximations for pulse expansion functions are examined in the next section and those for inverse square root expansion functions are detailed in Section 4.2.2.

4.2.1 Matrix Element Approximations for Pulse Basis Functions

Matrix elements for the edge pulse expansion function may be written in the form

$$p_j = \int_0^H H_0^{(1)}(|D_j - t|) dt, \quad j = 1, 2, \dots, N, \quad (2.1)$$

and those for expansion functions away from the edge may be written in the form

$$t_j = \int_{-H}^H H_0^{(1)}(|D_j - t|) dt, \quad j = 1, 2, \dots, N, \quad (2.2)$$

where N is the number of subsections, H is the subsection half-width, and $D_j = 2(j-1)H$. For $D = D_1 = 0$, the integrals become

$$p_1 = \int_0^H H_0^{(1)}(t) dt \quad \text{and} \quad t_1 = \int_{-H}^H H_0^{(1)}(|t|) dt = 2 \int_0^H H_0^{(1)}(t) dt. \quad (2.3)$$

These matrix elements are called the self terms. All other matrix elements are called mutual terms. Integrals like (2.3) may be approximated in terms of Chebyshev polynomial series by

$$\int_0^x J_0(t) dt = \sum_{n=0}^{\infty} a_n T_{2n+1}(x/8), \quad -8 \leq x \leq 8, \quad (2.4)$$

and

$$\int_0^x Y_0(t) dt = (2/\pi) [\gamma + \ln(x/2)] \int_0^x J_0(t) dt - \sum_{n=0}^{\infty} b_n T_{2n+1}(x/8), \quad (2.5)$$

$$0 \leq x \leq 8,$$

where $\gamma = 0.57721\ 56649 \dots$ is Euler's constant. The coefficients a_n and b_n are given by Luke (1969, Volume II, Table 27, p. 334). The specific range of validity of these equations is dictated by the available coefficients. The use of a Chebyshev series minimizes the maximum error over the interval of approximation. That is, if $G(x) = \sum_{n=0}^N a_n T_n(x)$ is a proper Chebyshev approximation to $f(x)$, then

$$\max_{-1 \leq x \leq 1} |f(x) - G(x)|$$

will be minimized over the set of all polynomials of degree N or less. If a sufficient number of terms are included in (2.4) and (2.5), these integrals may be evaluated to any desired accuracy. Various self term approximations are derived and compared to the above in Appendix B.

For $D_j \neq 0$, the mutual terms may be written as

$$\int_{-H}^H H_0^{(1)}(D_j - t) dt = \int_a^b H_0^{(1)}(t) dt \quad (2.6)$$

where $a = D_j - H$ and $b = D_j + H$. The mutual terms are evaluated by using either the Chebyshev series in (2.4) and (2.5) or the Chebyshev series

$$\int_x^{\infty} H_0^{(1)}(t) dt = \left(\frac{2}{\pi x}\right)^{\frac{1}{2}} e^{i(x+\pi/4)} \sum_{n=0}^{\infty} c_n T_n^*(5/x), \quad x \geq 5, \quad (2.7)$$

where T_n^* is the shifted Chebyshev polynomial of the first kind given by $T_n^*(x) = T_n(2x-1)$. The complex coefficients c_n are given by Luke (1969, Volume II, Table 27, p. 335). The Chebyshev series of (2.4), (2.5), and (2.7) are truncated after about 18 terms. This gives full double precision (15 digit) accuracy. The mutual terms are evaluated using either (2.4) and (2.5) or (2.7) in either

$$\int_a^b H_0^{(1)}(t)dt = \int_0^b H_0^{(1)}(t)dt - \int_0^a H_0^{(1)}(t)dt \quad (2.8)$$

or

$$\int_a^b H_0^{(1)}(t)dt = \int_a^\infty H_0^{(1)}(t)dt - \int_b^\infty H_0^{(1)}(t)dt, \quad (2.9)$$

respectively. Careful study of the results indicates that for $b = a+0.1$ approximately two digits of accuracy are lost in taking the difference. Another way of saying this is that for $b = a+0.1$ the first two digits of each of the integrals on the right-hand sides of (2.8) and (2.9) are approximately the same. This allows about 12 or 13 decimal places of accuracy for each pulse basis function mutual term matrix element computed in this way in double precision. Various numerical approximations for the mutual terms are compared in Appendix B.

4.2.2 Matrix Elements Associated with the Inverse Square Root Basis Function

Matrix elements associated with the $t^{-\frac{1}{2}}$ edge expansion function may be written in the form

$$r_j = \int_0^H t^{-\frac{1}{2}} H_0^{(1)}(|D_j - t|)dt. \quad (2.10)$$

The self term is the value for $D = D_1 = 0$ and the mutual terms are the values for $D_j > 0$.

The self term takes the form

$$r_1 = \int_0^H t^{-\frac{1}{2}} H_0^{(1)}(t) dt. \quad (2.11)$$

This integral may be written in terms of series of Chebyshev polynomials as

$$\int_0^x t^{-\frac{1}{2}} J_0(t) dt = \sqrt{x} \sum_{n=0}^{\infty} a_n T_{2n}(x), \quad 0 \leq x \leq 1, \quad (2.12)$$

and

$$\int_0^x t^{-\frac{1}{2}} Y_0(t) dt = \frac{2}{\pi} [\gamma + \ln(x/2)] \int_0^x t^{-\frac{1}{2}} J_0(t) dt + \sqrt{x} \sum_{n=0}^{\infty} b_n T_{2n}(x), \quad (2.13)$$

$$0 \leq x \leq 1.$$

The coefficients a_n and b_n are given to thirty decimal places in Appendix C along with a discussion of their computation. Various numerical approximations to this self term are given in Appendix B.

The mutual terms for the edge expansion function may be written in the form

$$r_j = \int_0^H t^{-\frac{1}{2}} H_0^{(1)}(D_j - t) dt. \quad (2.14)$$

Expanding $H_0^{(1)}(D_j - t)$ in a series of products of Bessel and Hankel functions according to Neumann's difference theorem for Bessel functions

$$H_0^{(1)}(D - t) = \sum_{k=-\infty}^{\infty} H_k^{(1)}(D) J_k(t), \quad |D| > |t|, \quad (2.15)$$

as given by Olver (1964, p. 363) and integrating with respect to $t^{-\frac{1}{2}}$, one obtains

$$\int_0^H t^{-\frac{1}{2}} H_0^{(1)}(D-t) dt = \sum_{k=0}^{\infty} \epsilon_k H_k^{(1)}(D) J_{i_{-\frac{1}{2}, k}}(H) \quad (2.16)$$

where

$$\epsilon_k = \begin{cases} 1 & k = 0 \\ 2 & k > 0 \end{cases} \quad (2.17)$$

and

$$J_{i_{\mu, \nu}}(H) = \int_0^H t^{\mu} J_{\nu}(t) dt \quad (2.18)$$

as given by Luke (1962, p. 42). This same result may also be obtained by expanding $H_0^{(1)}(D-t)$ in a Taylor series. For a particular formulation, H is fixed and so the J_i 's need to be computed only once. D , on the other hand, varies and so the $H_k^{(1)}$'s need to be computed for many points. This does not present any problem because the $H_k^{(1)}$'s are very easily and quickly computed using special algorithms. The J_k 's are computed using the algorithm of Blanch (1964) and the Y_k 's are computed directly from the recurrence relation. A brief description of Blanch's method is given in Section 4.3.2.

The $J_{i_{-\frac{1}{2}, k}}$'s are computed using a power series given by Luke (1962, p. 44). The series is

$$J_{i_{-\frac{1}{2}, k}}(z) = \sqrt{z} \frac{\left(\frac{z}{2}\right)^k}{k!} \sum_{n=0}^{\infty} \frac{(-)^n \left(\frac{z}{2}\right)^{2n}}{n! (k+1)_n (2n+k+\frac{1}{2})}. \quad (2.19)$$

This function is computed economically using the relations

$$(k+1)_n = (k+n)(k+1)_{n-1}, \quad (2.20)$$

$$k! = (k)(k-1)!, \quad (2.21)$$

and

$$z^k = (z)z^{k-1}. \quad (2.22)$$

These relations are used to generate the next term in the power series from the present one and also to generate $Ji_{-\frac{1}{2},k+1}(z)$ from $Ji_{-\frac{1}{2},k}(z)$. Since H is usually much less than one, the power series (2.19) is rapidly convergent.

The series (2.16) for the matrix elements is computed to an accuracy of at least ten decimal places with 32 terms. Various numerical approximations for the mutual terms due to the $t^{-\frac{1}{2}}$ expansion function are compared in Appendix B.

4.3 The Right-Hand Side

The right-hand side of the integral equation under study here is given in (1.8) and is

$$\text{RHS} = \frac{2}{z_0} \sin\theta e^{-ikz} \cos\theta \int_{kz}^{\infty} e^{it \cos\theta} H_0^{(1)}(t) dt, \quad z > 0. \quad (3.1)$$

With the help of the identity

$$\int_0^{\infty} e^{it \cos\theta} H_0^{(1)}(t) dt = \frac{2}{\pi} \frac{\theta}{\sin\theta}, \quad 0 \leq \theta < \pi, \quad (3.2)$$

Equation (3.1) becomes

$$\text{RHS} = \frac{4\theta}{\pi z_0} e^{-ikz} \cos\theta - \frac{2}{z_0} \sin\theta e^{-ikz} \cos\theta \int_0^{kz} e^{it \cos\theta} H_0^{(1)}(t) dt \quad (3.3)$$

for $z > 0$. An infinite series representation for the last integral in (3.3) is given by Luke (1962, pp. 239-240). One part of this representation is

$$\int_0^x e^{it \cos \theta} J_0(t) dt = 2e^{ix \cos \theta} \sum_{k=0}^{\infty} (-i)^k U_k(\cos \theta) J_{k+1}(x) \quad (3.4)$$

where

$$U_k(\cos \theta) = \frac{\sin(k+1)\theta}{\sin \theta} \quad (3.5)$$

is the Chebyshev polynomial of the second kind and $J_k(x)$ is the Bessel function of the first kind and order k . The other part of this representation is

$$\begin{aligned} \int_0^x e^{it \cos \theta} Y_0(t) dt &= \frac{2}{\pi} [\gamma + \ln(x/2)] \int_0^x e^{it \cos \theta} J_0(t) dt \\ &\quad - \frac{4}{\pi} e^{ix \cos \theta} \sum_{k=0}^{\infty} (-i)^k U_k(\cos \theta) S_k(x) \end{aligned} \quad (3.6)$$

where

$$S_k(x) = \frac{(x/2)^{k+1}}{(k+1)!} \sum_{m=0}^{\infty} \frac{(-)^m (x/2)^{2m}}{m! (k+2)_m} h_{m+k+1}. \quad (3.7)$$

In (3.7), $h_0 = 0$, $h_k = \psi(k+1) - \psi(1) = \sum_{r=1}^k \frac{1}{r}$, $\psi(1) = -\gamma$, $(z)_k$ is Pochhammer's symbol and ψ is the psi function. The use of "S" to represent this function is not standard, but is used to simplify (3.6).

4.3.1 Computation of the U_k 's

Values of higher order Chebyshev polynomials may be calculated from the recurrence relation

$$U_{n+1}(x) = 2x U_n(x) - U_{n-1}(x) \quad (3.8)$$

using the initial terms

$$U_0(x) = 1 \quad (3.9)$$

$$\text{and} \quad U_1(x) = 2x. \quad (3.10)$$

This relation is given by Luke (1969, Volume I, p. 297). The use of this relation is desirable because it is faster to evaluate an array of U_k 's in this manner than it is to evaluate them using (3.5). Equation (3.8) proves to be reasonably stable in the forward direction. Values for U_{90} generated by this method are accurate to about 10 decimal places.

4.3.2 Computation of the J_k 's

The method of Blanch (1964) for the computation of the J_k 's is based on the basic recurrence relation for Bessel's functions of the first kind

$$G_n(x) = \frac{1}{\frac{2n}{x} - G_{n+1}(x)} \quad (3.11)$$

where

$$J_n(x) = G_n(x) J_{n-1}(x). \quad (3.12)$$

The k^{th} continuation of (3.11) yields the continued fraction expansion

$$G_n(x) = \frac{1}{\frac{2n}{x} - \frac{1}{\frac{2n+2}{x} - \dots - \frac{1}{\frac{2n+2k}{x} - G_{n+k+1}(x)}}}. \quad (3.13)$$

Since the forward use of the recurrence relation (3.11) for $n > x$ results in severe accuracy loss, the continued fraction method is used in the backward direction as follows: $G_{n_{\max}}(x)$ is evaluated using (3.13) with $k = 15$ or more and $G_{n+k+1}(x) = 0$. The other $G_n(x)$ are computed from (3.11) for $n = n_{\max}-1, n_{\max}-2, \dots, 2$. Finally, the Bessel functions $J_n(x)$ are evaluated from (3.12) for $n = 2, 3, \dots, n_{\max}$ using $J_0(x)$ and $J_1(x)$ which have been computed with Chebyshev polynomials. Blanch gives an algorithm for carrying out these manipulations with minimal accuracy loss. Her algorithm is used because Hart et al. (1968, p. 146) say, "her discussion should be consulted by those requiring an algorithm for computing Bessel functions of the first kind to maximum accuracy."

4.3.3 The Computation of the S_k 's

The $S_k(x)$ functions of (3.7) are computed economically by using the relations

$$(k+2)_m = (k+1+m)(k+2)_{m-1}, \quad (3.14)$$

$$m! = m(m-1)!, \quad (3.15)$$

$$h_{m+k+1} = h_{m+k} + \frac{1}{m+k+1}, \quad (3.16)$$

and
$$(z)^m = z(z)^{m-1}. \quad (3.17)$$

The relations are used to generate the next term in the power series from the present one and also to generate $S_{k+1}(x)$ from $S_k(x)$.

4.3.4 Final Remarks on RHS

For the case $\theta = 90^\circ$, (3.1) reduces to

$$\text{RHS} = \frac{2}{Z_0} \int_{kz}^{\infty} H_0^{(1)}(t) dt \quad (3.18)$$

which is written in series of Chebyshev polynomials in Equations (2.4), (2.5), and (2.7). Table 4.1 gives the accuracy of the approximations (3.4) and (3.6) for $\theta = 90^\circ$ using the Chebyshev polynomial expansions for (3.18) as the standard. The term "Digits of Accuracy" is explained in Appendix A. This table shows that the real part of RHS is very accurate, but that the accuracy of the imaginary part decreases rapidly with increasing argument. The rapid deterioration of accuracy for the right-hand side for arguments greater than 20 requires that the limits of integration of the integral equation (1.9) be set at 20 or less. Graphs of RHS for $\theta = 45^\circ, 90^\circ, 135^\circ$, and 180° and for arguments between zero and twenty are shown in Figure 4.2.

4.4 The Efficient Inversion of the Almost-Toeplitz Matrix

Throughout this section, the notation

$$\underline{x} = \begin{bmatrix} x_1 \\ x_2 \\ \dots \\ x_N \end{bmatrix} \quad (4.1)$$

is used to represent a column vector \underline{x} and its elements. An efficient algorithm for the inversion of Toeplitz matrices has been developed by

Table 4.1

Digits of Accuracy for RHS by Double Precision Evaluation
of Equations (3.4) and (3.6)

x	Digits of accuracy	
	Real Part	Imag. Part
5.0	15.0	14.1
10.0	15.1	12.1
20.0	14.6	7.6
30.0	13.3	3.4
40.0	13.5	0.9

- Notes:
1. 16 digit accuracy possible.
 2. All summations truncated after 85 terms.
 3. For x greater than 40, the imaginary part becomes very large.
 4. RHS is given by Equation (3.3).

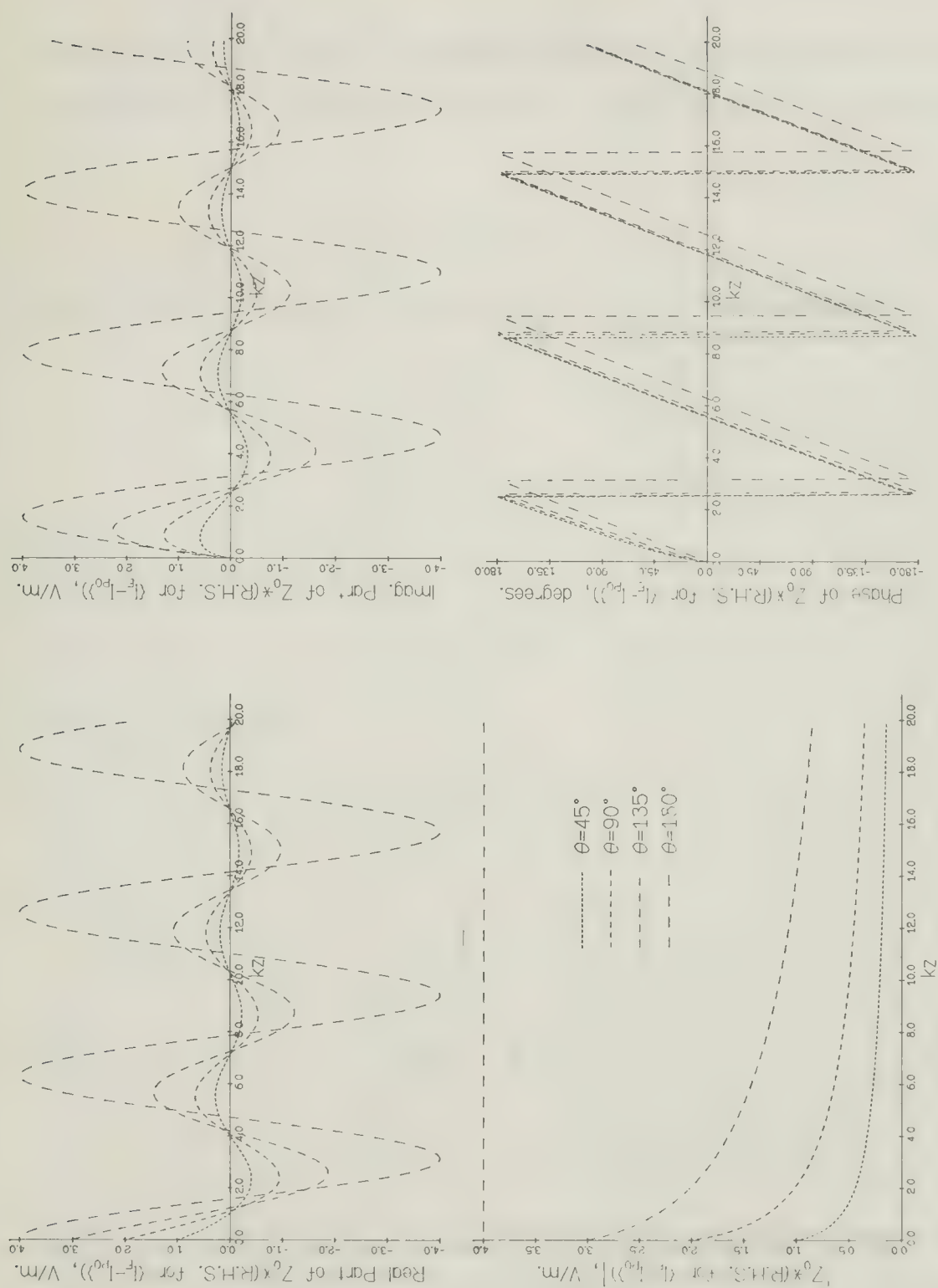


Figure 4.2. Plots of Z_0^*RHs for Angles of Incidence of $45^\circ, 90^\circ, 135^\circ,$ and 180° .

Preis (1972). An earlier discussion of Toeplitz matrix inversion is given by Bareiss (1969). The matrix equations (1.12) and (1.13) may be written as

$$(T + L)\underline{x} = \underline{y} \quad (4.2)$$

where, in the notation of Section 4.1.3, T is the Toeplitz matrix

$$T = \begin{bmatrix} t_1 & t_2 & \cdots & t_N \\ t_2 & t_1 & \cdots & t_{N-1} \\ \cdots & \cdots & \cdots & \cdots \\ t_N & t_{N-1} & \cdots & t_1 \end{bmatrix} \quad (4.3)$$

and L is the matrix

$$L = \begin{bmatrix} \underline{\ell} & \underline{0} & \underline{0} & \cdots & \underline{0} \end{bmatrix} \quad (4.4)$$

with

$$\underline{\ell} = \begin{bmatrix} z_1 - t_1 \\ z_2 - t_2 \\ \cdots \\ z_N - t_N \end{bmatrix} \quad \text{and} \quad \underline{0} = \begin{bmatrix} 0 \\ 0 \\ \cdots \\ 0 \end{bmatrix} \quad (4.5)$$

Here z_i is either r_i or p_i . These are given by (1.15) and (1.16), respectively. t_i is given by (1.17). Multiplying (4.2) by T^{-1} , the inverse of T , one obtains

$$(I + M)\underline{x} = \underline{c} \quad (4.6)$$

where I is the identity matrix, M is the matrix

$$M = \begin{bmatrix} \underline{m} & \underline{0} & \underline{0} & \cdots & \underline{0} \end{bmatrix} \quad (4.7)$$

with

$$\underline{m} = T^{-1} \underline{\ell} , \quad (4.8)$$

and \underline{c} is the vector

$$\underline{c} = T^{-1} \underline{y} . \quad (4.9)$$

Solving (4.6) for \underline{x} obtains

$$x_i = c_i - \frac{m_i c_1}{1+m_1} . \quad (4.10)$$

After \underline{m} and \underline{c} are obtained using the efficient Toeplitz matrix inversion routine, the solution vector \underline{x} is readily obtained from (4.10).

4.5 The Results

The integral equation (1.9) for the E-polarization half-plane current $\{I_E - I_{PO}\}(z')$ is solved here by the method of moments using the almost-Toeplitz matrix inversion algorithm. Two expansion function sets are used. Results due to a hybrid expansion function set are compared with results due to an all-pulse expansion function set. The expansion function sets are described in Section 4.1.3. The standard approximation to which both will be compared is obtained by subtracting (1.5) from Equation (3.3) of Chapter 3. After careful study of this standard, the subsection half-width

H is chosen to be

$$H = 0.05. \quad (5.1)$$

This is small enough that

$$\frac{1}{\sqrt{H}} \approx \frac{e^{iH}}{\sqrt{H}}, \quad (5.2)$$

so that the edge expansion function closely approximates the actual current over its range of applicability. The diminishing accuracy of the imaginary part of (3.3) for arguments greater than 20 requires the upper limit of integration to be about 20. For a total of 200 subsections, this upper limit becomes 19.95. A total of 200 subsections are used for both the hybrid and the all-pulse expansion function sets. For each of these sets, computations are carried out for the four angles of incidence $\theta = 45^\circ$, 90° , 135° , and 180° .

4.5.1 Accuracy of the Moment Method Results

The solution vectors for the hybrid expansion are plotted on top of the standard in Figures 4.3 through 4.6 for the angles of incidence $\theta = 45^\circ$, 90° , 135° , and 180° , respectively. The standard is computed using the Chebyshev polynomial expansion for the Fresnel integral given by Luke (1969, Volume II, Table 24, pp. 328-329). Agreement between the hybrid expansion moment method solution and the standard is generally excellent. Difficulties do occur, however, around $kz = 20$ at least to some degree for all angles of incidence. Comparison of results for truncation points of 15 and 20 shows that the same behavior is exhibited around 15 for the former case as is exhibited around 20 for the latter. Therefore, it seems valid to say

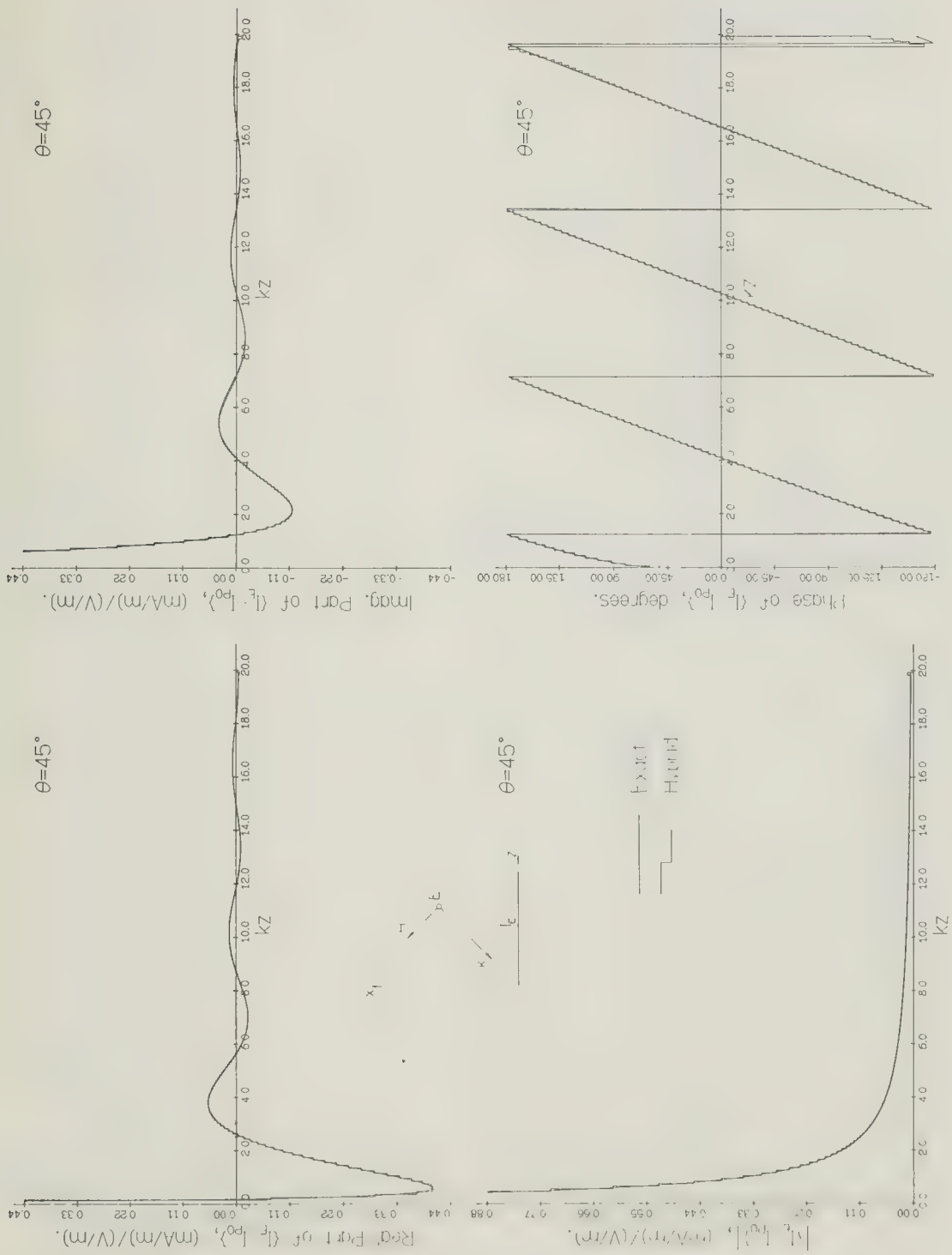


Figure 4.3. Comparison of the Exact with the Hybrid Expansion Moment Method Solution for $\theta = 45^\circ$.

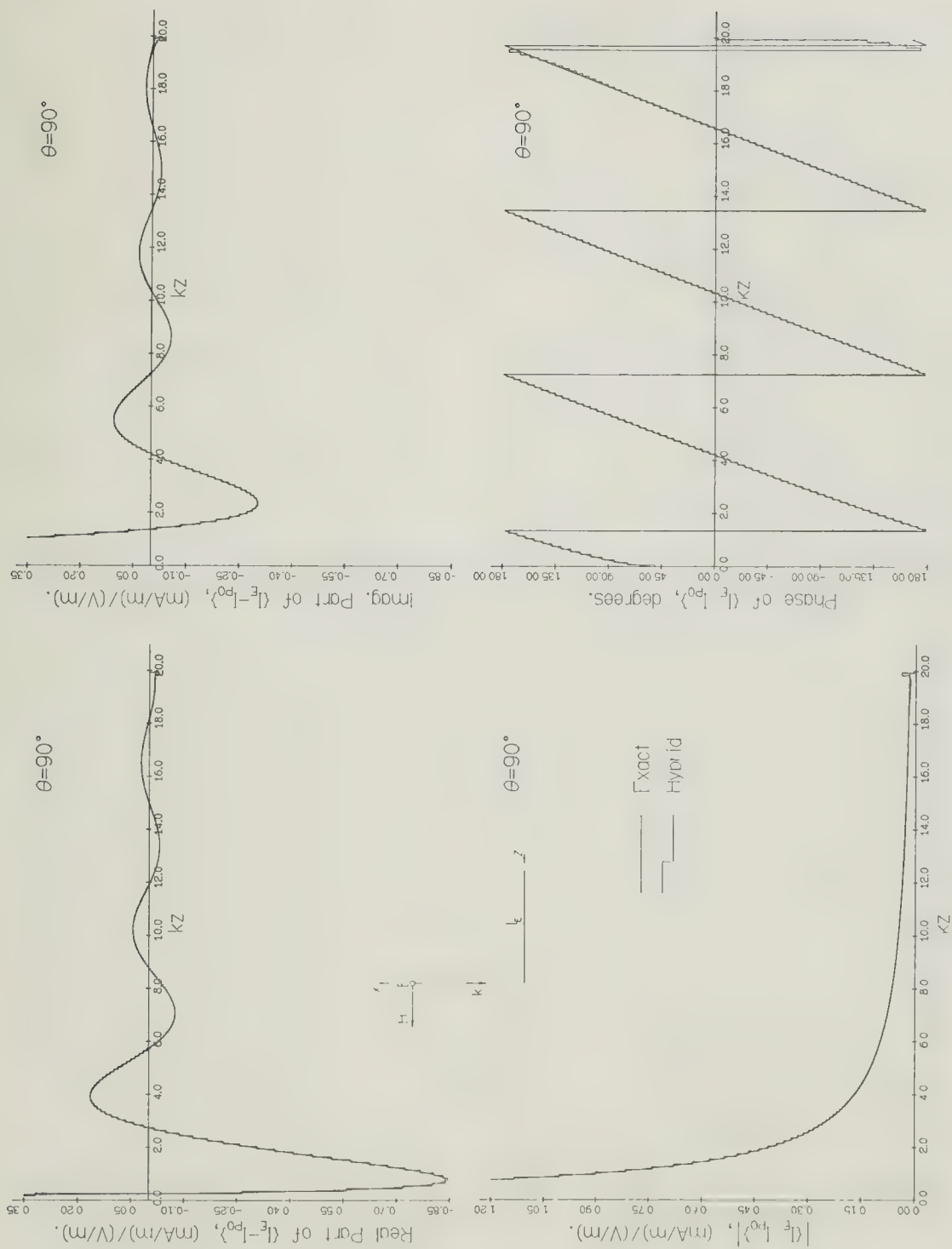


Figure 4.4. Comparison of the Exact with the Hybrid Expansion Moment Method Solution for $\theta = 90^\circ$.

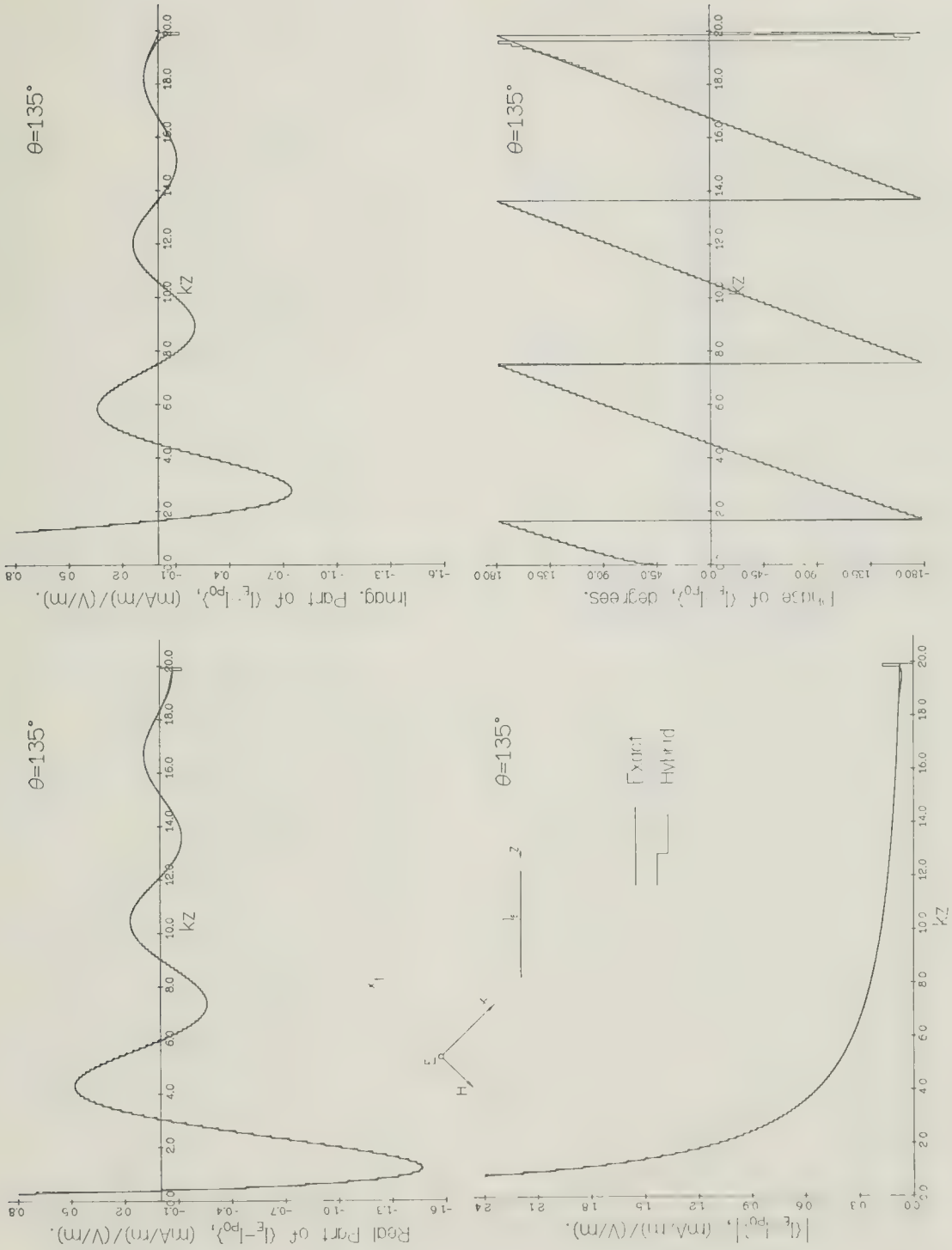


Figure 4.5. Comparison of the Exact with the Hybrid Expansion Moment Method Solution for $\theta = 135^\circ$.

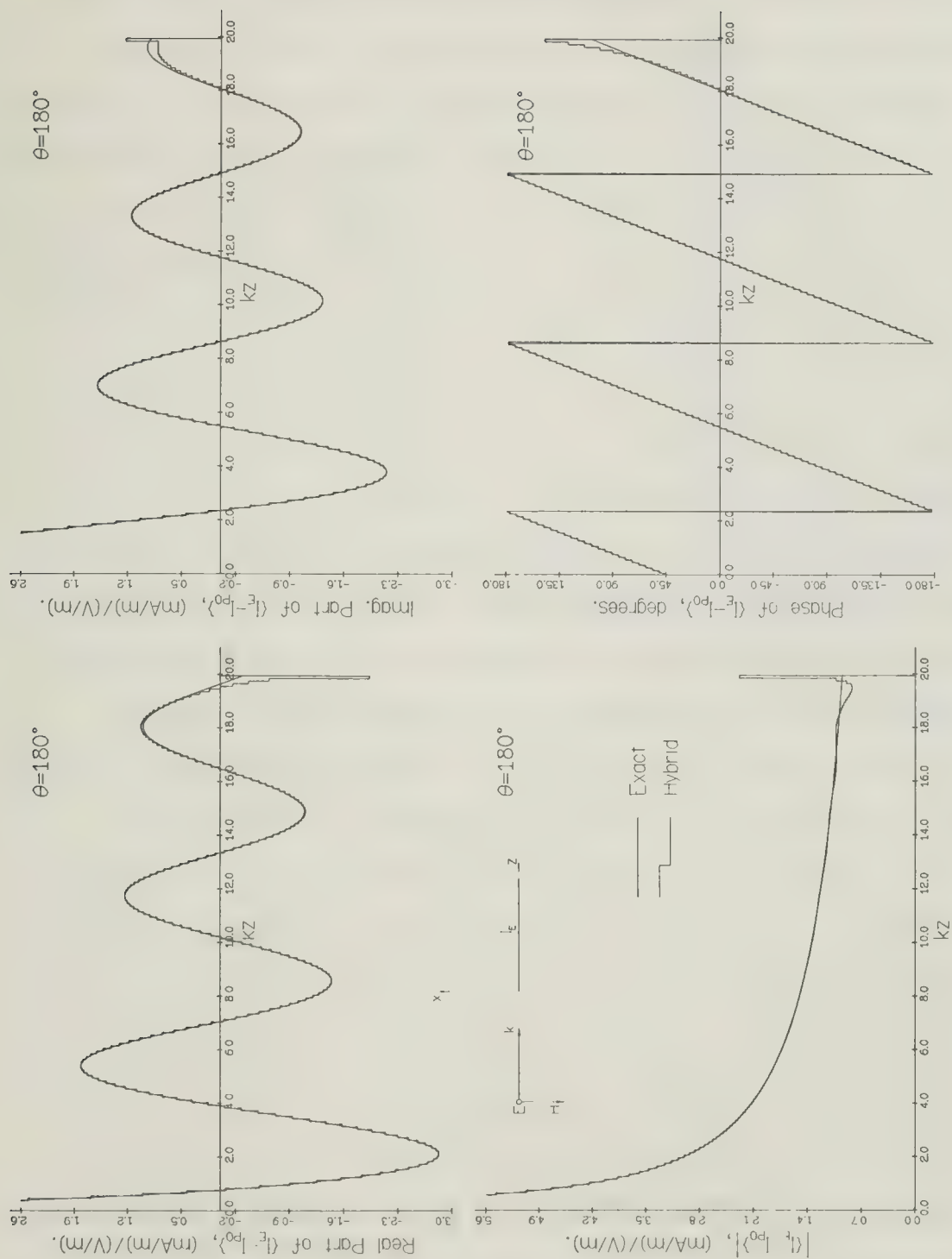


Figure 4.6. Comparison of the Exact with the Hybrid Expansion Moment Method Solution for $\theta = 180^\circ$.

that the inaccuracies around 20 in these figures are due to the truncation of the integral at 20. The results for the all-pulse expansion function set away from the edge are similar to those for the hybrid expansion. The hybrid expansion is much better than the all-pulse expansion for points close to the edge. Figures 4.7 and 4.8 emphasize the behavior of the two approximations near the edge for $\theta = 45^\circ$ and 180° , respectively. For both angles of incidence, the solution vector for the hybrid expansion is a better approximation to the standard than that for the all-pulse expansion. It is obvious that the inverse square root expansion function is a better approximation to the standard than is the edge pulse expansion function. It is not clear whether the height of this edge pulse has any significance. Relations between the all-pulse expansion solution and the hybrid expansion solution for the first two elements are derived in Section 4.5.2.

The explicit edge behavior of the solutions are compared to the standard in Figures 4.9 and 4.10 for $\theta = 45^\circ$ and 180° , respectively. For $\theta = 45^\circ$ the agreement of the hybrid expansion solution with the standard is acceptable. For $\theta = 180^\circ$ it is excellent. This is because for $\theta = 180^\circ$ the Fresnel integral term in (3.3) of Chapter 3 drops out. Table 4.2 gives the accuracy of the edge coefficients for all four angles of incidence. The accuracy of the real part for $\theta = 45^\circ$ is quite low because, as Figure 4.9 shows, the moment method attempts to fit the standard over the subsection width in some average sense. The low accuracy is also due to the fact that the standard is computed at the edge, while the numerical solution is some type of fit over the subsection width. This makes meaningful comparisons difficult, but this table does show relevant trends in the accuracy of the fit.

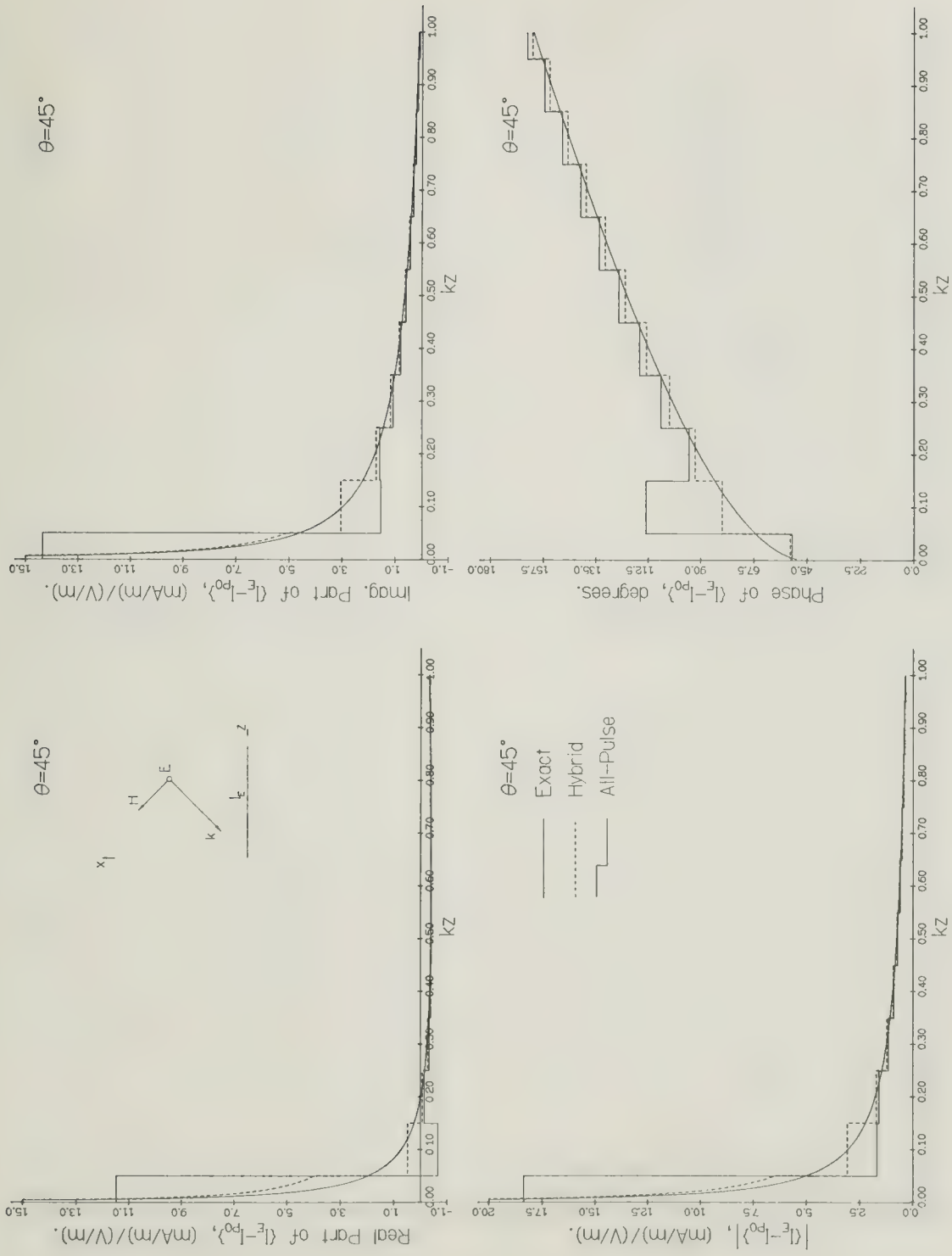


Figure 4.7. Comparison of the Exact with the Hybrid Expansion Solution and the All-Pulse Expansion Solution for the First Eleven Subsections and $\theta = 45^\circ$

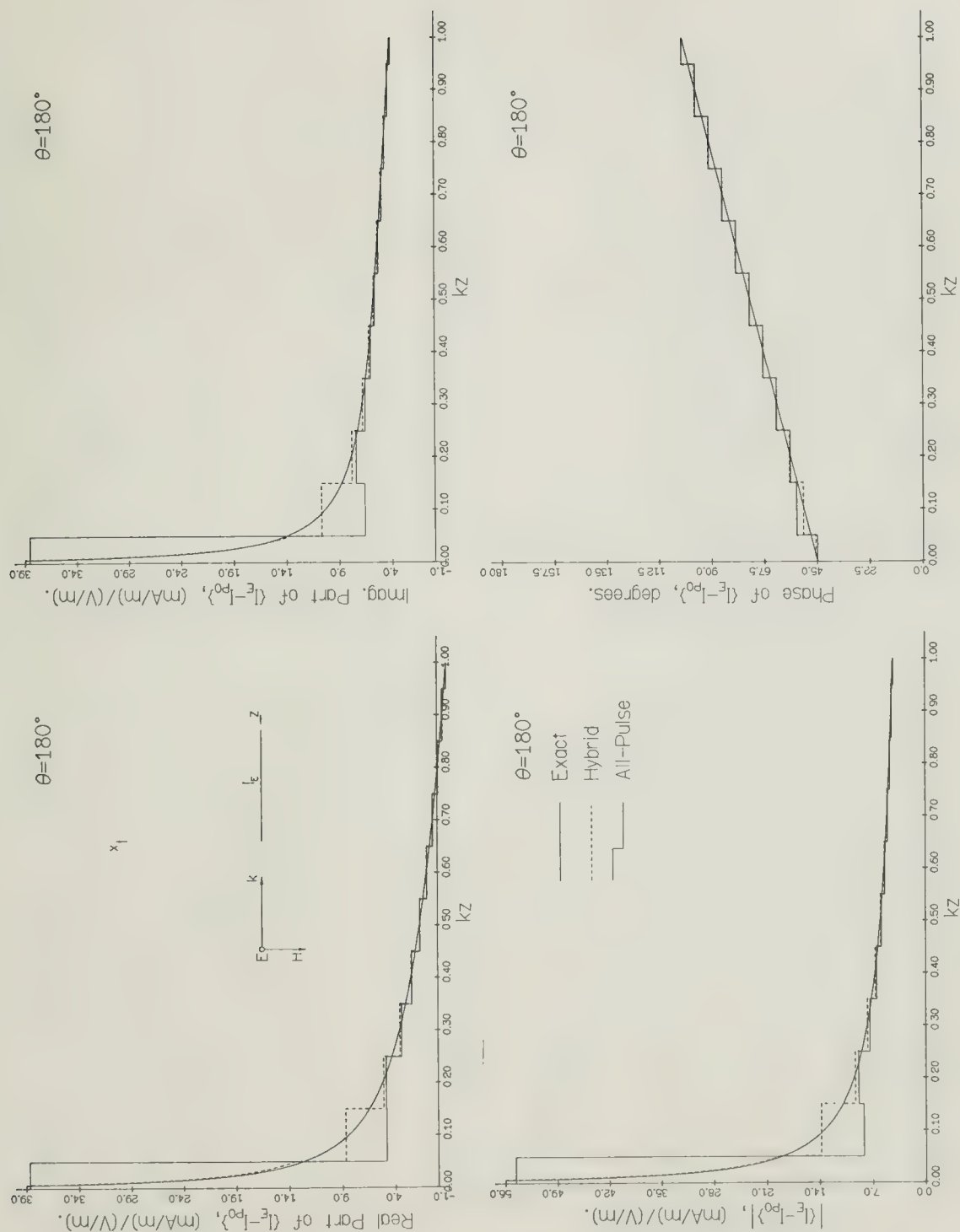


Figure 4.8. Comparison of the Exact with the Hybrid Expansion Solution and the All-Pulse Expansion Solution for the First Eleven Subsections and $\theta = 180^\circ$.

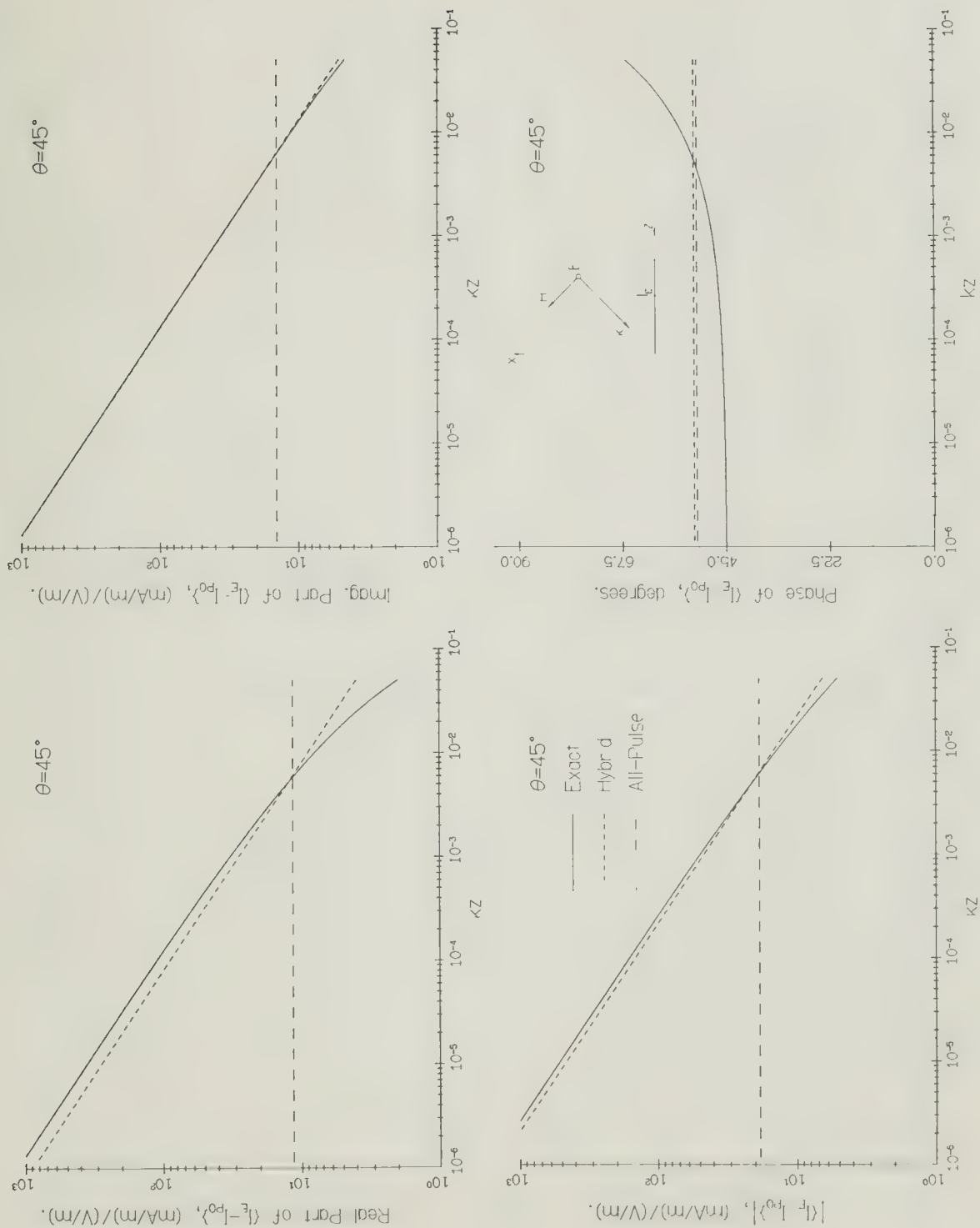


Figure 4.9. Comparison of the Exact with the Hybrid Expansion Solution and the All-Pulse Expansion Solution for $\theta = 45^\circ$ and the Edge Subsection.

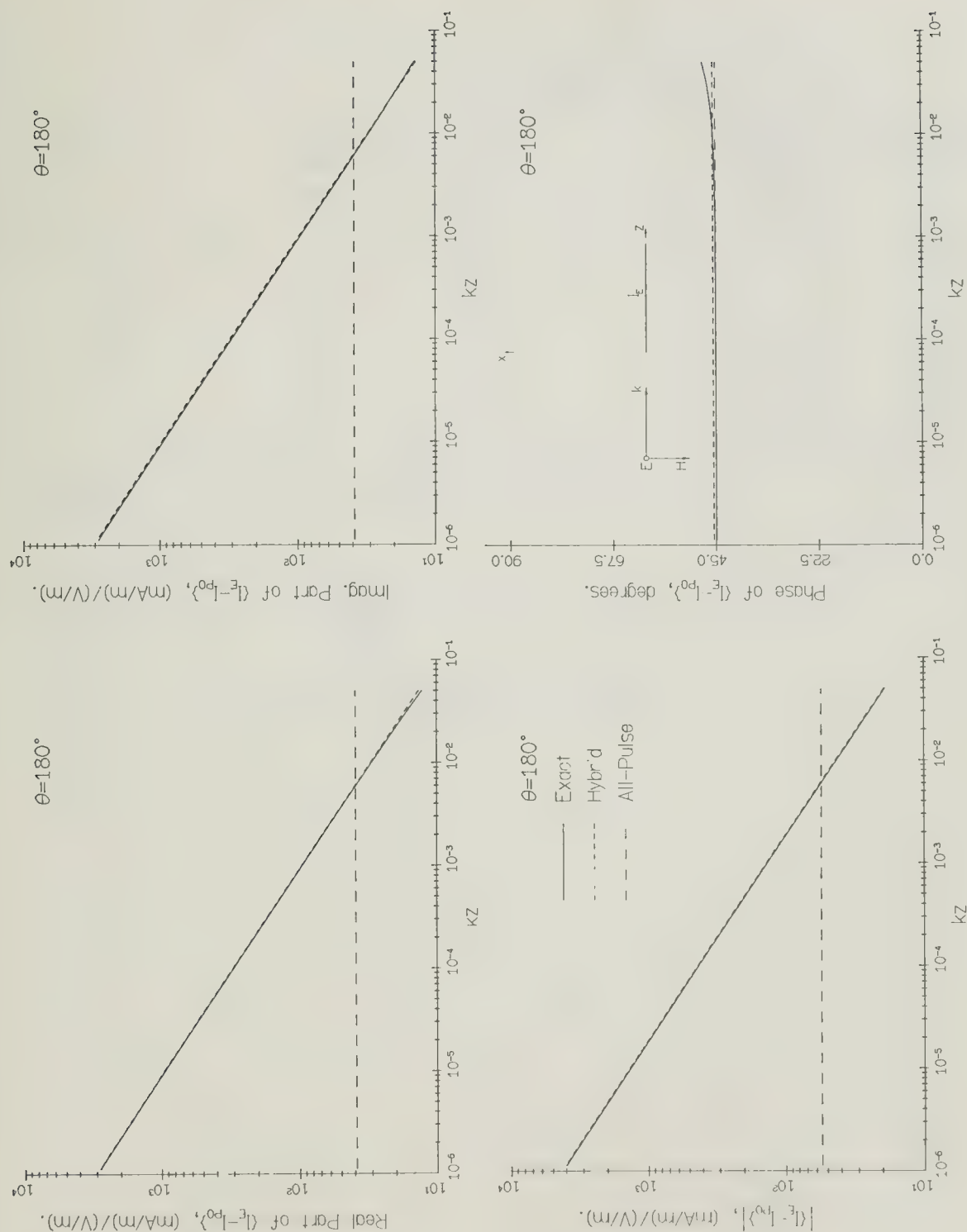


Figure 4.10. Comparison of the Exact with the Hybrid Expansion Solution and the All-Pulse Expansion Solution for $\theta = 180^\circ$ and the Edge Subsection.

Table 4.2

Accuracy of the Inverse Square Root Expansion Function
Coefficient

	Digits of Accuracy		Decimal Offset Factor	
	Real	Imag.	Real	Imag.
45°	0.7	2.1	0.4	0.4
90°	0.8	2.4	0.1	0.1
135°	1.0	1.8	-0.02	-0.02
180°	2.3	1.6	-0.05	-0.05

Notes: 1. Standard is computed at the edge and is

$$\frac{2 \sin \frac{\theta}{2}}{Z_0 \sqrt{\pi}} (1 + i) .$$

2. Subsection half-width H is 0.05.

The relative accuracies of the moment method solutions are compared to the standard for the hybrid expansion and for the all-pulse expansion in Tables 4.3 and 4.4, respectively. Numbers for the case of normal incidence are shown, but similar numerical trends appear for the other angles of incidence as well. The relative error is found at each match point except the first by comparing the moment method solution with the standard evaluated at the subsection midpoint. At some points the error is found to be very large. With the standard very small and the moment method solution several orders of magnitude larger, but still near zero, the relative error is quite large. This often occurs around zero crossing points because the moment method does not give answers as close to zero as the standard does. The average relative error is computed excluding errors greater than 15% for the top half of each table and excluding errors greater than 1% for the bottom half. The 15% and 1% figures correspond to 0.8 digits and 2.0 digits of accuracy, respectively. The term "Digits of Accuracy" is explained in Appendix A. With proper exclusions, the average relative error over each range given is found and the digits of accuracy figure given is $-\log_{10}$ of this. Also given (preceded by a slash) is the total number of points included in taking the average. Four ranges of subsections for averaging are used. The accuracy of the moment method solution in the neighborhood of the edge is checked over subsections 2 through 6. Figures are also given for subsection ranges 2 through 150, 151 through 200, and 2 through 200. These figures show the effect of truncation of the infinite integral. Over the range 151 through 200, the accuracy of the hybrid expansion solution and that of the all-pulse expansion solution are very

Table 4.3

Average Digits of Accuracy for the Hybrid Expansion
Solution Over Several Ranges

Range of subsections for averaging	Total S.S.	Real	Imag.	Mag.	Phase
<u>Data with less than 0.8 digits of accuracy excluded in average</u>					
2 - 6	/5	1.2 /3	1.9 /5	2.1 /5	1.8 /5
2 - 150	/149	2.3 /145	2.1 /148	2.6 /149	2.4 /149
151 - 200	/50	1.4 /46	1.6 /42	1.6 /49	1.7 /45
2 - 200	/199	1.8 /191	1.9 /190	2.1 /198	2.1 /194
<u>Data with less than 2.0 digits of accuracy excluded in average</u>					
2 - 6	/5	--- /0	2.3 /3	2.6 /3	2.2 /3
2 - 150	/149	2.7 /130	2.4 /118	2.6 /147	2.7 /138
151 - 200	/50	2.2 /23	2.3 /15	2.3 /25	2.3 /21
2 - 200	/199	2.6 /153	2.4 /133	2.6 /172	2.6 /159

Notes: 1. $\theta = 90^\circ$, $H = 0.05$.

2. The number preceded by a slash is the number of conforming data points included in the average.

3. The digits of accuracy figure used here is $-\log_{10}$ (average relative error).

4. 3 digits = 0.1%, 2 digits = 1%; 1 digit = 10%.

Table 4.4

Average Digits of Accuracy for the All-Pulse Expansion
Solution Over Several Ranges

Range of subsections for averaging	Total S.S.	Real	Imag.	Mag.	Phase
<u>Data with less than 0.8 digits of accuracy excluded in average</u>					
2 - 6	/5	1.0 /2	1.1 /4	1.2 /4	1.5 /4
2 - 150	/149	1.5 /134	1.5 /135	2.2 /148	1.7 /143
151 - 200	/50	1.4 /47	1.4 /40	1.6 /49	1.5 /43
2 - 200	/199	1.5 /181	1.4 /175	1.9 /197	1.6 /186
<u>Data with less than 2.0 digits of accuracy excluded in average</u>					
2 - 6	/5	--- /0	--- /0	--- /0	--- /0
2 - 150	/149	2.3 /40	2.3 /33	2.6 /130	2.1 /45
151 - 200	/50	2.3 /9	2.3 /10	2.3 /26	2.3 /8
2 - 200	/199	2.3 /49	2.3 /43	2.5 /156	2.1 /53

- Notes:
1. $\theta = 90^\circ$, $H = 0.05$.
 2. The number preceded by a slash is the number of conforming data points included in the average.
 3. The digits of accuracy figure used here is $-\log_{10}$ (average relative error)
 4. 3 digits = 0.1%; 2 digits = 1%; 1 digit = 10%.

close to each other, while over the range 2 through 150 they are somewhat different. This seems to indicate that truncation most seriously limits the accuracy of those elements in its vicinity and allows us to say that the truncation has negligible effect over subsections 2 through 150.

Comparison of the results over the range 2 through 150 shows that the answers for the hybrid expansion are much better than those for the all-pulse expansion. Consider the bottom portion of each table where accuracies of less than two digits are excluded in the average. Although the figures for digits of accuracy appear to be comparable, the true story is told by the number of terms included in the respective averages. For the hybrid expansion, 130, 118, 147, and 138 points are included out of a possible total in each case of 149 while for the all-pulse expansion, only 40, 33, 130, and 45 points are included for the real part, imaginary part, magnitude and phase, respectively. Note that the magnitude of the all-pulse expansion is accurate to nearly the same degree as is that of the hybrid expansion. Inaccuracies in the phase for the all-pulse expansion seems to spoil it.

The accuracy of the hybrid expansion is much better in the vicinity of the edge than is the all-pulse expansion as the numbers for the range 2 through 6 show. This is consistent with conclusions drawn from visual study of Figures 4.7 and 4.8.

4.5.2 The Relation Between the Hybrid Expansion Solution and the All-Pulse Expansion Solution

It is often asked, "What is the significance of the value of the solution for the edge pulse in the all-pulse expansion and how does it relate

to the value for the hybrid expansion?" The answer to this question is discussed here.

The matrix equation for the hybrid expansion is

$$A^r \underline{x}^r = \underline{y} \quad (5.3)$$

and that for the all-pulse expansion is

$$A^p \underline{x}^p = \underline{y}. \quad (5.4)$$

A^r and A^p are the matrices given by (1.14). \underline{x}^r and \underline{x}^p are the solution vectors for each expansion and \underline{y} is the right-hand side common to both equations. Subtracting (5.3) from (5.4), one obtains

$$A^r \underline{x}^r = A^p \underline{x}^p \quad (5.5)$$

$$\text{or} \quad (R + T_L) \underline{x}^r = (P + T_L) \underline{x}^p \quad (5.6)$$

$$\text{where} \quad R = \begin{bmatrix} \underline{r} & \underline{0} & \underline{0} & \cdots & \underline{0} \end{bmatrix} \quad (5.7)$$

$$P = \begin{bmatrix} \underline{p} & \underline{0} & \underline{0} & \cdots & \underline{0} \end{bmatrix} \quad (5.8)$$

and

$$T_L = T - \begin{bmatrix} \underline{t} & \underline{0} & \underline{0} & \cdots & \underline{0} \end{bmatrix}. \quad (5.9)$$

Here T is the Toeplitz matrix of (4.3) and \underline{t} is the first column of this matrix. \underline{r} and \underline{p} correspond to the first column of A^r and A^p as given by (1.14), respectively. After multiplying by T^{-1} and simplifying, Equation (5.6) becomes

$$(T^{-1}R + I_L) \underline{x}^r = (T^{-1}P + I_L) \underline{x}^p \quad (5.10)$$

where I_L is the identity matrix I except that the first element in the first row is zero instead of one. Solving for \underline{x}^r yields

$$x_1^r = \frac{(T^{-1}\underline{p})_1}{(T^{-1}\underline{r})_1} x_1^p \quad (5.11)$$

and

$$x_j^r = x_j^p + \left[(T^{-1}\underline{p})_j - \frac{(T^{-1}\underline{p})_1}{(T^{-1}\underline{r})_1} (T^{-1}\underline{r})_j \right] x_1^p, \quad j > 1. \quad (5.12)$$

Here the notation $(T^{-1}\underline{w})_n$ represents the n^{th} element in the column vector $T^{-1}\underline{w}$.

If $(T^{-1}\underline{p})_1$, $(T^{-1}\underline{r})_1$, and x_1^p are known, then the first element in the hybrid expansion solution, x_1^r , may be found from (5.11). Similarly, the rest of the elements in the hybrid expansion solution may be found from the elements of the all-pulse expansion solution by using (5.12).

Figure 4.11 gives plots of the results near the edge for $\theta = 135^\circ$. Identical plots, except for $\theta = 45^\circ$ and 180° , are given in Figures 4.9 and 4.10. It is interesting to note that all three curves cross at about the same point in these figures. It is not known if there is some simple explanation for this. The crossing point in these figures is located at about $\sqrt{H/8}$ where H is the width of the edge subsection and is 0.05 in this case. This makes

$$x_1^r \approx \sqrt{H/8} x_1^p. \quad (5.13)$$

Hypothesizing that this relation holds for all H and experimenting with subsection size gives the results presented in Table 4.5. The accuracy of

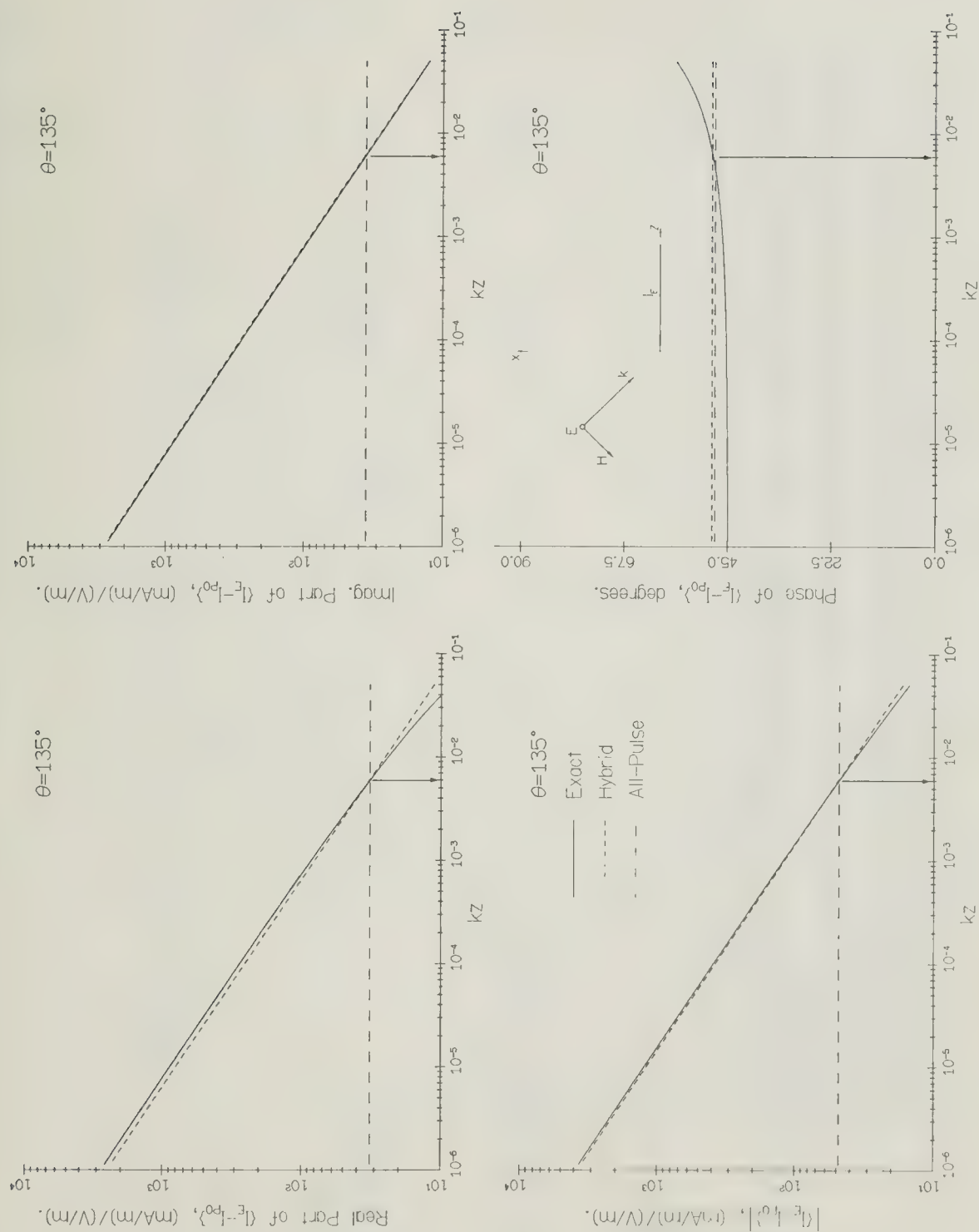


Figure 4.11. Comparison of the Exact with the Hybrid Expansion Solution and with the All-Pulse Expansion Solution for the Edge Subsection, $\theta = 135^\circ$, and $H = 0.05$.

Table 4.5

A Relation Between the Coefficient for the Inverse Square Root Basis Function and the Edge Coefficient for the All-Pulse Expansion

	H = 0.05		H = 0.1		H = 0.4	
	Real	Imag.	Real	Imag.	Real	Imag.
Hybrid expansion coefficient x_1^r	0.9416	1.0593	0.8912	1.0596	0.7034	1.0386
All-pulse expansion coefficient times $\sqrt{H/8} = \sqrt{H/8} x_1^p$	0.9573	1.0553	0.9174	1.0457	0.7872	0.9725
Number of matching digits	1.8	2.4	1.5	1.9	0.9	1.2

- Notes:
1. The factor $\sqrt{H/8}$ was obtained experimentally.
 2. Results shown are for $\theta = 135^\circ$, but numerical trends are the same for all angles of incidence.
 3. The number of matching digits is calculated using the hybrid expansion coefficient as the standard.
 4. For exact agreement at the edge, the above coefficients should be $1.0425 (1 + i)$.
 5. The above coefficients must be divided by $Z_0 = 376.731\Omega$ to correspond to the text.

the coefficient for the inverse square root edge expansion function is compared with $\sqrt{H/8}$ times the coefficient of the edge pulse in the all-pulse expansion. For values of H of 0.05, 0.1, and 0.4, the relative error in making the approximation of (5.13) is about 1%, 3%, and 10%, respectively. For many purposes, and especially for small subsection size, use of (5.13) proves to be an adequate approximation to (5.11).

Study of the numerical results and of Figures 4.7 and 4.8 indicates that a correction to the all-pulse solution for the second subsection may also be necessary, but that a correction is probably not needed for the other subsections. Explicitly writing (5.12) for the second subsection gives

$$x_2^r = x_2^p + \left[(T^{-1}_p)_2 - \frac{(T^{-1}_p)_1}{(T^{-1}_r)_1} (T^{-1}_r)_2 \right] x_1^p. \quad (5.14)$$

Hypothesizing that each of the terms in the bracket are simple functions of H , the subsection half-width, results in the empirical formulas

$$(T^{-1}_r)_1 = \frac{\pi^{\frac{1}{4}}}{H^{\frac{1}{2}}} (1 - i[H/3]), \quad (5.15)$$

$$(T^{-1}_r)_2 = -\frac{3^{\frac{1}{2}} \pi^{\frac{1}{4}}}{15 H^{\frac{1}{2}}} e^{i\sqrt{5/3} H}, \quad (5.16)$$

$$(T^{-1}_p)_1 = (5\pi - 1 + \sqrt{6/\pi} H^2)/10\pi - i(\pi/13) H^2 [1 - (\pi/13) H^2], \quad (5.17)$$

and

$$(T^{-1}_p)_2 = \frac{\sqrt{8\pi}}{100} [1 + (1.36H)^2] - i \frac{1.4\sqrt{\pi}}{100} H [1 - (1.8H)^2]. \quad (5.18)$$

These are obtained using standard curve fitting techniques applied at two points. The equations are written using constants and operations that are readily available on an HP-45 calculator. When the actual numbers are used, values computed at other points often match to 6 digits. Much better curve fits could certainly be given using six digit numerical values instead of the simple values given above.

The accuracies of the empirical formulas are compared to the actual numerical values in Tables 4.6 through 4.9 for four values of H . As these tables show, the agreement is very good.

The form of Equations (5.15) through (5.18) is not completely surprising. Study of the first row of T^{-1} shows that $\text{Im}(T^{-1})_{1i}$ is roughly proportional to $\frac{1}{H}$. The results of Appendix B show that the elements of \underline{r} and \underline{p} are proportional to \sqrt{H} and H , respectively, at least in some approximate sense. This makes the elements of $T^{-1}\underline{r}$ proportional to $H^{-\frac{1}{2}}$ and those of $T^{-1}\underline{p}$ to 1. That $(T^{-1}\underline{p})_1$ is close to 0.5 might be guessed by remembering that the range of integration for the elements of \underline{p} is H while that of \underline{t} is $2H$. Since $(T^{-1}\underline{t})_1 = 1$, it makes sense that $(T^{-1}\underline{p})_1 \approx 0.5$.

Substituting the empirical formulas in (5.11) and (5.14) gives

$$x_1^r = q_1(H) x_1^p \quad (5.19)$$

and

$$x_2^r = x_2^p + q_2(H) x_1^p \quad (5.20)$$

where

$$q_1(H) = \frac{(5\pi - 1 + \sqrt{6/\pi} H^2)/10\pi - i(\pi/13)^2 H [1 - \pi(\pi/13)^2 H^2]}{\pi^{\frac{1}{4}}(1 - i[H/3])} H^{\frac{1}{2}} \quad (5.21)$$

Table 4.6

Comparison of the Empirical Formula for $(T^{-1}_{\underline{r}})_1$
with Numerical Results

H	Numerical value of $(T^{-1}_{\underline{r}})_1$	Number of matching decimal places		Number of matching digits	
		Real	Imag.	Real	Imag.
0.005	18.8263	2.8	2.8	4.1	1.4
	-i0.0328				
0.05	5.9527	2.9	3.7	3.7	2.7
	-i0.0990				
0.1	4.2091	3.0	3.6	3.6	2.7
	-i0.1401				
0.4	2.1033	2.8	3.5	3.1	2.9
	-i0.2810				

Empirical formula: $(T^{-1}_{\underline{r}})_1 = \frac{\pi^{1/4}}{H^{1/2}} (1 - i[H/3])$

- Notes: 1. The numerical value is used as the standard for the calculation of matching digits.
2. These numbers are approximately independent of matrix order for orders greater than ten.

Table 4.7

Comparison of the Empirical Formula for $(T^{-1}\underline{r})_2$
with Numerical Results

H	Numerical value of $(T^{-1}\underline{r})_2$	Number of matching decimal places		Number of matching digits	
		Real	Imag.	Real	Imag.
0.005	-2.1725	2.8	4.8	3.2	3.0
	-i0.0141				
0.05	-0.6853	3.1	2.7	3.0	1.3
	-i0.0421				
0.1	-0.4804	2.8	2.5	2.5	1.3
	-i0.0593				
0.4	-0.2009	2.0	1.9	1.3	0.9
	-i0.1068				

Empirical formula: $(T^{-1}\underline{r})_2 = -\frac{3^{1/2}\pi^{1/4}}{15 H^{1/2}} e^{i \sqrt{5/3} H}$

- Notes: 1. The numerical value is used as the standard for the calculation of matching digits.
2. These numbers are approximately independent of matrix order for orders greater than ten.

Table 4.8

Comparison of the Empirical Formula for $(T^{-1}_P)_1$
with Numerical Results

H	Numerical value of $(T^{-1}_P)_1$	Number of matching decimal places		Number of matching digits	
		Real	Imag.	Real	Imag.
0.005	0.468196	4.6	4.9	4.3	1.4
	-i0.000305				
0.05	0.468283	5.3	5.6	5.0	3.1
	-i0.002916				
0.1	0.468606	5.6	5.3	5.3	3.1
	-i0.005825				
0.4	0.475197	5.0	4.6	4.6	3.0
	-i0.022651				

Empirical formula: $(T^{-1}_P)_1 = (5\pi - 1 + \sqrt{6/\pi} H^2)/10\pi$

$$- i\left(\frac{\pi}{13}\right)^2 H [1 - \pi\left(\frac{\pi}{13}\right)^2 H^2]$$

- Notes: 1. The numerical value is used as the standard for the calculation of matching digits.
2. These numbers are approximately independent of matrix order for orders greater than ten.

Table 4.9

Comparison of the Empirical Formula for $(T^{-1}_P)_2$
with Numerical Results

H	Numerical value of $(T^{-1}_P)_2$	Number of matching decimal places		Number of matching digits	
		Real	Imag.	Real	Imag.
0.005	0.050147	4.9	5.2	3.6	1.3
	-i0.000131				
0.05	0.050370	5.3	5.8	4.0	2.8
	-i0.001232				
0.1	0.051065	5.3	5.6	4.0	3.0
	-i0.002404				
0.4	0.064024	3.0	4.9	1.8	2.6
	-i0.004793				

Empirical formula: $(T^{-1}_P)_2 = \frac{\sqrt{8\pi}}{100} [1 + (1.36H)^2] - i \frac{1.4\sqrt{\pi}}{100} H[1 - (1.8H)^2]$

- Notes: 1. The numerical value is used as the standard for the calculation of matching digits.
2. These numbers are approximately independent of matrix order for orders greater than ten.

and

$$q_2(H) = \frac{\sqrt{8\pi}}{100} [1 + (1.36H)^2] - i \frac{1.4\sqrt{\pi}}{100} H [1 - (1.8H)^2] \\ + q_1(H) \left(\frac{3^{\frac{1}{2}} \pi^{\frac{1}{4}}}{15 H^{\frac{1}{2}}} e^{i \sqrt{5/3} H} \right). \quad (5.22)$$

Table 4.10 compares the numerical results for x_1^r and x_2^r with $q_1(H)x_1^p$ and $x_2^p + q_2(H)x_1^p$, respectively. Comparisons are given for four subsection sizes. The error is generally less than 1% and in some cases is less than 0.1%. For most purposes, these formulas give answers that are more accurate than they need to be in light of the fact that the error introduced in using the moment method is often quite large.

The empirical formulas (5.15) through (5.18) are also useful for obtaining x_1^r , x_2^r , x_1^p , and x_2^p from x_1^t and x_2^t . \underline{x}^t is the solution of

$$T \underline{x}^t = \underline{y} \quad (5.23)$$

where T is the Toeplitz matrix in (4.3). Using the facts that $(T^{-1}\underline{t})_1 = 1$ and $(T^{-1}\underline{t})_2 = 0$, it may be shown that

$$x_1^r = x_1^t / (T^{-1}\underline{r})_1, \quad (5.24)$$

$$x_1^p = x_1^t / (t^{-1}\underline{p})_1, \quad (5.25)$$

$$x_2^r = x_2^t - [(T^{-1}\underline{r})_2 / (T^{-1}\underline{r})_1] x_1^t, \quad (5.26)$$

$$\text{and} \quad x_2^p = x_2^t - [(T^{-1}\underline{p})_2 / (T^{-1}\underline{p})_1] x_1^t. \quad (5.27)$$

Although these formulas look simpler than those relating \underline{x}^r and \underline{x}^p , the accuracy of the solution \underline{x}^t is less than that of \underline{x}^p which is less than that

Table 4.10

Comparison of the Values of the First Two Elements in the Solution Vector for the Hybrid Expansion with the Values Obtained Using the Corresponding Elements for the All-Pulse Expansion and the Empirical Formulas

H	Number of matching digits			
	x_1^r compared to $q_1(H)x_1^p$		x_2^r compared to $x_2^p + q_2(H)x_1^p$	
	Real	Imag.	Real	Imag.
0.005	1.8	1.9	2.4	2.5
0.05	3.6	3.7	3.0	3.1
0.1	3.6	3.7	2.5	2.7
0.4	3.6	3.0	2.3	1.5

Notes: 1. $\theta = 135^\circ$ for comparisons, but result does not depend on θ .

2. The numerical values of x_1^r and x_2^r are used as the standard for the calculation of matching digits.

of \underline{x}^r . For this reason, it is very desirable to use the almost-Toeplitz algorithm to obtain \underline{x}^p , at least, instead of the Toeplitz algorithm to obtain \underline{x}^t . If only \underline{x}^t is available, Table 4.11 gives the accuracy that would be obtained if (5.24) through (5.27) and the empirical formulas were used to modify the values of the first two elements. For the case given, the relative error is less than 0.1%.

If the right-hand side of the matrix equation (5.23) is peaked around the first element, then approximations to x_1^t may be easily obtained. The right-hand side of the integral equation, given by (3.1), is such a function (see Figure 4.2). Table 4.12 gives the values of the first few elements of T^{-1} along with the number of matching digits for various orders of matrices. The inverse is clearly peaked around the first element and rapidly decreases away from this element. If the right-hand side \underline{y} also decreases away from the first element, then because of rapid convergence properties it is acceptable to use only a few terms to evaluate $(T^{-1}\underline{y})_1$ instead of the full number of terms. Reasonable answers for $(T^{-1}\underline{y})_1$ are obtained for a matrix of order ten, and surprisingly good answers are obtained for matrix orders between ten and three.

Following the above argument, it can be seen that terms of the form $(T^{-1}\underline{r})_n$ or $(T^{-1}\underline{p})_n$, as given in (5.11) and (5.12), are approximately independent of the order of the matrix T , at least for the first few elements (small n). It is this property that allows the empirical formulas (5.15) through (5.18) to be given as functions of H only. The empirical formulas are approximately independent of matrix order as long as the matrix order is ten or more and two or three digit accuracy is sufficient.

Table 4.11

Comparison of the Values of the First Two Elements in
the Hybrid and All-Pulse Expansion Solution Vectors
with the Values Obtained Using the Corresponding
Elements in the Toeplitz Solution Vector

Comparison	Number of matching digits	
	Real	Imag.
$x_1^r : \frac{x_1^t}{(T^{-1}_r)_1}$	3.8	3.7
$x_1^p : \frac{x_1^t}{(T^{-1}_p)_1}$	4.0	4.6
$x_2^r : x_2^t - \frac{(T^{-1}_r)_2}{(T^{-1}_r)_1} x_1^t$	3.0	3.1
$x_2^p : x_2^t - \frac{(T^{-1}_p)_2}{(T^{-1}_p)_1} x_1^t$	3.4	4.3

Notes: 1. $H = 0.05$ and $\theta = 135^\circ$ for all comparisons. The empirical formulas are used to compute all T^{-1}_r and T^{-1}_p terms.

2. x_i^r : hybrid solution

x_i^p : all-pulse solution

x_i^t : Toeplitz solution

3. The numerical values of x_i^r and x_i^p are used as the standard for calculation of matching digits.

Table 4.12

Number of Matching Digits in the Magnitudes of Elements of T^{-1} as Matrix Order is Varied

Element	Number of matching digits				Numerical values of T-1 (200 order matrix)
	100	50	Order of matrix		
			20	10	6
t'_{11}	5.8	4.8	3.7	3.0	2.5
					5.80269 <u>/+ 87.135°</u>
t'_{12}	5.8	4.9	3.8	2.9	2.7
					3.32929 <u>/- 87.874°</u>
t'_{13}	5.0	4.3	3.2	2.1	2.4
					0.494128 <u>/- 78.493°</u>
t'_{14}	4.9	4.3	3.2	1.9	1.9
					0.320888 <u>/- 75.192°</u>
t'_{15}	4.8	4.4	3.8	1.7	1.1
					0.201240 <u>/- 69.240°</u>

Notes: 1. Subsection half-width H is 0.05 for all orders of matrices.

2. $t'_{1i} = (T^{-1})_{1i}$.

3. The t'_{1i} values for matrix order of 200 are used as the standard for the calculation of matching digits.

4.6 Conclusion

For the E-polarization, the CSF approach and the ordinary approach are virtually the same. In both cases, the same integral equation must be solved by the method of moments. A comparison of the moment method results for the induced current with the exact results shows that the moment method is reasonably accurate. It is also shown that the use of the hybrid expansion yields better accuracy than does the use of the all-pulse expansion. For many purposes, however, the all-pulse expansion solution will suffice as long as the values of the first two elements are corrected using the empirical formulas. The complete computer program for the E-polarization half-plane problem is given in Appendix D. The results of this chapter are used in the next chapter to generate results for the H-polarization by using the current source-function technique.

5. THE NUMERICAL SOLUTION OF THE HALF-PLANE PROBLEM BY THE CURRENT SOURCE-FUNCTION TECHNIQUE: H-POLARIZATION

The closed form solution of the half-plane problem with H-polarized incident field by the CSF technique is presented in Chapter 3. Numerical procedures for the application of the CSF technique to this same problem are described here. The numerical results for $\{I_E - I_{PO}\}$ that are described in the previous chapter are used to obtain numerical results for $\{I_H - I_{po}\}$, the H-polarization current minus the H-polarization physical optics current. Mayes (1972) and Prettie and Dudley (1974) have worked on the numerical solution of the problem of scattering of a plane wave from a cylindrical rod using the CSF technique. Some unresolved questions about their results further motivated the present work on the half-plane problem which has been discussed elsewhere by Hanson and Mayes (1975).

5.1 The Current Source-Function Technique Applied to the Half-Plane Problem

The configuration for the H-polarization half-plane problem with plane wave incidence is given in Figure 2.1(b). The CSF technique, as is described previously, is a two step process. In the application to the half-plane problem, the first step is to solve the integral equation

$$\text{Fp} \int_0^{\infty} u_H(z') H_0^{(1)}(k|z-z'|) dz' = \frac{4k}{Z_0} \sin\theta e^{-ikz \cos\theta}, \quad z > 0, \quad (1.1)$$

for $u_H(z')$. The second step is to find the current I_H from

$$I_H(z) = \int_0^{\infty} u_H(z') g(z, z') dz', \quad -\infty < z < \infty. \quad (1.2)$$

In the numerical work at hand, the solution for $\{I_E - I_{PO}\}$, given in the last chapter, is used to find I_H . This is necessary because the moment method results for the difference $\{I_E - I_{PO}\}$ are available directly.

5.1.1 The Physical Optics Current for the H-polarization, I_{po}

The physical configuration of the H-polarization physical optics problem is just that given by Figure 2.1(b) except that the conductor extends to infinity in all directions. Although the CSF technique does not require that a solution be found in terms of $\{I_H - I_{po}\}$, this difference is used because it is of the same form as the solution $\{I_E - I_{PO}\}$ for the E-polarization is. Following steps similar to those outlined in Section 4.1.1 for the E-polarization case, the H-polarization physical optics current becomes

$$I_{po} = \frac{2}{Z_0} e^{-ikz \cos\theta}. \quad (1.3)$$

Lower case "po" is always used to indicate the H-polarization physical optics current while upper case "PO" is always used for the E-polarization.

5.1.2 The Solution for u_H , the Current Source-Function, in Terms of $\{I_E - I_{PO}\}$

The rigorous solution for u_H , the H-polarization current source-function, is given in Chapter 3. Recall that u_H is a solution of the integral equation

$$Fp \int_0^{\infty} u_H(z') H_0^{(1)}(k|z-z'|) dz' = \frac{4k}{Z_0} \sin\theta e^{-ikz \cos\theta}, \quad z > 0, \quad (1.4)$$

where $u_H(z')$ satisfies the edge condition

$$u_H(z') = O(z'^{-\frac{3}{2}}) \quad \text{as } z' \rightarrow 0. \quad (1.5)$$

Also recall that the solution of this integral equation, given by (4.2) of Chapter 3, is made up of two parts. The first part is the one that reproduces the right-hand side. This part is simply the locally integrable solution to the integral equation and is

$$\begin{aligned} \sin\theta \, v(z') &= k^2 \sin\theta \, I_E^\theta(z') l_+(z') = \\ &= k^2 \sin\theta \{I_E^\theta - I_{PO}^\theta\}(z') l_+(z') + k^2 \sin\theta \, I_{PO}^\theta(z') l_+(z'). \end{aligned} \quad (1.6)$$

The second equality is obtained by adding and subtracting $k^2 \sin\theta \, I_{PO}^\theta l_+$ in the first equality.

The other part of the solution to the integral equation (1.4) is the part that does not violate the edge condition (1.5) and satisfies the homogeneous finite part integral equation

$$\text{Fp} \int_0^\infty w(z') H_0^{(1)}(k|z-z'|) dz' = 0, \quad z > 0. \quad (1.7)$$

A solution to this homogeneous equation may be obtained by differentiating the integral equation [see Section 3.3.3] for I_E for normal incidence which, upon adding and subtracting $I_{PO}^\perp l_+$ in the unknown, becomes

$$k^2 \int_{-\infty}^\infty \left\{ \{I_E^\perp - I_{PO}^\perp\} l_+(z') + I_{PO}^\perp l_+(z') \right\} H_0^{(1)}(k|z-z'|) dz' = \frac{4k}{Z_0}, \quad z > 0, \quad (1.8)$$

where the superscript \perp indicates the quantity is evaluated for $\theta = 90^\circ$. Differentiating both sides of this equation with respect to z and using

(4.12) of Chapter 2 gives

$$k^2 \int_{-\infty}^{\infty} \left\{ \{I_E^\perp - I_{PO}^\perp\} 1_+(z') + I_{PO}^\perp 1_+(z') \right\} \frac{\partial}{\partial z'} H_0^{(1)}(k|z-z'|) dz' = 0, \quad z > 0, \quad (1.9)$$

Integrating by parts and utilizing the properties of the finite part yields

$$\begin{aligned} k^2 \int_0^{\infty} \left\{ \{I_E^\perp - I_{PO}^\perp\} + I_{PO}^\perp \right\} \frac{\partial}{\partial z'} H_0^{(1)}(k|z-z'|) dz' &= \\ &= -k^2 I_{PO}(0) H_0^{(1)}(k|z|) - k^2 \text{Fp} \int_0^{\infty} \left\{ \frac{\partial}{\partial z'} \{I_E^\perp - I_{PO}^\perp\} + \frac{\partial I_{PO}^\perp}{\partial z'} \right\} H_0^{(1)}(k|z-z'|) dz' \\ &= -k^2 \text{Fp} \int_{-\infty}^{\infty} \left\{ \left\{ \frac{\partial}{\partial z'} \{I_E^\perp - I_{PO}^\perp\} + \frac{\partial I_{PO}^\perp}{\partial z'} \right\} 1_+(z') + I_{PO}^\perp \delta(z') \right\} H_0^{(1)}(k|z-z'|) dz' \end{aligned} \quad (1.10)$$

Thus,

$$w(z') = k^2 \text{Pf} \left\{ \frac{\partial}{\partial z'} \{I_E^\perp - I_{PO}^\perp\} \right\} 1_+(z') + k^2 I_{PO}^\perp \delta(z') \quad (1.11)$$

since the $\partial I_{PO}^\perp / \partial z'$ term vanishes. This is a solution of (1.7) which satisfies the edge condition. A complete solution of (1.4) is then

$$\begin{aligned} u_H(z) &= A w(z) + \sin\theta v(z) = \\ &= k^2 A \text{Pf} \left\{ \left(\frac{\partial}{\partial z} \{I_E^\perp - I_{PO}^\perp\} \right) 1_+(z) \right\} + k^2 A I_{PO}^\perp \delta(z) \\ &\quad + k^2 \sin\theta \{I_E^\theta - I_{PO}^\theta\} 1_+(z) + k^2 \sin\theta I_{PO}^\theta 1_+(z) \end{aligned} \quad (1.12)$$

where A is a constant.

It is interesting to note the behavior of u_H as the argument approaches infinity. The first three terms in (1.12) vanish leaving

$$u_H(z) \sim k^2 \sin\theta I_{PO}^\theta(z) \quad \text{as } z \rightarrow \infty. \quad (1.13)$$

This makes

$$u_{po} = \frac{2}{Z_0} k^2 \sin^2\theta e^{-ikz \cos\theta}. \quad (1.14)$$

Substituting the expression (1.3) for I_{po} in the equation for u_H ,

$$u_H = \frac{d^2 I_H}{dz^2} + k^2 I_H, \quad \text{gives}$$

$$u_{po} = \frac{2k^2}{Z_0} \sin^2\theta e^{-ikz \cos\theta}. \quad (1.15)$$

It is reassuring to obtain the same result in each of these two ways.

The solution for u_H must satisfy the consistency condition in order to obtain a unique solution for I_H . From Equation (4.13) of Chapter 3, the consistency condition simply states that

$$\int_{-\infty}^{\infty} u_H(z') e^{ikz'} dz' = 0. \quad (1.16)$$

Substituting the expression (1.12) in the above equation and solving for ikA gives

$$ikA = \frac{i \frac{4}{Z_0} \cos^2(\theta/2) + k \sin\theta \int_0^{\infty} \{I_E^\theta - I_{PO}^\theta\} e^{ikz} dz}{i \frac{2}{Z_0} + k \int_0^{\infty} \{I_E^1 - I_{PO}^1\} e^{ikz} dz}. \quad (1.17)$$

This is the value that must be used for A in (1.12). For normal incidence, $ikA = 1$. This agrees with (4.19) of Chapter 3.

5.1.3 The Solution for $\{I_H - I_{PO}\}$ in Terms of $\{I_E - I_{PO}\}$

The closed form solution for I_H is given by (5.14) in Chapter 3.

It is shown that

$$I_H(z) = \int_0^{\infty} u_H(z') g(z, z') dz', \quad -\infty < z < \infty, \quad (1.18)$$

where

$$g(z, z') = \frac{1}{2ik} \left(e^{ik|z-z'|} - e^{ik(z+z')} \right). \quad (1.19)$$

Substituting (1.12) into (1.18) yields

$$\begin{aligned} I_H = & k^2 A \int_{-\infty}^{\infty} \text{Pf} \left(\frac{\partial}{\partial z'} \{I_E^{\perp} - I_{PO}^{\perp}\} \right) l_+(z') g(z, z') dz' \\ & + k^2 A I_{PO}^{\perp}(0) \int_{-\infty}^{\infty} \delta(z') g(z, z') dz' + k^2 \sin\theta \int_0^{\infty} \{I_E^{\theta} - I_{PO}^{\theta}\} g(z, z') dz' \\ & + k^2 \sin\theta \int_0^{\infty} I_{PO}^{\theta} g(z, z') dz'. \end{aligned} \quad (1.20)$$

By integrating by parts, the first integral above becomes

$$\int_{-\infty}^{\infty} \text{Pf} \left(\frac{\partial}{\partial z'} \{I_E^{\perp} - I_{PO}^{\perp}\} \right) l_+(z') g(z, z') dz' = - \int_0^{\infty} \{I_E^{\perp} - I_{PO}^{\perp}\} \frac{\partial}{\partial z'} g(z, z') dz'. \quad (1.21)$$

The second integral is zero since $g(z, 0) = 0$. The third integral remains unchanged. The last integral becomes

$$\int_0^{\infty} I_{PO}^{\theta}(z') g(z, z') dz' = \frac{2}{z_0 \sin\theta k^2} \left(e^{-ikz \cos\theta} - e^{ikz} \right). \quad (1.22)$$

after using (1.5) of Chapter 4. These equalities are valid for $z > 0$ only. Equation (1.20) becomes

$$I_H = -k^2 A \int_0^\infty \{I_E^\perp - I_{PO}^\perp\} \frac{\partial}{\partial z'} g(z, z') dz' + k^2 \sin\theta \int_0^\infty \{I_E^\theta - I_{PO}^\theta\} g(z, z') dz' + \frac{2}{z_0} (e^{-ikz} \cos\theta - e^{ikz}). \quad (1.23)$$

The first part of the third term in this equation is just I_{po} . Taking this term to the other side of the equation and letting $h(z, z') = \frac{\partial}{\partial z'} g(z, z')$ gives

$$\{I_H^\theta - I_{po}^\theta\} = -k^2 A \int_0^\infty \{I_E^\perp - I_{PO}^\perp\} h(z, z') dz' + k^2 \sin\theta \int_0^\infty \{I_E^\theta - I_{PO}^\theta\} g(z, z') dz' - \frac{2}{z_0} e^{ikz}, \quad (1.24)$$

where A is the constant given by (1.17). Each of the integrals on the right-hand side of (1.24) is approximated using the numerical results of Chapter 4 for $\{I_E - I_{PO}\}$ weighted with either $h(z, z')$ or $g(z, z')$. These numerical integrations are detailed in the next section.

5.2 The Numerical Evaluation of $\{I_H - I_{po}\}$

The moment method numerical results of Chapter 4 for $\{I_E - I_{PO}\}$ are used here to obtain the numerical results for $\{I_H - I_{po}\}$ by applying (1.24). Two integrals have to be evaluated numerically. From (1.24), these are

$$k^2 \int_0^L \{I_E^\perp - I_{PO}^\perp\} h(z, z') dz' \quad (2.1)$$

and

$$k^2 \int_0^L \{I_E^\theta - I_{PO}^\theta\} g(z, z') dz' \quad (2.2)$$

where the upper limit is set to $L = 19.95/k$ [see (1.9) of Chapter 4]

instead of infinity because the integral equation for $\{I_E^\theta - I_{PO}^\theta\}$ is

truncated at $z = L$. Making the change of variable $z' = y'/k$ and letting $y = kz$ in (2.1) and (2.2), one obtains

$$k \int_0^{kL} \{I_E^I - I_{PO}^I\} h(y, y') dy' \quad (2.3)$$

$$k \int_0^{kL} \{I_E^\theta - I_{PO}^\theta\} g(y, y') dy' \quad (2.4)$$

where

$$g(y, y') = \frac{1}{2ik} (e^{i|y-y'|} - e^{i(y+y')}) , \quad (2.5)$$

and

$$h(y, y') = \frac{\partial}{\partial z'} g(z, z') = k \frac{\partial}{\partial y'} g(y, y') . \quad (2.6)$$

It is convenient to break $h(y, y')$ and $g(y, y')$ into two parts, one for $y' < y$ and the other for $y' > y$. These expressions become

$$g(y, y') = \begin{cases} g_{<y}(y, y') & y' < y \\ g_{>y}(y, y') & y' > y \end{cases} \quad (2.7)$$

and

$$h(y, y') = k \frac{\partial}{\partial y'} g(y, y') = \begin{cases} h_{<y}(y, y') & y' < y \\ h_{>y}(y, y') & y' > y \end{cases} \quad (2.8)$$

where

$$k g_{<y}(y, y') = -e^{iy} \sin(y'), \quad (2.9)$$

$$k g_{>y}(y, y') = -e^{iy'} \sin(y), \quad (2.10)$$

$$h_{<y}(y, y') = -e^{iy} \cos(y'), \quad (2.11)$$

and

$$h_{>y}(y, y') = -i e^{iy'} \sin(y). \quad (2.12)$$

This notation is used throughout this section. In order to simplify the numerical evaluation of the integrals of (2.1) and (2.2) when a value of y is given, it is desirable to determine the number of the subsection that y ($=kz$) is in. If this number is called K , it may be found from the equation

$$K = \left[\frac{(y/H) + 1}{2} \right] + 1 \quad (2.13)$$

where the notation $[x]$ represents the integer portion of x . Expressions for the integrals (2.3) and (2.4) for both the hybrid expansion and the all-pulse expansion are obtained.

The hybrid expansion for $\{I_E - I_{PO}\}$, shown in Figure 4.1(a), is

$$\{I_E - I_{PO}\}(y) = \begin{cases} x_1^r y^{-\frac{1}{2}} & 0 < y < H \\ x_j^r & D_j^{-H} < y < D_j^{+H} \quad N \geq j \geq 2. \end{cases} \quad (2.14)$$

The all-pulse expansion for $\{I_E - I_{PO}\}$, shown in Figure 4.1(b), is

$$\{I_E - I_{PO}\}(y) = \begin{cases} x_1^p & 0 < y < H \\ x_j^p & D_j^{-H} < y < D_j^{+H}, \quad N \geq j \geq 2. \end{cases} \quad (2.15)$$

where the x_j 's in both expressions are constants and

$$D_j = 2(j-1)H \quad (2.16)$$

is the midpoint of the j^{th} subsection. The expressions for K and D_j are used throughout this section.

5.2.1 The Evaluation of the Integral Weighted by $h(y, y')$

The integral (2.3) may be written in the form

$$k \int_0^y f(y') h_{<y}(y, y') dy' + k \int_y^{D_N+H} f(y') h_{>y}(y, y') dy' \quad (2.17)$$

where N ($=200$) is the total number of subsections, $kL = D_N+H$, and $f(y')$ is given by (2.14) and (2.15) for the hybrid expansion and for the all-pulse expansion, respectively. The numerical evaluation of this integral for the hybrid expansion is aided by the identities

$$\int_0^x t^{-\frac{1}{2}} h_{<y}(y, t) dt = -2 e^{iy} \operatorname{Re}[F_2(x)], \quad (2.18)$$

$$\int_0^x t^{-\frac{1}{2}} h_{>y}(y, t) dt = -2i \sin(y) F_2(x) \quad (2.19)$$

$$\int_{D_j-H}^{D_j+H} h_{<y}(y, y') dy' = -2 e^{iy} \sin(H) \cos(D_j), \quad (2.20)$$

$$\int_y^{D_j+H} h_{<y}(y, y') dy' = -2 e^{iy} \sin\frac{1}{2}(y-D_j+H) \cos\frac{1}{2}(y+D_j-H), \quad (2.21)$$

$$\int_{D_j-H}^{D_j+H} h_{>y}(y, y') dy' = -2i \sin(y) \sin\frac{1}{2}(D_j+H-y) e^{i\frac{1}{2}(D_j+H+y)}, \quad (2.22)$$

and

$$\int_{D_j-H}^{D_j+H} h_{>y}(y, y') dy' = -2i \sin(y) \sin(H) e^{iD_j} \quad (2.23)$$

where F_2 is given by (5.13) of Chapter 3. The evaluation for the all-pulse expansion requires the additional identities

$$\int_0^x h_{<y}(y, y') dy' = -e^{iy} \sin(x), \quad (2.24)$$

and

$$\int_y^H h_{>y}(y, y') dy' = -2i \sin(y) \sin\frac{1}{2}(H-y) e^{i\frac{1}{2}(H+y)}. \quad (2.25)$$

Substituting the hybrid expansion (2.14) in (2.3) and using the identities above yields

$$\begin{aligned} & -\frac{1}{2} \int_0^{D_N+H} \{I_E^1 - I_{PO}^1\} h(y, y') dy' = x_1^r e^{iy} \operatorname{Re}[F_2(y)] \\ & + i \sin(y) \{x_1^r [F_2(H) - F_2(y)] + \sin(H) \sum_{j=2}^N x_j^r e^{iD_j}\}, \quad 0 < y < H, \end{aligned} \quad (2.26)$$

and

$$\begin{aligned} & -\frac{1}{2} \int_0^{D_N+H} \{I_E^1 - I_{PO}^1\} h(y, y') dy' = e^{iy} \left[x_1^r \operatorname{Re}[F_2(H)] \right. \\ & \left. + (K_{\geq 3}) \sin(H) \sum_{j=2}^{K-1} x_j^r \cos(D_j) + x_K^r \sin\frac{1}{2}(y-D_K+H) \cos\frac{1}{2}(y+D_K-H) \right] \\ & + i \sin(y) \left[x_K^r \sin\frac{1}{2}(D_K+H-y) e^{i\frac{1}{2}(D_K+H+y)} + (K_{\leq N-1}) \sin(H) \sum_{j=K+1}^N x_j^r e^{iD_j} \right], \\ & y > H. \end{aligned} \quad (2.27)$$

In the above formulas, \underline{x}^r is the moment method hybrid expansion solution vector for $\{I_E^1 - I_{PO}^1\}$ that is obtained in Chapter 4. The corresponding formulas for the all-pulse expansion (2.15) are obtained using (2.24) and (2.25) to replace the terms involving the Fresnel integral. The logical expressions preceding the summations are equal to one, if true, and equal to zero, otherwise.

5.2.2 The Evaluation of the Integral Weighted by $g(y,y')$

The integral (2.4) may be written in the form

$$k \int_0^y f(y') g_{<y}(y,y') dy' + k \int_y^{D_N+H} f(y') g_{>y}(y,y') dy' \quad (2.28)$$

where $f(y')$ is given by (2.14) for the hybrid expansion and by (2.15) for the all-pulse expansion. The numerical evaluation of this integral for the hybrid expansion uses the identities

$$k \int_0^x t^{-\frac{1}{2}} g_{<y}(y,t) dt = -2 e^{iy} \operatorname{Im}[F_2(x)], \quad (2.29)$$

$$k \int_0^x t^{-\frac{1}{2}} g_{>y}(y,t) dt = -2 \sin(y) F_2(x), \quad (2.30)$$

$$k \int_{D_j-H}^{D_j+H} g_{<y}(y,y') dy' = -2 e^{iy} \sin(H) \sin(D_j), \quad (2.31)$$

$$k \int_{D_j-H}^y g_{<y}(y,y') dy' = -2 e^{iy} \sin^{\frac{1}{2}}(y-D_j+H) \sin^{\frac{1}{2}}(y+D_j-H), \quad (2.32)$$

$$k \int_{D_j-H}^{D_j+H} g_{>y}(y,y') dy' = -2 \sin(y) \sin^{\frac{1}{2}}(D_j+H-y) e^{i\frac{1}{2}(D_j+H+y)}, \quad (2.33)$$

and

$$k \int_{D_j-H}^y g_{>y}(y,y') dy' = -2 \sin(y) \sin(H) e^{iD_j} \quad (2.34)$$

where F_2 is given by (5.13) of Chapter 3. The evaluation for the all-pulse expansion uses the additional identities

$$k \int_0^x g_{<y}(y,y') dy' = -2 e^{iy} \sin^2(x/2) \quad (2.35)$$

and

$$k \int_y^H g_{>y}(y, y') dy' = -2 \sin(y) \sin \frac{1}{2}(H-y) e^{i \frac{1}{2}(H+y)}. \quad (2.36)$$

Substituting the hybrid expansion (2.14) in (2.4) and using the above identities yields

$$\begin{aligned} -\frac{k}{2} \int_0^{D_N+H} \{I_E^\theta - I_{PO}^\theta\} g(y, y') dy' &= x_1^r \operatorname{Im} [F_2(y)] e^{iy} \\ &+ \{x_1^r [F_2(H) - F_2(y)] + \sin(H) \sum_{j=2}^N x_j^r e^{iD_j}\} \sin(y), \quad 0 < y < H, \end{aligned} \quad (2.37)$$

and

$$\begin{aligned} -\frac{k}{2} \int_0^{D_N+H} \{I_E^\theta - I_{PO}^\theta\} g(y, y') dy' &= e^{iy} \left[x_1^r \operatorname{Im} [F_2(H)] \right. \\ &+ (K_{\geq 3}) \sin(H) \sum_{j=2}^{K-1} x_j^r \sin(D_j) + x_K^r \sin \frac{1}{2}(y - D_K + H) \sin \frac{1}{2}(y + D_K - H) \left. \right] \\ &+ \sin(y) \left[x_K^r \sin \frac{1}{2}(D_K + H - y) e^{i \frac{1}{2}(D_K + H + y)} + (K_{\leq N-1}) \sin(H) \sum_{j=K+1}^N x_j^r e^{iD_j} \right], \end{aligned} \quad (2.38)$$

y > H.

In the above, \underline{x}^r is the moment method hybrid expansion solution vector for $\{I_E^\theta - I_{PO}^\theta\}$ solved for in Chapter 4. The corresponding formulas for the all-pulse expansion of (2.15) are obtained using (2.35) and (2.36) to replace the terms involving the Fresnel integral.

5.2.3 The Numerical Evaluation of the Integrals Used to Find A, the Consistency Constant

The consistency constant, A, is given in (1.17) in terms of two integrals, each of which may be written in the form

$$F_{kL}(\theta) = \int_0^L \{I_E^\theta - I_{PO}^\theta\} e^{ikz} dz = \frac{1}{k} \int_0^{kL} \{I_E^\theta - I_{PO}^\theta\}(y) e^{iy} dy \quad (2.39)$$

where the upper limit has been reduced from infinity to kL because the integral equation for $\{I_E - I_{PO}\}$, Equation (1.9) of Chapter 4, is truncated at kL . Substituting the hybrid expansion (2.14) in the above yields

$$\frac{1}{2} \int_0^{kL} \{I_E^\theta - I_{PO}^\theta\} e^{iy} dy = x_1^r F_2(H) + \sin(H) \sum_{j=2}^N x_j^r e^{iD_j}. \quad (2.40)$$

The corresponding expression using the all-pulse expansion is

$$\frac{1}{2} \int_0^{kL} \{I_E^\theta - I_{PO}^\theta\} e^{iy} dy = x_1^p \sin(H/2) e^{i(H/2)} + \sin(H) \sum_{j=2}^N x_j^p e^{iD_j}. \quad (2.41)$$

The closed form evaluation of (2.39) may be carried out using the known analytic solution for $\{I_E^\theta - I_{PO}^\theta\}$ to obtain

$$F_\infty(\theta) = \int_0^\infty \{I_E^\theta - I_{PO}^\theta\} e^{ikz} dz = \frac{2i}{kZ_0} \left(\frac{1 - \cos(\theta/2)}{\sin(\theta/2)} \right). \quad (2.42)$$

This equation is used in the next section to check the accuracy of the numerical evaluation.

5.3 The Numerical Results for I_H

In this section the formulas of the preceding sections are used to find $\{I_H - I_{PO}\}$ from $\{I_E - I_{PO}\}$. Results due to both the hybrid expansion and the all-pulse expansion for $\{I_E - I_{PO}\}$ are compared to the standard for angles of incidence $\theta = 45^\circ$, 90° , and 135° . The standard is computed from the closed form results. Only the moment method results for $H = 0.05$,

$kL = 19.95$ (200 subsections) and $\theta = 45^\circ, 90^\circ$, and 135° are used. The current for $\theta = 180^\circ$ is zero. The computer program used to generate these results is given in Appendix D.

5.3.1 Accuracy of the Numerical Results for the Consistency Constant, A

In this section the accuracy of the numerical integration (2.39) for $F_{kL}(\theta)$ is tabulated. The accuracy of the numerical evaluation of the consistency constant A , also referred to as A_θ , is also tabulated.

Consider the expressions for $F_{kL}(\theta)$ in (2.40) and (2.41). It is helpful to watch the convergence of the series on the right-hand side of both equations as the series is summed. Study of this progression indicates that the real part, which should be zero, oscillates around zero when the hybrid expansion solution for $\{I_E - I_{P0}\}$ is used, but does not when the all-pulse expansion solution is used. This seems to indicate that the hybrid expansion solution gives better answers than the all-pulse expansion solution does. Table 5.1 gives the accuracy of the numerical results using each solution, and verifies the superiority of the hybrid expansion solution, but only for the real part. Note that the imaginary part, the most important part, is more accurate for the all-pulse expansion solution. It should also be noted, however, that the accuracy of the magnitude of the all-pulse expansion result is about the same as that of the hybrid expansion result. The phase of the latter result is much better than that of the former because the real and imaginary parts of the result for the hybrid expansion are accurate to about the same number of decimal places while those for the all-pulse expansion are not. For these reasons, it may be said that the result due

Table 5.1

Accuracy of the Numerical Results for $kZ_0 F_{kL}(\theta)$

	Decimal places of accuracy				Numerical value of standard
	Hybrid expansion results used for		All-pulse expansion results used for		
	$I_E^\theta - I_{PO}^\theta$		$I_E^\theta - I_{PO}^\theta$		
	Real	Imag.	Real	Imag.	
$kZ_0^F_{kL}(45^\circ)$	2.5	2.5	1.5	3.2	0.0 +i0.3978
$kZ_0^F_{kL}(90^\circ)$	2.5	2.3	1.3	3.0	0.0 +i0.8284
$kZ_0^F_{kL}(135^\circ)$	3.5	2.3	1.1	3.1	0.0 +i1.3364
$kZ_0^F_{kL}(180^\circ)$	1.9	1.9	1.1	1.8	0.0 +i2.0

Notes: 1. Decimal places = $-\log_{10}|s-a|$ as defined in Appendix A.

2. All standard real parts are zero, so the numbers under "Real" are = $-\log_{10}|a|$.

3. Standard:

$$kZ_0 F_\infty(\theta) = Z_0 \int_0^\infty (I_E^\theta - I_{PO}^\theta) e^{iy} dy = 2i \frac{1 - \cos(\theta/2)}{\sin(\theta/2)}.$$

to the hybrid expansion is slightly better than the result due to the all-pulse expansion. The poor accuracy obtained for the $\theta = 180^\circ$ case might be expected because in Figure 4.6 $\{I_E - I_{PO}\}$ is not negligibly small at the truncation point of $kL = 19.95$.

The accuracies of the $F_{kL}(\theta)$ described above become important when these numbers are used to obtain A_θ , the consistency constant, from Equation (1.17). Table 5.2 gives the decimal places of accuracy for ikA_θ . The two cases shown are for $\theta = 45^\circ$ and $\theta = 135^\circ$. For all angles of incidence, the imaginary part of ikA_θ is, in theory, zero. It is seen that ikA_θ obtained from the hybrid expansion exhibits accuracy to about the same number of decimal places in both the real and the imaginary part, while that for the all-pulse expansion does not. As is argued above for $F_{kL}(\theta)$, this means that the ikA_θ that is evaluated from the hybrid expansion is slightly better than that evaluated from the all-pulse expansion. In conclusion, it may be said that the numerical formulas for ikA_θ seem to converge quite well to the actual values.

5.3.2 Accuracy of the Numerical Results for $\{I_H - I_{PO}\}$

The numerical results for $\{I_H - I_{PO}\}$ are plotted along with the standard in Figures 5.1 through 5.3 for the angles of incidence of 45° , 90° , and 135° , respectively. The standard or "exact" $\{I_H - I_{PO}\}$ is obtained from (5.14) of Chapter 3 and (1.3). For each case, two dashed curves are plotted along with the standard. The fine dashed curve is the $\{I_H - I_{PO}\}$ that is obtained from (1.24) when the hybrid expansion moment method results for $\{I_E - I_{PO}\}$ are used. The coarse dashed curve is that obtained when the all-pulse numerical results are used.

Table 5.2

Accuracy of the Numerical Results for ikA_θ , the
Consistency Constant

	Decimal places of accuracy				Numerical values of standard ikA_{θ}
	Hybrid expansion results used for		All-pulse expansion results used for		
	$I_E^{\theta} - I_{PO}^{\theta}$		$I_E^{\theta} - I_{PO}^{\theta}$		
	Real	Imag.	Real	Imag.	
$ikA_{45^{\circ}}$	2.8	3.0	3.2	1.7	1.3066
$ikA_{135^{\circ}}$	3.7	3.2	3.8	2.1	0.5412

Notes: 1. $ikA_{90^\circ} = 1.0$ and $ikA_{180^\circ} = 0.0$ exactly.

2. All standard imaginary parts are zero, so the numbers under "Imag." are $= -\log_{10}|a|$.

3. Standard:

$$ikA_\theta = \frac{2 \cos^2(\theta/2) + \sin \theta (kZ_0 F_\infty(\theta)/2i)}{1 + (kZ_0 F_\infty(\pi/2)/2i)} = \sqrt{2} \cos(\theta/2) .$$

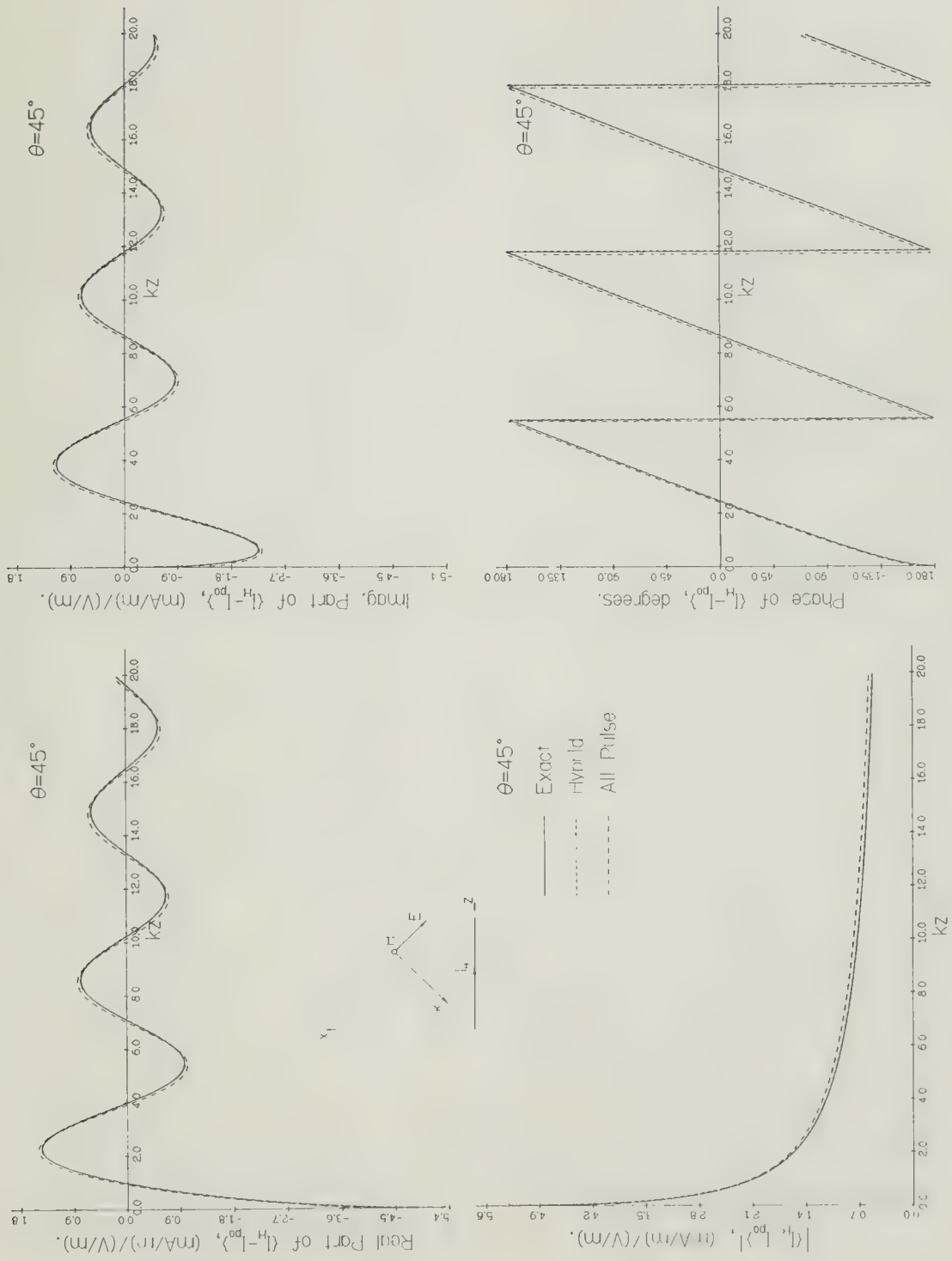


Figure 5.1. Comparison of the Exact with the Numerical Results Corresponding to the Hybrid and the All-Pulse Expansion Solutions for $\theta = 45^\circ$.

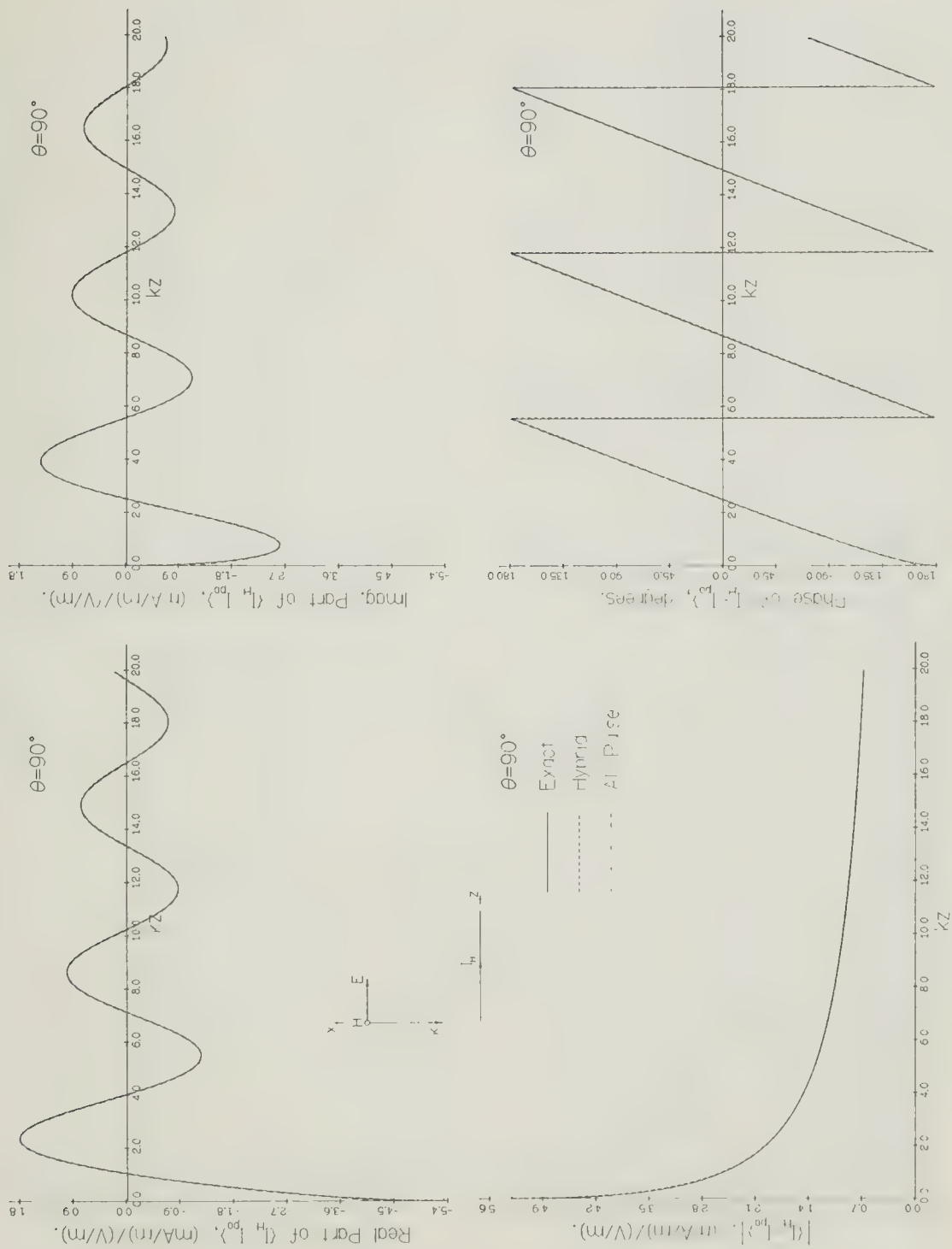


Figure 5.2. Comparison of the Exact with the Numerical Results Corresponding to the Hybrid and the All-Pulse Expansion Solutions for $\theta = 90^\circ$.

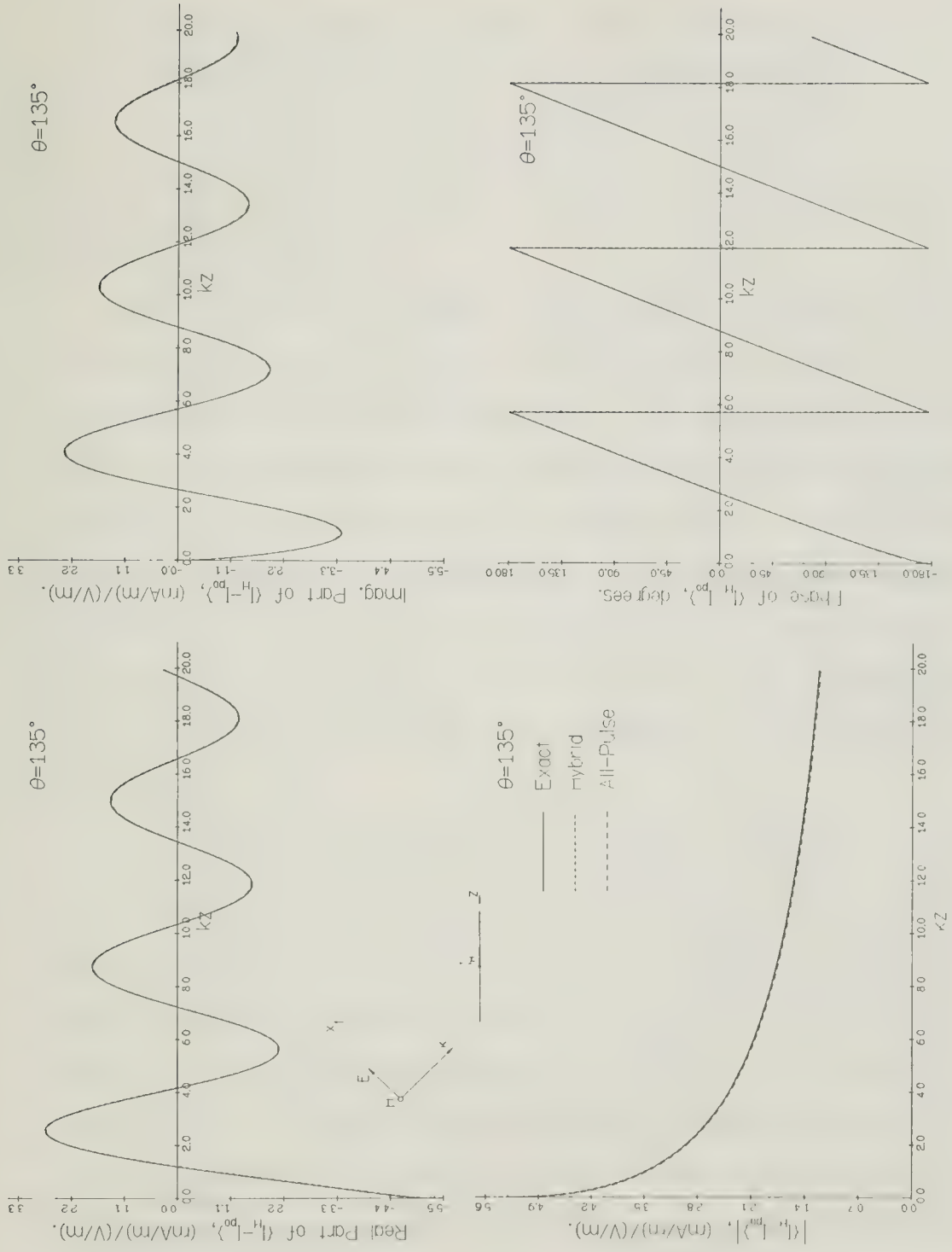


Figure 5.3. Comparison of the Exact with the Numerical Results Corresponding to the Hybrid and the All-Pulse Expansion Solutions for $\theta = 135^\circ$.

For all three angles of incidence, the finely dashed curve is indistinguishable from the standard. The coarsely dashed curve, on the other hand, visibly departs from the standard for $\theta = 45^\circ$. This suggests that the hybrid expansion gives better answers for $\{I_H - I_{po}\}$ than the all-pulse expansion does.

It is interesting to observe the edge behavior of $\{I_H - I_{po}\}$ when the two expansions for $\{I_E - I_{po}\}$ are used in (1.24). Figures 5.4 and 5.5 show plots of the edge behavior for $\theta = 45^\circ$ and 90° , respectively. Results corresponding to the hybrid and all-pulse expansions are shown with finely and coarsely dashed lines, respectively. It is clear that the hybrid expansion result is much better than the all-pulse result and that the former result has $z^{\frac{1}{2}}$ edge behavior whereas the latter does not. This is not surprising in light of the fact that the hybrid expansion for $\{I_E - I_{po}\}$ has $z^{-\frac{1}{2}}$ edge behavior whereas the all-pulse expansion does not.

It is desirable to compare the form of these results for $\{I_H - I_{po}\}$ with those that would be obtained if a moment method solution for I_H were found directly. As the graphs of Figures 5.1 through 5.5 show, the CSF method produces continuous currents. A pulse expansion moment method solution of an E-field integral equation would not have produced continuous currents. For essentially the work of solving what is a pulse expansion moment method problem, the final result takes the form of a sine expansion function except with the important difference that both the phase and the magnitude vary continuously. In all probability, the current source-function method described here reproduces a local phase

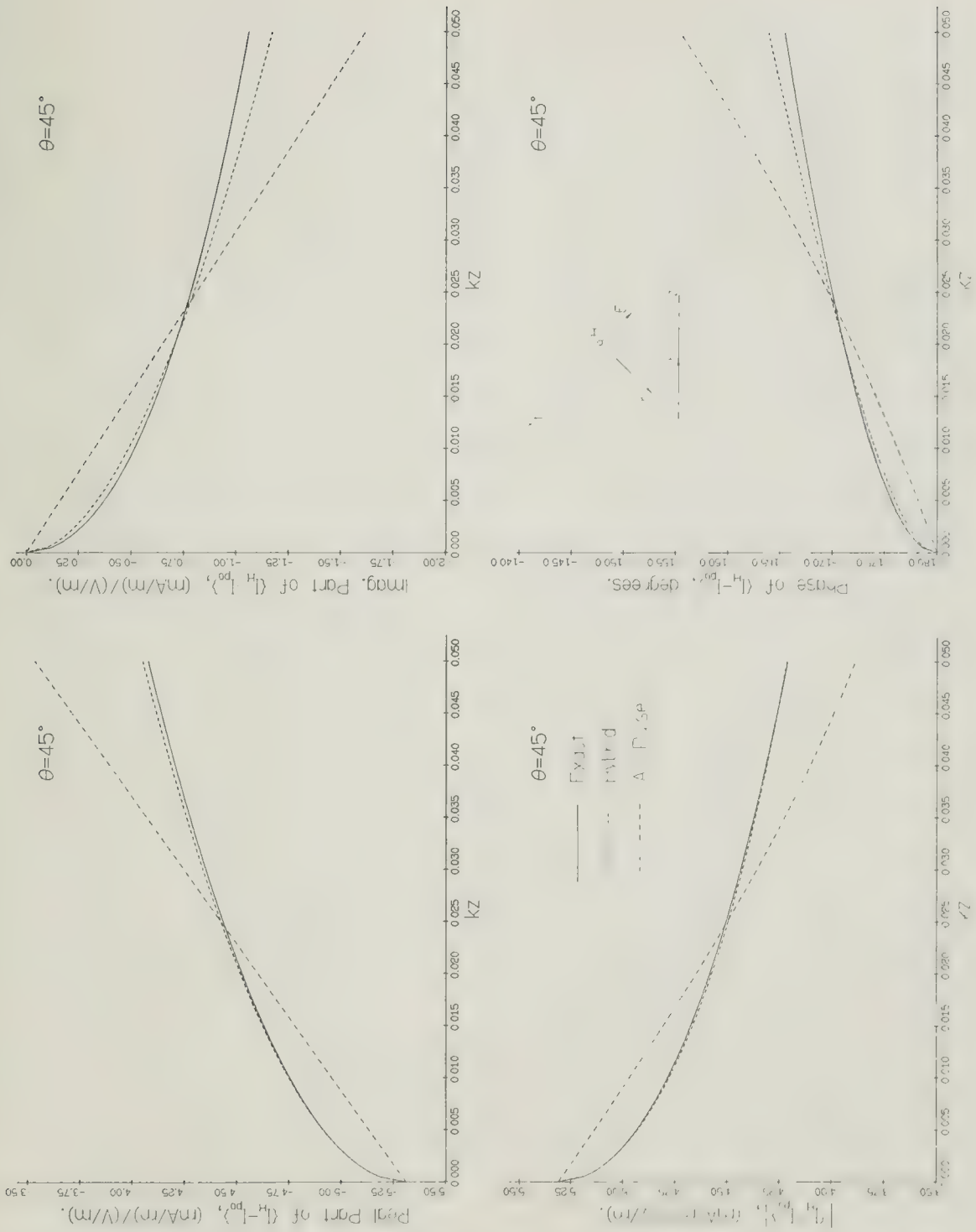


Figure 5.4. Comparison of the Exact Edge Behavior for $\{I_H - I_{po}\}$ with that of the Numerical Results Corresponding to the Hybrid and the All-Pulse Expansion Solutions for $\theta = 45^\circ$.

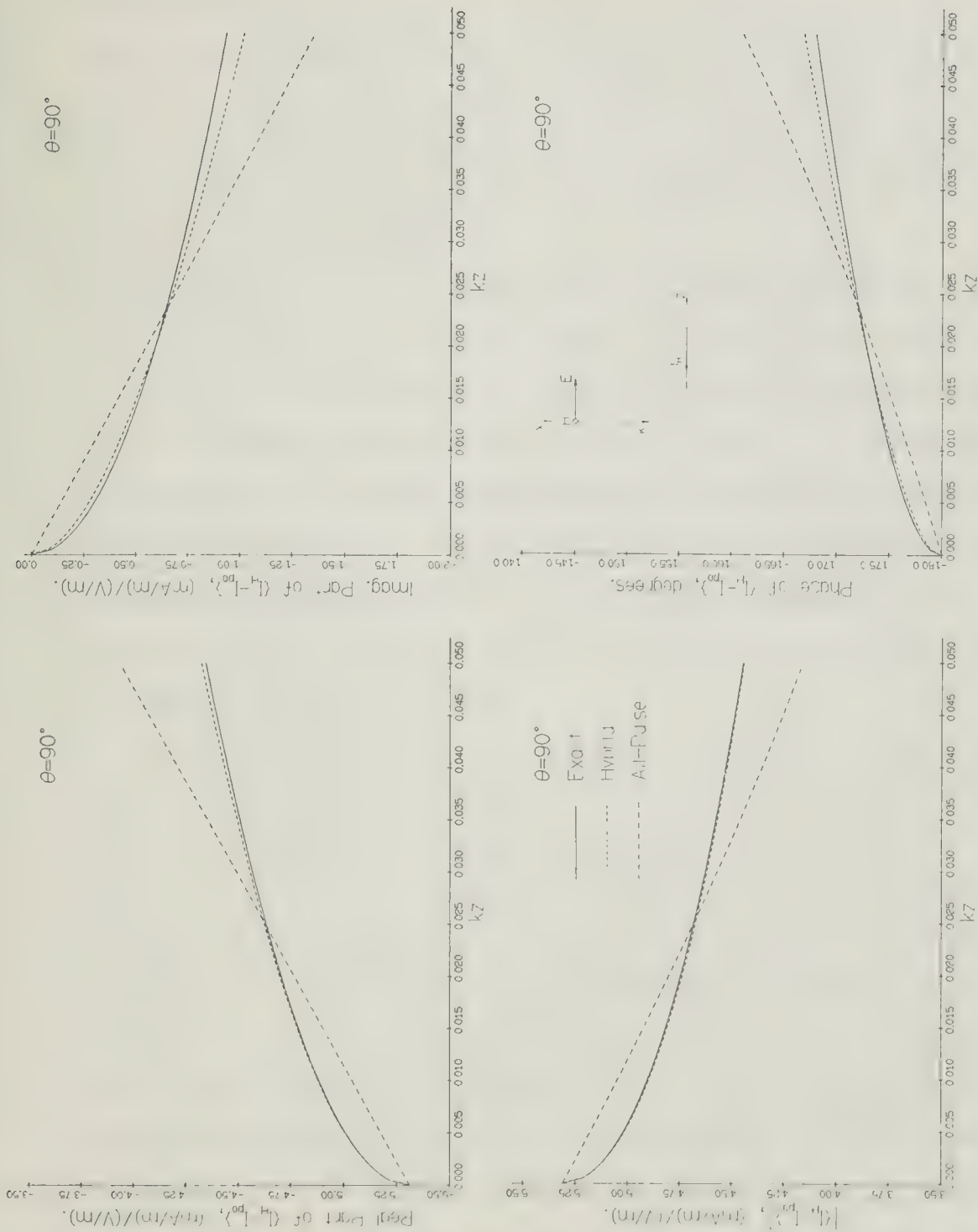


Figure 5.5. Comparison of the Exact Edge Behavior for $\{I_H - I_{po}\}$ with that of the Numerical Results Corresponding to the Hybrid and the All-Pulse Expansion Solutions for $\theta = 90^\circ$.

behavior which is more accurate than could have been anticipated in the choice of basis functions. That this is the case can be clearly seen by looking at the phase in Figures 5.4 and 5.5. This contrasts with the moment method which requires that an initial guess be made in the selection of expansion functions.

Although it is clear from the graphs of Figures 5.1 through 5.5 that the hybrid expansion gives better answers than does the all-pulse solution, it is not clear exactly how much better the one is over the other. Table 5.3 compares the average accuracies of $Z_0\{I_H - I_{po}\}$ for the hybrid expansion and for the all-pulse expansion. Two ranges and two angles of incidence are considered. For each angle, the average accuracy of a group of points near the edge and of an overall group of points is given. Averages are tabulated for $\theta = 45^\circ$ and $\theta = 90^\circ$. The averages for $\theta = 135^\circ$ are similar to those for $\theta = 90^\circ$.

Generally speaking, Table 5.3 shows that the results for the hybrid expansion are about one digit better than those for the all-pulse expansion. This means that if the hybrid results are good to an average of 1%, then the all-pulse results are good to only 10%. The results for $\theta = 90^\circ$ are better than those for $\theta = 45^\circ$ by an average of 0.5 digit. This inaccuracy for $\theta = 45^\circ$ is clearly visible in Figure 5.1. Thus, while both the hybrid and the all-pulse results for $\theta = 90^\circ$ and $\theta = 135^\circ$ appear to be equally accurate in the graphs, this is not true. The hybrid results are always more accurate than the all-pulse results. This underscores the need for using a hybrid expansion if the best possible results are desired.

Table 5.3

Accuracy of $Z_0\{I_H - I_{PO}\}$ for $\theta = 45^\circ$ and $\theta = 90^\circ$

	Edge		Overall	
	Hybrid	All-Pulse	Hybrid	All-Pulse
<u>Average decimal places of accuracy</u>				
<u>$\theta = 45^\circ$</u>				
Real	2.5	1.3	2.8	1.8
Imag.	2.0	1.3	2.7	1.8
Mag.	2.8	1.3	2.5	1.8
<u>Average digits of accuracy</u>				
Phase	2.7	1.9	3.3	1.3
<u>Average decimal places of accuracy</u>				
<u>$\theta = 90^\circ$</u>				
Real	2.6	1.4	3.3	2.4
Imag.	2.1	1.4	3.3	2.4
Mag.	2.8	1.5	3.1	3.4
<u>Average digits of accuracy</u>				
Phase	2.8	2.0	3.0	1.8

- Notes: 1. "Hybrid" and "All-Pulse" refer to the expansion used for $\{I_E - I_{PO}\}$.
2. "Edge" refers to 100 points equally spaced between 0 and 0.05 (see Figures 5.4 and 5.5).
3. "Overall" refers to 399 points equally spaced between 0.05 and 19.95 (see Figures 5.1, 5.2, and 5.3).
4. The standard is given by (5.14) of Chapter 3 and (1.3).

5.4 Conclusion

The results shown here demonstrate that the current source-function technique is suitable for numerical application. Even more important is the fact that this technique gives a numerical result that is continuous. The numerical result is also identically equal to zero outside of the domain of application. The technique, although relying on the moment method solution of an integral equation, yields a result for the current for any desired argument rather than at a finite number of points. The phase of the CSF solution exhibits a good approximation to the actual local behavior. Accurate detailed information about the behavior of the unknown current is available from the CSF solution by simply evaluating the superposition integral at a larger number of points. This does not require increasing the number of basis functions used to represent the current as is the case with the moment method solution of Pocklington's or Hallén's equations.

6. SCHWARTZ DISTRIBUTION THEORY AND THE STRIP PROBLEM

This chapter applies the CSF technique to the problem of electromagnetic scattering of an incident plane wave by a finite width perfectly conducting strip. Although the analytic procedures developed for the half-plane problem would seem to be applicable to this problem a complete description of the solution is still to be found. To complete the procedure, an even solution of the homogeneous finite part integral equation is required. The CSF technique for the strip problem is described in terms of Schwartz distribution theory. This insures that each procedural step has a well-defined meaning. De Jager (1969, p. 78) comments that (instead of using the finite part) supersonic wing theory "can be developed in a much shorter and more elegant way by employing the theory of distributions."

Section 6.1 presents the formulation of the strip problem and results of some previous studies. Section 6.2 introduces the concepts of distribution theory which are employed in the CSF approach to the strip problem. The remaining sections present the results obtained so far in applying the CSF technique to the strip problem.

6.1 The Strip Problem

The problem of scattering of a plane wave by a conducting strip is well-known. The geometry for the strip problem is the same as that for the half-plane problem, given in Figure 2.1, except that the metal extends from $-b$ to b , i.e., $-b < z < b$. The exact solution has been found by considering the strip as a limiting case of an elliptic cylinder. Unfortunately, this solution is in terms of an infinite series (of Mathieu

functions) which is not rapidly convergent. Descriptions of the exact solution to the strip problem are given by McLachlan (1947, p. 358) and Meixner and Schafke (1954, p. 373). Calculations of Mathieu function series for relatively narrow strips have been performed by Strutt (1931) and Morse and Rubenstein (1938). Moullin and Phillips (1952) use Morse and Rubenstein's expansions to calculate the current distribution on the strip. Miles (1949) gives the exact solutions of the integral equations for the current on the strip in terms of an infinite series of Mathieu functions. Dörr (1952) shows that the E-polarization strip integral equation has even Mathieu functions as eigenfunctions.

The E- and H-polarization integral equations for the currents $I_E(z)$ and $I_H(z)$ on the strip are, respectively,

$$\int_{-b}^b I_E(z') H_0^{(1)}(k|z-z'|) dz' = \frac{4}{kZ_0} e^{-ikz \cos\theta}, \quad |z| \leq b, \quad (1.1)$$

and

$$\left(\frac{d^2}{dz^2} + k^2 \right) \int_{-b}^b I_H(z') H_0^{(1)}(k|z-z'|) dz' = \frac{4k}{Z_0} \sin\theta e^{-ikz \cos\theta}, \quad |z| \leq b. \quad (1.2)$$

Cameron (1966) utilizes variational techniques to obtain an approximate solution to the strip integral equation for the E-polarization and develops integral equations for the even and odd parts of the solution. Methods for handling the $t^{-\frac{1}{2}}$ edge singularities in (1.1) in numerical solutions are given by Shafai (1971), Dmitriev and Zakhovov (1967), and Bolomey (1974), among others. Approximate solutions of the strip problem for narrow strips subjected to a normally incident plane wave have been obtained by Sommerfeld (1964, pp. 273-284) and Born and Wolf (1970, pp. 589-590). For the narrow

strip and the case of normal incidence, the H-polarization current $I_H(z)$ has z-dependence of the form

$$I_H(z) = c_1(b^2 - z^2)^{\frac{1}{2}}, \quad (1.3)$$

and the E-polarization current $I_E(z)$ has z-dependence of the form

$$I_E(z) = c_2(b^2 - z^2)^{-\frac{1}{2}}, \quad (1.4)$$

where c_1 and c_2 are constants. This solution for $I_E(z)$ may be obtained by approximating the Hankel function kernel in (1.1) by a logarithmic kernel. The integral equation

$$\int_{-1}^1 f(x') \ln|x-x'| dx' = 1 \quad (1.5)$$

has the exact solution $f(x) = -\frac{(1-x^2)^{-\frac{1}{2}}}{\pi \ln 2}$.

Solution techniques for singular integral equations with logarithmic and/or x^{-1} kernels have been given by Latta (1956), Erdogan (1969), Kanwal (1971), Muskhelishvili (1958), and Müller (1967), among others. The solution of the integral equation

$$\int_a^b P(t') \ln|t-t'| dt' = f(t) + \text{constant} \quad (1.6)$$

for an elasticity problem is given by Muskhelishvili (1958, pp. 305-309). Both sides of (1.6) are differentiated to obtain the solution. Kanwal (1971, p. 210) shows that a solution of

$$\int_{-1}^1 \frac{g(y)}{x-y} dy = 0 \quad (1.7)$$

is $g(x) = C(1 - x^2)^{-\frac{1}{2}}$, where C is any constant. This same solution is also obtained when both sides of (1.5) are differentiated.

An important consideration in a finite problem is symmetry. The solution can always be expressed as the sum of an even part and an odd part. Consider the equation

$$\int_{-b}^b f(x) H_0^{(1)}(k|x-y|) dx = g(y), \quad -b < y < b. \quad (1.8)$$

It may be shown that if $g(y)$ is odd, i.e., $g(y) = -g(-y)$, then $f(x)$ is also odd. If $g(y)$ is even, i.e., $g(y) = g(-y)$, then $f(x)$ is even. The derivative of an odd function is an even function and that of an even function is an odd function. These important properties are very useful.

6.2 Pertinent Concepts in Schwartz Distribution Theory

Schwartz's theory of distributions provides a rigorous justification for a number of manipulations that are otherwise unjustifiable, e.g., differentiating the unit step function to obtain the delta function. Operations of this type are only a small part of the total theory. Schwartz (1966a, pp. 38-44) utilized Hadamard's finite part in the development of the theory of distributions to define certain integrals which otherwise would not be defined. In recent years, several excellent textbooks on distribution theory have appeared, for example, Zemanian (1965), Schwartz (1966b), Gel'fand and Shilov (1964), Arsac (1966), Jones (1966), and Antosik, Mikusiński, and Sikorski (1973), among others. The discussion here will be directed toward the solution of the problem at hand and will therefore be quite limited. The theory of distributions provides the operations that are required to handle the strip problem.

6.2.1 The Definition of a Distribution

There are two equivalent ways in which a distribution may be defined. First, a distribution may be defined to be a continuous linear functional f on a space \mathcal{D} of testing functions $\varphi(x)$. This approach is used by Schwartz (1966a), Zemanian (1965), and Gel'fand and Shilov (1964). Second, a distribution may be defined as a limit of equivalent fundamental sequences of continuous functions. The sequential approach to the development of the theory of distributions is presented by Jones (1966) and Antosik, Mikusiński, and Sikorski (1973). To each distribution in the functional approach, there is one corresponding distribution in the sequential approach. The functional approach to distribution theory is used here because it is the approach that is most often used and therefore possesses a greater body of literature.

Definition: A distribution is a continuous linear functional on the space \mathcal{D} .

For our purposes, the space of testing functions \mathcal{D} consists of all complex-valued functions $\varphi(t)$ of a real variable t that possess derivatives of all orders (i.e., are infinitely smooth) and vanish outside of some finite interval. A functional f on \mathcal{D} is a rule that assigns a complex number $\langle f, \varphi \rangle$ to every member of \mathcal{D} . $\langle f, \varphi \rangle$ is sometimes written as $f(\varphi)$. A continuous linear functional f on \mathcal{D} possesses

- (1) linearity, that is, for any two testing functions φ_1 and φ_2 in \mathcal{D} and any complex number α

$$\langle f, \varphi_1 + \varphi_2 \rangle = \langle f, \varphi_1 \rangle + \langle f, \varphi_2 \rangle$$

$$\langle f, \alpha \varphi_1 \rangle = \alpha \langle f, \varphi_1 \rangle . \quad (2.1)$$

(2) continuity, that is, for any sequence $\{\varphi_\nu(t)\}_{\nu=1}^\infty$ in \mathcal{D} such that

$$\{\varphi_\nu\}_{\nu \rightarrow \infty} \rightarrow \varphi \text{ in } \mathcal{D},$$

then

$$\lim_{\nu \rightarrow \infty} |\langle f, \varphi \rangle - \langle f, \varphi_\nu \rangle| \rightarrow 0. \quad (2.2)$$

The space of all such distributions is denoted by \mathcal{D}' .

When $f(t)$ is locally integrable, a distribution f corresponding to $f(t)$ can be defined through the convergent integral

$$\langle f, \varphi \rangle \equiv \int_{-\infty}^{\infty} f(t) \varphi(t) dt. \quad (2.3)$$

Distributions corresponding to locally integrable functions are called regular distributions. Although distributions do not possess values at points, regular distributions may be associated with ordinary functions which do have point values. Zemanian (1965, pp. 6-9) shows that "a regular distribution determines the function producing it almost everywhere." He concludes that "without ambiguity we may consider an equivalence class of functions and its regular distribution as being the same entity." For this reason, both the regular distribution and the function that generates it will, at times, be referred to as "the" distribution.

All distributions that are not regular are called singular distributions. One example of a singular distribution is the delta functional which assigns the value

$$\langle \delta, \varphi \rangle = \varphi(0) \quad (2.4)$$

to every $\varphi \in \mathcal{D}$. If the integral (2.3) is divergent, a singular distribution may often be defined with the aid of Hadamard's finite part. In such

cases, f is called a pseudofunction and is identified with the letters Pf. A distribution corresponding to Pf[f] can be defined through the finite part integral

$$\langle \text{Pf}[f], \varphi \rangle = \text{Fp} \int_{-\infty}^{\infty} f(t) \varphi(t) dt. \quad (2.5)$$

At times, both a singular distribution and its corresponding pseudofunction will be referred to as "the" distribution. An example of a pseudofunction is

$$\text{Pf } t^{-\frac{3}{2}} 1_+(t). \quad (2.6)$$

The distribution corresponding to this pseudofunction is assigned the value

$$\langle \text{Pf } t^{-\frac{3}{2}} 1_+(t), \varphi(t) \rangle = \text{Fp} \int_0^{\infty} t^{-\frac{3}{2}} \varphi(t) dt \quad (2.7)$$

for every $\varphi \in \mathcal{D}$. Instead of introducing the finite part concept as Schwartz does, some authors, notably Gel'fand and Shilov, use a procedure called regularization to treat the divergent integrals that occur. This regularization is generally equivalent to taking the finite part.

The concept of a distribution can easily be extended to the n -dimensional case by introducing testing functions φ of n real variables that are infinitely smooth and that vanish outside of some bounded domain of the n -dimensional Euclidean space \mathcal{R}^n .

Definition: A distribution on \mathcal{R}^n is a continuous linear functional on the space \mathcal{D} of testing functions on \mathcal{R}^n .

A locally integrable function $f(\underline{t})$ generates a distribution on \mathcal{R}^n through the multiple integral

$$\langle f, \varphi \rangle = \int_{\mathcal{R}^n} f(\underline{t}) \varphi(\underline{t}) d\underline{t}, \quad \varphi \in \mathcal{D}, \quad (2.8)$$

where $\underline{t} = (t_1, t_2, \dots, t_n)$.

6.2.2 The Differentiation of a Distribution

Every distribution has derivatives of all orders. This is based on the fact that $\langle f, d\varphi/dt \rangle$ is meaningful even if df/dt does not exist. It is this observation that allows distribution theory to generalize the derivative. In fact, every distribution may be expressed as a finite order distributional derivative of an ordinary (locally integrable) function.

The first derivative df/dt of a distribution f is defined as the functional on \mathcal{D} given by

$$\langle df/dt, \varphi \rangle = - \langle f, d\varphi/dt \rangle, \quad \varphi \in \mathcal{D}. \quad (2.9)$$

This is a convenient definition because $d\varphi/dt$ itself is an infinitely differentiable testing function of finite support belonging to \mathcal{D} . First order partial derivatives $\partial f/\partial t_i$, $i=1,2,\dots,n$, of any distribution f defined over \mathcal{R}^n are the functionals on \mathcal{D} given by

$$\langle \partial f/\partial t_i, \varphi \rangle = - \langle f, \partial \varphi/\partial t_i \rangle, \quad \varphi \in \mathcal{D}. \quad (2.10)$$

As an example of the procedures involved in distributional differentiation, consider the distributional derivative of $g(t) = (b^2 - t^2)^{-\frac{1}{2}} 1_{-b}^b(t)$. The ordinary derivative is

$$\frac{dg}{dt} = \begin{cases} 0 & |t| > b \\ ? & |t| = b \\ t(b^2 - t^2)^{-\frac{3}{2}} & |t| < b. \end{cases} \quad (2.11)$$

The distributional derivative is found by applying (2.9).

$$\begin{aligned}
 \langle dg/dt, \varphi \rangle &= - \langle g, d\varphi/dt \rangle = - \lim_{\epsilon \rightarrow 0+} \int_{-(b-\epsilon)}^{b-\epsilon} (b^2-t^2)^{-\frac{1}{2}} \frac{d\varphi}{dt} dt = \\
 &= \lim_{\epsilon \rightarrow 0+} \left\{ \int_{-(b-\epsilon)}^{b-\epsilon} t(b^2-t^2)^{-\frac{3}{2}} \varphi dt - (2b\epsilon)^{-\frac{1}{2}} [\varphi(b) - \varphi(-b)] \right\} = \\
 &= \text{Fp} \int_{-b}^b t(b^2-t^2)^{-\frac{3}{2}} \varphi dt = \langle \text{Pf} [t(b^2-t^2)^{-\frac{3}{2}}] 1_{-b}^b(t), \varphi \rangle. \quad (2.12)
 \end{aligned}$$

The distributional derivative of g is the pseudofunction

$$\frac{dg}{dt} = \text{Pf} [t(b^2-t^2)^{-\frac{3}{2}}] 1_{-b}^b(t). \quad (2.13)$$

The sequential approach to the theory of distributions handles the definition of the derivative of g differently. A delta sequence is a sequence that converges to the delta function, i.e.,

$$\delta(x) = [\delta_n(x)] \quad (2.14)$$

where the square brackets $[]$ denote the limiting process. If the sequence $g_n(x) = \delta_n(x) * g(x)$ [$\delta_n(x)$ convolved with $g(x)$] converges to $g(x)$, then dg/dx is defined by the limiting sequence

$$\frac{dg}{dx} = \left[\frac{dg_n(x)}{dx} \right]. \quad (2.15)$$

A graph of dg_n/dx for fixed n gives an approximation of the distribution.

6.2.3 The Convolution of Distributions

For ordinary functions $f(x)$ and $g(x)$ defined for $-\infty < x < \infty$, the expression

$$(f * g)(x) = \int_{-\infty}^{\infty} f(\xi) g(x-\xi) d\xi \quad (2.16)$$

is called the convolution of f and g . The integral does not always exist. If one of the functions f or g has compact support and therefore vanishes outside of some finite interval, then $f * g$ exists for almost all values of x .

In the development of the convolution of two distributions, the concept of the direct product of the distributions must be introduced. If $\varphi(t, \tau)$ is a two-dimensional testing function in $\mathcal{D}_{t,\tau}$ and if $f(t)$ and $g(\tau)$ belong to the distribution spaces \mathcal{D}'_t and \mathcal{D}'_τ , respectively, then the direct product $f(t) \otimes g(\tau)$ is a distribution in $\mathcal{D}'_{t,\tau}$ defined by

$$\langle f(t) \otimes g(\tau), \varphi(t, \tau) \rangle \equiv \langle f(t), \langle g(\tau), \varphi(t, \tau) \rangle \rangle. \quad (2.17)$$

The direct product is commutative and associative for all distributions of interest here.

The rule that defines the convolution $h(t) = f * g$ of two distributions f and g is given by

$$\begin{aligned} \langle f * g, \varphi \rangle &\equiv \langle f(t) \otimes g(\tau), \varphi(t+\tau) \rangle \\ &\equiv \langle f(t), \langle g(\tau), \varphi(t+\tau) \rangle \rangle. \end{aligned} \quad (2.18)$$

A meaning can be assigned to the right-hand side if either f or g has bounded support. If g is taken to be the distribution with bounded support,

this requirement insures that $\langle g(\tau), \varphi(t+\tau) \rangle$ is itself a testing function in \mathcal{D} .

Since the current on a finite body is of finite support, the convolution of the current with another function is usually defined. The convolution of distributions can be defined under other conditions, but these are beyond the scope of the present discussion. Since the direct product is commutative, it follows that the convolution of two distributions is commutative, that is,

$$\langle f * g, \varphi \rangle = \langle g * f, \varphi \rangle, \quad \varphi \in \mathcal{D}. \quad (2.19)$$

Convolution is not in general associative, but it is associative if the supports of all of the distributions, except for at most one of them, are bounded. That is,

$$\langle f * (g * h), \varphi \rangle = \langle (f * g) * h, \varphi \rangle, \quad \varphi \in \mathcal{D}, \quad (2.20)$$

if the supports of at least two of the distributions f , g , and h are bounded.

The delta functional and its derivatives are very important in convolution. They exhibit the properties

$$\langle \delta * f, \varphi \rangle = \langle f, \varphi \rangle,$$

$$\langle \delta' * f, \varphi \rangle = \langle f', \varphi \rangle, \quad (2.21)$$

and

$$\langle \delta^{(n)} * f, \varphi \rangle = \langle f^{(n)}, \varphi \rangle, \quad \varphi \in \mathcal{D}.$$

The first derivative of the distribution f is the same as the convolution of f with the first derivative of δ . The derivative of the convolution obeys the property that

$$D(f * g) = (Df) * g = f * (Dg) \quad (2.22)$$

where $D = d/dx$. This is easily proved by using associativity and the fact that $Dh = \delta' * h$, that is,

$$D(f * g) = \delta' * (f * g) = (\delta' * f) * g = f * (\delta' * g). \quad (2.23)$$

This is true as long as either f or g is of finite support.

Properties of various distributions and their convolution with other distributions are given by De Jager (1970), Bremermann et al. (1967), De Jager (1969), Beltrami and Wohlers (1966), and Shilov (1968), among others.

6.2.4 Convolution Equations

Many of the differential, integral and integro-differential equations useful in solving electromagnetics problems may be written in the convolution form

$$h * y = f. \quad (2.24)$$

Here, h and f are given distributions and y is an unknown distribution. The equation is a differential equation when h is a linear combination of the derivatives of the delta functional. It is an integral equation when h has finite or infinite, but not vanishing, support. It may have a unique solution or no solution, or even an infinite number of solutions. The solution of (2.24) must satisfy

$$\langle h * y, \varphi \rangle = \langle f, \varphi \rangle \quad (2.25)$$

for every $\varphi \in \mathcal{D}$. For the strip problem integral equation, the support of the solution y is known. This restricts the possible classes of solutions

to those having the proper support.

An important concept in solving distributional differential equations is that of the fundamental solution. Consider the equation

$$\mathcal{L}y = f \quad (2.26)$$

where \mathcal{L} is any linear differential operator with constant coefficients, that is, \mathcal{L} is of the form

$$\mathcal{L} = a_n \frac{d^n}{dz^n} + \cdots + a_0. \quad (2.27)$$

Equation (2.26) may also be written as

$$(\mathcal{L}\delta) * y = f. \quad (2.28)$$

A fundamental solution for this equation, denoted by $E(z|\zeta)$ with pole at ζ satisfies the equation

$$\mathcal{L}E = \delta(z-\zeta). \quad (2.29)$$

Boundary conditions per se are not required. A distribution E is a solution of this equation if and only if

$$\langle \mathcal{L}E, \varphi \rangle = \langle E, \mathcal{L}^*\varphi \rangle = \varphi(\zeta) \quad (2.30)$$

for every $\varphi \in \mathcal{D}$. \mathcal{L}^* is the adjoint of \mathcal{L} . Any two fundamental solutions for \mathcal{L} differ by a solution of the homogeneous equation $\mathcal{L}v = 0$. When a fundamental solution E is known, a solution of (2.26) can be written as the convolution

$$y = f * E. \quad (2.31)$$

The convolution equation for the current source-function is obtained in the next section.

6.3 Maxwell's Equations and the Convolution Equation for the Current Source-Function

The fundamental relationship between the scattered electric field \underline{E}^S and the induced current \underline{J} is, from (1.10) of Chapter 3,

$$\nabla^2 \underline{E}^S + k^2 \underline{E}^S = - \frac{1}{\gamma} [\nabla \nabla \cdot \underline{J} + k^2 \underline{J}] \equiv - \frac{1}{\gamma} \underline{U}. \quad (3.1)$$

Here, \underline{E}^S is the electric field, \underline{J} is the current, and \underline{U} is the vector current source-function. A treatment of Maxwell's equations in a space of distributions is given by Schmidt (1968).

Let $\varphi(x,y,z)$ be a three-dimensional testing function with $\varphi \in \mathcal{D}$.

Then the equation

$$(\nabla^2 + k^2)\Phi = -\delta \quad (3.2)$$

must satisfy

$$\langle \Phi, (\nabla^2 + k^2)\varphi \rangle = -\varphi(0,0,0) \quad (3.3)$$

for all $\varphi \in \mathcal{D}$. Here, Φ is a fundamental solution for the operator $(\nabla^2 + k^2)$ and is

$$\Phi = \frac{e^{ikR}}{4\pi R} \quad (3.4)$$

where $R^2 = x^2 + y^2 + z^2$. This result is given, for example, by Stakgold (1967, Volume II, pp. 53-55). Since \underline{U} has finite support, the solution for \underline{E}^S may be written

$$- \frac{1}{\gamma} (\underline{U} * \Phi) = [(\nabla^2 + k^2)\underline{E}^S] * \Phi = \underline{E}^S * (\nabla^2 + k^2)\Phi = - \underline{E}^S * \delta = - \underline{E}^S(x,y,z)$$

or

$$\langle \underline{E}^S(x,y,z), \varphi \rangle = \frac{1}{\gamma} \langle (\underline{U} * \Phi), \varphi \rangle \quad (3.5)$$

for every $\varphi \in \mathcal{D}$.

For E- polarization in the strip problem, the current takes the form

$$\underline{J}_E = I_E(z) \underline{1}_{-b}^b(z) \delta(x) \hat{y} \quad (3.6)$$

and the current source-function becomes

$$\langle \underline{U}_E, \varphi \rangle = \langle \nabla \nabla \cdot \underline{J}_E + k^2 \underline{J}_E, \varphi \rangle = k^2 \langle \underline{J}_E, \varphi \rangle. \quad (3.7)$$

For the H-polarization, the current may be written as

$$\underline{J}_H = I_H(z) \underline{1}_{-b}^b(z) \delta(x) \hat{z} = \mathcal{J}_H \hat{z}. \quad (3.8)$$

The current source-function becomes

$$\begin{aligned} \langle \underline{U}_H, \varphi \rangle &= \langle \nabla \nabla \cdot \underline{J}_H + k^2 \underline{J}_H, \varphi \rangle = \\ &= \langle \frac{\partial^2 \mathcal{J}_H}{\partial x \partial z} \hat{x} + \left(\frac{\partial^2}{\partial z^2} + k^2 \right) \mathcal{J}_H \hat{z}, \varphi \rangle. \end{aligned} \quad (3.9)$$

Now

$$\begin{aligned} \langle \left(\frac{\partial^2}{\partial z^2} + k^2 \right) \mathcal{J}_H, \varphi \rangle &= \langle I_H(z) \underline{1}_{-b}^b(z), \left(\frac{\partial^2}{\partial z^2} + k^2 \right) \varphi(0, y, z) \rangle = \\ &= \int_{-b}^b I_H(z) \left(\frac{\partial^2}{\partial z^2} + k^2 \right) \varphi dz = - \int_{-b}^b \frac{dI_H}{dz} \frac{d\varphi}{dz} dz + k^2 \int_{-b}^b I_H \varphi dz = \\ &= \text{Fp} \int_{-b}^b \left(\frac{d^2}{dz^2} + k^2 \right) I_H(z) \varphi dz \end{aligned} \quad (3.10)$$

Therefore,

$$\left(\frac{\partial^2}{\partial z^2} + k^2 \right) \mathcal{J}_H = \delta(x) \underline{1}_{-b}^b(z) \left(\text{Pf} \frac{d^2}{dz^2} + k^2 \right) I_H(z) \equiv \delta(x) u(z) \quad (3.11)$$

where the subscript H has been left off u_H for convenience. This defines what will also be called the current source-function for the H-polarized case. The use of the notation $\text{Pf} \frac{d^2}{dz^2} I_H$ means that $d^2 I_H / dz^2$ is to be taken as a distribution, per se.

Using the property that $\delta(x) * f(x) = f(x)$ and substituting (3.7) in (3.5) gives

$$\begin{aligned} E_y^s(x, z) &= -\frac{kZ_0}{4} \{I_E(z) l_{-b}^b(z)\} * H_0^{(1)}(k[x^2 + z^2]^{\frac{1}{2}}) \\ &= -\frac{kZ_0}{4} \int_{-b}^b I_E(z') H_0^{(1)}(k[x^2 + (z-z')^2]^{\frac{1}{2}}) dz'. \end{aligned} \quad (3.12)$$

For the H-polarization, after using the same property and substituting (3.11) in (3.5), the tangential (z component) scattered field becomes

$$E_z^s(x, z) = -\frac{Z_0}{4k} \int_{-b}^b u(z') H_0^{(1)}(k[x^2 + (z-z')^2]^{\frac{1}{2}}) dz'. \quad (3.13)$$

The total tangential fields, for the E- and H-polarization, respectively, are

$$E_y^t(x, z) = E_y^s(x, z) + E_y^i(x, z), \quad (3.14a)$$

and

$$E_z^t(x, z) = E_z^s(x, z) + E_z^i(x, z) \quad (3.14b)$$

where

$$E_y^i = e^{-ik(z \cos\theta + x \sin\theta)} \quad (3.15a)$$

and

$$E_z^i = \sin\theta e^{-ik(z \cos\theta + x \sin\theta)}. \quad (3.15b)$$

By the boundary condition, the total tangential electric field on the conducting strip must vanish. Introducing the notation

$$a_s(x) = \begin{cases} a(x) & x \in s \\ 0 & x \notin s \end{cases} \quad \text{and} \quad a_{\hat{s}}(x) = \begin{cases} 0 & x \in s \\ a(x) & x \notin s \end{cases} \quad (3.16)$$

where \hat{s} denotes the collection of points not in $s = [-b, b]$, the total electric field along $x = 0$ may be expressed as

$$E^t(0, z) = 0_s + f_{\hat{s}}(z) \quad (3.17)$$

where $s = [-b, b]$ and f is an unknown function equal to the total field along $x = 0$ and in \hat{s} . The convolution equations for the E- and H-polarizations, respectively, become

$$I_{s,E}(z) * H_0^{(1)}(k|z|) = \frac{4}{kZ_0} (e^{-ikz \cos \theta} - f_{\hat{s},E}(z)) \quad (3.18)$$

and

$$u_{s,H}(z) * H_0^{(1)}(k|z|) = \frac{4k}{Z_0} (\sin \theta e^{-ikz \cos \theta} - f_{\hat{s},H}(z)). \quad (3.19)$$

The exact solution of the E-polarization equation for $I_E(z)$ may be expressed in terms of a series of Mathieu functions. Various approximate methods of solution have been discussed in the literature. The equation for $u(z)$, however, contains a pseudofunction and therefore can not be solved directly by expanding the unknown in a set of basis functions. The left side of this equation can also be written as

$$[(\delta'' + k^2 \delta) * (I_{H-b}^{(1)})] * H_0^{(1)}(k|z|). \quad (3.20)$$

This follows from (2.21) and (3.9). The next section details an unsuccessful attempt to solve (3.19) for $u(z)$.

6.4 An Attempt to Solve for $u(z)$

Consider the convolution equation

$$y_s * H_0^{(1)}(k|z|) = 1_s + f_{\hat{s}} \quad (4.1)$$

where y and f are unknown distributions with support $s = [-b, b]$ and \hat{s} , respectively. Assuming that $1_s + f_{\hat{s}}$ corresponds to a once-differentiable function, then

$$\frac{d}{dz} (1_s + f_{\hat{s}}) = 0_s + f'_{\hat{s}} \quad (4.2)$$

where the prime represents a new function (or distribution) which corresponds to the derivative of $f_{\hat{s}}$. Since

$$\frac{d}{dz} \{y_s * H_0^{(1)}(k|z|)\} = \left[\frac{dy_s}{dz} \right] * H_0^{(1)}(k|z|), \quad (4.3)$$

any constant times the pseudofunction $\frac{dy_s}{dz}$ may be added to the unknown in the convolution equation without affecting the right-hand side in the interval $[-b, b]$. This is seen to be equivalent to the case when the homogeneous finite part integral equation is solved by differentiating a locally integrable solution of the ordinary integral equation. The following discussion is based on this equivalence.

The integral equation for $u(z)$ may be written as

$$\text{Fp} \int_{-b}^b u(z') H_0^{(1)}(k|z-z'|) dz' = \frac{4k}{Z_0} \sin\theta e^{-ikz \cos\theta}, \quad z \in s = [-b, b]. \quad (4.4)$$

A solution for $u(z)$ of this finite part integral equation satisfies the distributional convolution equation of Equation (3.19) which is

$$\langle u_s(z) * H_0^{(1)}(k|z|), \varphi \rangle = \langle \frac{4k}{Z_0} [\sin\theta e^{-ikz \cos\theta} - f_{s,H}(z)], \varphi \rangle, \quad (4.5)$$

for all $\varphi \in \mathcal{D}$. Here, the emphasis is placed on trying to solve the finite part integral equation (4.4) and hence obtain a solution of (4.5).

It would seem reasonable to follow the same approach to solving (4.4) which proved successful in the case of the half-plane problem. Thus a solution of the form

$$u(z) = \sin\theta v(z) + A w_e(z) + B w_o(z) \quad (4.6)$$

is desired where $v(z)$ is the solution of the ordinary integral equation

$$\int_{-b}^b v(z') H_0^{(1)}(k|z-z'|) dz' = \frac{4k}{Z_0} e^{-ikz \cos\theta}, \quad z \in s, \quad (4.7)$$

and w_e and w_o are, respectively, even and odd (probably) pseudofunction solutions of the homogeneous finite part integral equation

$$\text{Fp} \int_{-b}^b w(z') H_0^{(1)}(k|z-z'|) dz' = 0, \quad z \in s, \quad (4.8)$$

subject to the edge condition $w(z) = O(z^{-\frac{3}{2}})$ as $z \rightarrow \pm b$. An odd solution $w_o(z)$ is easily found, but thus far, an even solution $w_e(z)$ with the proper edge behavior has not been determined.

To determine a solution of (4.8), consider the integral equation

$$\int_{-b}^b y(z') H_0^{(1)}(k|z-z'|) dz' = e^{-ikaz} - f_s(z), \quad -\infty < z < \infty, \quad (4.9)$$

where $a = \cos\theta$ and $f_s(z)$ is defined by (3.17). Rewriting the e^{-ikaz} factor on the right-hand side as $[\cos(kaz) - i \sin(kaz)]$ and using the

symmetry properties that are discussed in the last paragraph of Section 6.1, one finds that the solution $y(z')$ of (4.9) can be written as the sum of an even part $y_e(z')$ and an odd part $y_o(z')$. The integral equations for $y_e(z')$ and $y_o(z')$ are, respectively,

$$\int_{-b}^b y_e(z') H_0^{(1)}(k|z-z'|) dz' = \cos(kaz), \quad z \in s, \quad (4.10a)$$

and

$$\int_{-b}^b y_o(z') H_0^{(1)}(k|z-z'|) dz' = \sin(kaz), \quad z \in s. \quad (4.10b)$$

Applying the operator $L = (\frac{d}{dz} + ika)$ to (4.9) yields

$$\text{Fp} \int_{-b}^b \{Ly(z')\} H_0^{(1)}(k|z-z'|) dz' = 0_s - Lf_s, \quad -\infty < z < \infty. \quad (4.11)$$

A solution to the homogeneous finite part integral equation becomes

$$\begin{aligned} w(z) &= Ly = \left(\frac{d}{dz} + ika \right) (y_e - i y_o) = \\ &= \frac{d}{dz} y_e + ka y_o + i(ka y_e - \frac{d}{dz} y_o). \end{aligned} \quad (4.12)$$

At first, it may appear as if w has an even and an odd part. It may be shown, however, that the even part is identically zero. To do this consider the case when $a = 0$ in (4.10a) and (4.9) (the normal incidence case). The right-hand sides of both equations are unity. Since the edge behavior of $y(z)$ for this special case is $z^{-\frac{1}{2}}$, it follows that $y_e(z)$ has the same edge behavior for $a \in [-1, 1]$. Differentiating (4.10b) with respect to z , using (4.12) of Chapter 2, integrating by parts, and assuming that $y_o(\pm b) = 0$,

one obtains

$$\int_{-b}^b \frac{dy_o}{dz'} H_0^{(1)}(k|z-z'|) dz' = ka \cos(kaz), \quad z \in s. \quad (4.13)$$

Comparing this with (4.10a) and assuming that the homogeneous equation has only the trivial solution requires that

$$ka y_e - \frac{dy_o}{dz} = 0. \quad (4.14)$$

This is almost certainly true. More research needs to be carried out to prove that it is definitely true. Since y_e was assumed to have $z^{-\frac{1}{2}}$ edge behavior, the edge behavior of y_o appears to be $z^{\frac{1}{2}}$. This seems to verify the validity of the assumption that $y_o(\pm b) = 0$. Substituting (4.14) in (4.12) yields

$$w(z) = w_o(z) = \frac{d}{dz} y_e + ka y_o. \quad (4.15)$$

This is an odd function which apparently has edge behavior $z^{-\frac{3}{2}}$. The z variation of $w_o(z)$ must be the same for all $a \in [-1,1]$ in order for the present method to yield a unique solution. Since this is true for the half-plane problem, it seems reasonable that it also would be true for the strip, even though a proof of this has not been found. By differentiating this odd solution, an even solution is obtained. This even solution has $z^{-5/2}$ edge behavior and so is not allowed.

Although a non-zero even solution of the homogeneous finite part integral equation with the proper edge behavior has not been determined, one will optimistically be assumed to exist to facilitate the present discussion. If one does not exist, then the problem does not have a solution.

That an even solution is required may be seen by considering the special case of normal incidence. For a narrow strip, the current distribution may be approximated as

$$I_H = c_1 (b^2 - z^2)^{\frac{1}{2}} I_{-b}^b(z). \quad (4.16)$$

The current source-function $u(z) = (d^2/dz^2 + k^2)I_H$ is seen to be an even function with $z^{-\frac{3}{2}}$ edge behavior. Clearly, an even function with $z^{-\frac{3}{2}}$ edge behavior is required to reconstruct the proper current source-function.

Assuming the existence of an even solution with suitable edge behavior, the current source-function may be written in the form expressed by (4.6). This formula contains two coefficients which remain to be determined. The procedure for evaluating these constants depends upon a consistency condition which is presented in the next section.

6.5 The Consistency Condition

Consider the homogeneous, inhomogeneous, and adjoint homogeneous systems for $-b \leq z \leq b$:

The homogeneous system

$$\mathcal{L}\rho = 0 \quad \rho(-b) = \rho(b) = 0 \quad (5.1a)$$

The inhomogeneous system

$$\mathcal{L}\eta = f \quad \eta(-b) = \eta(b) = 0 \quad (5.1b)$$

and

The adjoint homogeneous system

$$\mathcal{L}^*\psi = 0 \quad (5.1c)$$

where $\mathcal{L} = \mathcal{L}^* = (d^2/dz^2 + k^2)$. When $\mathcal{L}\eta$ is a pseudofunction in the neighborhood of the edges, boundary conditions on the adjoint homogeneous system are not required. Consistency conditions, however, must be satisfied for the existence of a unique solution. Multiplying (5.1b) by ψ and (5.1c) by η , subtracting, and integrating, one obtains

$$\int_{-b}^b \{\psi \mathcal{L}\eta - \eta \mathcal{L}^*\psi\} dz = \int_{-b}^b f(z) \psi(z) dz \quad (5.2)$$

for every ψ which is a solution of (5.1c). The integral on the left is zero. This may be seen by performing integration by parts on the first term on the left. The integral on the left becomes

$$\left(\psi \frac{d\eta}{dz} - \eta \frac{d\psi}{dz} \right) \Big|_{-b}^b. \quad (5.3)$$

If $d\eta/dz$ is finite at the end points, then the adjoint problem has the boundary conditions

$$\psi(-b) = \psi(b) = 0. \quad (5.4)$$

If, on the other hand, $d\eta/dz$ approaches infinity at the end points, then no boundary conditions on ψ are required because the divergent terms may be made part of a finite part integral. Using the fact that

$$\text{Fp} \int_{-b}^b \psi \mathcal{L}\eta dz = \lim_{\epsilon \rightarrow 0+} \left[\int_{-(b-\epsilon)}^{b-\epsilon} \psi \mathcal{L}\eta dz - \psi \frac{d\eta}{dz} \Big|_{-(b-\epsilon)}^{b-\epsilon} \right], \quad (5.5)$$

the left-hand side of (5.2) becomes

$$- \eta \frac{d\psi}{dz} \Big|_{-b}^b \quad (5.6)$$

The boundary condition in (5.1b) makes this zero. Thus, in order for (5.1b) to have a solution, the consistency conditions

$$\int_{-b}^b f(z) \psi_1(z) dz = 0 \quad (5.7a)$$

and

$$\int_{-b}^b f(z) \psi_2(z) dz = 0 \quad (5.7b)$$

must be satisfied where $\psi_1 = e^{ikz}$ and $\psi_2 = e^{-ikz}$ or $\psi_1 = \sin(kz)$ and $\psi_2 = \cos(kz)$. These are necessary conditions.

The solution to (5.1b) depends on whether (5.1a) has a non-zero solution. When it does, the system is resonant and an arbitrary multiple of the resonant solution of (5.1a) can be added to the solution for η . The following theorem, similar to one given by Stakgold (1967, Volume I, p. 85), is useful.

Theorem: System (5.1b) has no solution unless the consistency conditions (5.7) are satisfied for every function ψ which is a solution of (5.1c).

This theorem is true only if the derivative of η , the unknown, approaches infinity as the edge is approached. This eliminates the adjoint boundary conditions. If the adjoint boundary conditions are required, the consistency condition is usually satisfied automatically since the adjoint homogeneous system (5.1c) would usually have only the trivial solution. Assuming that the current source-function u may be expressed by (4.6),

$$u(z) = \sin\theta v(z) + A w_e(z) + B w_o(z), \quad (5.8)$$

the constants A and B may be found by using the consistency conditions with $\psi_1 = \psi_e = \cos(kz)$ and $\psi_2 = \psi_o = \sin(kz)$. "e" and "o" subscripts denote even and odd functions, respectively. Since the integral of an odd function is zero, the expressions for A and B become

$$A = \frac{-\sin\theta \int_{-b}^b v(z) \cos(kz) dz}{\int_{-b}^b w_e(z) \cos(kz) dz}, \quad (5.9)$$

and

$$B = \frac{-\sin\theta \int_{-b}^b v(z) \sin(kz) dz}{\int_{-b}^b w_o(z) \sin(kz) dz}. \quad (5.10)$$

6.6 The Solution for the Current

6.6.1 Off Resonance

If an appropriate even solution $w_e(z)$ of the homogeneous finite part integral equation can be found, then the current source-function $u(z)$ is given by (4.6) and the current is related to the current source-function by the convolution equation

$$(\delta'' + k^2 \delta) * I_H = u(z). \quad (6.1)$$

This equation can be solved using a fundamental solution of the operator $(d^2/dz^2 + k^2)$. A fundamental solution satisfies the equation

$$(\delta'' + k^2 \delta) * E = \delta(z - \zeta) \quad (6.2)$$

as was discussed in Section 6.2.4. One such fundamental solution is

$$E(z) = \frac{e^{ik|z|}}{2ik} . \quad (6.3)$$

This is given by Stakgold (1967, Volume II, p. 55). The solution for the current $I_H(z)$ is

$$I_H(z) = u(z) * E(z). \quad (6.4)$$

Substituting this in (6.1) gives

$$u(z) * (\delta'' + k^2 \delta) * E(z) = u(z) * \delta(z) = u(z). \quad (6.5)$$

This shows that (6.4) is indeed a solution for the current.

The consistency conditions may be used to show that $I_H(z)$ as given by (6.4) is zero for $z \notin (-b, b)$. Assuming that (6.4) may also be interpreted as a finite part integral,

$$I_H(z) = \frac{1}{2ik} \int_{-b}^b u(z') e^{ik|z-z'|} dz' \\ = \frac{1}{2ik} \begin{cases} e^{-ikz} \int_{-b}^b u(z') e^{ikz'} dz' = 0 & z < -b \\ e^{ikz} \int_{-b}^b u(z') e^{-ikz'} dz' = 0 & z > b. \end{cases} \quad (6.6)$$

Thus, as long as the consistency conditions hold, $I_H(z)$ is given by (6.4) for all values of the argument z . For a Green's function with boundary conditions $g(\pm b, z') = 0$,

$$g(z, z') = \frac{\sin[k(z' \pm b)] \sin[k(z \mp b)]}{k \sin(2kb)}, \quad z \gtrless z', \quad (6.7)$$

it may be shown that

$$\int_{-b}^b u(z') g(z, z') dz' = \int_{-b}^b u(z') E(z - z') dz' \quad (6.8)$$

as long as the consistency conditions are satisfied. This proves that the expression for the current derived by conventional Green's function techniques is the same as that given by (6.4) provided that the consistency conditions are satisfied.

6.6.2 The Case of Resonance

When the frequency of the incident plane wave is such that

$$k = \frac{n\pi}{2b}, \quad n = 1, 2, \dots, \quad (6.9)$$

Equation (5.1a) has a nontrivial solution. For even n , the solution is $\sin(kz)$ and for odd n , it is $\cos(kz)$. At resonance, (6.2) has no solution because the consistency condition $\int_{-b}^b \delta(z - \zeta) \rho(\zeta) d\zeta = 0$ is not satisfied. Here, $\rho(\zeta)$ is the resonant nontrivial solution to (5.1a).

At resonance, a modified Green's function must be used. Discussions of the modified Green's function are given by Stakgold (1967, Volume I, p. 89) and Lanczos (1961, pp. 270-275). The modified Green's function satisfies

$$\mathcal{L}^* g_M(z | \zeta) = \delta(z - \zeta) + C \rho(z) \rho(\zeta) \quad (6.10)$$

where $\rho(z)$ is a solution to (5.1a). The consistency condition

$$\int_{-b}^b [\delta(z-\zeta) + C \rho(z) \rho(\zeta)] \rho(\zeta) d\zeta = 0$$

is applied to find the constant C ,

$$C = - \left\{ \int_{-b}^b \rho^2(\zeta) d\zeta \right\}^{-1} = - \frac{1}{b}, \quad \text{all } n. \quad (6.11)$$

This insures that a solution for g_M exists.

Boundary conditions on g_M are not required if pseudofunctions which are singular at the ends are present in the current source-function. A suitable modified Green's function appears to be

$$g_M(z|\zeta) = \frac{e^{ik|z-\zeta|}}{2ik} - \frac{z}{2kb} \begin{pmatrix} -\cos \\ \sin \end{pmatrix} (kz) \begin{pmatrix} \sin \\ \cos \end{pmatrix} (k\zeta), \quad n = \begin{cases} \text{even} \\ \text{odd.} \end{cases} \quad (6.12)$$

This may be verified directly by applying \mathcal{L}^* . Any constant times $\rho(z)$ can be added to this Green's function to obtain another one.

The solution for the current corresponding to (6.6) becomes

$$I_H(\zeta) = \int_{-b}^b u(z) g_M(z|\zeta) dz + C \rho(\zeta) \quad (6.13)$$

where $\rho(\zeta)$ is the nontrivial solution to (5.1a) and C is any constant.

This result tends to suggest that, at resonance, a current can exist even though $u(z)$ is negligibly small or zero. The reader is referred to Stakgold or Lanczos for further comments.

6.7 Conclusion

So far, the results of this chapter are inconclusive. If an even function with the proper edge behavior can be found which satisfies (4.8),

or if additional techniques can be developed to find the distributional solutions of (4.5), then the current source-function technique may be used to find an exact solution to the strip problem. More research in this area needs to be performed.

Although time did not permit it here, the strip problem could be solved numerically and the results compared to the exact results to verify that the current source-function technique is useful in obtaining approximate solutions for finite problems. It would also be interesting to take the exact solution for the current I_H , to find $u = d^2 I_H / dz^2 + k^2 I_H$ and to compare this with I_E in order to determine the functions which must be added to I_E to obtain u .

7. THE THREE-DIMENSIONAL TIME-DEPENDENT CURRENT SOURCE-FUNCTION

The extension of the current source-function technique to the three-dimensional time-dependent case is straightforward. The steps in the development are briefly outlined here.

The previous chapters dealt with extreme cases of scatterers with sharp edges. The currents on smooth scattering objects without edges do not have singular behavior and therefore may be twice differentiable. Objects with sufficiently well-behaved currents would be expected to have a well-behaved current source-function. If this is the case, then the current source-function will be locally integrable, the concept of the finite part will not have to be introduced, and consistency conditions usually will be satisfied automatically.

7.1 Maxwell's Equations and the Current Source-Function

Maxwell's equations are

$$\nabla \times \underline{E} = - \frac{\partial \underline{B}}{\partial t} - \underline{K} \quad (1.1a)$$

$$\nabla \times \underline{H} = \frac{\partial \underline{D}}{\partial t} + \underline{J} \quad (1.1b)$$

$$\nabla \cdot \underline{D} = \rho \quad (1.2a)$$

$$\nabla \cdot \underline{B} = m \quad (1.2b)$$

where \underline{E} and \underline{H} are the electric and magnetic field intensities, \underline{J} and \underline{K} are densities of electric and magnetic currents, and ρ and m are the electric and magnetic charge densities. The charge and current are related by the

continuity equations

$$\nabla \cdot \underline{K} = - \frac{\partial m}{\partial t} , \quad (1.3a)$$

$$\nabla \cdot \underline{J} = - \frac{\partial \rho}{\partial t} . \quad (1.3b)$$

By combining Maxwell's equations, the currents and fields can be related directly. These expressions are

$$\left(\nabla^2 - \frac{1}{c^2} \frac{\partial^2}{\partial t^2} \right) \frac{\partial \underline{E}}{\partial t} = - \frac{1}{\epsilon} \left[\nabla \nabla \cdot \underline{J} - \frac{1}{c^2} \frac{\partial^2}{\partial t^2} \underline{J} \right] + \frac{\partial}{\partial t} \nabla \times \underline{K} \quad (1.4a)$$

and

$$\left(\nabla^2 - \frac{1}{c^2} \frac{\partial^2}{\partial t^2} \right) \frac{\partial \underline{H}}{\partial t} = - \frac{1}{\mu} \left[\nabla \nabla \cdot \underline{K} - \frac{1}{c^2} \frac{\partial^2}{\partial t^2} \underline{K} \right] - \frac{\partial}{\partial t} \nabla \times \underline{J}. \quad (1.4b)$$

If, for example, $\underline{K} = 0$, then the \underline{E} field is related to the current by

$$\left(\nabla^2 - \frac{1}{c^2} \frac{\partial^2}{\partial t^2} \right) \frac{\partial \underline{E}}{\partial t} = - \frac{1}{\epsilon} \left[\nabla \nabla \cdot \underline{J} - \frac{1}{c^2} \frac{\partial^2}{\partial t^2} \underline{J} \right] = - \frac{1}{\epsilon} \underline{U} \quad (1.5)$$

where \underline{U} , the current source-function, is given by

$$\underline{U} = \nabla \nabla \cdot \underline{J} - \frac{1}{c^2} \frac{\partial^2}{\partial t^2} \underline{J}. \quad (1.6)$$

7.2 The Expression for the Current in Terms of the Current Source-Function

If the current source-function \underline{U} is known, then the current is given by

$$\frac{1}{c^2} \frac{\partial^2}{\partial t^2} \underline{J} = (\nabla \times \nabla \times + \frac{1}{c^2} \frac{\partial^2}{\partial t^2}) [\underline{U} * \Phi] \quad (2.1a)$$

$$= [(\nabla \times \nabla \times + \frac{1}{c^2} \frac{\partial^2}{\partial t^2}) \underline{U}] * \Phi \quad (2.1b)$$

$$= \underline{U} * \left[(\nabla \times \nabla \times + \frac{1}{c^2} \frac{\partial^2}{\partial t^2}) \Phi \right] \quad (2.1c)$$

where ϕ is a solution of the equation

$$(\nabla^2 - \frac{1}{c^2} \frac{\partial^2}{\partial t^2}) \phi = \delta(\underline{r}, t) \quad (2.2)$$

and $\overline{[\quad]}$ represents a dyadic operator. For harmonic time dependence, $e^{-i\omega t}$, (2.1) becomes

$$k^2 \underline{J} = (-\nabla \times \nabla \times + k^2) [\underline{U} * \phi] \quad (2.3a)$$

$$= [(-\nabla \times \nabla \times + k^2) \underline{U}] * \phi \quad (2.3b)$$

$$= \overline{\underline{U} * [(-\nabla \times \nabla \times + k^2) \phi]} \quad (2.3c)$$

where ϕ is a solution of the equation

$$(\nabla^2 + k^2) \phi = \delta. \quad (2.4)$$

Equations (2.1a) and (2.3a) follow from (1.5) by using

$$\nabla \cdot \underline{J} = -\epsilon \frac{\partial}{\partial t} (\nabla \cdot \underline{E}) \quad (2.5)$$

and

$$\frac{\partial \underline{E}}{\partial t} = -\frac{1}{\epsilon} [\underline{U} * \phi]. \quad (2.6)$$

Equations (2.1b) and (2.3b) may be verified by substituting \underline{U} from (1.6) and using

$$\begin{aligned} \langle [(\nabla^2 - \frac{1}{c^2} \frac{\partial^2}{\partial t^2}) \underline{F}] * \phi, \varphi \rangle &= \langle \underline{F} * [(\nabla^2 - \frac{1}{c^2} \frac{\partial^2}{\partial t^2}) \phi], \varphi \rangle \\ &= \langle \underline{F} * \delta, \varphi \rangle = \langle \underline{F}, \varphi \rangle \end{aligned} \quad (2.7)$$

where $\varphi(\underline{r}, t)$ is a testing function in \mathcal{D} and \underline{F} is a distribution of finite support in the spatial variables and of semi-infinite support along the

positive time axis. Equations (2.1c) and (2.3c) follow either from the associativity of convolution in distribution theory or from the theory of systems of partial differential equations in distribution theory. The dyadic inverse of the $(\nabla\nabla\cdot - \frac{1}{c^2} \frac{\partial^2}{\partial t^2})$ operator in (1.6) may be found by utilizing the concepts presented by Latta (1974, pp. 621-623). Tai (1971) discusses similar dyadic Green's functions.

7.3 Conclusions

It appears that the direct relation (1.5) between the current and the electric field can be used to solve for the current on a scatterer without introducing the vector potential, at least for those obstacles with sufficiently well-behaved current distributions. The current source-function technique shows promise for treating the time-domain scattering from smooth objects. Vector and scalar potentials would not be required. More research needs to be carried out to verify the usefulness of this technique.

8. CONCLUSION AND SUGGESTIONS FOR FURTHER DEVELOPMENT

The current source-function (CSF) technique has been applied to the problems of scattering of electromagnetic waves from simple planar obstacles. Techniques were developed for treating the singular behavior of the current and its source-function when the scatterers have sharp edges. In the case of the half-plane, an exact solution was obtained using the CSF technique. The currents induced on the half-plane were also obtained by using the moment method to solve the CSF integral equation numerically. An attempt to solve the strip problem exactly using the CSF technique remains incomplete for lack of an even solution of the homogeneous finite part integral equation with proper edge behavior. However, the numerical solution of the strip problem using the CSF technique remains to be investigated.

The CSF technique shows promise for solving integral equations with a logarithmic singularity both on the right-hand side and in the kernel. An antenna with a δ gap excitation (i.e., magnetic current $\underline{K} = \delta(z) \delta(r-a) \hat{\phi}$) produces an electric field with a logarithmic singularity. The CSF technique also shows promise for handling arrays of scattering or radiating objects. The interactions between elements would be accounted for in the current source-function which would simplify the moment method solution. Once the current source-function was known, the current on an element could be found from the current source-function associated with that element alone.

The general nature of the CSF technique has been indicated in a brief outline of how a current source-function might be defined for three-dimensional time-domain problems (Chapter 7). Thus, there are many

possibilities for application of the CSF technique which remain to be explored. Only after further development will it be possible to make a meaningful comparison between the moment method solutions of the CSF integral equation and the electric field integral equations of Pocklington and Hallén. However, one advantage of the two-step CSF approach is that even though the current source-function may be approximated by a discontinuous function, the current, being calculated by integration, is continuous. Other possible advantages, mentioned previously, such as efficiency due to a simpler kernel and fewer basis functions, need to be investigated further.

APPENDICES

A. ANALYSIS OF ACCURACY

If a is a numerical approximation to the value of some function whose true ("standard") numerical value is s , then,

$$\text{Absolute error} = |s - a| \quad (\text{A.1})$$

and

$$\text{Relative error} = \left| \frac{s - a}{s} \right|. \quad (\text{A.2})$$

Relative error is often used when the approximate value a is obtained through floating point arithmetic. The exponent scaling present in floating point arithmetic makes relative error the most natural criterion to use for describing the accuracy of such a numerical procedure. The relative error must not be used when the standard is equal to zero or in the neighborhood of zero. This limits the usefulness of relative error.

By their very nature, some numerical approximations are naturally absolute decimal approximations and absolute error criteria must be used. Power series, for example, are sometimes of this type. If relative error is used instead of the absolute error for such approximations, enormous errors are obtained in the vicinity of a null or near-zero. For example, if a numerical approximation generates

$$a = 0.0003927$$

when the true value of the function at that point is

$$s = 0.000000721$$

then

$$\text{Absolute error} = 0.000391979$$

and

$$\text{Relative error} = 543.66.$$

This number for relative error is not particularly meaningful and may be misunderstood if the values of a and s are not given. The absolute error may also be misinterpreted unless the maximum value of the approximated function is given.

The proper choice of using either the relative error or the absolute error must often be made by computing both and choosing the most meaningful one. The "typical" or median relative error is used sometimes to describe the relative accuracy of a numerical approximation to some function. This provides a measure of error which is easily understood, but eliminates from consideration large relative errors occurring around nulls and near-zeroes.

Hart et al. (1968, p. 162) define

$$\text{Precision index} = -\log_{10} \epsilon_{\max} \quad (\text{A.3})$$

where ϵ_{\max} is the maximum relative or absolute error. For many of the numerical approximations studied in this work, pointwise, average or median relative error is preferred to maximum relative error. For this reason, the definition

$$\text{Digits of Accuracy} = -\log_{10} \left| \frac{s - a}{s} \right| \quad (\text{A.4})$$

is made where s and a are numbers corresponding to a standard approximation and to an approximation under study, respectively. The "digits of accuracy" factor defined above is applicable only at a point and is related to the pointwise percent error through the \log_{10} function. Its name is derived from the fact that it tends to represent the actual number of digits for which the approximate value matches the standard value. For

example, 2.42 is accurate to 1.3 digits when the standard is 2.54 and 0.0044721 is accurate to 3.9 digits when the standard is 0.0044716. The estimated median digits of accuracy is sometimes used to indicate general trends that an approximation to some function exhibits over some finite range of arguments. The median is used instead of the maximum because of the losses of digits of accuracy occurring at nulls or near-zeroes. If it is desired to compare two numbers, neither of which is known to be correct, then the "number of matching digits" is given. This is obtained by assuming that one or the other of the numbers is most correct and using it as the standard for the "digits of accuracy". In some cases, an average of the "digits of accuracy" is used.

For some comparisons, a measure of the number of decimal places of accuracy (or of the absolute error) is useful or necessary. For this reason, it is helpful to define

$$\text{Decimal Offset Factor} = -\log_{10}|s|. \quad (\text{A.5})$$

If the decimal offset factor is given, an estimate of the magnitude of the standard is obtained from

$$|s| \approx 10^{-\text{Decimal Offset Factor}}. \quad (\text{A.6})$$

A measure of the number of decimal places of accuracy is obtained from the equation

$$\begin{aligned} \text{Decimal Places of Accuracy} &= -\log_{10}|s - a| \\ &= -\left(\log_{10}\left|\frac{s - a}{s}\right| + \log_{10}|s|\right) \\ &= \text{Digits of Accuracy} + \text{Decimal Offset Factor} \end{aligned} \quad (\text{A.7})$$

For a standard of 2.54, the decimal offset factor is -0.4 and for a standard of 0.0044716 the decimal offset factor is +2.3. From the above equation, 2.42 is accurate to 0.9 decimal places with a standard of 2.54 and 0.0044721 is accurate to 6.3 decimal places with a standard of 0.0044716.

A measure of decimal places of accuracy which seems to agree with visual expectations better than (A.7) is

$$\begin{aligned} \text{Apparent Decimal Places of Accuracy} = \\ = \text{Digits of Accuracy} + \text{Decimal Offset Factor} - 0.5. \quad (\text{A.8}) \end{aligned}$$

This is not used in this thesis. Where large groups of data are involved, an estimated median decimal offset factor is given. In most cases, the decimal places of accuracy figure is given per se.

The concept of digits of accuracy, decimal offset factor, and decimal places of accuracy are quite useful when comparisons between two or more approximations to some function are being made. In general, it is sufficient to simply compare the digits of accuracy figures. In certain cases where the values of the standards are not close to each other, it is necessary to keep the respective decimal offset factors in mind in order to obtain a meaningful absolute comparison. Either (A.7) or (A.8) may be used for this.

B. APPROXIMATIONS TO THE MATRIX ELEMENTS

The matrix elements for the moment method solution of integral equations with a Hankel function $H_0^{(1)}$ kernel are integrals of the Hankel function weighted with the expansion functions. Numerical approximations for these matrix elements have often been made without stating the absolute or relative accuracy of these approximations. Excellent approximations, accurate to at least ten decimal places, for the matrix elements are given in the text and will be used as the standards to which the approximations given here are compared. The accuracies of the approximations derived here are given in terms of "digits of accuracy" and "decimal offset factor." These terms are defined and explained in Appendix A. Further references and another discussion of matrix element approximation for the Hankel function kernel are given by Harrington (1968, pp. 43-44, 47-49).

The crudest approximations for the self terms are derived from the formula

$$J_0(t) \approx 1 \quad (\text{B.1})$$

for small t . Better approximations are derived from the formula

$$J_0(t) \approx \cos(t/\sqrt{2}) \quad (\text{B.2})$$

for small t . Using the fact that

$$H_0^{(1)}(t) = J_0(t) + i(2/\pi)[\gamma + \ln(x/2)] J_0(t) + i(4/\pi)J_2(t) + iO(t^4). \quad (\text{B.3})$$

and substituting (B.1) and (B.2) in (B.3), one obtains

$$H_0^{(1)}(t) \approx 1 + i(2/\pi)[\gamma + \ln(t/2)] \quad (\text{B.4})$$

and

$$H_0^{(1)}(t) \approx \cos(t/\sqrt{2}) + i(2/\pi)[\gamma + \ln(t/2)] \cos(t/\sqrt{2}). \quad (\text{B.5})$$

after neglecting higher order terms. Self term approximations given here are based on (B.4) and (B.5).

Matrix element approximations involving the Hankel function with a difference argument are derived from the expansion

$$H_0^{(1)}(D-t) = \sum_{k=-\infty}^{\infty} H_k^{(1)}(D) J_k(t) \quad |D| > |t| \quad (\text{B.6})$$

as is given by Olver (1964, p. 363). Use of this infinite series allows the D and t dependence to be separated. Mutual term approximations given here are based on (B.1), (B.2), and (B.6).

B.1 The Self Terms for a Pulse Basis Function

Self term matrix elements for pulse expansion functions are proportional to

$$\int_0^H H_0^{(1)}(t) dt = \int_0^H J_0(t) dt + i \int_0^H Y_0(t) dt \quad (\text{B.7})$$

where $J_0(t)$ and $Y_0(t)$ are the Bessel functions of the first and second kinds. Two numerical approximations to this integral will be compared using the approximation given by (2.4) and (2.5) of Chapter 4 as the standard. Substituting (B.4) and (B.5) in (B.7) yields the approximations

$$\int_0^H H_0^{(1)}(t) dt \approx H + i(2/\pi)[\gamma + \ln(H/2) - 1]H \quad (\text{B.8})$$

and

$$\int_0^H H_0^{(1)}(t) dt \approx \sqrt{2} \sin(H/\sqrt{2}) + i(2/\pi) [\gamma + \ln(H/2)] \sqrt{2} \sin(H/\sqrt{2}) - i(2/\pi) H [\sin(H/\sqrt{8}) / (H/\sqrt{8})]^2. \quad (B.9)$$

Table B.1 summarizes the accuracy of these approximations. (B.8) is good to three digits for H less than 0.1. The usefulness of (B.9) is limited by its imaginary part which is good to three digits for H less than 0.2. In conclusion, it appears that (B.9) gives roughly the same accuracy at $2H$ as (B.8) does at H .

B.2 The Mutual Terms for a Pulse Basis Function

Mutual term matrix elements for pulse expansion functions are written as

$$\int_{-H}^H H_0^{(1)}(D-t) dt \quad (B.10)$$

where $2H$ is the subsection width and $D = 2nH$ for $n = 1, 2, \dots$. Several approximations to (B.10) are studied. Substituting (B.6) in (B.10), one obtains

$$\int_{-H}^H H_0^{(1)}(D-t) dt = 2 \sum_{k=0}^{\infty} \epsilon_k H_{2k}^{(1)}(D) \int_0^H J_{2k}(t) dt \quad (B.11)$$

where

$$\epsilon_k = \begin{cases} 1 & k = 0 \\ 2 & k > 0. \end{cases} \quad (B.12)$$

Retaining the first two terms gives the approximation

$$\int_{-H}^H H_0^{(1)}(D-t) dt \approx 2 H_0^{(1)}(D) \int_0^H J_0(t) dt + 4 H_2^{(1)}(D) \int_0^H J_2(t) dt. \quad (B.13)$$

Table B.1

Digits of Accuracy and Decimal Offset Factors for Pulse Expansion Function
Self Term Matrix Element Approximations

Approximations to $\int_0^H H_0^{(1)}(t)dt$	H = 0.05		H = 0.1		H = 0.2		H = 0.4	
	Real	Imag.	Real	Imag.	Real	Imag.	Real	Imag.
A	3.7	3.6	3.1	3.0	2.5	2.4	1.9	1.8
B	8.2	4.4	7.0	3.7	5.8	3.0	4.6	2.3
decimal offset factor	1.30	0.88	1.00	0.66	0.70	0.46	0.40	0.29

$$A = H + i(2/\pi)[\gamma + \ln(H/2) - 1]H$$

$$B = \sqrt{2} \sin(H/\sqrt{2}) + i(2/\pi)[(\gamma + \ln \frac{H}{2}) \sqrt{2} \sin(H/\sqrt{2}) - H\{\sin(H/\sqrt{8})/(H/\sqrt{8})\}^2]$$

The integral of $J_2(t)$ may be approximated by remembering that

$$J_2(t) \approx \frac{1}{8} t^2 \cos(t/\sqrt{6}) \quad (\text{B.14})$$

for small t . Integrating by parts and dropping higher order terms, one obtains

$$\int_0^H J_2(t) dt \approx (H^3/24) \cos(H/\sqrt{6}) \quad (\text{B.15})$$

for small H . Using this in (B.13) yields the first approximation

$$\int_{-H}^H H_0^{(1)}(D-t) dt \approx 2H_0^{(1)}(D) \int_0^H J_0(t) dt + H_2^{(1)}(D) \frac{H^3}{6} \cos(H/\sqrt{6}). \quad (\text{B.16})$$

All of the functions given on the right-hand side of the equal sign are evaluated to double precision accuracy using the appropriate subprograms.

The second approximation is obtained from (B.2) and (B.16) and is

$$\int_{-H}^H H_0^{(1)}(D-t) dt \approx 2\sqrt{2} H_0^{(1)}(D) \sin(H/\sqrt{2}) + H_2^{(1)}(D) \frac{H^3}{6} \cos(H/\sqrt{6}). \quad (\text{B.17})$$

The third and fourth approximations are obtained by dropping the $H_2^{(1)}(D)$ terms in (B.16) and (B.17). These are

$$\int_{-H}^H H_0^{(1)}(D-t) dt = (2H)H_0^{(1)}(D) \quad (\text{B.18})$$

and

$$\int_{-H}^H H_0^{(1)}(D-t) dt = 2\sqrt{2} \sin(H/\sqrt{2}) H_0^{(1)}(D) \quad (\text{B.19})$$

The four approximations are compared in Table B.2 by using (2.6) of Chapter 4 as the standard. Careful study of this table reveals that the imaginary

Table B.2

Digits of Accuracy and Decimal Offset Factors for Pulse Expansion Function
Matrix Element Approximations--the Mutual Terms

Approximations to $\int_{-H}^H H_0^{(1)}(D-t)dt$	subsection width	D = 2H		D ≈ 10H		D > 4 estimated median	
		Real	Imag.	Real	Imag.	Real	Imag.
$(2H)H_0^{(1)}(D)$	0.1	3.7	1.7	3.7	2.6	3.3	3.3
	0.4	2.5	1.4	2.7	2.1	2.1	2.1
$2\sqrt{2} \sin(H/\sqrt{2})H_0^{(1)}(D)$	0.1	6.6	1.7	5.2	2.6	3.5	3.5
	0.4	4.2	1.3	2.7	2.4	2.4	2.4
$2H_0^{(1)}(D) \int_0^H J_0(t)dt$	0.1	10.7	2.9	9.2	5.1	7.7	7.5
	0.4	7.0	2.4	5.2	4.9	5.4	5.4
$+ H_2^{(1)}(D)(H^3/6) \cos(H/\sqrt{6})$	0.1	8.2	2.9	8.2	5.1	7.9	7.6
	0.4	5.7	2.4	5.0	4.9	5.7	5.7
$2\sqrt{2} H_0^{(1)}(D) \sin(H/\sqrt{2})$	0.1	1.0	0.8	1.0	1.4	1.8	1.8
	0.4	0.4	0.6	0.7	0.8	1.2	1.2
decimal offset							
factor							

parts for adjacent elements are the least accurate. The expressions (B.16) and (B.17) are accurate to almost three digits while (B.18) and (B.19) are accurate to almost two digits. For accuracy to three digits, (B.16) or (B.17) should be used, if only for adjacent elements.

A final approximation is derived for the evaluation of adjacent elements. This is obtained by writing

$$\int_{-H}^H H_0^{(1)}(D-t)dt = \int_0^{D+H} H_0^{(1)}(t)dt - \int_0^{D-H} H_0^{(1)}(t)dt \quad (B.20)$$

and using either (B.8) or (B.9) to evaluate the integrals on the right. Table B.3 gives the accuracy of such a scheme for small H and D. These numbers show that (B.20) is slightly better for small D and small H than are (B.16) through (B.19), but that the error increases very rapidly as D or H is increased.

B.3 The Self Terms for an Inverse Square Root Basis Function

The self term due to an inverse square root expansion function is

$$\int_0^H t^{-\frac{1}{2}} H_0^{(1)}(t) dt. \quad (B.21)$$

Substituting (B.4) and (B.5) in (B.21), one obtains

$$\int_0^H t^{-\frac{1}{2}} H_0^{(1)}(t) dt = 2\sqrt{H} (1 + i(2/\pi)[\gamma + \ln(H/2) - 2]) \quad (B.22)$$

and

$$\begin{aligned} \int_0^H t^{-\frac{1}{2}} H_0^{(1)}(t) dt = & 2^{\frac{1}{4}} \text{Re} F_2(H/\sqrt{2}) + \\ & + i(4/\pi)[(\gamma + \ln \frac{1}{2} H) 2^{\frac{1}{4}} \text{Re} F_2(H/\sqrt{2}) - 2\sqrt{2} \text{Re} F_2(H/2)] \end{aligned} \quad (B.23)$$

where F_2 is a form of the Fresnel integral and is

Table B.3

Digits of Accuracy and Decimal Offset Factors for
Pulse Expansion Function Matrix Element Approximations
for Small H and D

Approximations to					
$\int_{-H}^H H_0^{(1)}(D-t)dt$	sub- section width	D = 2H		D = 4H	
	2H	Real	Imag.	Real	Imag.
1	0.1	2.6	2.4	2.0	1.8
	0.2	2.0	1.8	1.4	1.4
2	0.1	6.1	3.0	5.0	2.3
	0.2	4.9	2.3	3.8	1.5
decimal offset factor	0.1	1.0	0.8	1.0	1.0
	0.2	0.7	0.7	0.7	0.9

$$\int_{-H}^H H_0^{(1)}(D-t)dt = \int_0^{D+H} H_0^{(1)}(t)dt - \int_0^{D-H} H_0^{(1)}(t)dt$$

1: for $\int_0^x H_0^{(1)}(t)dt$ use Equation (B.8).

2: for $\int_0^x H_0^{(1)}(t)dt$ use Equation (B.9).

$$F_2(y) = \int_0^{\sqrt{y}} e^{it^2} dt. \quad (B.24)$$

The above approximations are compared in Table B.4 using the Chebyshev expansions of (2.12) and (2.13) of Chapter 4 as the standard. Equation (B.22) provides three digit accuracy for small H while (B.23) provides three digit accuracy for H as large as 0.4.

B.4 The Mutual Terms for an Inverse Square Root Basis Function

Mutual terms for an inverse square root expansion function may be written as

$$\int_0^H t^{-\frac{1}{2}} H_0^{(1)}(D-t) dt. \quad (B.25)$$

Substituting (B.6) in (B.25), one obtains

$$\int_0^H t^{-\frac{1}{2}} H_0^{(1)}(D-t) dt = \sum_{k=0}^{\infty} \epsilon_k H_k^{(1)}(D) \int_0^H t^{-\frac{1}{2}} J_k(t) dt \quad (B.26)$$

where ϵ_k is defined by (B.12). The first approximation is obtained by retaining only the first two terms of the series in (B.26). This yields

$$\int_0^H t^{-\frac{1}{2}} H_0^{(1)}(D-t) dt \approx H_0^{(1)}(D) \int_0^H t^{-\frac{1}{2}} J_0(t) dt + 2H_1^{(1)}(D) \int_0^H t^{-\frac{1}{2}} J_1(t) dt. \quad (B.27)$$

The second approximation uses (B.2) and the result

$$J_1(t) \approx \frac{t}{2} \cos(t/2), \quad (B.28)$$

for small t, in (B.27) to obtain

$$\int_0^H t^{-\frac{1}{2}} H_0^{(1)}(D-t) dt \approx 2^{\frac{1}{2}} H_0^{(1)}(D) \operatorname{Re} F_2(H/\sqrt{2}) + \frac{2}{3} H_1^{(1)}(D) H^{\frac{3}{2}} \cos(H/2). \quad (B.29)$$

Table B.4

Digits of Accuracy and Decimal Offset Factors for Inverse Square Root Expansion
Function Self Term Matrix Element Approximations

Approximations to $\int_0^H t^{-1/2} H_0^{(1)}(t) dt$	H = 0.05		H = 0.1		H = 0.2		H = 0.4	
	Real	Imag.	Real	Imag.	Real	Imag.	Real	Imag.
A	3.9	4.0	3.3	3.4	2.7	2.8	2.1	2.2
B	8.4	5.0	7.2	4.3	6.0	3.7	4.8	3.0
decimal offset factor	0.35	-0.16	0.20	-0.25	0.05	-0.33	-0.10	-0.38

$$A = 2\sqrt{H} (1 + i(2/\pi)[\gamma + \ln(H/2) - 2])$$

$$B = 2^{1/4} {}_2\text{ReF}_2(H/\sqrt{2}) + i(4/\pi)[(\gamma + \ln \frac{H}{2}) {}_2^{1/4}\text{ReF}_2(H/\sqrt{2}) - \sqrt{2} {}_2\text{ReF}_2(H/2)]$$

$$F_2(y) = \int_0^{\sqrt{y}} e^{it^2} dt ; \text{ReF}_2(y) = \int_0^{\sqrt{y}} \cos(t^2) dt$$

The $H^{5/2}$ term arising in integration by parts is neglected. The third and fourth approximations are obtained by dropping the $H_1^{(1)}(D)$ term in (B.27) and using (B.1) and (B.2) for $J_0(t)$. These approximations become

$$\int_0^H t^{-\frac{1}{2}} H_0^{(1)}(D-t) dt \approx 2 H^{\frac{1}{2}} H_0^{(1)}(D) \quad (\text{B.30})$$

and

$$\int_0^H t^{-\frac{1}{2}} H_0^{(1)}(D-t) dt \approx 2^{\frac{1}{4}} H^{\frac{1}{2}} H_0^{(1)}(D) \operatorname{Re} F_2(H/\sqrt{2}). \quad (\text{B.31})$$

The accuracy of the approximations (B.27), (B.29), (B.30), and (B.31) is compared in Table B.5. The standard for comparison is given by (2.16) of Chapter 4. It is clear that none of the one or two term approximations are suitable for calculating the imaginary part for adjacent elements to three digits. Equations (B.30) and (B.31) appear to be useless for almost any D or H . Equations (B.27) and (B.29) may be useful for non-adjacent elements, but it too exhibits loss of digits for adjacent elements. This certainly limits its usefulness.

Table B.5

Digits of Accuracy and Decimal Offset Factors for Inverse Square Root Expansion
Function Matrix Element Approximations--the Mutual Terms

Approximations to $\int_0^H t^{-1/2} H_0^{(1)}(D-t) dt$	subsection half- width		D = 2H		D ≈ 10H		D > 4 estimated median	
	H		Real	Imag.	Real	Imag.	Real	Imag.
$2\sqrt{H} H_0^{(1)}(D)$	0.05		3.1	1.1	2.4	1.3	1.8	1.8
	0.2		1.9	0.7	1.1	1.2	1.3	1.3
$2^{1/4} 2H_0^{(1)}(D) \operatorname{Re} F_2(H/\sqrt{2})$	0.05		3.1	1.1	2.4	1.3	1.8	1.8
	0.2		1.9	0.7	1.1	1.2	1.3	1.3
$H_0^{(1)}(D) \int_0^H t^{-1/2} J_0(t) dt$ $+ 2H_1^{(1)}(D) \int_0^H t^{-1/2} J_1(t) dt$	0.05		6.8	1.9	5.4	2.8	3.9	3.9
	0.2		4.4	1.5	2.6	2.6	2.7	2.7
$2^{1/4} 2H_0^{(1)}(D) \operatorname{Re} F_2(H/\sqrt{2})$ $+ (2/3) H_1^{(1)}(D) (H^{3/2}) \cos(H/2)$	0.05		6.5	1.9	5.3	2.8	3.9	3.9
	0.2		4.1	1.5	2.5	2.6	2.7	2.7
decimal offset	0.05		0.35	0.13	0.38	0.68	1.1	1.2
factor	0.2		0.1	0.2	0.4	0.5	0.8	0.8

C. THE CHEBYSHEV APPROXIMATION FOR $\int_0^H t^{-\frac{1}{2}} H_0^{(1)}(t) dt$

The Chebyshev coefficients for the integral

$$\int_0^x t^{-\frac{1}{2}} H_0^{(1)}(t) dt = 2 \int_0^{\sqrt{x}} H_0^{(1)}(t^2) dt \quad (C.1)$$

are derived using techniques presented by Luke (1969, Volume I, p. 316). For simplicity, the coefficients will be evaluated for x between zero and one. The first step is to expand the Hankel function $H_0^{(1)}(t)$ in terms of Chebyshev polynomials over the range from zero to one. Luke gives

$$J_0(ax) = \sum_{n=0}^{\infty} A_n T_{2n}(x), \quad 0 \leq x \leq 1, \quad (C.2)$$

and

$$Y_0(ax) = \frac{2}{\pi} [\gamma + \ln \frac{1}{2}(ax)] J_0(ax) + \sum_{n=0}^{\infty} B_n T_{2n}(x), \quad 0 < x \leq 1. \quad (C.3)$$

Luke (1969, Volume II, pp. 37-38) gives expressions for A_n and B_n . These are

$$A_n = \epsilon_n (-)^n J_n^2(a/2) \quad (C.4)$$

and

$$B_n = \frac{2 \epsilon_n \left(\frac{a}{4}\right)^{2n} (-)^{n+1}}{\pi (n!)^2} \sum_{k=0}^{\infty} \frac{(-)^k \left(\frac{a}{2}\right)^{2k} (n+\frac{1}{2})_k h_{n+k}}{(n+1)_k (2n+1)_k k!} \quad (C.5)$$

where $h_0=0$, $h_k=\psi(k+1)-\psi(1) = \sum_{r=1}^k \frac{1}{r}$, $\epsilon_k=2, k>0$, $\epsilon_0=1$, $(z)_k$ is Pochhammer's symbol and ψ is the psi function. These coefficients for $a=1$ have been evaluated and are presented to thirty decimal places in Table C.1. Integrating (C.3) with weighting function $t^{-\frac{1}{2}}$, one obtains

$$\int_0^x t^{-\frac{1}{2}} Y_0(t) dt = \frac{2}{\pi} [\gamma + \ln \frac{1}{2} x] \int_0^x t^{-\frac{1}{2}} J_0(t) dt - \frac{2}{\pi} \int_0^x \frac{1}{t} \int_0^t y^{-\frac{1}{2}} J_0(y) dy dt + \int_0^x t^{-\frac{1}{2}} y_s(t) dt \quad (C.6)$$

where

$$y_s(t) = \sum_{n=0}^{\infty} B_n T_{2n}(x). \quad (C.7)$$

After substituting the Chebyshev series for $J_0(x)$ and $y_s(x)$ in (C.6), all of the integrals on the right-hand side reduce to the general form

$$\int_0^x t^{-\frac{1}{2}} \sum_{n=0}^{\infty} a_n T_{2n}(t) dt. \quad (C.8)$$

Integrals of this type have been studied by Luke (1969, Volume I, p. 316), among others. It may be shown that

$$\int_0^x t^{-\frac{1}{2}} \sum_{n=0}^{\infty} a_n T_{2n}(t) dt = \sqrt{x} \sum_{n=0}^{\infty} \frac{e_n}{2} T_{2n}(x) \quad (C.9)$$

where the e_n 's are evaluated from the a_n 's with

$$\frac{3}{4} e_1 + \frac{1}{2} e_0 = 2 a_0 - a_1$$

and

$$(n + \frac{3}{4}) e_{n+1} + (n + \frac{1}{4}) e_n = a_n - a_{n+1} \quad (C.10)$$

with e_{n+1} initially set to zero. The coefficients $[e_n/2]$ computed in this manner for the first integral on the right-hand side of (C.6) are used to write the second integral in the form (C.8) also. The coefficients calculated in this fashion are displayed in Table C.2. These coefficients were

checked for accuracy by comparing the numerical values of the Chebyshev series with those of the power series representations for the same integrals evaluated at $0.1n$, $n=0,1,\dots,10$. The two expansions were carried out to 32 decimal places and they agreed to at least 31 decimal places for all eleven arguments. The power series representations that were used are given by Luke (1962, pp. 44-45) as his equations 2.3(1) and 2.3(4).

D. COMPUTER PROGRAMS

Computer Program for E-polarization Half-Plane Current.

These routines were written by
Donald Farness Hanson between
February, 1975 and June, 1975.

C The following MAIN program solves the classical half-plane
C problem with plane wave incidence for the E-polarization (E-vector
C parallel to the edge) current minus the so-called physical optics
C current, (IE-IPO). This computer program is written in FORTRAN IV
C for the IBM 360 computer at the University of Illinois. The entire
C program as given here requires 129 seconds of IBM 360/75 computer
C time from beginning to end (29 seconds of compile time; 100 seconds
C of execution time). It compares a hybrid expansion with a
C pulse-everywhere expansion for the numerical solution of the
C integral equation by the method of moments. The hybrid basis
C function set used is one with a $1/\sqrt{z}$ expansion function in a
C half-width segment at the edge and with 199 full-width pulse
C expansion functions away from the edge. The pulse-everywhere basis
C function set used is one with a half-width pulse expansion function
C at the edge and with full-width pulse expansion functions away from
C the edge. Matrix elements are evaluated using methods which yield
C at least 10 decimal place accuracy. The almost-Toeplitz nature of
C this matrix is utilized by LTPLZ to cut down on required computer
C time. MAIN reserves storage locations for arrays which are passed
C as arguments through several levels of subprograms. ISPMOM sets up
C the required matrices and right-hand-side, and LTPLZ uses these
C matrices to form an inverse and generate the result. PNTOWT takes
C the result and compares it with the known analytic solution by
C printing out the respective real parts, imaginary parts, magnitudes,
C and phases along with their differences. PNTOWT also stores the
C results on disk for later use. MAIN calls ISPMOM, PULMOM, LTPLZ,
C and PNTOWT directly and many other subprograms indirectly. Refer to
C each of these routines for a list of the subprograms that they in
C turn call. The RESULTS of MAIN must be divided by $Z_0=376.731$ ohms
C in order to give units of (A/m)/(V/m).

C -----
C Dimension large arrays.
C -----

COMPLEX*16 IH0(200), ISRTH0(200), RHS(800), RESULT(800), Z1(200),
1 A(200), A1(200), IEMPO(200), HN1(32)
REAL*8 JN(88), JIN(32), SK(88), UN(88), TAD(4), DEZ, KZ(200),
1 XNORM, H
INTEGER NCASES, NSIZE, NH, NMAX, PNTOPT, IER, I
LOGICAL GORH(88), ROOT

C -----
C Set up angles of incidence for calculation.
C -----

DATA TAD/45.D0, 90.D0, 135.D0, 180.D0 /

C -----
C Set up parameters for run.
C -----

Computer Program for E-polarization Half-Plane Current.

Page 2

```

NSIZE=200
DEZ = 10.D0
NCASES=4
NH = 32
NMAX = 85
PNTOPT = 0

```

```

C-----
C   Set up matrices for hybrid expansion and evaluate
C   Right-Hand Sides.
C-----
      CALL ISPMOM(NCASES,TAD,DEZ,NSIZE,KZ,IH0,ISRTH0,RHS,NH,HN1,NMAX,
1 JN, JIN, SK, UN, GORH, PNTOPT )
C-----
C   Print values of matrix elements.
C-----
      PRINT 1, (KZ(I), IH0(I), ISRTH0(I), I=1, NSIZE )
1 FORMAT('1',T12,'MATRIX ELEMENTS '//T9,'X',T35,'IH0',T89,'ISRTH0'/
1 (T2,0PF10.3,T13,'<',1PD23.15,' ',1X,D23.15,'>',5X,'<',D23.15,
2 ' ',1X,D23.15,'>' ) )
C-----
C   Evaluate (IE-IPO) by matrix inversion for hybrid expansion.
C-----
      CALL LTPLZ( ISRTH0,IH0,Z1,A,A1,NSIZE,RHS,RESULT,NCASES,XNORM,IER)
      IF( IER .NE. 0 ) GO TO 10
      ROOT = .TRUE.
      H = 1.D0/(2.D0*DEZ)
C-----
C   Print out results for (IE-IPO) for hybrid expansion.
C-----
      CALL PNTOWT( TAD, NSIZE, NCASES, KZ, IEMPO, RHS, RESULT, ROOT, H )
C-----
C   Set up matrices for pulse-everywhere expansion.
C-----
      CALL PULMOM( DEZ, NSIZE, KZ, IH0, ISRTH0 )
C-----
C   Print values of matrix elements.
C-----
      PRINT 1, (KZ(I), IH0(I), ISRTH0(I), I=1, NSIZE )
C-----
C   Evaluate (IE-IPO) by matrix inversion for pulse-everywhere
C   expansion.
C-----
      CALL LTPLZ(ISRTH0,IH0,Z1,A,A1,NSIZE,RHS,RESULT,NCASES,XNORM,IER)
      IF( IER .NE. 0 ) GO TO 10
C-----
C   Print out results for (IE-IPO) for pulse-everywhere expansion.
C-----
      ROOT = .FALSE.
      CALL PNTOWT( TAD, NSIZE, NCASES, KZ, IEMPO, RHS, RESULT, ROOT, H)
      STOP
10 PRINT 5
5 FORMAT('0CAME TO 10 IN MAIN.' )
      STOP
      END

```


C Subroutine ISPMOM fills the matrices that are required as input
 C to the matrix inversion routine LTPLZ for the hybrid basis function
 C case. These arrays are ISRTH0, IH0, and RHS. All other parameters
 C in the parameter list are either inputs or dimensioned arrays. IH0
 C is an output vector of length NSIZE which is filled with numbers
 C corresponding to the first column of the Toeplitz matrix which
 C results when double-wide pulses are used throughout as basis
 C functions. ISRTH0 is an output vector of length NSIZE which is
 C filled with numbers corresponding to the $1/\text{SQRT}(z)$ half-wide initial
 C subsection. RHS is an output array of length NC*NSIZE which is
 C filled with the values of the Right-Hand Side for (IE-IPO) for each
 C of the angles of incidence THETAD=45, 90, 135, and 180. KZ is an
 C output array of length NSIZE and contains the values of the match
 C points. NC, TAD, DEZ, NSIZE, NH, NMAX, and PNTOPT are all input
 C parameters. NC is the number of cases or angles to be
 C considered(NC=4). TAD is an array of the angles and is of length
 C NC. DEZ is one over the subsection width. NSIZE is the number of
 C subsections. NH is the number of terms to be taken in sums of
 C weighted Hankel functions and must be 32 or less. NMAX is the
 C number of terms to be taken in sums of Bessel functions. PNTOPT is
 C the underflow/overflow printing option(see HANKEL). HN1 and JIN are
 C arrays of length NH(see GTJN, HANKEL). JN, GORH, SK, and UN are
 C arrays of length NMAX(see BESSEL, SKS, and UNS). ISPMOM directly
 C calls GTJN, SELFTM, SELFSN, SUMINC, IA2BH0, BESSEL, HANKEL, SKS,
 C SUMHJI, and UNS. Refer to each of these routines for a list of the
 C subprograms that each in turn calls.

```

C-----
SUBROUTINE ISPMOM(NC,TAD,DEZ,NSIZE,KZ,IH0,ISRTH0,RHS,NH,HN1,NMAX,
1 JN,JIN,SK,UN,GORH,PNTOPT)
  COMPLEX*16 SELFTM, SELFSN, IH0(1), ISRTH0(1), ESUM, RHS(1),H01,
1 HN1(1), IA2BH0, SUM, IZIH01
  REAL*8 H, JI0, JIN(1), ZETA, KZ(1), THETAD, TAD(1), UPLIM, LOWLIM,
1 FN, DFLOAT, J0, JN(1), S0, SK(1), UN(1), DEZ, TDEZ
  INTEGER NM, NMAX, PNTOPT, PN, OFFSET, J, NH, N, NP1, NPNP1, NSIZE,
1 NC, I, NSM1
  LOGICAL GORH(1), T/.TRUE./
  TDEZ = 2.D0*DEZ
  H = 1.D0/TDEZ
  PN = PNTOPT
  NM = NMAX
  NSM1 = NSIZE-1
  
```

C-----
 C Calculate values of JIN for later use in SUMHJI.
 C-----

```

CALL GTJN( H, NH, JI0, JIN, PN )
ZETA = 0.D0
KZ(1) = 0.D0
  
```

C-----
 C Fill IH0 and ISRTH0 matrices.
 C-----

```

  IH0(1) = SELFTM(H)
  ISRTH0(1) = SELFSN(H)
  DO 1 J = 1, NC
    OFFSET = (J-1)*NSIZE
    THETAD = TAD(J)
  
```



```

      CALL SUMINC(ZETA, THETAD, 1, UN, JN, S0, SK, ESUM, PN )
1  RHS( OFFSET + 1 ) = ESUM
      UPLIM = H
      DO 2 N=1, NSM1
      NP1 = N+1
      NPNP1 = N+N+1
      FN = DFLOAT( NPNP1 )
      ZETA = DFLOAT(N)/DEZ
      KZ(NP1) = ZETA
      LOWLIM = UPLIM
      UPLIM = FN/TDEZ
      IH0(NP1) = IA2BH0(LOWLIM, UPLIM )
C-----
C      Calculate matrix element corresponding to 1/SQRT(z) initial
C      subsection, ISRTH0.
C-----
      CALL HANKEL( ZETA, NH, T, H01, HN1, &100, PN )
      CALL SUMHJI( NH, H01, HN1, JI0, JIN, SUM, PN )
      ISRTH0(NP1) = SUM
C-----
C      Calculate values of the Right-Hand Side.
C-----
      CALL BESSEL( ZETA, NM, GORH, J0, JN, &100, PN )
      CALL SKS( ZETA, NM, S0, SK, PN )
      DO 2 J=1, NC
      OFFSET = (J-1)*NSIZE
      THETAD = TAD(J)
      CALL UNS( THETAD, NM, UN )
      CALL SUMINC( ZETA, THETAD, NM, UN, JN, S0, SK, ESUM, PN )
2  RHS( OFFSET+NP1) = ESUM
      RETURN
100 PRINT 3
3  FORMAT( '0FROM ISPMOM, WENT TO 100.' )
      STOP
      END

```


C Subroutine PULMOM fills the matrices that are required as input
 C to the matrix inversion routine LTPLZ for the pulse-everywhere basis
 C function case. DEZ, NSIZE, and KZ are inputs and IH0 and IHWH0 are
 C outputs. DEZ is one over delta z, the subsection width. NSIZE is
 C the number of subsections. KZ is an array of length NSIZE of the
 C match points. IH0 is the same as in ISPMOM. IHWH0 is an array of
 C length NSIZE filled with numbers corresponding to the half-width
 C pulse initial subsection. PULMOM directly calls SELFTM and IA2BH0.
 C Refer to these routines for a list of their called subprograms.

```
C-----
SUBROUTINE PULMOM( DEZ, NSIZE, KZ, IH0, IHWH0 )
  INTEGER NSIZE
  COMPLEX*16 IH0(NSIZE), IHWH0(NSIZE), SELFTM, IZIH01, IA2BH0
  REAL*8 DEZ, KZ(NSIZE), H, FN, DFLOAT, ZETA, LOWLIM, UPLIM
  INTEGER I, N, NP1, NPNP1, NSM1, OFFSET
  H = 1.D0/(2.D0*DEZ)
```

```
C-----
C Fill IH0 and IHWH0.
```

```
C-----
  IH0(1) = SELFTM(H)
  IHWH0(1) = IH0(1)/2.D0
  UPLIM = H
  NSM1 = NSIZE - 1
  DO 2 N=1, NSM1
    NP1 = N+1
    NPNP1 = N+N+1
    FN = DFLOAT( NPNP1 )
    ZETA = KZ( NP1 )
    LOWLIM = UPLIM
    UPLIM = FN/(2.D0*DEZ)
    IH0(NP1) = IA2BH0( LOWLIM, UPLIM )
  2 IHWH0( NP1 ) = IA2BH0( ZETA-H, ZETA )
  RETURN
END
```


C Subroutine SUMHJI calculates a matrix element associated with
 C the $1/\sqrt{z}$ edge expansion function for the hybrid case. SUM is
 C given by

$$\text{SUM} = \text{JI0} * \text{H01} + 2 \sum_{\text{N}=1}^{\text{NMAX}} (\text{JIN} * \text{HN1})$$

C where JI0 and JIN are the outputs of GTJN, and H01 and HN1 are the
 C outputs of HANKEL. NMAX must be 1 or more, but 32 or less (see
 C HANKEL). PNTOPT is the underflow printing option (see HANKEL).
 C SUMHJI calls UNDRFL.

```

C-----
SUBROUTINE SUMHJI(NMAX, H01, HN1, JI0, JIN, SUM, PNTOPT )
COMPLEX*16 SUM, H01, HN1(1), S(2), CBAR, ZERO/(0.D0,0.D0)/
REAL*8 JI0, JIN(1), CC(2)
INTEGER NMAX, KB, K, PNTOPT, PNTOP
LOGICAL UFL
EQUIVALENCE( CBAR, CC )
EXTERNAL UNDRFL
COMMON/$2/ UFL
COMMON/$3/ PNTOP
UFL = .FALSE.
PNTOP = PNTOPT
IF( PNTOP-1 ) 100, 102, 100
100 CALL ERRSET( 208, 320, -1, 1, UNDRFL )
GO TO 1
102 CALL ERRSET( 208, 320, 0, 0, UNDRFL )
1 UFL = .TRUE.
S(1) = JI0*H01
S(2) = ZERO
  
```

C Sum in the BACKWARD direction.

```

C-----
DO 2 K=1, NMAX
KB = NMAX - K + 1
  
```

C If JIN is zero, do not sum for this K.

```

C-----
IF( JIN(KB) .EQ. 0.D0 ) GO TO 2
  
```

C If the overflow flag for the imaginary part of HN1 is detected,
 C skip this term.

```

C-----
CBAR = HN1(KB)
IF( CC(2) .EQ. -1.D70 ) GO TO 2
S(2) = S(2) + HN1(KB)*JIN(KB)
2 CONTINUE
UFL = .FALSE.
SUM = S(1) + S(2) + S(2)
RETURN
END
  
```


C Subroutine SUMINC evaluates the right-hand side for (IE-IPO)
 C for a given displacement X and angle of incidence THETAD. The
 C right-hand side is evaluated as sums of Chebyshev polynomials UN
 C weighted with Bessel functions JN and with a function whose name was
 C coined as S. ESUM is evaluated using equations 10.3(3) and
 C 10.3(10), pages 239 and 240, of Luke's, "Integrals of Bessel
 C Functions." UN is the output array of UNS for angle THETAD. JN
 C is the output array of BESSEL and S0 and SK are the outputs of SKS.
 C Refer to these routines for the details. PNTOPT is the underflow
 C printing option(see HANKEL). NMAX is the number of terms to be
 C taken and must be 2 or more. Accurate results to about 10 decimal
 C places are generated for NMAX=85 and X=20. Results for X between 20
 C and 40 are accurate to at least one decimal place when NMAX=85.
 C SUMINC calls UNDRFL.

```

C-----
      SUBROUTINE SUMINC( X, THETAD, NMAX, UN, JN, S0, SK, ESUM, PNTOPT )
      COMPLEX*16 DCMPLX, ESUM, T1, T2, IB, I/(0.D0,1.D0)/,
1     ZERO/(0.D0,0.D0)/
      REAL*8 X, THETAD, UN(1), JN(1), S0, SK(1), SJ(2), SY(2), DLOG,
1     DABS, DSIN, DCOS, PRODJ, PRODY, THETA, CTA, STA, ARG
      REAL*8 TWOPI/0.63661977236758134308D0/,
1     GAMMA/0.57721566490153286061D0/,PI/3.14159265358979323846D0/
      INTEGER NMAX, KB, K, PNTOPT, PNTOP, NMML, MOD, L1
      LOGICAL UFL
      EXTERNAL UNDRFL
      COMMON/$2/ UFL
      COMMON/$3/ PNTOP
      IF( X .EQ. 0.D0 ) GO TO 7
      UFL = .FALSE.
      PNTOP = PNTOPT
      IF( PNTOP-1 ) 100, 102, 100
100 CALL ERRSET( 208, 320, -1, 1, UNDRFL )
      GO TO 1
102 CALL ERRSET( 208, 320, 0, 0, UNDRFL )
      1 NMML = NMAX-1
      SJ(1) = 0.D0
      SY(1) = 0.D0
      SJ(2) = 0.D0
      SY(2) = 0.D0

```

```

C-----
C     Perform sums in BACKWARD direction.
C-----

```

```

      DO 6 K = 1, NMML
      KB = NMML-K+1
      UFL = .TRUE.
      PRODJ = UN(KB)*JN(KB+1)
      PRODY = UN(KB)*SK(KB)
      UFL = .FALSE.

```

```

C-----
C     Treat i**K by making appropriate jumps.
C-----

```

```

      L1 = MOD(KB, 4 ) + 1
      GO TO (2,3, 4,5), L1
      PRINT 10
10  FORMAT('0', 75X, 'BAD GO TO IN SUMINC.' )

```



```

      STOP
2  SJ(1) = SJ(1) + PRODJ
   SY(1) = SY(1) + PRODY
   GO TO 6
3  SJ(2) = SJ(2) - PRODJ
   SY(2) = SY(2) - PRODY
   GO TO 6
4  SJ(1) = SJ(1) - PRODJ
   SY(1) = SY(1) - PRODY
   GO TO 6
5  SJ(2) = SJ(2) + PRODJ
   SY(2) = SY(2) + PRODY
6  CONTINUE
   SJ(1) = SJ(1) + JN(1)
   SY(1) = SY(1) + S0
C-----
C   Complete the evaluation of ESUM.
C-----
      THETA = (THETAD/180.D0)*PI
      CTA = DCOS( THETA )
      IF( THETAD .EQ. 90.D0 ) CTA = 0.D0
      STA = DSIN( THETA )
      T1 = DCMLPX( SJ(1), SJ(2) )
      T2 = DCMLPX( SY(1), SY(2) )
      IB = T1+TWOPI*I*((GAMMA+DLOG(X/2.D0))*T1 - T2 )
      ARG = X*CTA
      ESUM = 4.D0*((THETAD/180.D0)*DCMLPX(DCOS(ARG),-DSIN(ARG)) - STA*IB)
      RETURN
C-----
C   Treat the special case X=0.
C-----
7  ESUM = DCMLPX( 4.D0*(THETAD/180.D0), 0.D0 )
   RETURN
END

```



```

C      Subroutine UNS evaluates the Chebyshev polynomials
C      UN( cos(THETA) ) for N from one to NMAX (U0(cos(THETA))=1). The
C      recursion relation 3.5.1(14) from Luke's book, "The Special
C      Functions and Their Approximations" is used. The result accumulates
C      error quickly, so special measures were taken to insure 10 decimal
C      place accuracy for NMAX up to 85 and for any THETA between 0 and 180
C      degrees which is an exact multiple of 15 degrees. THETA is the
C      angle of incidence in degrees. NMAX is the order of the highest
C      order Chebyshev polynomial to be found. UN is an array of length
C      NMAX containing the values of UN( cos(THETA) ). These numbers are
C      used in SUMINC. UNS is complete by itself. It calls no other
C      subprograms.

```

```

C-----
      SUBROUTINE UNS( THETA, NMAX, UN )
      REAL*8 THETA, X, DCOS, F, UN(1), TA, RTA
      REAL*8 PI/3.141592653589793D0/
      INTEGER NMAX, I, ITHETA, MOD, ICHECK
      RTA = PI*(THETA/180.D0)
      X = DCOS(RTA)
      UN(1) = X + X
      IF( THETA .EQ. 90.D0 ) UN(1) = 0.D0
      IF( NMAX .EQ. 1) RETURN
      F = UN(1)
      UN(2) = F*F - 1.D0
      IF( THETA .EQ. 60.D0 ) UN(2) = 0.D0
      IF( NMAX .EQ. 2 ) RETURN

```

```

C-----
C      Determine if THETA is a multiple of 15.
C-----

```

```

      ITHETA = THETA
      TA = ITHETA
      IF( (THETA-TA) .NE. 0.D0 ) GO TO 2
      IF( MOD(ITHETA, 15) .NE. 0 .OR. MOD(ITHETA,180) .EQ. 0 ) GO TO 2
      ICHECK = ITHETA + ITHETA + ITHETA

```

```

C-----
C      Evaluate UN for THETA multiple of 15.
C-----

```

```

      DO 1 I=3, NMAX
      ICHECK = ICHECK + ITHETA
      UN(I) = F*UN(I-1) - UN(I-2)
      IF( MOD(ICHECK, 180) .EQ. 0 ) UN(I) = 0.D0
1 CONTINUE
      RETURN

```

```

C-----
C      Evaluate UN for THETA not a multiple of 15.
C-----

```

```

      2 DO 3 I = 3, NMAX
      3 UN(I) = F*UN(I-1) - UN(I-2)
      RETURN
      END

```


C Subroutine SKS evaluates the terms which don't depend on THETA
 C of the non-logarithmic term of the integral from zero to X of
 C $\exp(it\cos(\text{THETA}))Y_0(t)dt$ as given by 10.3(10a) on page 240 of Luke's
 C "Integrals of Bessel Functions." This is an infinite power series
 C depending on m and k(see Luke). The function name was coined to be
 C $S(K,X)$. S_0 is the value of this function for $K=0$ and SK is an array
 C of values for K from 1 to NMAX. These numbers are used in SUMINC.
 C For X less than 20, NMAX should be at least 51 for convergence.
 C PNTOPT is the underflow printing option(see HANKEL). SKS was
 C checked by comparison of these results with those obtained by
 C expanding S in a series of Bessel functions, eq. 10.3(10b) of Luke.
 C SKS calls UNDRFL.

```
C-----
      SUBROUTINE SKS( X, NMAX, S0, SK, PNTOPT )
      REAL*8 X, S0, SK(1), KFACTR, HMF, XO2, XO2SQ, H0, FK, H, P,
1    MFACTR, FM, FMK1, DABS, DFLOAT
      INTEGER NMAX, PNTOPT, PNTOP, KP1, K, M, NMP1
      EXTERNAL UNDRFL
      LOGICAL UFL
      COMMON/$2/ UFL
      COMMON/$3/ PNTOP
      UFL = .FALSE.
      PNTOP = PNTOPT
      IF( PNTOP - 1 ) 100, 102, 100
100  CALL ERRSET(208, 320, -1, 1, UNDRFL )
      GO TO 1
102  CALL ERRSET( 208, 320, 0, 0, UNDRFL )
      1 NMP1 = NMAX+1
      XO2 = X/2.D0
      XO2SQ = XO2*XO2
      KFACTR = 1.D0
      H0 = 0.D0
      DO 5 KP1 = 1, NMP1
      K = KP1 - 1
      FK = DFLOAT(K)
      IF( KFACTR.EQ. 0.D0 ) GO TO 3
      H0 = H0 + 1.D0/(FK+1.D0)
      H = H0
      P = H0
      MFACTR = 1.D0
      M=1
      2 FM = DFLOAT(M)
      FMK1 = FM+FK+1.D0
      H = H + 1.D0/FMK1
      MFACTR = -MFACTR*(XO2SQ/(FM*FMK1))
      HMF = H*MFACTR
      P = P + HMF
C-----
```

C Test for convergence to 15 decimal places.

```
C-----
      IF( DABS( HMF ) .LT. 1.D-15 ) GO TO 3
      M = M + 1
      GO TO 2
      3 UFL = .TRUE.
      KFACTR = KFACTR*(XO2/(FK+1.D0))
```


Computer Program for E-polarization Half-Plane Current.

Page 11

```
UFL = .FALSE.
```

```
C-----  
C    Catch underflow before it occurs(possibly).  
C-----
```

```
    IF( DABS(KFACTR) .LT. 1.D-70) KFACTR = 0.D0  
    IF( K .NE. 0 ) GO TO 4  
    S0 = P*KFACTR  
    GO TO 5  
4 SK(K) = P*KFACTR  
5 CONTINUE  
    RETURN  
    END
```


C Function I0XH01 evaluates the integral from zero to X of
 C H01(t)dt using Chebyshev polynomials as given in Table 27 on page
 C 334 of Volume II of Luke's book, "The Special Functions and Their
 C Approximations." This routine is used to evaluate elements in the
 C matrix for pulse expansion functions. I0XH01 is used by IA2BH0,
 C IZIH01, and SELFTM. I0XH01 calls EAT2Pl.

```

C-----
      COMPLEX FUNCTION I0XH01*16(X)
      IMPLICIT REAL*8 (D)
      COMPLEX*16 DCMPLX
      REAL*8 XX, X, XO8, GAMMA, TWOPI, IJ0, SUMY, A(17), B(17)
      DATA A/0.00150D-15, -0.09949D-15, 5.79477D-15, -0.0029408710D-10,
1 0.1286892765D-10, -4.7960704238D-10, 0.001500207418186D-5,
2 -0.038695337761818D-5, 0.805230017147464D-5, -13.148973200727470D
3 -5, 0.00162455576482273217D0, -0.01444107253850054169D0,
4 0.08576038744155828731D0, -0.30180691211699830875D0,
5 0.50821888566078927112D0, -0.36520274074158537488D0,
1 1.29671754121052984167D0/, B/0.00324D-15, -0.21031D-15,
2 11.99595D-15, -0.0059495975D-10, 0.2537749742D-10,
3 -9.1898449486D-10, 0.002781957053702D-5, -0.069083540549799D-5,
4 1.374382109086322D-5, -21.244292114418655D-5,
5 0.00244754014990944840D0, -0.01978679701180859820D0,
6 0.10180664216242309366D0, -0.27450260739390063315D0,
7 0.19604604501712995275D0, 0.16707193818110339620D0,
8 1.52325892745358903192D0/
      DATA TWOPI/0.63661977236758134308D0/,
1 GAMMA/0.57721566490153286061D0/
      XX = DABS(X)
      IF( XX .GT. 8.D0 ) GO TO 2
      IF( XX .EQ. 0.D0 ) GO TO 1
      XO8 = XX*0.125D0
C-----
C        Sum the Chebyshev series.
C-----
      CALL EAT2Pl(XO8, 16, A, IJ0 )
      CALL EAT2Pl( XO8, 16, B, SUMY )
      I0XH01 = DCMPLX(IJ0, TWOPI*(GAMMA+DLOG(XX*0.5D0) ) * IJ0 - SUMY )
      RETURN
C-----
C        Treat the special case X=0.
C-----
1 I0XH01 = DCMPLX( 0.D0, 0.D0 )
      RETURN
C-----
C        STOP if X is greater than 8.
C-----
2 PRINT 3, XX
3 FORMAT('0',70X,'I0XH01 WAS CALLED WITH ARGUMENT X=',G20.12,'.'//)
      STOP
      END

```


Computer Program for E-polarization Half-Plane Current.

Page 13

C Function IZIH01 evaluates the integral from X to infinity of
 C H01(t)dt using Chebyshev polynomials as given in Table 27 on page
 C 335 of Volume II of Luke's book, "The Special Functions and Their
 C Approximations." This routine is used to evaluate elements in the
 C matrix for pulse expansion functions. IZIH01 is used by IA2BH0.
 C IZIH01 calls EATSTR.

```

C-----
      COMPLEX FUNCTION IZIH01*16(X)
      IMPLICIT REAL*8(D)
      COMPLEX*16 DCMPLX, I0XH01, IOZ, EOR, ONE/(1.D0,0.D0)/
      REAL*8 XX, X, FOX, PIO4, R2OPI, XPPIO4, RC(26), IC(26), RECT, IECT
      DATA RC/-.03489D-15, 0.16683D-15, -.051320D-15, 1.07730D-15,
1 -0.80559D-15, -5.70713D-15, 36.07236D-15, -127.37706D-15,
2 288.66165D-15, -151.48359D-15, -.0242797151D-10,
3 0.1490480479D-10, -.05151791688D-10, 0.8916779341D-10,
4 2.3353692269D-10, -27.8292764282D-10, 128.5294903326D-10,
5 -268.5706468353D-10, -.010699959818439D-5, 0.141140889467207D-5,
6 -.0682861017202808D-5, -.0208371347609414D-5, 36.927699265513937D-5,
7 -.00327411179733924011D0, -.01622955223898783538D0,
8 0.98740761581488426270D0/, IC/ -.05463D-15, 0.07387D-15,
1 0.09161D-15, -1.06272D-15, 4.39396D-15, -12.15265D-15,
2 19.76575D-15, 17.95082D-15, -292.98739D-15, 0.0133843845D-10,
3 -.0382166065D-10, 0.0480015078D-10, 0.2163344301D-10,
4 -1.8616117165D-10, 7.5741249246D-10, -15.3672496861D-10,
5 -37.8906539485D-10, 0.005344509822653D-5, -.026476639696766D-5,
6 0.043762392901943D-5, 0.496153395628297D-5, -5.462157649813484D-5,
7 0.19647777633032259D-3, 0.240404107087261157D-2,
8 -.05561793742411522950D0, -.05776667474099451444D0 /
      DATA PIO4/.78539816339744830962D0/, R2OPI/.79788456080286535588D0/
      XX = DABS(X)
      IF( XX .LT. 7.D0 ) GO TO 1
      XPPIO4 = XX+PIO4
      EOR = R2OPI*DCMPLX(DCOS(XPPIO4),DSIN(XPPIO4))/DSQRT(XX)
      FOX = 5.D0/XX

```

C-----
 C Sum the Chebyshev series.
 C-----

```

      CALL EATSTR( FOX, 25, RC, RECT )
      CALL EATSTR( FOX, 25, IC, IECT )
      IZIH01 = EOR*DCMPLX(RECT, IECT)
      RETURN

```

C-----
 C Treat the case when X is less than 7.
 C-----

```

1 IOZ = I0XH01(XX)
  IZIH01 = ONE-IOZ
  RETURN
END

```


C Function IA2BH0 evaluates matrix elements for pulse expansion
 C functions by taking the difference between I0XH01 evaluated at B and
 C A or between IZIH01 evaluated at A and B. Approximately two decimal
 C places of accuracy are lost in taking this difference for B=A+0.1.
 C More or less decimal places will be lost depending on the actual
 C relation between A and B. IA2BH0 is used by ISPMOM and PULMOM.
 C IA2BH0 calls either IZIH01 or I0XH01.

C-----
 C COMPLEX FUNCTION IA2BH0*16(A, B)
 C COMPLEX*16 X, Y, IZIH01, I0XH01
 C REAL*8 A, B, AA, BB, DABS
 C AA = DABS(A)
 C BB = DABS(B)
 C I = IDINT(AA*0.14D0)
 C J = IDINT(BB*0.14D0)

C-----
 C Check to see if A and B are greater or less than 7.
 C-----
 C IF(I+J .EQ. 0) GO TO 027
 7200 X = IZIH01(AA)
 Y = IZIH01(BB)
 IA2BH0 = X-Y
 RETURN
 027 X = I0XH01(BB)
 Y = I0XH01(AA)
 IA2BH0 = X-Y
 RETURN
 END

C Function SELFTM evaluates the self terms for the double-wide
 C pulse expansion functions of width 2A with match point in the
 C center. SELFTM is used by ISPMOM and PULMOM.

C-----
 C COMPLEX FUNCTION SELFTM*16(A)
 C COMPLEX*16 X, IZIH01, I0XH01, ONE/(1.D0,0.D0)/, TWO/(2.D0,0.D0)/
 C REAL*8 A, AA, DABS
 C AA = DABS(A)
 C I = IDINT(AA*0.14D0)
 C IF(I .EQ. 0) GO TO 027
 7200 X = IZIH01(AA)
 SELFTM = TWO*(ONE-X)
 RETURN
 027 SELFTM = TWO*I0XH01(AA)
 RETURN
 END

C Function SELFSN evaluates the integral from 0 to H of
 C $(1/\sqrt{t})H_0(t)dt$. The Chebyshev coefficients were derived by
 C methods given by Luke in "The Special Functions and Their
 C Approximations." The coefficients are given elsewhere in this work.
 C SELFSN is used in ISPMOM.

C-----

```

      COMPLEX FUNCTION SELFSN*16(H)
      COMPLEX*16 DCMPLX
      REAL*8 DSQRT, H, A(7), B(7), GAMMA, TWOPI, DLOG, Y(2), HSQ
      DATA A/      0.000000000000001811537D0,   -0.0000000000001239581279D0,
1     0.0000000000610822490741D0,   -0.000000203737032104096D0,
2     0.00042168076965671394D0,   -0.04829484254633680521D0,
3     1.95128143319304658436D0      /
      DATA B/      -0.000000000000002915405D0,   0.0000000000001874935286D0,
1     -0.0000000000854475942331D0,   0.000000257078475742030D0,
2     -0.00046027182338672611D0,   0.04269902252343120894D0,
3     -2.50331721577521205291D0      /
      DATA TWOPI/0.63661977236758134308D0/,
1     GAMMA/0.57721566490153286061D0/
      IF( H .EQ. 0.D0 ) GO TO 2
      IF( H .GT. 1.D0 ) GO TO 10
      HSQ = H*H

```

C-----

C Perform evaluation of Chebyshev series.

C-----

```

      CALL EATSTR( HSQ, 6, A, Y(1) )
      CALL EATSTR( HSQ, 6, B, Y(2) )
      SELFSN=DCMPLX(Y(1),TWOPI*(GAMMA+DLOG(H/2.D0))*Y(1)+Y(2))*DSQRT(H)
      RETURN
2     SELFSN= DCMPLX( 0.D0, 0.D0 )
      RETURN
10    PRINT 1, H
      1    FORMAT( '0', 75X, 'SELFSN WAS CALLED WITH ARG=', 1PD12.4/)
      STOP
      END

```


C Subroutine GTJN is used in evaluating matrix elements for the
 C $1/\sqrt{z}$ expansion function present in the hybrid expansion and is
 C used with SUMHJI and HANKEL. GTJN evaluates the integral from 0 to
 C H of $(1/\sqrt{t})JN(t)dt$ for N from 0 to NMAX. ITJ0 is the value for
 C N=0 and ITJN is an array of length NMAX which contains the values
 C for N=1 to NMAX. PNTOPT is the underflow printing option (see
 C HANKEL). The power series expansion given by 2.2(1) on page 44 of
 C Luke's, "Integrals of Bessel Functions" is used for these
 C evaluations. Numbers were checked by comparison of this power
 C series with Luke's equivalent expansion in series of Bessel
 C functions, eq. 2.4(1), page 51 of "Integrals of Bessel Functions."
 C GTJN calls UNDRFL and EATSTR.

```

C-----
      SUBROUTINE GTJN( H, NMAX, ITJ0, ITJN, PNTOPT )
      REAL*8 ITJ0, ITJN(1), H, HO2, HO2SQ, P, Q, R, DSQRT, SH, AK, AN,
1 DFLOAT, QP, DABS, A(7)
      INTEGER N, K, NMAX, PNTOPT, PNTOP
      LOGICAL UFL
      COMMON/$2/ UFL
      COMMON/$3/ PNTOP
      DATA A/      0.0000000000000001811537D0,    -0.000000000001239581279D0,
1      0.0000000000610822490741D0,    -0.000000203737032104096D0,
2      0.00042168076965671394D0,    -0.04829484254633680521D0,
3      1.95128143319304658436D0      /
      PNTOP = PNTOPT
      IF( PNTOP-1 ) 100, 102, 100
100 CALL ERRSET( 208, 32, -1, 1, UNDRFL )
      GO TO 104
102 CALL ERRSET( 208, 32, 0, 0, UNDRFL )
104 R = H*H
      SH = DSQRT(H)
      HO2 = H/2.D0
      HO2SQ = HO2*HO2
C-----
C      If H is greater than 1.D0, STOP.
C-----
      IF( H .GT. 1.D0 ) GO TO 10
C-----
C      Evaluate ITJ0 in a series of Chebyshev polynomials.
C-----
      CALL EATSTR( R, 6, A, ITJ0 )
      ITJ0 = ITJ0*SH
      IF( NMAX .EQ. 0 ) RETURN
      P = 1.D0
      UFL = .TRUE.
      DO 4 N=1, NMAX
      AN = DFLOAT(N)
      P = P*HO2/AN
      R = 2.D0/(AN+AN+1.D0)
      Q = 1.D0
      K=1
2 AK = DFLOAT(K)
      Q = -Q*HO2SQ/(AK*(AN+AK))
      QP = Q/(AK+AK+AN+0.5D0)
      R=R+QP

```



```

C-----
C    Check for convergence to 15 decimal places.
C-----
      IF( DABS(QP) .LT. 1.D-15 ) GO TO 3
      K=K+1
      GO TO 2
3    ITJN(N) = SH*P*R
C-----
C    Catch underflow before it occurs(possibly).
C-----
      IF( DABS( ITJN(N) ) .GT. 1.D-70 ) GO TO 4
      ITJN(N) = 0.D0
      P=0.D0
      Q=0.D0
      R=0.D0
4    CONTINUE
      UFL = .FALSE.
      RETURN
10  PRINT 1, H
1   FORMAT( '0', 75X, 'GTJN WAS CALLED WITH ARG=', 1PD12.4/)
      STOP
      END

```


C Subroutine BESSEL evaluates the Bessel functions JN for
 C argument X and for orders N from zero through NMAX. BESSEL is used
 C in ISPMOM to provide values for SUMINC. Extreme numerical problems
 C occur when the recurrence relation is used directly in the forward
 C direction. For this reason, the recurrence relation is used in the
 C backward direction to form a continued fraction expansion. The
 C details are too lengthy to describe here. The method is due to G.
 C Blanch, "SIAM Review", V.6, no. 4, Oct. 1964. GORH is a logical
 C array of length NMAX that is required by Blanch's method. J0 is the
 C value of J0 and JN is an array of length NMAX containing the values
 C of JN for N from 1 to NMAX. * is a label to where the calling
 C program should jump when either X or NMAX is less than zero. PNTOPT
 C is the underflow printing option(see HANKEL). BESSEL is accurate to
 C at least 12 decimal places. BESSEL calls UNDRFL, H01S, H11S, and
 C GORHVU.

```

C-----
SUBROUTINE BESSEL( X, NMAX, GORH, J0, JN, *, PNTOPT )
IMPLICIT REAL*8(A-H, O-Z, $), INTEGER( I-N )
COMPLEX*16 H01S, H11S, HC
REAL*8 J0, JN(1), F(2)
INTEGER V, PNTOPT, PNTOP, VP1
LOGICAL GORH(1), LP, UFL
EQUIVALENCE( HC, F )
EXTERNAL UNDRFL
COMMON/$2/ UFL
COMMON/$3/ PNTOP
UFL = .FALSE.
DO 1 I = 1, NMAX
1 GORH(I) = .FALSE.
NM = NMAX
NM1 = NM-1
XX = X
PNTOP = PNTOPT
IF( XX.LT. 0.D0 .OR. NM.LT. 0 ) RETURN1
IF( XX.EQ. 0.D0 ) GO TO 44

```

C-----
 C Evaluate J0 using Chebyshev polynomial expansion.
 C-----

```

HC = H01S(XX)
J0 = F(1)
IF( NM.EQ. 0 ) RETURN

```

C-----
 C Evaluate JN(1) using Chebyshev polynomial expansion.
 C-----

```

HC = H11S(XX)
JN(1) = F(1)
IF( NM.EQ. 1 ) RETURN
A = 2.D0/XX

```

C-----
 C A maximum of 32 underflows may occur before program termination.
 C-----

```

IF( PNTOP-1 ) 100, 102, 100
100 CALL ERRSET( 208, 32, -1, 1, UNDRFL )
GO TO 8
102 CALL ERRSET( 208, 32, 0, 0, UNDRFL )

```



```

8 J = IDINT( XX )
  IF( J .LT. NM ) J = NM
  I = J
10 M = I
  IF( A*DFLOAT(I) .GE. 2.5D0 ) GO TO 12
  I = I + 1
  GO TO 10

```

```

C-----
C   NPJCNV is N+J such that convergence is obtained. See Blanch
C   paper.
C-----

```

```

12 N = M + 5
  P = 0.D0
  NPJCNV = M
14 N = N + 5
  Q = P
  P = 0.D0
  DO 15 J = NPJCNV, N
    M1 = N + NPJCNV - J
15 P = 1.D0/(DFLOAT(M1)*A - P)
16 IF( DABS(P-Q) .GT. (1.D-15)*DABS(P) ) GO TO 14
  GHP = P
  LP = .FALSE.
  NPJML = NPJCNV - 1
  IF( NPJCNV .EQ. NM ) GO TO 20

```

```

C-----
C   Evaluate G(NMAX) or H(NMAX) from G(NPJCNV). See Blanch paper.
C-----

```

```

DO 18 J = NM, NPJML
  M1 = NM + NPJML - J
18 CALL GORHVU( M1, A, GHP, LP )
20 JN(NM) = GHP
  GORH(NM) = LP
  IF(NM .EQ. 2) GO TO 24
  DO 22 J=3, NM
    M1 = NM+3-J
    M1M1 = M1-1
    GHP = JN(M1)
    LP = GORH(M1)
    CALL GORHVU( M1M1, A, GHP, LP )
    JN(M1M1) = GHP
22 GORH(M1M1) = LP

```

```

C-----
C   Evaluate JN(2). See Blanch paper.
C-----

```

```

24 UFL = .TRUE.
  IF( GORH(2) ) GO TO 26
  JN(2) = JN(1)*JN(2)
  GO TO 29
26 IF( DABS(J0) .GT. DABS(JN(1) ) ) GO TO 28
  JN(2) = JN(1)/JN(2)
  GO TO 29
28 JN(2) = J0/(JN(2)*A - 1.D0 )
29 IF( DABS(JN(2) ) .LT. 1.D-70) JN(2) = 0.D0

```



```

C-----
C      Evaluate JN(VP1), VP1=3,...,NMAX.  See Blanch paper.
C-----
      DO 36 V = 2, NMM1
      VP1 = V+1
      IF( GORH(VP1) ) GO TO 30
      JN(VP1) = JN(V)*JN(VP1)
      GO TO 34
30 IF( DABS(JN(V-1)) .GT. DABS(JN(V)) ) GO TO 32
      JN(VP1) = JN(V)/JN(VP1)
      GO TO 34
32 JN(VP1) = JN(V-1)/(JN(VP1)*A*DFLOAT(V) - 1.D0)
C-----
C      Abort possible later underflows.
C-----
34 IF( DABS(JN(VP1)) .LT. 1.D-70 ) JN(VP1) = 0.D0
36 CONTINUE
      UFL = .FALSE.
      RETURN
C-----
C      Treat the special case X=0.
C-----
44 P=0.D0
      J0 = 1.D0
      DO 45 V=1, NM
45 JN(V) = P
      RETURN
      END

```


C Subroutine HANKEL evaluates the Hankel functions HN1 for
 C argument X and for orders N from zero through NMAX. HANKEL is used
 C in ISPMOM to provide values for SUMHJI. In the following,
 C HN1=J(n)+iY(n). The recurrence relation is used for the J's from
 C J(2) through J(K=X) and Blanch's continued fraction method is used
 C for the J's from J(K=X) through J(NMAX)(see BESSEL). The recurrence
 C relation is used for all Y's from Y(2) through Y(NMAX). Should
 C overflow occur the resultant Y and all higher order Y's are set to
 C -1.D70. Due to internal array dimensioning NMAX must be 32 or
 C less(BESSEL was written to avoid this). JORH is the JN or HN1
 C return option: JORH = .TRUE.: Return the Hankel functions HN1;
 C JORH = .FALSE.: Return the Bessel functions JN and set YN to zero.
 C H01 is the value of H01. HN1 is an array of values of HN1(X) for N
 C from one to NMAX. * is a label to which the calling program jumps
 C when either X or NMAX is less than zero. PNTOPT is the
 C overflow/underflow printing option:
 C PNTOPT=0: Print nothing; PNTOPT=1: Print complete statistics;
 C PNTOPT=2: Print one liner.
 C HANKEL is accurate to at least 12 decimal places. HANKEL calls
 C UNDRFL, OVERFL, H01S, H11S, and GORHVU.

```

C-----
SUBROUTINE HANKEL( X, NMAX, JORH, H01, HN1, *, PNTOPT )
IMPLICIT REAL*8(A-H, O-Z, $), INTEGER( I-N )
COMPLEX*16 DCMPLX, H01, HN1(1), H01S, H11S, HC
REAL*8 JN(33), YN(33), GH(33), F(2)
INTEGER V, PNTOPT, PNTOP, VP1
LOGICAL GCRH(33), OBOY, YLOOP, LP, UFL, JORH, JORHS
EQUIVALENCE( HC, F )
EXTERNAL OVERFL, UNDRFL
COMMON/$1/ OBOY, YLOOP
COMMON/$2/ UFL
COMMON/$3/ PNTOP
OBOY = .FALSE.
YLOOP = .FALSE.
UFL = .FALSE.
DO 1 I = 1, 33
1 GORH(I) = .FALSE.
NM = NMAX
NMPL = NM+1
XX = X
JORHS = JORH
PNTOP = PNTOPT
IF( XX.LT. 0.D0 .OR. NM.LT. 0 ) RETURN1
IF( XX.EQ. 0.D0 ) GO TO 44
K = IDINT( XX )
IF( K.GT. NM ) K=NM

```

C-----
 C Evaluate H01 using Chebyshev polynomial expansion.
 C-----

```

H01 = H01S(XX)
HC = H01
JN(1) = F(1)
YN(1) = F(2)
IF( NM.EQ. 0 ) RETURN

```



```

C-----
C      Evaluate H11 using Chebyshev polynomial expansion.
C-----
      HN1(1) = H11S(XX)
      HC = HN1(1)
      JN(2) = F(1)
      YN(2) = F(2)
      IF( NM .EQ. 1 ) RETURN
      A = 2.D0/XX
      KML = K-1
      IF( KML .LT. 1 ) GO TO 4
C-----
C      Evaluate the J's up to J(K=X) using the recurrence relation.
C-----
      6 DO 7 V = 1, KML
        AV = DFLOAT( V )
      7 JN(V+2) = JN(V+1)*A*AV - JN(V)
      4 IF( K .EQ. NM ) GO TO 32
C-----
C      A maximum of 32 underflows may occur before program termination.
C-----
      IF( PNTOP-1 ) 100, 102, 100
      100 CALL ERRSET( 208, 32, -1, 1, UNDRFL )
      GO TO 8
      102 CALL ERRSET( 208, 32, 0, 0, UNDRFL )
C-----
C      Evaluate the rest of the J's by Blanch's method.
C-----
      8 J = IDINT( XX )
      IF( J .LT. NM ) J = NM
      I = J
      10 M = I
      IF( A*DFLOAT(I) .GE. 2.5D0 ) GO TO 12
      I = I + 1
      GO TO 10
C-----
C      NPJCNV is N+J such that convergence is obtained. See Blanch
C      paper.
C-----
      12 N = M + 5
      P = 0.D0
      NPJCNV = M
      14 N = N+ 5
      Q = P
      P = 0.D0
      DO 15 J = NPJCNV, N
      M1 = N + NPJCNV - J
      15 P = 1.D0/(DFLOAT(M1)*A - P)
      16 IF( DABS(P-Q) .GT. (1.D-15)*DABS(P) ) GO TO 14
      GHP = P
      LP = .FALSE.
      NPJM1 = NPJCNV - 1
      IF( NPJCNV .EQ. NM ) GO TO 20

```



```

C-----
C      Evaluate G(NMAX) or H(NMAX) from G(NPJCNV).  See Blanch paper.
C-----
      DO 18 J = NM, NPJM1
      M1 = NM + NPJM1 - J
18 CALL GORHVU( M1, A, GHP, LP )
20 GH(NMP1) = GHP
   GORH( NMP1 ) = LP
   KP1 = K+1
   KP2 = K+2
   IF( KP2 .GT. NM ) GO TO 24
   DO 22 J = KP2, NM
   M1 = NM + KP2 - J
   M1P1 = M1+1
   M1M1 = M1-1
   GHP = GH(M1P1)
   LP=GORH(M1P1)
   CALL GORHVU( M1M1, A, GHP, LP )
   GH(M1) = GHP
22 GORH(M1) = LP
24 UFL = .TRUE.
   DO 30 V = KP1, NM
   IF( V .LE. 1 ) GO TO 30
   VP1 = V+1
   IF( GORH(VP1) ) GO TO 26
   JN( VP1 ) = JN(V)*GH(VP1)
   GO TO 29
26 IF( DABS(JN(V-1)) .GT. DABS( JN(V) ) ) GO TO 28
   JN(VP1) = JN(V)/GH(VP1)
   GO TO 29
28 JN(VP1) = JN(V-1)/(GH(VP1)*A*DFLOAT(V) - 1.D0 )
C-----
C      Abort possible later underflows.
C-----
29 IF( DABS( JN(VP1) ) .LT. 1.D-70 ) JN(VP1) = 0.D0
30 CONTINUE
32 UFL = .FALSE.
   I1 = 3
   IF( JORHS ) GO TO 105
   DO 103 J = 1, NMP1
103 YN(J) = 0.D0
   H01 = DCMPLX(JN(1), YN(1) )
   HN1(1) = DCMPLX( JN(2), YN(2) )
   GO TO 40
C-----
C      A maximum of 32 overflows may occur before program termination.
C-----
105 IF( PNTOP-1 ) 104, 106, 104
104 CALL ERRSET( 207, 32, -1, 1, OVERFL )
   GO TO 33
106 CALL ERRSET( 207, 32, 0, 0, OVERFL )
33 YLOOP = .TRUE.

```



```

C-----
C      Evaluate the Y's using the recurrence relation.
C-----
      DO 34 J = 2, NM
      I1 = J+1
      YN(I1) = YN(J)*A*DFLOAT(J-1) - YN(J-1)
C-----
C      Catch first overflow and set subsequent Y's to -1.D70.
C-----
      IF( OBOY ) GO TO 36
      IF( DABS(YN(I1)) .GT. 1.D70 ) GO TO 36
34  CONTINUE
      YLOOP = .FALSE.
      GO TO 40
36  DO 38 J = I1, NMPI
38  YN(J) = -1.D70
      YLOOP = .FALSE.
      OBOY = .FALSE.
C-----
C      Evaluate the Hankel functions to be returned.
C-----
      40 DO 42 J = 2, NM
      JPI = J+1
      42 HN1(J) = DCMLPX( JN(JPI), YN(JPI) )
      RETURN
C-----
C      Treat the special case X=0.
C-----
      44 P = 1.D0
      Q = 0.D0
      A = -1.D70
      H01 = DCMLPX( P, A )
      DO 45 J = 1, NM
      45 HN1(J) = DCMLPX( Q, A )
      RETURN
      END

```


C Subroutine GORHVU is required as part of Blanch's method given
 C in "SIAM Review", V. 6, no. 4, Oct. 1964. It is used in BESSEL and
 C HANKEL. For further details, see the Blanch paper.

```

C-----
      SUBROUTINE GORHVU( K, A, GH, L )
      REAL*8 GH, A, BK, YD, ZD, DABS, DFLOAT, H1
      INTEGER K
      LOGICAL L
      BK = A*DFLOAT(K)
      IF(L) GO TO 10
      YD = BK-GH
      IF(DABS(BK) .GE. 2.D0 ) GO TO 1
      IF( DABS(YD) .GT. 1.D0 ) GO TO 1
      L = .TRUE.
      GH = YD
      RETURN
1  L = .FALSE.
      GH = 1.D0/YD
      RETURN
10 ZD = BK*GH - 1.D0
      H1 = GH
      IF( DABS(ZD) .GE. DABS(GH) ) GO TO 100
      L = .TRUE.
      GH = ZD/H1
      RETURN
100 L = .FALSE.
      GH = H1/ZD
      RETURN
      END
  
```


C Subroutine UNDRFL is called when an underflow occurs. If an
 C underflow occurs when UFL is .TRUE., the result register will be set
 C to zero and program execution will continue. Otherwise, the program
 C will terminate. D is the result register. I is a dummy variable.
 C UNDRFL is used in BESSEL, HANKEL, GTJN, SKS, SUMINC, and SUMHJI.

```

C-----
      SUBROUTINE UNDRFL( D, I )
      REAL*8 D
      INTEGER PNTOPT
      LOGICAL UFL
      COMMON/$2/ UFL
      COMMON/$3/ PNTOPT
      IF( PNTOPT .GE. 2 ) PRINT 1
1  FORMAT( ' ', 75X, 'UNDERFLOW OCCURRED. RESULT REGISTER WAS SET TO
1  ZERO.' )
      D = 0.D0
      IF( UFL ) RETURN
      CALL ERRSET( 208, 1, 0, 0 )
      STOP
      END
  
```

C Subroutine OVERFL is called when an overflow occurs. If an
 C overflow occurs when YLOOP is .TRUE., the result register will be
 C set to -1.D70, OBOY will be set to .TRUE., and program execution
 C will continue. Otherwise, the program will terminate. D is the
 C result register. I is a dummy variable. OVERFL is used in HANKEL.

```

C-----
      SUBROUTINE OVERFL(D, I )
      REAL*8 D
      INTEGER PNTOPT
      LOGICAL OBOY, YLOOP
      COMMON/$1/ OBOY, YLOOP
      COMMON/$3/ PNTOPT
      OBOY = .TRUE.
      IF( PNTOPT .GE. 2 ) PRINT 1
1  FORMAT( ' ', 75X, 'OVERFLOW OCCURRED. RESULT REGISTER WAS SET TO
1  -1.D70.' )
      D = -1.D70
      IF( YLOOP ) RETURN
      CALL ERRSET( 207, 1, 0, 0 )
      STOP
      END
  
```


C Function H01S evaluates the Hankel function H01 for argument X.
 C A Chebyshev polynomial expansion is used for X less than 7 and
 C another is used for X greater than 7. The coefficients are from
 C Table 25 on page 331 of Volume II of Luke's book, "The Special
 C Functions and Their Approximations." The routine is called by
 C HANKEL and BESSEL.

```

C-----
      COMPLEX FUNCTION H01S*16(X)
      COMPLEX*16 DCMLPX, DIST
      REAL*8 X, XX, DABS, A(16), B(16), CR(16), CI(16), DSQRT, FOX,
1 OOSRTX, AGL, DLOG, RECT, IECT, XO8, X2, EAT, EBT, PIO4, R2OPI,
2 TWOOPI, GAMMA, DSIN, DCOS
      DATA PIO4/0.7853981633974483D0/, R2OPI/0.7978845608028654D0/,
1 TWOOPI/0.6366197723675813D0/, GAMMA/0.5772156649015329D0/
      DATA A/-0.758D-15, 0.00041253D-10, -0.01943835D-10, 0.78486963D-10,
1 -0.0002679253530D-5, 0.0076081635924D-5, -0.1761946907762D-5,
2 3.2460328821005D-5, -0.000460626166206275D0, 0.004819180069467604D0
3, -0.034893769411408885D0, 0.158067102332097261D0,
4 -0.37009499387264977D0, 0.26517861320333680D0,
5 -0.00872344235285222D0, 0.15772797147489011D0 /
      DATA B/1.58D-15, -84.42D-15, 0.03882867D-10, -1.5258285D-10,
1 50.5105437D-10, -0.013845718123D-5, 0.307649328810D-5,
2 -5.392507972293D-5, 71.911740375230D-5, -0.00693228629152318D0,
3 0.04462137954066928D0, -0.16563598171365041D0,
4 0.23425274610902180D0, 0.19860563470255416D0,
5 -0.27511813304351879D0, -0.02150511144965755D0 /
      DATA CR/0.59D-15, -3.61D-15, 8.73D-15, 41.91D-15, -0.0055909D-10,
1 0.0253535D-10, 0.0323797D-10, -1.3916619D-10, 9.2676248D-10,
2 14.5492807D-10, -0.009077010153D-5, 0.069154234914D-5,
3 0.8511232210656D-5, -0.00031878987806189D0, -0.00133842854997185D0
4, 0.99898808985896515D0 /
      DATA CI/0.46D-15, 0.75D-15, -16.77D-15, 92.31D-15, -0.0012255D-10,
1 -0.0230489D-10, 0.2169571D-10, -0.6062738D-10, -6.8334751D-10,
2 96.4642133D-10, -0.002724405341D-5, -0.085180664442D-5,
3 1.365557049035D-5, 9.649418499342D-5,
4 -0.01224949628125947D0, -0.01233152057854414D0 /
      XX = DABS(X)
      IF( XX .LT. 7.D0 ) GO TO 1
      OOSRTX = 1.D0/DSQRT( XX )
      AGL = XX - PIO4
      DIST = OOSRTX*R2OPI*DCMLPX( DCOS(AGL), DSIN(AGL) )
      FOX = 5.D0/XX

```

```

C-----
C        Sum the Chebyshev series.
C-----
      CALL EATSTR( FOX, 15, CR, RECT )
      CALL EATSTR( FOX, 15, CI, IECT )
      H01S = DCMLPX( RECT, IECT )*DIST
      RETURN
1 IF( XX .EQ. 0.D0 ) GO TO 2
      XO8 = 0.125D0*XX
      X2 = XO8*XO8
C-----
C        Sum the Chebyshev series.
C-----

```


Computer Program for E-polarization Half-Plane Current.

Page 28

```

CALL EATSTR( X2, 15, A, EAT )
CALL EATSTR( X2, 15, B, EBT )
H01S = DCMPLX( EAT, TWOOP1*(GAMMA+DLOG(0.5D0*XX))*EAT + EBT )
RETURN

```

```

C-----
C   Treat the special case X=0.
C-----

```

```

2 H01S = DCMPLX( 1.D0, -1.D70 )
RETURN
END

```

```

C   Function H11S evaluates the Hankel function H11 for argument X.
C   A Chebyshev polynomial expansion is used for X less than 7 and
C   another is used for X greater than 7. The coefficients are from
C   Table 26 on pages 332 and 333 of Volume II of Luke's book, "The
C   Special Functions and Their Approximations." The routine is called
C   by HANKEL and BESSEL.
C-----

```

```

COMPLEX FUNCTION H11S*16(X)
COMPLEX*16 DCMPLX, DIST
REAL*8 X, XX, DABS, DSQRT, DLOG, XO8, DR(16), DI(16), A(16),
1 C(16), OOSRTX, FOX, EAT, REDT, IEDT, ECT, PIO4, R2OPI, TWOOP1,
2 GAMMA, TPIO4, AGL, DSIN, DCOS
DATA PIO4/0.7853981633974483D0/, R2OPI/0.7978845608028654D0/,
1 TWOOP1/0.6366197723675813D0/, GAMMA/0.5772156649015329D0/
DATA A /-0.096D-15, 5.59D-15, -0.0028317D-10, 0.1235175D-10,
1 -4.5857003D-10, 0.001427732438D-5, -0.036613085523D-5,
2 0.756263022969D-5, -12.227868505432D-5, 0.00148991289666763D0,
3 -0.01296762731173517D0, 0.07426679621678703D0,
4 -0.24186740844740748D0, 0.31327508236156718D0,
5 0.04809646915823037D0, 0.05245819033465648D0 /
DATA C/ 0.20D-15, -0.0001157D-10, 0.0057261D-10, -0.2434327D-10,
1 8.7803011D-10, -0.002645073717D-5, 0.065284795235D-5,
2 -1.288585329924D-5, 19.706230270154D-5, -0.00223561929448509D0,
3 0.01763670300316313D0, -0.08667169705694852D0,
4 0.20664454101749051D0, -0.02271924442841773D0,
5 -0.44444714763055806D0, -0.04017294654441407D0 /
DATA DR/ -0.63D-15, 3.97D-15, -10.132D-15, -43.161D-15,
1 0.0061781D-10, -0.0293217D-10, -0.0283045D-10, 1.5763723D-10,
2 -11.1490594D-10, -12.9439892D-10, 0.011103267712D-5,
3 -0.094690138239D-5, -1.117946189540D-5, 54.321648750801D-5,
4 0.00225557284656117D0, 1.00170223485382100D0 /

```



```

DATA DI/ -0.52D-15, -0.70D-15, 18.12D-15, -103.38D-15,
1 0.0015619D-10, 0.0249389D-10, -0.2475278D-10, 0.7547607D-10,
2 7.5973309D-10, -0.001162872327D-5, 0.003830526171D-5,
3 0.107001405738D-5, -1.985129468759D-5, -13.726323820190D-5,
4 0.03714532247980768D0, 0.03726171500053765D0 /

```

```

TPIO4 = 3.D0*PIO4

```

```

XX = DABS(X)

```

```

IF( XX .LT. 7.D0 ) GO TO 1

```

```

OOSRTX = 1.D0/DSQRT( XX )

```

```

AGL = XX - TPIO4

```

```

DIST = OOSRTX*R2OPI*DCMPLX( DCOS(AGL), DSIN(AGL) )

```

```

FOX = 5.D0/XX

```

```

C-----

```

```

C Sum the Chebyshev series.

```

```

C-----

```

```

CALL EATSTR( FOX, 15, DR, REDT )

```

```

CALL EATSTR( FOX, 15, DI, IEDT )

```

```

H11S = DIST*DCMPLX( REDT, IEDT )

```

```

RETURN

```

```

1 IF( XX .EQ. 0.D0 ) GO TO 2

```

```

X08 = XX*0.125D0

```

```

C-----

```

```

C Sum the Chebyshev series.

```

```

C-----

```

```

CALL EAT2P1( X08, 15, A, EAT )

```

```

CALL EAT2P1( X08, 15, C, ECT )

```

```

H11S = DCMPLX( EAT, TWOOPI*(GAMMA+DLOG(0.5D0*XX)) *EAT-TWOOPI/XX+

```

```

1 ECT )

```

```

RETURN

```

```

C-----

```

```

C Treat the special case X=0.

```

```

C-----

```

```

2 H11S = DCMPLX( 0.D0, -1.D70 )

```

```

RETURN

```

```

END

```


C Subroutine EAT2Pl evaluates the Chebyshev series: $Y = \text{Sum of}$
 C $A(k)T(2k+1)(X)$ over k from zero to N for argument X . "E" in EAT2Pl
 C denotes Sigma(Sum of). N is the upper index of the summation. The
 C index goes from zero to N . $N+1$ coefficients are required. A is the
 C coefficient vector of length $N+1$ written in REVERSE order: $A(N),$
 C $A(N-1), \dots, A(0)$. Y is the result of the sum. The recurrence
 C algorithm is given on page 329 of Volume I of Luke's book, "The
 C Special Functions and Their Approximations."

```

C-----
SUBROUTINE EAT2Pl( X, N, A, Y )
REAL*8 X, A(1), Y, U, PA, PB, PC, XX
INTEGER N, I, NN
XX = X
U = 4.D0*XX*XX -2.D0
PB = 0.D0
PA = 0.D0
NN = N+1
DO 1 I = 1, NN
PC = U*PB - PA + A(I)
PA = PB
1 PB = PC
Y = XX*(PB-PA)
RETURN
END

```

C Subroutine EATSTR evaluates the Chebyshev series: $Y = \text{Sum of}$
 C $A(k)T^*(k)(X)$ over k from zero to N with argument X , or the Chebyshev
 C series: $Y = \text{Sum of } A(k)T(2k)(X)$ over k from zero to N for argument
 C X when the routine is called with argument $X*X$ (X -squared) instead
 C of X . N is the upper index of summation. The index goes from zero
 C to N . $N+1$ coefficients are required. A is the coefficient vector
 C of length $N+1$ written in REVERSE order: $A(N), A(N-1), \dots, A(0)$. Y
 C is the result of the sum. The recurrence algorithm is given on page
 C 329 of Volume I of Luke's book, "The Special Functions and Their
 C Approximations."

```

C-----
SUBROUTINE EATSTR( X, N, A, Y )
REAL*8 X, A(1), Y, U, PA, PB, PC, XX
INTEGER N, I, NN
XX = X
U = 4.D0*XX -2.D0
PB = 0.D0
PA = 0.D0
NN = N
DO 1 I = 1, NN
PC = U*PB - PA + A(I)
PA = PB
1 PB = PC
Y = 2.D0*XX*PB - (PA+PB) + A(NN+1)
RETURN
END

```



```

C      Subroutine LTPLZ finds the solution vector VOUT for an
C      almost-Toeplitz matrix whose first (Left) column is different from
C      what it would be if the matrix were completely Toeplitz. ZTAU is
C      the input vector of values for the left column. TAU is the input
C      vector of the values that the left-most column would take on if the
C      matrix were completely Toeplitz. If T is the Toeplitz matrix
C      corresponding to TAU, and if ZTAM and TAM are matrices whose
C      left-most columns are ZTAU and TAU, respectively, and whose other
C      columns are all zero, then the matrix equation may be written as
C      ( T + (ZTAM - TAM) )VOUT = VIN.
C      Z1, A, and A1 are working storage vectors and are each of length NZ.
C      NZ is the order of the matrix system. VIN is a one-dimensional
C      vector of length (NZ*MM) containing the MM concatenated excitation
C      vectors. VOUT is a one-dimensional vector of length (NZ*MM)
C      containing the MM concatenated solution vectors. MM is the number
C      of excitation and solution vectors. XNORM is the infinite norm of
C      the inverse of the Toeplitz matrix T(not of T+(ZTAM-TAM)). IER is
C      an error code returned: IER=0 means no error; IER=N means an error
C      occurred on the N'th iteration of working vector A. Both TAU and
C      ZTAU are destroyed. LTPLZ was modified from TPLZ which was written
C      by Chuck Klein. The basic Toeplitz algorithm is due to D. H.
C      Preis, IEEE Transactions on Antennas and Propagation, V. AP-20,
C      1972, Page 204.
C-----
      SUBROUTINE LTPLZ(ZTAU,TAU,Z1,A,A1,NZ,VIN,VOUT,MM,XNORM,IER)
      IMPLICIT COMPLEX*16 (A-H,O-Z)
      COMPLEX*16 ZTAU(NZ),TAU(NZ),Z1(1),A(1),A1(1),VIN(1),VOUT(1)
      COMPLEX*16 ONE/(1D0,0D0)/,ZERO/(0D0,0D0)/
      REAL*8 ONNE/1D0/,ZRR0/0D0 /
      REAL*8 XNM,XNORM
C-----
C      Take the difference between ZTAU and TAU and store the result in
C      ZTAU.
C-----
      DO 100 II=1,NZ
100  ZTAU(II) = ZTAU(II) - TAU(II)
      N=NZ-1
      IER=0
C-----
C      Normalize input matrix TAU by dividing all elements by TAU(1).
C-----
      TAU1=TAU(1)
      DO 2000 II=1,N
2000  TAU(II)=TAU(II+1)/TAU1
C-----
C      Calculate the iterative variables to obtain A(N) and ALMDA.
C-----
      ALMDA=ONE - TAU(1)*TAU(1)
      A(1)=-TAU(1)
      I=2
1  KK=I-1
      ALPHA=ZERO
      DO 2 M=1,KK
      LL=I-M
2  ALPHA=ALPHA+A(M)*TAU(LL)

```



```

ALPHA=-(ALPHA+TAU(I))
IF ( CDABS(ALPHA) .EQ. 0.00) GO TO 15
COEF=ALPHA/ALMDA
ALMDA=ALMDA-COEF*ALPHA
DO 3 J=1, KK
L=I-J
3 A(J)=A(J)+COEF*A(L)
DO 7 J=1, KK
7 A(J)=A(J)
A(I)=COEF
IF (I .GE. N) GO TO 5
4 I=I+1
GO TO 1

```

C-----
C Compute the values of each element of the inverse of T.
C-----

```

5 NH=(NZ+1)/2
FAC=ALMDA*TAU1
XNORM=ZRRO
NP=NZ+1
DO 51 I=1, NH
XNM=ZRRO
IF(I .NE. 1) GO TO 52
A1(1)= ONE/FAC
XNM=CDABS(A1(1))
DO 53 J=2, NZ
A1(J)=A(J-1)/FAC
53 XNM=CDABS(A1(J))+XNM
GO TO 54
52 XNM=ZRRO
C1=A(I-1)
C2=A(NP-I)
DO 55 JJ=1, N
J=NP-JJ
A1(J)=A1(J-1)+(C1*A(J-1)-C2*A(NP-J))/FAC
55 XNM=CDABS(A1(J))+XNM
A1(1)=A(I-1)/FAC
XNM=XNM+CDABS(A1(1))
54 IF(XNM .GT. XNORM) XNORM=XNM

```

C-----
C Obtain Z1 from ZTAU' and A1 by matrix multiplication.
C (ZTAU' = ZTAU - TAU).
C-----

```

V=ZERO
V1 = ZERO
DO 60 J=1, NZ
V2 = ZTAU(J)
V = V+V2*A1(J)
60 V1 = V1+V2*A1(NP-J)
Z1(I)=V
Z1(NP-I) = V1

```

C-----
C Evaluate VOUT due to the completely Toeplitz matrix T for each
C input excitation vector.
C-----


```

      DO 56 II=1,MM
      ID=(II-1)*NZ
      V=ZERO
      V1=ZERO
      DO 57 J=1,NZ
      V2=VIN(ID+J)
      V=V+V2*A1(J)
57  V1=V1+V2*A1(NP-J)
      VOUT(ID+I )=V
56  VOUT(ID+NP-I )=V1
51  CONTINUE
C-----
C      Modify VOUT as required to arrive at the solution for the
C      almost-Toeplitz matrix using Z1 calculated above.
C-----
      DO 62 II = 1, MM
      ID = (II-1)*NZ
      V = VOUT(ID+1)/(ONE+Z1(1) )
      VOUT(ID+1) = V
      DO 62 J=2, NZ
62  VOUT(ID+J) = VOUT(ID+J) - (Z1(J)*V)
      RETURN
15  PRINT 700
700 FORMAT('0',75X,'ERROR HAS OCCURRED.  MATRIX IS NOT STRONGLY NONSIN
1G.'/)
      IER=I
      RETURN
      END

```



```

C      Subroutine PNTOWT calculates the "exact" current (IE-IPO) and
C      compares it with the approximate solution obtained by the method of
C      moments. TAD, NSIZE, NCASES, KZ, RHS, RESULT, ROOT, and H are
C      inputs. IEMPO is a dimensioned array of length NSIZE which is
C      filled with the "exact" values of (IE-IPO) for each match point KZ.
C      RHS, TAD, NSIZE, NCASES, and KZ are the same as RHS, TAD, NSIZE, NC,
C      and KZ as described in ISPMOM. RESULT is an array of length
C      NCASES*NSIZE which contains the values of (IE-IPO) obtained by the
C      method of moments. ROOT is a logical variable which must be
C      .TRUE. for PNTOWT to handle the hybrid case and .FALSE. to handle
C      the pulse case. H is the half-subsection width. PNTOWT calls
C      XIEMPO and SEP directly.

```

```

C-----
      SUBROUTINE PNTOWT(TAD,NSIZE,NCASES,KZ,IEMPO,RHS,RESULT,ROOT,H)
      COMPLEX*16 IEMPO(1),EXACT,ANS,DIFF,RESULT(1),RHS(1),COEFF,SP(20)
      REAL*8 KZ(1), TAD(1), H, Z(20), DFLOAT,DSQRT, THETAD, DELZ, AX(4)
      1, AA(4), ZM(3,4)
      INTEGER NCASES, NSIZE, J, K, IC(4)/' RE=', ' IM=', 'MAG=', 'AGL='/,
      1 JJ, KK, OFFSET
      LOGICAL ROOT
      DO 3 J=1, NCASES
      OFFSET = (J-1)*NSIZE
      THETAD = TAD(J)

```

```

C-----
C      Obtain array of "exact" (IE-IPO); store in IEMPO.
C-----

```

```

      CALL XIEMPO( NSIZE, KZ, THETAD, IEMPO )
C-----

```

```

C      Write results in appropriate disk file: ROOT=.TRUE. for hybrid
C      expansion; ROOT=.FALSE. for pulse expansion.
C-----

```

```

      IF( ROOT ) GO TO 21
      WRITE(22) THETAD, NSIZE, H, (KZ(K), K=1, NSIZE),
      1 (RESULT(OFFSET+K), K=1, NSIZE )
      GO TO 20
21 WRITE(21) THETAD, H, (KZ(K), K=1, NSIZE), (IEMPO(K), K=1, NSIZE)
      1 (RHS(OFFSET+K), K=1, NSIZE), (RESULT(OFFSET+K), K=1, NSIZE)
20 PRINT 5, THETAD
      5 FORMAT('1', 'THETAD=', F9.2//T4, 'KZ', T18, 'EXACT', T38, 'ANS', T55,
      1 'DIFF', T76, 'EXACT', T96, 'ANS', T113, 'DIFF' )
C-----

```

```

C      Compare "exact" with moment solution and print results.
C-----

```

```

      DO 2 K=1, NSIZE
      EXACT = IEMPO(K)
      ANS = RESULT( OFFSET + K)
C-----

```

```

C      Separate EXACT, ANS into real part, imaginary part, magnitude and
C      phase, A(1), A(2), A(3), and A(4), respectively.
C-----

```

```

      CALL SEP( EXACT, AX )
      CALL SEP( ANS, AA )

```



```

      DO 10 I=1, 4
      ZM(1,I) = AX(I)
      ZM(2, I) = AA(I)
10  ZM(3, I) = AX(I) - AA(I)
      2 PRINT 4, KZ(K), (IC(I), (ZM(JJ,I), JJ=1,3), I=1,4), RHS(OFFSET+K)
      4 FORMAT(' ', T2, 0PF7.4, T9, 2(A4, '<', 1PD17.10, '/', D17.10, '>', D17.10,
1 2X)/T9, A4, '<', D17.10, '/', D17.10, '>', D17.10, 2X, A4, '<', 0PF17.10,
2  '/' , F17.10, '>', F17.10/T71, 'RHS=(', 1PD23.15, ',', 1X, D23.15, '); ')
C-----
C      Print out selected values across the 1/SQRT subsection, if
C      applicable.
C-----
      IF( .NOT. ROOT ) GO TO 3
      COEFF = RESULT( OFFSET + 1 )
      PRINT 12, COEFF
12  FORMAT('0', 5X, 'COEFF=(', 1PD23.15, ',', 2X, D23.15, ')')
      DELZ = H/20.D0
      DO 7 JJ=1, 20
      7 Z(JJ) = DELZ*DFLOAT(JJ)
      CALL XIEMPO(20, Z, THETAD, SP )
      DO 6 JJ = 1, 20
      EXACT = SP(JJ)
      ANS = COEFF/DSQRT(Z(JJ))
      CALL SEP( EXACT, AX )
      CALL SEP( ANS, AA )
      DO 8 K=1, 4
      ZM(1,K) = AX(K)
      ZM(2,K) = AA(K)
      8 ZM(3,K) = AX(K) - AA(K)
      6 PRINT 4, Z(JJ), (IC(I), (ZM(K,I), K=1,3), I=1,4)
      3 CONTINUE
      RETURN
      END

```


C Subroutine XIEMPO calculates the "exact" half-plane current,
 C (IE-IPO), from the well-known analytic result, for NSIZE points. KZ
 C is an array of length NSIZE containing the values of argument for
 C which (IE-IPO) is to be found. THETAD is the angle of incidence in
 C degrees. IEMPO is an array of length NSIZE containing the values of
 C (IE-IPO) corresponding to arguments KZ. XIEMPO calls FRESNL and is
 C called by PNTOWT.

```

-----
      SUBROUTINE XIEMPO( NSIZE, KZ, THETAD, IEMPO )
      COMPLEX*16 DCMPLX, IEMPO(1), FRESNL, IEIKZ, SEKC
      REAL*8 KZ(1), X, THETAD, THETA, TAO2, DCOS, DSIN, STA, STA2 ,
1  CTA2, CTA, TSRX, PI, PIO4, SRTPI, DSQRT, XP4, XCP4, CTA2SQ, XC
      DATA PI/3.14159265358979323846D0/,
1SRTPI/1.77245385090551602730D0/,PIO4/0.78539816339744830962D0/
      INTEGER NSIZE, NS, I
      THETA = (THETAD/180.D0)*PI
      TAO2 = THETA/2.D0
      CTA = DCOS( THETA )
      STA = DSIN( THETA )
      IF( THETAD .EQ. 180.D0 ) STA = 0.D0
      STA2 = DSIN( TAO2 )
      CTA2 = DCOS( TAO2 )
      IF( THETAD .EQ. 180.D0 ) CTA2 = 0.D0
      CTA2SQ = CTA2*CTA2
      DO 1 I = 1, NSIZE
      X = KZ(I)
      IF( X .NE. 0.D0 ) GO TO 2
      IEMPO(I) = DCMPLX( 1.D70, 1.D70 )
      GO TO 1
2  TSRX = DSQRT(2.D0*X)
      XP4 = X + PIO4
      XC = X*CTA
      XCP4 = XC + PIO4
      IEIKZ = STA2*DCMPLX(DCOS(XP4), DSIN(XP4))/TSRX
      SEKC = STA*DCMPLX(DCOS(XCP4),-DSIN(XCP4) )
      IEMPO(I)=(4.D0/SRTPI)*(IEIKZ+SEKC*FRESNL(2.D0*X*CTA2SQ)) - 2.D0*
1  STA*DCMPLX(DCOS(XC),-DSIN(XC))
1  CONTINUE
      RETURN
      END

```


C Function FRESNL evaluates a form of the Fresnel Integral for
 C argument X, specifically, the integral from zero to SQRT(X) of
 C exp(it**2)dt. A Chebyshev polynomial expansion is used for X less
 C than 7 and another is used for X greater than 7. The coefficients
 C are from Table 24, page 328 and 329 of Volume II of Luke's book,
 C "The Special Functions and Their Approximations." The coefficients
 C given here are simply those in the book divided by two. FRESNL is
 C called by XIEMPO and by a subprogram used in finding (IH-Ipo).

```

C-----
      COMPLEX FUNCTION FRESNL*16(X)
      COMPLEX*16 DCMPLX
      REAL*8 X, DSQRT, DSIN, DCOS, RPIO2, A(16), B(16), RC(25), IC(25),
1     Y(2), XX, DABS, XO8, FOX, XO8SQ
      DATA RPIO2/1.25331413731550025121D0/
      DATA A/
1     -0.000000000000000008751D0,    0.0000000000000000493266D0,
2     -0.000000000000000024172016D0,    0.0000000000000001018666274D0,
3     -0.000000000000000036450810593D0,    0.0000000000000001090829227466D0,
4     -0.000000000000000026804669944621D0,    0.000000000000000528698828191630D0,
5     -0.000008132488809443773D0,    0.000093927711719911009D0,
6     -0.00773262242230690979D0,    0.04208022660438467689D0,
7     -0.13486655169193555514D0,    0.21644099989863326527D0,
      -0.21567773773830089656D0,    0.38217569332093000094D0/
      DATA B/
1     -0.00000000000000000001109D0,    0.000000000000000000066819D0,
2     -0.000000000000000003516208D0,    0.000000000000000160024212D0,
3     -0.000000000000000006224915109D0,    0.000000000000000204124865848D0,
4     -0.00000000000000005549420920434D0,    0.000000000000000122560374961649D0,
5     -0.000002143535766051002D0,    0.00002872747598448683D0,
6     -0.000282281738566095449D0,    0.001911127889316504347D0,
7     -0.08124744577254783707D0,    0.18808586321671828312D0,
      -0.21172255702852666772D0,    0.31520702157285269620D0/
      DATA RC/
1     0.000000000000000000002612D0,    0.000000000000000000003239D0,
2     -0.0000000000000000000037573D0,    0.00000000000000000000155347D0,
3     -0.000000000000000000000429646D0,    0.000000000000000000000698781D0,
4     0.000000000000000000000634657D0,    -0.0000000000000000000010357825D0,
5     0.00000000000000000000047315709D0,    -0.00000000000000000000135101335D0,
6     0.000000000000000000000169738230D0,    0.000000000000000000000764304404D0,
7     -0.0000000000000000000006578827233D0,    0.00000000000000000000026775038355D0,
8     -0.00000000000000000000054407240611D0,    -0.000000000000000000000133275825051D0,
9     0.0000000000000000000001887764024651D0,    -0.0000000000000000000009382910042642D0,
      0.00000000000000000000015767650161726D0,    0.000000000000000000000174661432988653D0,
      -0.000001956652043150792D0,    0.0000007326700129053392D0,
      0.000087714356982572662D0,    -0.002249606510061970698D0,
      -0.02327889936875822803D0 /
      DATA IC/
1     -0.000000000000000000005898D0,    0.00000000000000000000018144D0,
2     -0.00000000000000000000038087D0,    0.000000000000000000000028479D0,
3     0.0000000000000000000000201778D0,    -0.0000000000000000000001275308D0,
4     0.00000000000000000000004503197D0,    -0.00000000000000000000010204942D0,
5     0.00000000000000000000005356182D0,    0.00000000000000000000085821900D0,
6     -0.000000000000000000000526846515D0,    0.0000000000000000000001821160947D0,
7     -0.0000000000000000000003153985690D0,    -0.0000000000000000000008238645529D0,
8     0.00000000000000000000098311801633D0,    -0.00000000000000000000045439864633D0,
9     0.000000000000000000000953974378644D0,    0.0000000000000000000003754635868605D0,
      -0.0000000049952763318406D0,    0.0000000244184087696664D0,
      0.000000053953449370317D0,    -0.000013304747632362367D0,
      0.00124137141155653017D0,    0.00609175491573949873D0,
  
```



```

      B          -0.49528023968674877433D0  /
      XX = DABS(X)
      IF( XX .LT. 7.D0 ) GO TO 1
      FOX = 5.D0/XX
C-----
C      Sum the Chebyshev series.
C-----
      CALL EATSTR( FOX, 24, RC, Y(1) )
      CALL EATSTR( FOX, 24, IC, Y(2) )
      FRESNL = DCMPLX(0.5D0,0.5D0)*RPIO2+DCMPLX(Y(1),Y(2))*
1      DCMPLX( DCOS(XX),DSIN(XX))/DSQRT(XX)
      RETURN
1  XO8 = XX/8.D0
   XO8SQ = XO8*XO8
C-----
C      Sum the Chebyshev series.
C-----
      CALL EATSTR( XO8SQ, 15, A, Y(1) )
      CALL EAT2P1( XO8, 15, B, Y(2) )
      FRESNL = DCMPLX( Y(1), Y(2) ) *DSQRT(XX)
      RETURN
      END

C      Subroutine SEP is used to separate C, a COMPLEX*16 variable,
C      into its real part, imaginary part, magnitude and phase. These
C      results are stored in A(1) through A(4), respectively. A is an
C      array of length 4 and of type REAL*8. SEP is used in PNTOWT.
C-----
      SUBROUTINE SEP(C, A )
      COMPLEX*16 C, CC
      REAL*8 C2(2), A(4), CDABS, O80OPI,PI, DATAN2
      DATA PI/3.14159265358979323846D0/
      EQUIVALENCE(CC,C2)
      O80OPI = 180.D0/PI
      CC=C
      A(1) = C2(1)
      A(2) = C2(2)
      A(3) = CDABS(CC)
      A(4) = O80OPI*DATAN2( C2(2), C2(1) )
      RETURN
      END

```


Computer Program for H-polarization Half-Plane Current.

These routines were written by
Donald Farness Hanson, June, 1975.

C The following MAIN program evaluates the H-polarization
C (H-vector parallel to the edge) half-plane current minus the
C physical optics current, (IH-Ipo), from the values of (IE-IPO) found
C previously by the method of moments. For each point along the
C half-plane, two numerical integrations must be performed. For the
C first, the values of (IE-IPO) must be known for angle of incidence
C THETAD=90 degrees and for the second, (IE-IPO) must be known for the
C angle of incidence for which (IH-Ipo) is to be found. The details
C of this method are presented elsewhere in this work. MAIN reads
C RESULT vectors written on the disk by the moment method program for
C (IE-IPO) and operates upon them in the appropriate fashion. Results
C are written on the disk for THETAD=45, 90, 135, and 180 degrees
C respectively. Results due to the hybrid expansion are read from
C disk file 21 and those due to the pulse-everywhere expansion are
C read from disk file 22. The approximate results for (IH-Ipo) due to
C the numerical integrations are stored in IHMPOA by SUBROUTINE AIHMPO
C and the "exact" results due to the analytic expression are stored in
C IHMPOX by SUBROUTINE XIHMPO. MAIN calls YARRAY, AIHMPO, XIHMPO, and
C PNTOUT directly. A list of the subprograms called by each of these
C routines is given among the respective routine descriptions. This
C routine requires 132 seconds of IBM 360/75 execution time, and 9
C seconds of compile time.

```

C-----
      COMPLEX*16 DCMPLX, A(200), B1(200), B2(200), EIKZ(200), IHMPOA(499
1      ), IHMPOX(499)
      REAL*8 Y(499), KZ(200), H, THETAD, TA(2), DCOS, DSIN
      INTEGER I, J, NPTS, NSIZE
      LOGICAL HYORPS
      NSIZE = 200
      NPTS = 499

```

```

C-----
C      Read hybrid expansion RESULT arrays for 45 and 90 degrees into A
C      and B1, respectively.
C-----

```

```

      READ(21) TA(1), H, KZ, A, A, A
      READ(21) TA(2), H, KZ, B1, B1, B1

```

```

C-----
C      Set up an array Y of points at which to evaluate the current
C      (IH-Ipo).
C-----

```

```

      CALL YARRAY( NPTS, KZ, NSIZE, H, Y )

```

```

C-----
C      Write these points on disk file 25.
C-----

```

```

      WRITE(25) NPTS, H, Y

```



```

C-----
C      Fill an array with often used numbers to make the program more
C      efficient.
C-----
      DO 1 I=1, NSIZE
1 EIKZ(I) = DCMPLX( DCOS(KZ(I) ), DSIN( KZ(I) ) )
      THETAD = TA(1)
      HYORPS = .TRUE.
C-----
C      Evaluate the current (IH-Ipo) for 45 degrees using the hybrid
C      expansion.
C-----
      CALL AIHMPO( NPTS, Y, A, B1, KZ, EIKZ, NSIZE, H, THETAD, HYORPS,
1 IHMPOA )
      CALL XIHMPO( NPTS, Y, THETAD, IHMPOX )
C-----
C      Compare with "exact."
C-----
      CALL PNTOUT( THETAD, NPTS, Y, IHMPOA, IHMPOX, HYORPS )
C-----
C      Read pulse-everywhere expansion RESULT arrays for 45 and 90
C      degrees into A and B2, respectively.
C-----
      READ(22) TA(1), NSIZE, H, KZ, A
      READ(22) TA(2), NSIZE, H, KZ, B2
      HYORPS = .FALSE.
C-----
C      Evaluate the current (IH-Ipo) for 45 degrees using
C      pulse-everywhere expansion.
C-----
      CALL AIHMPO( NPTS, Y, A, B2, KZ, EIKZ, NSIZE, H, THETAD, HYORPS,
1 IHMPOA )
C-----
C      Compare with "exact."
C-----
      CALL PNTOUT( THETAD, NPTS, Y, IHMPOA, IHMPOX, HYORPS )
      HYORPS = .TRUE.
C-----
C      Read B1 into A.
C-----
      DO 2 I=1, NSIZE
2 A(I) = B1(I)
      THETAD = TA(2)
C-----
C      Calculate the current (IH-Ipo) for 90 degrees using the hybrid
C      expansion.
C-----
      CALL AIHMPO( NPTS, Y, A, B1, KZ, EIKZ, NSIZE, H, THETAD, HYORPS,
1 IHMPOA )
      CALL XIHMPO( NPTS, Y, THETAD, IHMPOX )
      CALL PNTOUT( THETAD, NPTS, Y, IHMPOA, IHMPOX, HYORPS )
      HYORPS = .FALSE.
C-----
C      Read B2 into A.
C-----

```


Computer Program for H-polarization Half-Plane Current.

Page 3

```

      DO 3 I=1, NSIZE
3 A(I) = B2(I)
      THETAD = TA(2)
C-----
C      Calculate the current (IH-Ipo) for 90 degrees using the
C      pulse-everywhere expansion.
C-----
      CALL AIHMPO(NPTS, Y, A, B2, KZ, EIKZ, NSIZE, H, THETAD, HYORPS,
1          IHMPOA )
      CALL PNTOUT( THETAD, NPTS, Y, IHMPOA, IHMPOX, HYORPS )
      DO 4 J=3, 4
      HYORPS = .TRUE.
C-----
C      Read hybrid expansion RESULT array for 135(J=3) and 180(J=4)
C      degrees and calculate the current (IH-Ipo).
C-----
      READ(21) THETAD, H, KZ, A, A, A
      CALL AIHMPO( NPTS, Y, A, B1, KZ, EIKZ, NSIZE, H, THETAD, HYORPS,
1          IHMPOA )
      CALL XIHMPO( NPTS, Y, THETAD, IHMPOX )
      CALL PNTOUT( THETAD, NPTS, Y, IHMPOA, IHMPOX, HYORPS )
      HYORPS = .FALSE.
C-----
C      Read pulse-everywhere expansion RESULT array for 135(J=3) and
C      180(J=4) degrees and calculate the current (IH-Ipo).
C-----
      READ(22) THETAD, NSIZE, H, KZ, A
      CALL AIHMPO( NPTS, Y, A, B2, KZ, EIKZ, NSIZE, H, THETAD, HYORPS,
1          IHMPOA )
      CALL PNTOUT( THETAD, NPTS, Y, IHMPOA, IHMPOX, HYORPS )
4 CONTINUE
      STOP
      END

```


C Subroutine YARRAY generates the points at which it is desired
 C to calculate the current (IH-Ipo). NPTS is used here to dimension
 C array Y only; otherwise, it is not used. KZ is the array of match
 C points that was used in the method of moment solution for (IE-IPO).
 C H is the half subsection width ($H=0.05$) and Y is the output array of
 C points. One hundred points are equally spaced $H/100$ apart within
 C the interval (0:H) and 399 points are equally spaced H apart on the
 C interval (H:19.95). These points were chosen to provide the details
 C of the current near the edge as well as the general form away from
 C the edge.

C-----

```

SUBROUTINE YARRAY( NPTS, KZ, NSIZE, H, Y )
  INTEGER NPTS, NSIZE
  REAL*8 KZ(NSIZE), H, Y(NPTS), DZ, DFLOAT
  INTEGER I, OFFSET, J
  Y(1) = KZ(1)
  DZ = H/100.D0

```

C-----

C Evaluate Y for points near the edge.

C-----

```

DO 1 I=1, 100
1 Y(I+1) = DFLOAT(I)*DZ
  OFFSET = 98

```

C-----

C Evaluate Y for points away from the edge.

C-----

```

DO 2 I=2, NSIZE
  J = OFFSET + I + I
  Y(J) = KZ(I)
2 Y(J+1) = KZ(I) + H
  RETURN
END

```


C Subroutine AIHMPO calculates the current (IH-Ipo) at the NPTS
C points contained in array YVALU by the Green's function method
C applied to (IE-IPO). A and B are arrays of values of (IE-IPO) for
C angles of incidence THETAD and 90 degrees, respectively. KZ is the
C array of match points used in obtaining A and B. EIKZ is an array
C of values of $\exp(iKZ)$ which is used to increase program efficiency
C by calculating the numbers once and storing them for later use.
C Arrays A, B, KZ, and EIKZ are all of length NSIZE. H is the
C subsection half-width that was used for (IE-IPO). HYORPS (HYbrid OR
C Pulse) is a logical variable which is .TRUE. when the A and B arrays
C correspond to the hybrid expansion for (IE-IPO) and is .FALSE. for
C the pulse-everywhere expansion. IHMPOA is the output array of
C (IH-Ipo) values and is of length NPTS. AIHMPO calls either
C IFGHP(pulse) or IFGHSH(hybrid). The "exact" value of the
C consistency constant is used for convenience.

```

C-----
      SUBROUTINE AIHMPO( NPTS, YVALU, A, B, KZ, EIKZ, NSIZE, H, THETAD,
1      HYORPS, IHMPOA )
      INTEGER NPTS, NSIZE
      COMPLEX*16 DCMLPX, A(NSIZE), B(NSIZE), EIKZ(NSIZE), IHMPOA(NPTS)
1,   HSUME, HSUMS, GSUMS, ITIMES, EIY
      REAL*8 H, THETAD, KZ(NSIZE), YVALU(NPTS), DSIN, DCOS, DSQRT, STA,
1   CTA2, PI/3.14159265358979323846D0/, THETA, SY, CY, Y, SRT2
      INTEGER I
      LOGICAL HYORPS
      SRT2 = DSQRT( 2.D0 )
      THETA = (THETAD/180.D0)*PI
      STA = DSIN( THETA )
      CTA2 = DCOS( THETA/2.D0 )
      IF( THETAD .EQ. 180.D0 ) CTA2 = 0.D0
      DO 2 I=1, NPTS
      Y = YVALU(I)
      SY = DSIN(Y)
      CY = DCOS(Y)
      EIY = DCMLPX( CY, SY )
      IF( HYORPS ) GO TO 1
      CALL IFGHP(Y, A, B, KZ, EIKZ, NSIZE, H, GSUME, GSUMS, HSUME, HSUMS)
      GO TO 2
1   CALL IFGHSH(Y, A, B, KZ, EIKZ, NSIZE, H, GSUME, GSUMS, HSUME, HSUMS)
2   IHMPOA(I) = EIY*(SRT2*CTA2*ITIMES(HSUME) + STA*GSUME - 2.D0)
1   + SY*(SRT2*CTA2*ITIMES(HSUMS) + STA*GSUMS)
      RETURN
      END

```


C Subroutine IFGHSH and entry subroutine IFGHP evaluate four
 C numerical integrations that are required by AIHMPO to evaluate the
 C current (IH-Ipo) from the current (IE-IPO). The internal logical
 C variable HORP (Hybrid OR Pulse) is set to .TRUE. if IFGHSH is called
 C and to .FALSE. if IFGHP is called. Y is the point at which the
 C current (IH-Ipo) is to be evaluated. A, B, KZ, and EIKZ are the
 C same as described in the write-up for AIHMPO and are arrays of
 C length NNSIZE. H is the subsection half-width for (IE-IPO).
 C Outputs GSUME, GSUMS, HSUME, and HSUMS are the values of the
 C numerical integrations. Prefixes of "G" and "H" are used to specify
 C results associated with the A and B vectors, respectively. Suffixes
 C of "E" and "S" are used to specify that the results need to be
 C multiplied by $\exp(iY)$ and $\sin(Y)$, respectively. Either IFGHSH or
 C IFGHP is used by AIHMPO.

```

C-----
      SUBROUTINE IFGHSH( Y, A, B, KZ, EIKZ, NNSIZE, H, GSUME, GSUMS,
1      HSUME, HSUMS )
      INTEGER NNSIZE
      COMPLEX*16 A(NNSIZE), B(NNSIZE), EIKZ(NNSIZE), GSUME, GSUMS,
1      HSUME, HSUMS, FRESNL, DCMLPX, TMP, ZRO/(0.D0,0.D0)/, SAEKZ,
2      SBKZ, FDI
      REAL*8 Y, YY, H, HH, KZ(NNSIZE), TEMP(2), SH, DSIN, DCOS, DABS,
1      SNKZ, CSKZ, SP, SM, ARG, PT, TWO/2.D0/
      INTEGER I, J, K, NYSM1, NYS, NYSPl, IDINT, NSIZE
      LOGICAL HORP
      EQUIVALENCE( TMP, TEMP)

```

```

C-----
C      Initialize HORP(.TRUE. for hybrid, .FALSE. for pulse).
C-----

```

```

      HORP = .TRUE.
      GO TO 1
      ENTRY IFGHP( Y, A, B, KZ, EIKZ, NNSIZE, H, GSUME, GSUMS, HSUME,
1      HSUMS )
      HORP = .FALSE.
1  NSIZE = NNSIZE
      YY = DABS(Y)
      HH = H
      SH = DSIN(HH)

```

```

C-----
C      NYS is the number of the subsection that Y is in.
C-----

```

```

      NYSM1 = IDINT( (YY/HH+1.D0)/TWO )
      NYS = NYSM1 + 1
      NYSPl = NYSM1+2

```

```

C-----
C      See if Y is or is not within the first subsection and respond
C      accordingly.
C-----

```

```

      IF(HORP) GO TO 3
      IF(NYS.EQ.1) GO TO 2
      PT = DSIN(HH/TWO)
      PT = PT*PT
      GSUME = A(1)*PT
      HSUME = B(1)*SH/TWO
      GO TO 5

```


Computer Program for H-polarization Half-Plane Current.

Page 7

```

2 PT = DSIN(YY/TWO)
  PT = PT*PT
  GSUME=A(1)*PT
  HSUME=B(1)*DSIN(YY)/TWO
  ARG=(HH-YY)/TWO
  SM = DSIN(ARG)
  ARG = (HH+YY)/TWO
  TMP = DCMPLX( DCOS(ARG), DSIN(ARG) )
  GSUMS = A(1)*SM*TMP
  HSUMS = B(1)*SM*TMP
  GO TO 8
3 IF( NYS .EQ. 1 ) GO TO 4
  TMP = FRESNL( HH )
  GSUME = A(1)*TEMP(2)
  HSUME = B(1)*TEMP(1)
  GO TO 5
4 TMP = FRESNL(YY)
  GSUME = A(1)*TEMP(2)
  HSUME = B(1)*TEMP(1)
  FDIF = FRESNL(HH)
  FDIF = FDIF - TMP
  GSUMS = A(1)*FDIF
  HSUMS = B(1)*FDIF
  GO TO 8

```

C Integrate from subsection 2 through (NYS-1).

```

5 IF( NYSM1 .LT. 2 ) GO TO 7
  SAEKZ = ZRO
  SBKZ = ZRO
  DO 6 I=2, NYSM1
    J = NYSM1-I+2
    TMP = EIKZ(J)
    SNKZ = TEMP(2)
    CSKZ = TEMP(1)
    SAEKZ = SAEKZ + A(J)*SNKZ
6  SBKZ = SBKZ + B(J)*CSKZ
    GSUME = GSUME + SH*SAEKZ
    HSUME = HSUME + SH*SBKZ

```

C Treat subsection NYS.

```

7 ARG = (YY + KZ(NYS) - HH)/TWO
  SNKZ = DSIN(ARG)
  CSKZ = DCOS( ARG )
  SM = DSIN( (YY-KZ(NYS)+HH)/TWO)
  GSUME = GSUME + A(NYS)*(SM*SNKZ)
  HSUME = HSUME + B(NYS)*(SM*CSKZ)
  ARG = (YY+KZ(NYS)+HH)/TWO
  TMP= DCMPLX( DCOS(ARG), DSIN(ARG) )
  SM = DSIN( (KZ(NYS)+HH-YY)/TWO )
  GSUMS = A(NYS)*SM*TMP
  HSUMS = B(NYS)*SM*TMP

```



```

C-----
C      Integrate from subsection (NYS+1) through NSIZE.
C-----
      8 IF( NSIZE .LT. NYSP1 ) GO TO 10
        SAEKZ = ZRO
        SBEKZ = ZRO
        DO 9 I= NYSP1, NSIZE
          J= NSIZE - I + NYSP1
          SAEKZ = SAEKZ + A(J)*EIKZ(J)
        9 SBEKZ = SBEKZ + B(J)*EIKZ(J)
          GSUMS = GSUMS + SH*SAEKZ
          HSUMS = HSUMS + SH*SBEKZ
      10 TMP = HSUMS
        HSUMS = DCMPLX( -TEMP(2), TEMP(1) )
C-----
C      Multiply all sums by a common factor of -2.
C-----
        HSUMS = -TWO*HSUMS
        GSUMS = -TWO*GSUMS
        HSUME = -TWO*HSUME
        GSUME = -TWO*GSUME
        RETURN
        END

```

```

C      Function ITIMES takes "i" times the argument S. ITIMES is
C      called by AIHMPO, IFGHSH, and IFGHP.
C-----

```

```

      COMPLEX FUNCTION ITIMES*16(S)
      COMPLEX*16 S, SS, DCMPLX
      REAL*8 SS2(2)
      EQUIVALENCE( SS, SS2 )
      SS = S
      ITIMES = DCMPLX( -SS2(2), SS2(1) )
      RETURN
      END

```


Computer Program for H-polarization Half-Plane Current.

Page 9

C Subroutine XIHMPO calculates the current (IH-Ipo) at the NPTS
 C points stored in array KZ by the analytic or "exact" formula. The
 C output is returned in array IHMPOX. KZ and IHMPOX are arrays of
 C length NPTS. THETAD is the angle of incidence in degrees. XIHMPO
 C calls FRESNL and is called by MAIN.

```

C-----
      SUBROUTINE XIHMPO( NPTS, KZ, THETAD, IHMPOX)
      INTEGER NPTS
      COMPLEX*16 DCMPLX, IHMPOX(NPTS), FRESNL, EIKZC
      REAL*8 KZ(NPTS), Y, THETAD, THETA, DCOS, DSIN, CTA, CTA2SQ,
1 PI, PIO4, SQRTPI, YC, YCP4
      DATA PI/3.14159265358979323846D0/,
1 SQRTPI/1.77245385090551602730D0/,
2 PIO4/0.78539816339744830962D0/
      INTEGER I
      THETA = ( THETAD/180.D0)*PI
      CTA = DCOS( THETA)
      CTA2SQ = DCOS(THETA/2.D0 )
      IF( THETAD .EQ. 180.D0 ) CTA2SQ = 0.D0
      CTA2SQ = CTA2SQ*CTA2SQ
      DO 1 I=1, NPTS
      Y= KZ(I)
      YC = Y*CTA
      YCP4 = YC + PIO4
      EIKZC = DCMPLX( DCOS(YCP4), -DSIN(YCP4) )
1 IHMPOX(I) = (4.D0/SQRTPI)*(EIKZC*FRESNL(2.D0*Y*CTA2SQ) )
1 -2.D0*DCMPLX(DCOS(YC),-DSIN(YC) )
      RETURN
      END

```


C Subroutine PNTOUT writes results in disk file 25 and also
 C prints out the "exact" and the approximate real part, imaginary
 C part, magnitude and phase of (IH-Ipo). THETAD is the angle of
 C incidence in degrees. Y, IHMPOA, and IHMPOX are arrays of length
 C NPTS. IHMPOA and IHMPOX have been filled by subprograms AIHMPO and
 C XIHMPO, respectively, with values of approximate and "exact"
 C (IH-Ipo) evaluated at the points contained in Y. HYORPS is .TRUE.
 C when the numbers corresponding to the hybrid expansion are being
 C passed.

```

C-----
      SUBROUTINE PNTOUT( THETAD, NPTS, Y, IHMPOA, IHMPOX, HYORPS )
      INTEGER NPTS
      COMPLEX*16 IHMPOA(NPTS), IHMPOX(NPTS), EXACT, ANS
      REAL*8 SA(4), SX(4), ZM(3, 4), Y(NPTS), THETAD
      INTEGER J, K, IC(4)/' RE=', ' IM=', 'MAG=', 'AGL='/, I
      LOGICAL HYORPS
      PRINT 1, THETAD
1  FORMAT('1', 'THETAD=', F9.4//T5, 'KZ', T19, 'EXACT', T38, 'ANS', T56,
1  'DIFF', T76, 'EXACT', T97, 'ANS', T114, 'DIFF' )
C-----
C      Write results on disk.
C-----
      WRITE(25) THETAD, IHMPOA
      IF(HYORPS) WRITE(25) IHMPOX
C-----
C      Print results.
C-----
      DO 3 K=1, NPTS
      EXACT = IHMPOX(K)
      ANS = IHMPOA(K)
      CALL SEP( EXACT, SX )
      CALL SEP( ANS, SA )
      DO 2 J=1, 4
      ZM(1,J) = SX(J)
      ZM(2,J) = SA(J)
2  ZM(3,J) = SX(J) - SA(J)
3  PRINT 4, Y(K), ( IC(I), (ZM(J,I), J=1,3), I=1,4 )
4  FORMAT(' ', T2, '0PF8.5,T10,2(A4,'<',1PD17.10,'/',D17.10,'>',D17.10
1  , 2X)/T10,A4,'<',D17.10,'/',D17.10,'>',D17.10,2X,A4,'<',0PF17.10,
2  '/',F17.10,'>',F17.10 )
      RETURN
      END

```


REFERENCES

- Abramowitz, M. and Stegun, I. A. (1964). Handbook of Mathematical Functions, National Bureau of Standards, AMS 55, United States Dept. of Commerce, Washington.
- Antosik, P., Mikusiński, J., and Sikorski, R. (1973). Theory of Distributions, The Sequential Approach, Elsevier Publishing Co., New York.
- Arsac, J. (1966). Fourier Transforms and The Theory of Distributions, Prentice-Hall, Inc., Englewood Cliffs, N.J.
- Bareiss, E. H. (1969). "Numerical Solution of Linear Equations with Toeplitz and Vector Toeplitz Matrices," Numer. Math. 13, pp. 404-424.
- Beltrami, E. J., and Wohlers, M. R. (1966). Distributions and the Boundary Values of Analytic Functions, Academic Press, New York.
- Belward, J. A. (1972). "Solutions of some Fredholm Integral Equations Using Fractional Integration, with an Application to a Forced Convection Problem," J. Appl. Math. Phys. (ZAMP) 23, pp. 901-917.
- Blanch, G. (1964). "Numerical Evaluation of Continued Fractions," SIAM Review 6, #4 (Oct. 1964), pp. 383-421.
- Boehme, T. K. (1963). "Operational Calculus and the Finite Part of Divergent Integrals," Trans. Amer. Math. Soc. 106, #2 (Feb. 1963), pp. 346-368.
- Balomey, J. Ch. (1974). "Methodes Numeriques en Electromagnetisme," Computing Methods in Applied Sciences and Engineering, Part 2, Lecture Notes in Computer Science, Volume 11, Springer-Verlag, New York, pp. 261-288.
- Born, M., and Wolf, E. (1970). Principles of Optics, Fourth Edition, Pergamon Press, New York.
- Bouwkamp, C. J. (1946). "A Note on Singularities Occurring at Sharp Edges in Electromagnetic Diffraction Theory," Physica 12, #7 (Oct. 1946), pp. 467-474.
- Bouwkamp, C. J. (1954). "Diffraction Theory," Rept. Progr. Phys. 17, pp. 35-100.
- Bremermann, H. J., et al. (1967). The Applications of Generalized Functions, Studies in Applied Mathematics, Volume 2, Soc. Ind. and Appl. Math., Philadelphia, Penn. Reprinted from SIAM J. on Appl. Math. 15, pp. 771-1111.

- Bromwich, T. J. I'A. (1915). "Diffraction of Waves by a Wedge," Proc. London Math. Soc. 14, (May 13, 1915), pp. 450-463.
- Bureau, F. J. (1955). "Divergent Integrals and Partial Differential Equations," Comm. Pure Appl. Math. 8, pp. 143-202.
- Butzer, P. L. (1959). "Singular Integral Equations of Volterra Type and the Finite Part of Divergent Integrals," Arch. Rational Mech. Anal. 3, pp. 194-205.
- Cameron, N. (1966). "The Numerical Solution of the Singular Integral Equation for Diffraction by a Soft Strip," Quart. Journ. Mech. and Appl. Math. 19, Part I, pp. 93-105.
- Cauchy, A. L. (1826). "Sur un nouveau genre d'integrales," Oeuvres Complètes d'Augustin Cauchy, Series II, Volume 6, pp. 78-88; also, "Diverses propriétés de la fonction $\Gamma(x)$," Oeuvres Complètes d'Augustin Cauchy, Series II, Volume 7, pp. 121-123, Gauthier-Villars, Paris, 1938.
- Collin, R. E. (1960). Field Theory of Guided Waves, McGraw-Hill Book Company, New York.
- Copson, E. T. (1946). "On an Integral Equation Arising in the Theory of Diffraction," Quart. J. Math. 17, pp. 19-34.
- Copson, E. T. (1950). "Diffraction by a Plane Screen," Proceedings of the Royal Society 202, Series A, pp. 277-284.
- De Jager, E. M. (1969). Applications of Distributions in Mathematical Physics, Mathematisch Centrum, Amsterdam.
- De Jager, E. M. (1970). "Theory of Distributions," Chapter II of Deschamps et al. (1970).
- Deschamps, G. A., et al. (1970). Mathematics Applied to Physics, Springer-Verlag, New York.
- Dmitriev, V. I., and Zakharov, E. V. (1967). "Diffraction of a Plane Electromagnetic Field by an Ideally Conducting Strip in a Layered Medium," Akademiia Nauk SSSR--Izvestiia, Physics of the Solid Earth 1967, #5, pp. 304-308.
- Dörr, J. (1952). "Two Integral Equations of the First Kind, which Themselves Aid in Yielding Mathieu Function Solutions," Zeit. f. Angewandte Math. Phys. (ZAMP) 3, #6 (Nov. 1952), pp. 427-439.
- Erdogan, F. (1969). "Approximate Solutions of Systems of Singular Integral Equations," SIAM J. Appl. Math. 17, #6 (Nov. 1969), pp. 1041-1059.

- Friedlander, F. G. (1951). "On the Half-plane Diffraction Problem," Quart. Journ. Mech. and Appl. Math. 4, Part 3, pp. 344-357.
- Gel'fand, I. M., and Shilov, G. E. (1964). Generalized Functions, Properties and Operations, Volume I, Academic Press, New York.
- Hadamard, J. (1923). Lectures on Cauchy's Problem in Linear Partial Differential Equations, Yale University Press, New Haven.
- Hallén, E. (1938). "Theoretical Investigations into the Transmitting and Receiving Qualities of Antennae," Nova Acta Regiae Soc. Sci. Upsaliensis 11, Series IV, pp. 1-44.
- Hanson, D. F., and Mayes, P. E. (1975). "Use of a Hybrid Expansion in Moment Method to Incorporate Edge Conditions," URSI Program and Abstract Digest, (Oct. 1975), Boulder, Colorado.
- Hart, J. F., et al. (1968). Computer Approximations, John Wiley and Sons, New York.
- Harrington, R. F. (1968). Field Computation by Moment Methods, Macmillan Company, New York.
- Jones, D. S. (1966). Generalised Functions, McGraw-Hill Book Company, New York.
- Kanwal, R. P. (1971). Linear Integral Equations, Academic Press, New York.
- Karp, S. N. (1950). "Wiener-Hopf Techniques and Mixed Boundary Value Problems," Comm. Pure Appl. Math. 3, pp. 411-426.
- Lanczos, C. (1961). Linear Differential Operators, Van Nostrand Company, New York.
- Latta, G. E. (1956). "The Solution of a Class of Integral Equations," J. Rational Mech. Anal. 5, #5, pp. 821-834.
- Latta, G. E. (1974). "Transform Methods," Chapter 11 of Pearson (1974).
- Lavoine, J. (1963). Transformation de Fourier des Pseudo-fonctions avec Tables de Nouvelles Transformées, Centre National de la Recherche Scientifique, Paris.
- Lebedev, N. N., Skal'skaya, I. P., and Uflyand, Ya. S. (1966). Problems in Mathematical Physics, Pergamon Press, New York.
- Li, T.-S. (1972). "A Spectral Domain Approach to the Numerical Solution of Electromagnetic Scattering Problems," University of Illinois Ph.D. Thesis (Feb. 1972).

- Luke, Y. L. (1962). Integrals of Bessel Functions, McGraw-Hill Book Co., New York.
- Luke, Y. L. (1969). The Special Functions and Their Approximations, Volumes I and II, Academic Press, New York.
- Magnus, W. (1941). "Über die Beugung elektromagnetischer Wellen an einer Halbebene," Zeitschrift für Physik 117, pp. 168-179.
- Mayes, P. E. (1972). "A New Integral Equation Technique for Electromagnetic Scattering," URSI Program and Abstract Digest (Dec. 1972), Williamsburg, Virginia.
- McLachlan, N. W. (1947). Theory and Applications of Mathieu Functions, Corrected Edition 1951, Oxford University Press, London.
- Meixner, J., and Schafke, F. W. (1954). Mathieu Functions and Spheroidal Functions with Applications to Physical and Technical Problems, Springer-Verlag, Berlin.
- Mittra, R., and Lee, S. W. (1971). Analytical Techniques in the Theory of Guided Waves, Macmillan Company, New York.
- Mittra, R. (1973). Computer Techniques for Electromagnetics, Pergamon Press, New York.
- Miles, J. W. (1949). "On Certain Integral Equations in Diffraction Theory," J. Math. Phys. 28, pp. 223-226.
- Morse, P. M., and Rubenstein, P. J. (1938). "The Diffraction of Waves by Ribbons and by Slits," Phys. Rev. 54, (Dec. 1, 1938), pp. 895-898.
- Moullin, E. B., and Phillips, F. M. (1952). "On the Current Induced in a Conducting Ribbon by the Incidence of a Plane Electromagnetic Wave," Proc. Institution Elec. Engrs. 99, Part IV, #3 (July 1952), pp. 137-150.
- Müller, H. N. (1967). "On a Singular Integral Equation of the First Kind with a Difference Kernel," Math. Nachr. 35, pp. 57-74.
- Muskhelishvili, N. I. (1958). Singular Integral Equations, Wolters-Noordhoff Publishing, Groningen, The Netherlands; Reprinted 1972.
- Noble, B. (1958). Methods Based on the Wiener-Hopf Technique for the Solution of Partial Differential Equations, Pergamon Press, New York.
- Oldham, K. B., and Spanier, J. (1974). The Fractional Calculus, Academic Press, New York.

- Olver, F. W. J. (1964). "Bessel Functions of Integer Order," Chapter 9 of Abramowitz and Stegun (1964).
- Pearson, C. E. (1974). Handbook of Applied Mathematics, Van Nostrand Reinhold, New York.
- Pearson, L. W. (1975). Private Communication.
- Pocklington, H. C. (1897). "Electrical Oscillations in Wire," Camb. Phil. Soc. Proc. 9, pp. 324-332.
- Preis, D. H. (1972). "The Toeplitz Matrix: Its Occurrence in Antenna Problems and a Rapid Inversion Algorithm," IEEE Trans. Antennas Propagation AP-20, pp. 204-206.
- Prettie, C. W., and Dudley, D. G. (1974). "A Re-examination of the Pocklington Formulation for the Currents on a Wire Scatterer," Private Communication.
- Rayleigh, Lord. (1897). "On the Passage of Waves through Apertures in Plane Screens, and Allied Problems," Phil. Mag. 43, Series 5, #263 (April 1897), pp. 259-272.
- Schmidt, G. (1968). "Spectral and Scattering Theory for Maxwell's Equations in an Exterior Domain," Arch. Rational Mech. Anal. 28, pp. 284-322.
- Schwartz, L. (1966a). Théorie des Distributions, Hermann, Paris.
- Schwartz, L. (1966b). Mathematics for the Physical Sciences, Hermann, Paris.
- Shafai, L. (1971). "Currents Induced on a Conducting Strip," Canadian Journal of Physics 49, pp. 495-498.
- Shilov, G. E. (1968). Generalized Functions and Partial Differential Equations, Gordon and Breach, New York.
- Sommerfeld, A. (1896). "Mathematische Theorie der Diffraction," Math. Ann. 47, pp. 317-374.
- Sommerfeld, A. (1964). Lectures on Theoretical Physics, Volume IV--Optics, Academic Press, New York.
- Stakgold, I. (1967). Boundary Value Problems of Mathematical Physics, Volumes I and II, Macmillan Company, New York.
- Strutt, M. J. O. (1931). "Beugung einer ebenen Welle an einem Spalt von endlicher Breite," Z. Phys. 69, pp. 597-617.

- Tai, C.-T. (1971). Dyadic Green's Functions in Electromagnetic Theory, Intext Educational Publishers, Scranton, Penn.
- Wiener, K. (1962). "Lineare Integralgleichungen mit Hadamard-Integralen," Wiss. Z. M.-L. Univ. Halle--Wittenberg 11, pp. 567-580.
- Woods, B. D. (1957). "The Diffraction of A Dipole Field by a Half-plane," Quart. Journ. Mech. and Appl. Math. 10, part 1, pp. 90-100.
- Zemanian, A. H. (1965). Distribution Theory and Transform Analysis, McGraw-Hill Book Company, New York.

VITA

Donald Farness Hanson was born March 5, 1946 in Urbana, Illinois. His middle name stands for Farnes, Norway, where his father's mother was born. In 1956, while returning from a trip to Italy with his family, his ship, the Andrea Doria, was struck by another ship and sank. Fortunately, he survived. After graduating from high school, he spent three years at Iowa State University in Ames, Iowa. While there, he developed an interest in the theatre and became a member of the Iowa State Players. During his last quarter at I.S.U., he was Co-Chairman of the Electrical Engineering Open House and Chairman of the Robot Project. The six-foot nine-inch tall robot was completely radio controlled. He transferred to the University of Illinois for his senior year, earning his B.S. in Electrical Engineering with honors in February of 1969. From June 1968 through February 1969, he was a systems programmer for the Translator Writing System of the ILLIAC IV computer.

In February 1969, he entered graduate school and did research in the area of digital and analog electronics under Dr. W. J. Poppelbaum. For his Masters degree, he improved the AUTOMATIC TRICOLOR CARTOGRAPH. This machine is an interactive color television display system that automatically colors the inside of a boundary when an interior point is designated. The work was funded by the Atomic Energy Commission. He obtained his M.S. in Electrical Engineering in June 1972 with a thesis entitled Outlining and Shading Generation for a Color Television Display. During much of the time he was working on his Masters Degree he worked one night a week at the student radio station, WPGU-FM, as an announcer and engineer for a

classical music program. After finishing his Masters, he began to work on his Ph.D. in the area of electromagnetic theory under Dr. P. E. Mayes. As a teaching assistant in Electrical Engineering, he was asked to design an automated integrated circuit tester to test digital integrated circuits with an immediate verdict appearing at the push of a button. This project, which is still in use, resulted in the Electrical Engineering report entitled A Digital Integrated Circuit Tester. For the 1973/74 school year, the Architecture Department at the University of Illinois asked him to teach their senior-level course in practical lighting and wiring design. As a Lecturer in Architecture, he was in charge of 50 students in the fall and 165 students in the spring. For the last two years, he has been teaching E. E. 379, an analog and digital electronics laboratory course. For the last year, he has been an Instructor in Electrical Engineering.

Mr. Hanson is a member of the IEEE.

UNIVERSITY OF ILLINOIS-URBANA

537.12H19I

C001

AN INVESTIGATION OF THE CURRENT SOURCE-F



3 0112 007454082